AN INTRODUCTION TO STRUCTURAL OPTIMIZATION PROBLEMS

by

BRIAN MAXWELL ELMO DE SILVA

M.A.(Cambridge), B.Sc.(London), A.F.I.M.A.

A Doctoral Thesis

submitted in partial fulfilment of the requirements

for the award of

Doctor of Philosophy of the Loughborough University of Technology

JUNE 1972

SUMMARY

The object of the research described in this thesis is to examine the possibilities of developing analytical and computational procedures for a class of structural optimization problems in the presence of behaviour and side constraints. These are essentially optimal control problems based on the maximum principle of Pontryagin and dynamic programming formalism of Bellman. They are characterised by inequality constraints on the state and control variables giving rise to systems of highly complex differential equations which present formidable difficulties both in the construction of the appropriate boundary conditions and subsequent development of solution procedures for these boundary value probelms. Therefore an alternative approach is used whereby the problem is discretised leading to a non-linear programming approximation. The associated non-linear programs are characterised by non-analytic "black box" type representations for the behaviour constraints. The solutions are based on a "steepest descent - alternate step" mode of travel in design space.

The thesis is in two parts: Part I considers structural optimization from a nonlinear programming standpoint and begins by reviewing some constrained problems based on plastic and elastic redesign concepts. This is followed by the development and discussion of procedures applicable to problems with "black box" type behaviour constraints. They are illustrated with reference to the optimal design of a steam turbine disc idealisation subject to stress and vibration constraints.

Part II describes the continuous formulation of the disc problem

based on the formalism of optimal control theory. These problems are characterised by inequality constraints on the state and control variables. Considerable progress has been made in studying these problems using purely analytical techniques embodied in the maximum principle of Pontryagin. This has led to the scope of optimal control theory being extended to include a more general class of structural optimization problem than considered hitherto. Part II includes a derivation of the Principles of Pontryagin and Bellman using a first variation technique in conjunction with generalised Lagrange multipliers.

The thesis concludes with a brief statement of some structural optimization problems under investigation by the author.

ACKNOWLEDGEMENT

The author expresses his appreciation and gratitude to:

Professor C. Storey, Department of Mathematics, Loughborough University of Technology, for his continuing interest and encouragement during the period leading up to the preparation of this thesis. His careful reading of the original typescript and subsequent suggestions contributed significantly to the success of this undertaking.

Dr. R.K. Livesley, Department of Engineering, University of Cambridge, and Professor R.L. Fox, Department of Engineering, Case Western Reserve University, USA, who also read the draft version and made helpful comments.

Mrs. J. Russell for her careful typing.

CONTENTS

Part I - Nonlinear Programming Formulation

CHAPTER 1

SOME STRUCTURAL OPTIMIZATION PROBLEMS BASED ON ELASTIC AND PLASTIC DESIGN CONCEPTS

1.1 INTRODUCTION

The object of the research described in this thesis is to examine the possibility of developing computational and analytical procedures based on the methods of mathematical programming for a class of structural optimization problems in the presence of design constraints. These problems are essentially of a variational nature and are based on the formalism of optimal control theory. Exact solutions in general are impossible and recourse must be made to numerical procedures based on a discretised nonlinear programming approximation. The behaviour constraints are represented by functional constraints which correspond to nonanalytic constraints in the nonlinear programming formulation. For purposes of simplicity this initial investigation is restricted to a nonlinear programming representation.

The design requirements and specifications are represented by constraints on the behaviour and design variables. The behaviour variables describe the behaviour or response of the structure to the applied design loads and consist of structural variables such as stresses, vibrational frequencies, deformations, creep strains and so on, which are constrained to satisfy specified behaviour conditions in order to prevent failure of the structure. For example, the behaviour constraints may include statical constraints which constrain the stresses to lie below given yield stress levels, instability constraints which prevent failure under given buckling modes, dynamical constraints which constrain the vibrational frequencies to lie outside specified resonance bands and so on. Similarly, the design variables specify the design configuration of the structure and are constrained to satisfy prescribed side conditions in order to ensure physically reasonable design configurations. For example, the side constraints may impose restrictions on the dimensions of the structure which constrain the design variables to vary within prescribed bounds. The behaviour and side constraints are represented mathematically by a combination of equality and inequality constraints. The merit function to be optimised is usually the weight or cost of manufacture of the structure but other criteria such as some optimal combination of frequencies or structural efficiency may also be used. The problem can be formulated as a problem in nonlinear programming - optimizing a merit function in the presence of equality and inequality constraints. When these functions and conditions are obtainable as analytic functions of the design variables, the solutions can be based on standard nonlinear programming procedures.

Because of the variational nature of some problems, it is not always possible to use closed form analytical functions for describing the behaviour characteristics of the system. The behaviour variables are functions only in the sense that they are computer-oriented rules for determining the behaviour associated with a given design configuration. The behaviour variables may be regarded as a "black box" into which are put the design variables characterising a given design configuration and out of which comes the behaviour variables for that design. The box may contain such items as differential equations, matrices, numerical procedures, a digital computer and so on.

The synthesis is based on the concept of a design space which is the multi-dimensional Euclidean space spanned by the design variables. The behaviour and side constraints are represented by constraint hypersurfaces which separate the regions of feasible designs from regions of non-feasible designs. Since the behaviour variables are of a "black box" nature, the corresponding surfaces are unknown. The contours of constant merit are also surfaces in this space and the problem consists of determining the path to the optimum merit contour in the feasible regions. The synthesis commences from an initial (feasible) trial design which is systematically improved by an alternating iterative process of analysis and design modification. This automated synthesis capability generates motion in design space along paths on which the merit improves and consists essentially in the proper selection of the directions and distances of travel in design space.

The synthesis procedures specifically applicable to structural optimization problems in the presence of non-analytic constraints on the behaviour variables are those developed by Schmit and his co-workers for the minimum weight design of aerospace structures. Although the behaviour characteristics are described by analytical functions, the synthesis is independent of this analytical representation. Since these procedures are central to this investigation, they are briefly reviewed in this chapter and their applications considered in the following chapters. An attempt is also made to generalise and modify them to improve their computational efficiency and convergence rates and to develop further methods applicable to a wider range of problems. Other methods which have recently been used in the structural optimization area are based on the penalty function ideas of nonlinear programming [80,236,237] whereby a constrained problem is reduced to a series of unconstrained optimization problems which are solved using the techniques of Rosenbrock (hill-climbing), Powell (conjugate direction), Nelder-Mead (Simplex) and Davidon-Fletcher-Powell (variable metric).

The problems considered by way of illustration are: (Figure 2.1)

(1) weight minimistation of a steam turbine disc idealisation subject to specified behaviour and side constraints. For purposes of simplicity, the behaviour constraints are restricted to a consideration that the stresses everywhere should be below the yield stress for the material and the frequencies of vibration should lie outside specified frequency bands. The side constraints on the other hand impose restrictions on the dimensions and tolerances of the disc. The optimization is in two parts, based on a separate consideration of the stress and vibration constraints.

(2) calculation of the optimal vibrational modes of the disc, whereby some linear combination of the frequencies is optimized in the presence of a constraint on the total weight.

The problem consists essentially in determining an optimal thickness $h(r)$ where r is the radial distance from the axis of rotation, the thickness being measured parallel to the axis of rotation. The stresses are obtainable from a set of ordinary differential equations which contain h(r) and its derivatives. These equations are solvable only when h(r) is a specified function of r. Therefore the stresses are functionals of h(r) and correspond to "black box" type variables. The frequencies have essentially an eigenvalue structure corresponding to a functional differential operator, while the computations are based on a discretised transfer matrix method. The frequencies have again a "black box" type representation. The function h(r) which defines the design configuration is approximated by a discrete set of variables which define the design variables for the disc. These variables are read into standard programs for the stress and frequency calculations. The output from these programs determine the corresponding stresses and vibrational frequencies which must be subsequently checked against the behaviour constraints. The side constraints on the other hand ensure the non-negativity of h(r).

These problems are considered in detail in the following chapters. As a preliminary, this introductory chapter reviews some minimum weight structural optimization problems appearing in the technical literature with emphasis on nonlinear programming procedures of relevance to problems with non-analytic constraints. These problems are based on plastic and elastic design concepts and are briefly described below.

1.2 METHODS OF ANALYSIS

In the past engineers have judged the suitability of materials mainly in relation to their elastic range because a structure must be designed so as not to collapse under the design load system and it has been the custom to consider collapse to have occurred when the first yielding or permanent deformation has taken place. Lately, attention has been extended to the plastic regions in which permanent distortion occurs under stress. This is to enable a more efficient use of materials by obtaining a better understanding of the behaviour of the structure throughout the complete loading range leading up to final collapse, and also in order to understand the processes involved in the mechanics of formation such as the shaping and machining processes.

The theory of elasticity is based on the following assumptions:

(1) there is complete recovery of the initial unstrained configuration when the distorting forces or the externally derived strains are removed.

(2) the deformation of the body depends only on the final stresses not on the previous loading history or strain path.

(3) the stress-strain relations are given by a generalised Hooke's Law.

On the other hand none of these assumptions can be applied to a plastic body. There is no unique correspondence between stress and strain, and the corresponding equations have to be integrated by following the history of the deformation. Plasticity may be defined as that property which enables a material to be continuously and permanently deformed without rupture during the application of stresses exceeding those necessary to cause yielding of the material. Thus permanent distortion occurs under stress, and this distortion can build up to large amounts if the yield value is exceeded. The final deformation therefore depends not only on the final state of stress but also on the series of intermediate stress states from the initial state. The laws of plastic flow which relate the stress components and the corresponding deformations satisfy four main conditions:

(1) the volume of material remains constant under plastic deformation;

(2) hydrostatic pressure does not cause yielding;

(3) hyrdostatic component of a complex state of stress does not influence the point at which yielding occurs;

(4) a yield criterion must be formulated which will determine when yielding will start under a complex state of stress, given only the yield stress under a simple state of stress (e.g. uniaxial tension).

The yield criteria most frequently used are the Tresca maximum shear stress criterion and the Von Mises criterion. Further requirements must be satisfied in the case of work hardening materials. For problems in which the plastic strains are constrained to be of the same order as the elastic strains, the solutions in the elastic and plastic domains have to be solved side by side. In addition, various continuity conditions have to be satisfied along the elastic-plastic interface which is itself unknown. For a perfectly plastic material the stresses everywhere are less than, or equal to, the yield limit. Plastic collapse occurs when the design load system reaches a limiting value. As the loads approach their limiting value the deformations increase indefinitely and the body cannot sustain any additional loads. This critical load system can be determined using the theorems of limit analysis. Limit analysis is usually simpler to apply than an elastic analysis and may be used to obtain efficient designs resulting in considerable savings on weight and cost. An analysis based on the elastic-plastic regions is extremely complicated as it involves tracing the entire load history of the structure and a step-by-step integration of the equations of plastic flow. However, for designs based on a limit analysis the critical load system is independent of the previous loading program and may easily be determined using the theorems of limit analysis.

The general theory of minimum weight design may be based on either an elastic analysis or on a plastic analysis. The criterion of minimum weight design based on the theory of perfect plasticity is that the structure is on the verge of unrestricted flow under the applied loads and contains a minimum of material. The solutions are based on the theorems of plastic collapse formulated by Drucker, Prager and Greenberg [3] and applied to the minimum weight design of membranes, shells, plates and discs. These theorems provide bounds on the minimum weight solutions.

However, when it is undesirable to have any permanent plastic deformation and the structure is required to be reusable, the problem of minimum weight design must be formulated within the elastic range. The classical theory of optimal elastic design of structures was formulated by Michell [36] and extended by Cox [45], Hemp [38] and Chan [40,41], who showed that for statically determinate structures subject to a single load condition, the fully-stressed design criterion in which the stresses in the structural members were at their limiting values was equivalent to the minimum weight design. Later generalisations by Schmit and his associates [65-74] to structures under multiple load conditions in the presence of side constraints have shown that the fully-stressed design criterion in general is not always equivalent to weight minimisation.

1.3 PLASTIC DESIGN

The problem considered is that of determining the minimum weight of a structure capable of sustaining given design loads in the form of concentrated or continuously distributed force fields. The material is assumed to be perfectly plastic and of uniform density so that the condition of minimum weight is equivalent to minimum volume. The essential characteristics of plastic design are that it provides a first approximation to the behaviour of structural materials beyond their elastic range and provides a more realistic model for the behaviour of ductile materials. The minimum weight solutions are based on the plastic collapse theorems [1-3] where the geometrical changes of the body prior to and during the initial stages of collapse are neglected. They are valid for the initial motion of rigid perfectly plastic materials. The basic assumptions are:

(a) collapse occurs at constant load and at constant stress;

(b) plastic strains only take place.

These are equivalent to the following collapse theorems.

(1) *Upper bound theorem*

If an equilibrium distribution of stress exists which is everywhere below yield, then the structure will be safe against collapse at the given loads.

(2) *Lower bound theorem*

Collapse occurs when the rate at which the design loads do work exceeds the rate of internal plastic energy dissipation.

The yield condition for the structure is assumed to be of the form

$$f(\sigma_{ij}) = k^2 \tag{1.1}$$

The material behaves elastically for $f < k^2$ and plastic flow occurs when $f = k^2$. Stress fields for which $f > k^2$ are inadmissible. The yield condition defines a yield surface in stress space where the components of stress σ_{ij} are used as rectangular cartesian coordinates. The plastic strain rate tensor is then given by the external normal to the yield surface

$$e_{ij}^{(p)} = \lambda \frac{\partial f}{\partial \sigma_{ij}} \tag{1.2}$$

where λ is a small positive constant. At singular points there is no unique normal and the strain rates lie within the cone bounded by the normals to the yield surface at adjacent points. The dissipation rate per unit volume is given by

$$D(e_{ij}) = \sigma_{ij}\, e_{ij}\ {}^{*}$$

where the strain rates treated as purely plastic are defined by

$$e_{ij} = \frac{1}{2}\left(\frac{\partial u_i}{\partial x_j} + \frac{\partial u_j}{\partial x_i}\right)$$

where the u_i are velocities defining a compatible deformation field. The dissipation function can also be written in the equivalent form

$$D = \sum Q_i\, q_i$$

where Q_i are the generalised stresses corresponding to the generalised strains q_i. For admissible structures, the lower bound theorem gives

$$\int_S T_i\, u_i\, dS + \int_V F_i\, u_i\, dV \leqslant \int_V D\left(e_{ij}^{(p)}\right) dV$$

where rate of internal energy dissipation arises purely from the plastic strain rates.

---

* summation convention is used, where a repeated suffix denotes summation with respect to that suffix.

So that,

$$\int_V \Delta(u_i)dV \geq \int_S T_i\, u_i\, dS \qquad (1.3)$$

where

$$\Delta(u_i) = D(e_{ij}^{(p)}) - F_i\, u_i .$$

The surface S can be written in the form

$$S = S_T + S_U$$

where

S_T = part of the surface on which the non-vanishing surface tractions T_i are prescribed

S_U = part of the surface on which the velocity u_i vanishes.

Hence,

$$\int_S T_i\, u_i\, dS = \int_{S_T} T_i\, u_i\, dS$$

For a structure on the verge of collapse

$$\int_{V_c} \Delta\left(u_i^{(c)}\right)dV = \int_{S_T} T_i\, u_i^{(c)}\, dS$$

For any other admissible structure V_s

$$\int_{V_s} \Delta\left(u_i^{(c)}\right)dV \geq \int_{S_T} T_i\, u_i^{(c)}\, dS$$

This implies

$$\int_{V_s} \Delta\left(u_i^{(c)}\right) dV \geq \int_{V_c} \Delta\left(u_i^{(c)}\right) dV$$

Let $\Delta\left(u_i^{(c)}\right)$ = constant throughout the bounding volume. This means

$$V_s \geq V_c$$

and

$$V_c = V_m \tag{1.4}$$

where V_m is the absolute minimum volume. Therefore a structure designed for such a continuous collapse mode will be of minimum weight. Some applications of the condition Δ = constant, are considered below. Consider first the minimum weight solutions for a circular disc [4] for which the inner radius a_1 is assumed stress-free while the outer radius a_m is subjected to a tensile load T per unit circumferential length. The material is assumed to obey the Tresca maximum shear condition (Figure 1.1a)

$$\max(|\sigma_r|, |\sigma_\theta|, |\sigma_r - \sigma_\theta|) = \sigma_o \tag{1.5}$$

where σ_o = yield stress.

The equation of dynamic equilibrium is given by [136]

$$\frac{d}{dr}\left(h\sigma_r\right) + \frac{h}{r}(\sigma_r - \sigma_\theta) + \rho\omega^2 rh = 0 \tag{1.6}$$

where ω is the angular velocity. This equation has been derived on the assumption of radially symmetric plane stress. This simplifying assumption in which the influence of the shear stresses has been disregarded is sufficiently accurate if the thickness does not vary too abruptly and does not become too large in comparison with the diameter. The plastic minimum weight condition becomes

$$\Delta \equiv \sigma_r e_r + \sigma_\theta e_\theta - \rho\omega^2 ru = \text{constant} \tag{1.7}$$

where the strain rates e_r, e_θ are given in terms of the radial velocity u by the relationships

$$\left.\begin{aligned} e_r &= \frac{du}{dr} \\ e_\theta &= \frac{u}{r} \end{aligned}\right\} \tag{1.8}$$

The stress state cannot lie on the sides AF or CD because the normality condition (1.2) requires $e_r = 0$, $e_\theta = \lambda$ and condition (1.7) cannot be satisfied in view of (1.8). Sides BC, FE are also prohibited because $e_\theta = 0$ and this implies $u = 0$. The normality condition for sides AB, ED gives

$$\left.\begin{aligned} e_r &= -e_\theta \\ |\sigma_r - \sigma_\theta| &= \sigma_o \end{aligned}\right\} \tag{1.9}$$

From (1.7)

$$ke_r - \rho\omega^2 ru = \text{constant} \quad (k = \pm\sigma_o) \tag{1.10}$$

From (1.8, 1.9)

$$u = \frac{A}{r} \tag{1.11}$$

where A is a constant of integration. From equations (1.10, 1.11)

$$e_r = B \qquad \text{(constant)}.$$

Therefore from (1.8)

$$u = Br + C \tag{1.12}$$

where C is a constant of integration. Equations (1.11, 1.12) lead to a contradiction. Therefore the solutions must lie at the vertices of the hexagon. The corners A, D are not permissible because $\sigma_r = 0$ and equation (1.6) gives $h = 0$. The stresses everywhere are tensile so that the vertices B, C are prohibited. The vertex E is also inadmissible as it gives a negative radial velocity at the inner radius a_1. Therefore the remaining vertex F must define the solution

$$\sigma_r = \sigma_\theta = \sigma_o$$

Substituting this in (1.6) and using the loading condition at $r = a_m$ gives

$$h = \frac{T}{\sigma_o} \exp \frac{\rho\omega^2}{2\sigma_o}(a_m^2 - r^2)$$

The condition $\sigma_r = 0$ at $r = a_1$ can be satisfied by defining the optimal thickness as follows (Figure 1.1b)

$$\left.\begin{aligned} h(r) &= \frac{T}{\sigma_o} \exp \frac{\rho\omega^2}{2\sigma_o}(a_m^2 - r^2) \qquad a_2 < r \leq a_m \\ &= b_1 \qquad\qquad\qquad\qquad\qquad a_1 \leq r \leq a_2 \end{aligned}\right\} \tag{1.13}$$

where b_1 is some specified upper bound on the thickness and the radius a_2 is to be determined. The stresses within the region $a_1 \leq r \leq a_2$ are represented by points on the side AF of the hexagon for which $\sigma_\theta = \sigma_o$, $0 \leq \sigma_r < \sigma_o$, so that equation (1.6) becomes on simplification

$$\sigma_r = \frac{1}{r}\left[\sigma_o(r - a_1) - \frac{1}{3}\rho\omega^2(r^3 - a_1^3)\right] \tag{1.14}$$

The radial load at a_1 is continuous, therefore

$$b_1(\sigma_r)_{r=a_2-0} = h(a_2 + 0)\sigma_o$$

and

$$\frac{b_1}{a_2}\left[\sigma_o(a_2 - a_1) - \frac{1}{3}\rho\omega^2(a_2^2 - a_1^3)\right] = T \exp \frac{\rho\omega^2}{2\sigma_o}(a_m^2 - a_2^2) \tag{1.15}$$

This equation can be used to determine the hub radius a_2.* The thickness is discontinuous at a_2. The analysis can be extended to include a thickness distribution of the form

$$\left.\begin{aligned} h(r) &= b_1 && a_1 \leqslant r \leqslant a_2 \\ &= h_o \exp\left(\frac{-\rho\omega^2}{2\sigma_o} r^2\right) && a_2 < r < a_{m-1} \\ &= b_m && a_{m-1} \leqslant r \leqslant a_m \end{aligned}\right\} \tag{1.16}$$

where b_1, b_m, a_1, a_m, a_{m-1} h_o are constants, b_1, b_m, being the thickness at the inner and outer radii respectively assumed constant. The stresses at these edges are given by

$$\left.\begin{aligned} (\sigma_r)_{r=a_1} &= s < 0 \\ (\sigma_r)_{r=a_m} &= S > 0 \end{aligned}\right\} \tag{1.17}$$

where s, S are constants.

---

* A more general analysis based on limit theorems in the presence of side constraints is given by Kowlowski and Mroz [226]

The calculation of a_2 proceeds along lines similar to that considered earlier. A point r_o is first considered where $a_1 < r_o < a_2$, such that $\sigma_r \leqslant 0$ in $a_1 \leqslant r \leqslant r_o$ and $\sigma_r \geqslant 0$ in $r_o \leqslant r \leqslant a_2$.

Let r_o be the radius at which $\sigma_r = 0$. The stress states within the region $r_o \leqslant r \leqslant a_2$ are represented by points on the side FA of the hexagon where

$$\left.\begin{aligned} \sigma_\theta &= \sigma_o \\ 0 \leqslant \sigma_r &\leqslant \sigma_o \end{aligned}\right\} \qquad (1.18)$$

Solving the differential equation (1.6) gives

$$\sigma_r = \sigma_o\left(1 - \frac{r_o}{r}\right) - \frac{\rho\omega^2 r^2}{3}\left(1 - \frac{r_o^3}{r^3}\right) \quad \text{when} \quad r_o \leqslant r \leqslant a_2 \qquad (1.19)$$

Again, $\sigma_\theta - \sigma_r = \sigma_o$ where $a_1 \leqslant r \leqslant r_o$

This corresponds to stress states on the branch BA of the hexagon. Solving (1.6) using the condition $\sigma_r = s$ at $r = a_1$ gives

$$s = \sigma_o \ln \frac{a_1}{r_o} - \frac{\rho\omega^2}{2}(a_1^2 - r_o^2) \qquad (1.20)$$

This equation enables r_o to be calculated. The radial load at a_2 is continuous, which implies

$$b_1(\sigma_r)_{a_{2-0}} = h(a_2 + 0)\sigma_o$$

From (1.16 , 1.19),

$$b_1\left[\sigma_o\left(1 - \frac{r_o}{a_2}\right) - \frac{\rho\omega^2}{3a_2}(a_2^3 - r_o^3)\right] = h_o\sigma_o \exp\left\{-\frac{\rho\omega^2}{2\sigma_o} a_2^2\right\} \qquad (1.21)$$

For $a_{m-1} \leq r \leq a_m$, the stress states are represented by points on the side AF.

$$\left.\begin{aligned} 0 \leq \sigma_r &\leq \sigma_o \\ \sigma_\theta &= \sigma_o \end{aligned}\right\} \qquad (1.22)$$

Using (1.6) in conjunction with $\sigma_r = S$ at $r = a_m$ gives

$$\sigma_r = \sigma_o\left(1 - \frac{a_m}{r}\right) + \frac{a_m}{r} S + \frac{\rho\omega^2}{3r}\left(a_m^3 - r^3\right),$$

$$\text{when} \quad a_{m-1} \leq r \leq a_m \qquad (1.23)$$

The radial load at $r = a_{m-1}$ is continuous, therefore

$$b_m(\sigma_r)_{a_{m-1+0}} = h(a_{m-1} - 0)\sigma_o$$

Hence,

$$b_m\left[\sigma_o\left(1 - \frac{a_m}{a_{m-1}}\right) + \frac{a_m}{a_{m-1}} S + \frac{\rho\omega^2}{3a_{m-1}}\left(a_m^3 - a_{m-1}^3\right)\right] = \sigma_o h_o \exp\left\{\frac{-\rho\omega^2}{2\sigma_o} a_{m-1}^2\right\} \qquad (1.24)$$

From (1.21, 1.24)

$$\frac{b_m}{b_1} \; \frac{\sigma_o\left(1 - \frac{a_m}{a_{m-1}}\right) + \frac{a_m}{a_{m-1}} S + \frac{\rho\omega^2}{3a_{m-1}}\left(a_m^3 - a_{m-1}^3\right)}{\sigma_o\left(1 - \frac{r_o}{a_2}\right) - \frac{\rho\omega^2}{3a_2}\left(a_2^3 - r_o^3\right)} = \exp\left(\frac{-\rho\omega^2}{2\sigma_o}\right)\left(a_{m-1}^2 - a_2^2\right) \qquad (1.25)$$

Equations (1.20, 1.25) enable a_2 to be determined. Some numerical computations based on this analysis are considered. The computations were performed for a standard turbine disc of the type considered in this investigation. The results are summarised below:

DATA $a_1 = 14\cdot 0''$, $a_m = 32\cdot 3''$, $a_{m-1} = 30\cdot 3''$, $b_1 = 9\cdot 0''$

$b_m = 3\cdot 0''$, $m = 7$, $\rho = 0\cdot 283$ lb/in^3, $\sigma_o = 6 \times 10^4$ lb/in^2

TABLE 1

RADIUS (ins)	OPTIMAL THICKNESS (ins)
$a_2 = 15\cdot 58$	$7\cdot 053 \times 10^{-2}$
$21\cdot 313$	$6\cdot 618 \times 10^{-2}$
$22\cdot 813$	$6\cdot 487 \times 10^{-2}$
$29\cdot 5$	$5\cdot 838 \times 10^{-2}$
$30\cdot 3$	$5\cdot 755 \times 10^{-2}$

MINIMUM WEIGHT = $0\cdot 7463 \times 10^3$ lbs

The corresponding results based on an elastic analysis are also included in this chapter for purposes of comparative study. These optimal designs have been derived in the absence of side constraints. The modifications in the presence of side constraints are considered in Chapters 2 and 3. Further applications of the optimality condition Δ = constant are considered below. In the absence of body forces ($F_i = 0$) the minimum weight condition reduces to

$$\Delta(u_i) \equiv D(e_{ij}) = \text{constant}$$

This means that the designs must be based on a constant dissipation rate per unit volume over the entire structure.

For thin plates [4,5], the dissipation rate is linear over the thickness, thus precluding the possibility of D = constant everywhere. The strain rates are given by

$$e_{\alpha\beta} = \frac{2z}{h} e^{o}_{\alpha\beta}$$

where z is measured from the undeformed middle surface and $e^{o}_{\alpha\beta}$ is the maximum value of the strain rate. The rate of internal energy dissipation is given by

$$D(e_{\alpha\beta}) = \frac{2|z|}{h} D^{o} \tag{1.26}$$

Suppose the plate is on the verge of collapse under a transverse load p per unit area. Therefore,

$$\int_A pW^{(c)}\, dA = \int_V D(e_{\alpha\beta})dV = \int_{A_c} \frac{2D^{o}}{h}\, dA \int_{-h/2}^{+h/2} |z|dz = \int_{A_c} \tfrac{1}{2}D^{o}_{c}\, h_c\, dA$$

This corresponds to the critical thickness $h = h_c$.
For a plate not on the verge of collapse

$$\int_A pW^{(c)} dA \leq \int_{A_s} \tfrac{1}{2}\, D^{o}_{s}\, h_s\, dA$$

Hence,

$$\int_{A_c} \tfrac{1}{2}\, D^{o}_{c}\, h_c\, dA \leq \int_{A_s} \tfrac{1}{2}\, D^{o}_{s}\, h_s\, dA \tag{1.27}$$

Consider a small perturbation in the critical configuration

$$\left.\begin{aligned} h_s &\approx h_c + \delta h \\ A_s &\approx A_c \end{aligned}\right\} \tag{1.28}$$

From (1.26)

$$\frac{D_s^o}{D_c^o} = \frac{h_s}{h_c} \tag{1.29}$$

From (1.27, 1.28), neglecting second order terms in δh

$$\therefore \int_{A_c} D_c^o \, \delta h \, dA \geq 0$$

Suppose D_c^o is a positive constant over A.

From (1.27),

$$\int_{A_c} h_c \, dA \leq \int_{A_s} h_s \, dA$$

Therefore plates which are compatible with a deflection rate for which D_c^o is a constant on the middle surface provide a relative minimum. An alternate formulation can be based on the bending moments $M_{\alpha\beta}$ and curvatures $k_{\alpha\beta}$ of the middle surface. The rate of dissipation per unit area is given by

$$M_{\alpha\beta} \, k_{\alpha\beta} = \int_{-h/2}^{h/2} D \, dz = \tfrac{1}{4} D^o h$$

Therefore the condition for a relative minimum becomes

$$\frac{M_{\alpha\beta} \, k_{\alpha\beta}}{h} = \text{constant} \tag{1.30}$$

This result was derived independently by Freiberger and Tekinalp [6] using the calculus of variations. The latter approach required far greater effort and there was no real indication that the solutions corresponded to an actual minimum.

They considered the case of a simply supported thin circular plate under a transverse load p(r). The generalised stresses were the principal bending moments M_r, M_θ while the generalised strain rates were the curvatures k_r, k_θ, in the radial and circumferential directions respectively. On account of radial symmetry these variables are functions of radial distance only. The equations of equilibrium were given by

$$\frac{d}{dr}(r\, M_r) - M_\theta + \int_0^r r\, p(r)dr = 0 \tag{1.31}$$

The yield condition for the plate was given by

$$F(M_r, M_\theta) = M_o^{\frac{1}{2}} \tag{1.32}$$

where M_o is the fully plastic moment of theplate defined by

$$M_o = \int_{-h/2}^{h/2} |z|\sigma_o\, dz = \frac{1}{4}\sigma_o\, h^2$$

where σ_o is the yield stress in simple tension or compression. The function F was assumed to be continuously differentiable and homogeneous of order $\frac{1}{2}$ in M_r, M_θ. The weight of the plate is proportional to

$$W = \int_0^R r\, M_o^{\frac{1}{2}}\, dr \tag{1.33}$$

where R is the radius of the plate. The minimum weight solutions are obtained by minimising (1.33), subject to the constraint conditions (1.31, 1.32). These are provided by the Euler-Lagrange equations which give on simplification

$$\frac{D}{h} = \text{constant} \tag{1.34}$$

where D is the rate of energy dissipation per unit area defined by

$$D = M_r k_r + M_\theta k_\theta$$

where

$$k_r = -\frac{d^2W}{dr^2} = \lambda \frac{\partial F}{\partial M_r}$$

$$k_\theta = -\frac{1}{r}\frac{dW}{dr} = \lambda \frac{\partial F}{\partial M_\theta}$$

Therefore,

$$D = \lambda\left(M_r \frac{\partial F}{\partial M_r} + M_\theta \frac{\partial F}{\partial M_\theta}\right) = \lambda . \frac{1}{2} F = \frac{1}{2} \lambda M_o^{\frac{1}{2}} \tag{1.35}$$

Equation (1.34) was derived on the assumption of a smooth yield surface. Therefore the analysis is applicable to the Von Mises yield condition but not to the Tresca yield condition. Equations (1.33, 1.35) indicate that for each plate element at collapse, the weight is proportional to the dissipation rate. This is a generalisation of a result obtained by Foulkes [7] for structural frames. The minimum weight solutions for the Tresca yield condition have been derived by Hopkins and Prager [8,9] using the concept of a hinge circle [10] to show that the radial and circumferential bending moments at each point are equal to the fully plastic bending moment at that point.

$$M_r = M_\theta = M_o(r) = \frac{1}{4}\sigma_o h^2(r) \tag{1.36}$$

This corresponds to the stress state represented by the point F of the Tresca hexagon (Figure 1.1a).

The concept of a hinge circle is a generalisation of the concept of a plastic hinge used in the theory of the plastic analysis of beams and frames. Substituting (1.36) in (1.31) gives

$$\frac{d}{dr}(rM_o) - M_o + \int_o^r r\,p(r)\,dr = 0 \tag{1.37}$$

where $M_o(R) = 0$ theplate being assumed to be simply supported at the outer edge. Therefore for a uniform pressure p this gives on integration

$$M_o(r) = \frac{pR^2}{4}\left(1 - \frac{r^2}{R^2}\right)$$

Therefore the optimal thickness is given by

$$h(r) = R\left(\frac{p}{\sigma_o}\right)^{\frac{1}{2}}\left(1 - \frac{r^2}{R^2}\right)^{\frac{1}{2}} \tag{1.38}$$

This plate design theory has seen significant improvements and modifications in recent years, details of which are given in references [11, 12, 196]. Megarefs [106-108] gives a comprehensive analysis of minimum weight plate theory based on the Tresca condition.

For shells [13,14] condition (1.34), becomes D/h = constant where h is now the thickness of the face sheets gives an absolute minimum weight solution. This result can also be derived using the calculus of variations [15,16]. This section on optimal plastic design is concluded by a brief discussion of the design of beams and frames. They are based on the limit theorems given at the beginning of this section. The minimum weight design of continuous beams and frames which derive their strength from a bending action is based on the concept of a plastic hinge and is characterised by a finite number of design variables. A linear relationship between bending moment and curvature is assumed for small values of the curvature. As the curvature is increased the bending moment tends to a maximum limiting value called the fully plastic moment and a plastic hinge is formed at the cross section where the bending moment attains this critical value. A plastic hinge allows a finite change of slope to occur at the place where it forms. The structure collapses when a sufficient number of hinges have formed to transform the structure, or any part of it, into a mechanism. This represents a deformation field corresponding to rotation at the hinges. The design is based on the assumption of a linear relationship between the weight per unit length (m) and the fully plastic moment M

$$m = a + bM$$

where a, b are constants over the entire frame. Therefore the total weight of the frame is given by

$$a \sum_i \ell_i + b \sum_i \ell_i M_i$$

where ℓ_i is the length of the i^{th} structural member and M_i is its fully plastic moment. Theproblem is that of minimising the weight function G defined by

$$G = \sum_i M_i \ell_i \tag{1.39}$$

where the constraint conditions are provided by the second collapse theorem

$$W \leqslant \sum_i M_i \theta_i \qquad (\theta_i = \text{hinge rotation})$$

where W is the work done by the applied loads, the right hand side representing the rate of internal energy dissipation at the plastic hinges. Hence,

$$\sum_i a_i M_i \geqslant 1$$

where

$$a_i = \frac{\theta_i}{W}$$

Therefore the behaviour characteristics of the frame are described by linear inequalities of the form

$$\sum_i a_{ji} M_i \geqslant 1 \qquad j \in J \tag{1.40}$$

where J is the set of all possible collapse mechanisms. Therefore the problem of minimising (1.39) when the non-negative variables M_i satisfy the constraint conditions (1.40) constitutes a linear programming problem.

Foulkes [7,17,18], Chan [198] have derived necessary and sufficient conditions for a minimum weight solution by representing the collapse mechanisms in a hyperspace whose coordinate axes are the fully plastic moments. The inequalities (1.40) define a polyhedron dividing the hyperspace into a feasible and a nonfeasible region. The minimum weight solutions lie at the vertices where the constant weight hyperplanes (1.39) touch the feasible region.

Methods of solution to the linear programming problem include: the method of inequalities developed by Neal and Symonds [19] for determining the load-carrying capacity of a frame. The method consists in the successive elimination of redundant variables and was applied by Heyman [20,21], Livesley [22] to the design of frames subject to single and multiple load conditions. Livesley [23] and Toakley [24] have proposed a modified simplex method of solution which is suitable for programming on a digital computer. Livesley starts from an initial trial design and uses a steepest descent technique to reach a vertex of the constraint set. The method then moves from vertex to vertex until a minimum is attained. Toakley, on the other hand, uses the dual simplex algorithm to obtain his solutions. Prager [25] uses network theory [26], and has also considered a weight function given by [27]

$$G = \sum_i \ell_i \, M_i^{\alpha} \tag{1.41}$$

where α is a positive exponent less than unity. This means that the function G is convex in the variables M_i and the problem of minimising (1.41) subject to the linear constraints (1.40) constitutes a convex programming problem. The weight contours are convex surfaces in the plastic moment space and the optimal design lies at a vertex of the constraint set where the tangent hyperplane to the weight contour contains the collapse mechanism associated with the vertex. Similar problems have been investigated by Chires [28], and Chan [199], amongst others. Brotchie [29] and Cohn [35] have discussed the practical design considerations involved in these minimum weight design problems.

The minimum weight design of beams of variable cross-section is based on a deflection shape which gives a constant rate of curvature [30,31]. Gross and Prager [32,33] have used this result to design beams under a single moving load assuming piecewise linear variation of the plastic moment along the length of the beam, thereby reducing the problem to a linear programming problem. Save and Prager [34] have extended the analysis to beams under the combined action of fixed and moving loads. More powerful procedures applicable to a wider class of problems have been developed by Megarefs and Sidhu [109], Gjelsrik [230], based on a different minimality criterion. The volume was expressed as a functional of the bending moment, giving rise to a variational problem.

1.4 ELASTIC DESIGN

Elastic minimum weight design is based on the assumption that the optimum lies at the intersection of the behaviour constraints in the absence of side constraints. Such problems include the design of aerospace structures with buckling constraints, and the design of discs, plates, pressure vessels and so on where the solutions have been based on the assumption that the material is everywhere at the yield stress. The presence of side constraints restricts the design variables to vary within specified bounds, the minimum weight solutions being based on the methods of nonlinear programming. A fully automated synthesis technology has been developed by Schmit and his associates [65-74] for such problems where they use a combination of steepest descent and random search procedures for the exploration of the feasible regions of design space. Modifications of these procedures have been applied by Gellatly and Gallagher [82,83,97], Best [84], and de Silva [179] amongst others to structural optimization problems. Taylor [90], Turner [85,86], Zarghamee [87,88] and de Silva [235] have used variational techniques to study the design vibrational characteristics of such problems. Recently the penalty function concept of nonlinear programming has been introduced into the structural optimization area to transform a constrained problem into a series of unconstrained optimization problems, which are solved using the minimisation techniques of Rosenbrock, Powell, Nelder-Mead and Davidon-Fletcher-Powell [80].

The introductory stages of this section sketch the historical development of optimal elastic design, followed by the modern nonlinear programming treatment of the subject.

The classical theory of elastic design was formulated by Michell [36], in 1904 for the minimum weight design of statically determinate structures under a single load condition. According to him, the weight of a structure is a minimum when the space which it occupies can be subjected to a virtual deformation such that the strain in the direction of each member is $\pm e$ $(e > 0)$ where the sign agrees with that of the end load carried by the member. No other member is to have an extension or compression numerically greater than e.

The deformation field which extends over the whole region of space occupied by the structure is characterised by an orthogonal system of curves along which the members of the optimal design lie. These curves remain orthogonal after the deformation and are lines of constant principal strain equal to ±e. For two-dimensional problems this condition is identical to that governing the slip lines for two-dimensional perfectly plastic flow [37,40]. Using this analogy*, Hemp [38, 200] and Chan [39,41] have made a comprehensive study of the Michell theory using the methods of linear programming to determine the optimal design. Schmidt [42] has extended the theory to problems with multiple load conditions, where optimal design is based on the assumption that each member of the structure reaches its maximum allowable stress in at least one load condition. Cox [43-46] has applied the fully stressed design criterion of the theory to the design of beams and frames. For statically indeterminate problems [47-49] a solution is obtained only after a sufficient number of redundant members have been removed to give a statically determinate structure. Further applications to problems with creep and vibration conditions are given by Hegemier and Prager [50]. The minimum weight of structures subject to buckling constraints is attained when all the possible buckling modes occur simultaneously [51,52]. The condition that all the possible failure modes are equally likely to occur under a single load condition is satisfied in the absence of side constraints and enables the determination of as many optimal design variables as

* See also recent work of Johnson et al [234]

there are failure modes. Gerard [153,211], Lakshmikantham and Gerard [152] have made an extensive study of these design concepts as applied to aerospace vehicles based on cylindrical shell concepts. Reference [153] includes an extensive literature survey of minimal weight based on stability considerations.

Hilton and Feigen [53], Moses and Kinser [54] have considered optimal design from a probabilistic standpoint. The strength properties of the material and the structure and also the magnitude of the loads obey statistical laws. Knowing the distribution of these quantities, the form of structural members can be determined from conditions connected with the minimum volume for the prescribed safety of the entire structure. The solutions are based on the assumption of Gaussian distribution and concern problems with multiple load conditions.* Kalaba [55] has solved a similar problem using the dynamic programming formalism of Bellman [56,57]. Further applications of the Bellman principle in the structural optimization area are given in [58,59].

The optimal design of circular discs is now considered. The radial and tangential stresses are assumed to be everywhere equal to the critical stress [60],

$$\sigma_r = \sigma_\theta = \sigma_o.$$

This corresponds to a state represented by the point F of the Tresca hexagon, Figure 1.1a.

---

* Further extensions of probability concepts to more complex structural systems are given by Heer and Yang [227]

From (1.6)

$$h = h_o \exp\left(-\frac{\rho\omega^2 r^2}{2\sigma_o}\right) \tag{1.42}$$

when h_o is a constant of integration. This result is of the same form as that derived for the plastic case (1.13). But the displacement for the elastic case is given by

$$\left.\begin{aligned} \sigma_r &= \frac{E}{1-\nu^2}(e_r + \nu e_\theta) \\ \sigma_\theta &= \frac{E}{1-\nu^2}(\nu e_r + e_\theta) \end{aligned}\right\} \tag{1.43}$$

where

$$\left.\begin{aligned} e_r &= \frac{du}{dr} \\ e_\theta &= \frac{u}{r} \end{aligned}\right\} \tag{1.43a}$$

where E is Young's modulus and ν is the Poisson ratio for the material. These equations give

$$u = \frac{(1-\nu)\sigma_0}{E} r \tag{1.44}$$

at the optimum. (Compare:

$$u = \frac{C}{r}\left[\exp\frac{\rho\omega^2}{2\sigma_o}(r^2 - a_2^2)(1 - \frac{2\rho\omega^2}{2\sigma_o}a_2^2) - 1\right] \quad \text{for plastic analysis}$$

based on a Δ = constant. This result is given in [4].)

As in the plastic case, the optimal thickness is assumed to be of the form

$$\left.\begin{aligned} h(r) &= b_1 & a_1 \leq r \leq a_2 \\ &= h_o \exp\left(-\frac{\rho\omega^2 r^2}{2\sigma_o}\right) & a_2 < r < a_{m-1} \\ &= b_m & a_{m-1} \leq r \leq a_m \end{aligned}\right\} \tag{1.45}$$

where b_1, b_m are constants, the boundary conditions being given by $(\sigma_r)_{a_1} = s < 0$, $(\sigma_r)_{a_m} = S > 0$. The problem is to determine the hub radius a_2, given a_1, a_{m-1}, a_m. The thickness is discontinuous at $r = a_2$, a_{m-1}.

For $a_1 \leqslant r \leqslant a_2$, equations (1.6) give, in conjunction with (1.43)

$$u = C_1 r + \frac{C_2}{r} - \frac{\rho}{8}\frac{\omega^2(1-\nu^2)}{E} r^3 \tag{1.46}$$

where C_1, C_2 are constants of integration. Substituting (1.46) in (1.43, 1.43a) gives on simplification

$$\left.\begin{aligned}
\sigma_r &= \left(\frac{EC_1}{1-\nu}\right) - \left(\frac{EC_2}{1+\nu}\right)\frac{1}{r^2} - \left(\frac{3+\nu}{8}\rho\omega^2\right)r^2 \\
\sigma_\theta &= \left(\frac{EC_1}{1-\nu}\right) + \left(\frac{EC_2}{1+\nu}\right)\frac{1}{r^2} - \left(\frac{1+3\nu}{8}\rho\omega^2\right)r^2
\end{aligned}\right\} \tag{1.47}$$

Elastic continuity conditions on radial load and displacement at a_2 give

$$\left.\begin{aligned}
b_1(\sigma_r)_{a_2-0} &= h(a_2+0)\sigma_o \\
C_1 a_2 + \frac{C_2}{a_2} - \frac{\rho}{8}\frac{\omega^2(1-\nu^2)}{E}a_2^3 &= \frac{(1-\nu)}{E}\sigma_o . a_2 \\
\text{and} \qquad \sigma_r = s \quad \text{at} \quad r &= a_1
\end{aligned}\right\} \tag{1.48}$$

The constants C_1, C_2 are eliminated using (1.47,1.48). This gives on simplification,

$$\frac{\frac{\rho\omega^2}{4}\left(a_2^2 - a_1^2\right)\left[\nu\left(a_2^2 - a_1^2\right) - \left(a_2^2 + 3a_1^2\right)\right] + \sigma_o(1-\nu)\left(a_2^2 - a_1^2\right) + 2sa_1^2}{(1-\nu)a_2^2 + (1+\nu)a_1^2} =$$

$$\frac{\sigma_o}{b_1} h_o \exp\left(-\frac{\rho\omega^2}{2\sigma_o} a_2^2\right) \qquad (1.49)$$

Similarly continuity conditions at a_{m-1} are given by

$$\frac{\frac{\rho\omega^2}{4}\left(a_m^2 - a_{m-1}^2\right)\left[\nu\left(a_m^2 - a_{m-1}^2\right) + \left(a_{m-1}^2 + 3a_m^2\right)\right] - \sigma_o(1-\nu)\left(a_m^2 - a_{m-1}^2\right) + 2Sa_m^2}{(1-\nu)a_{m-1}^2 + (1+\nu)a_m^2} =$$

$$\frac{\sigma_o}{b_m} h_o \exp\left(-\frac{\rho\omega^2}{2\sigma o} a_{m-1}^2\right) \qquad (1.50)$$

Eliminating h_o from equations (1.49, 1.50) gives an equation for determining a_2. Some numerical computations for a_2 are given below, the data being the same as in Table 1 for the plastic case.

TABLE 2

RADIUS (ins)	OPTIMAL THICKNESS (ins)
a_2 = 16·46	$1{\cdot}962 \times 10^{-1}$
21·313	$1{\cdot}857 \times 10^{-1}$
22·813	$1{\cdot}820 \times 10^{-1}$
29·5	$1{\cdot}638 \times 10^{-1}$
30·3	$1{\cdot}615 \times 10^{-1}$

MINIMUM WEIGHT = $1{\cdot}036 \times 10^3$ lbs

A comparison of Tables (1,2) shows that the plastic optimal design is lighter than the corresponding elastic design. The optimal thickness (1.42) was calculated on the a priori assumption that the stress state was characterised by $\sigma_r = \sigma_\theta = \sigma_o$. As before, the stresses must satisfy (1.6) which was derived on the assumption of radially symmetric plane stress, whereby the axial and shear stresses were neglected. Ranta [63] has derived optimal designs on the assumption of rotationally symmetric stress in conjunction with the condition σ_r/σ_θ = constant at the optimum.

Tadjbakhsh [61] has designed thin circular plates using the Tresca condition and assuming that at the optimum the plate begins to yield simultaneously along its top and bottom surfaces under the applied lateral pressure. The theory assumes rotational symmetry for which the equilibrium equation is given by

$$\frac{d}{dr}(r\,M_r) - M_\theta + \int_a^r rp(r)dr + V(a) = 0 \qquad (1.51)$$

where a is the inner radius of the plate and V(a) is the shear force (compare with equation 1.31 for the plastic case).

The bending moments M_r, M_θ are given by

$$\left.\begin{aligned} M_r &= \frac{Eh^3(r)}{12(1-\nu^2)}\left(\frac{d^2W}{dr^2} + \frac{\nu}{r}\frac{dW}{dr}\right) \\ M_\theta &= \frac{Eh\ (r)}{12(1-\nu^2)}\left(\nu\frac{d^2W}{dr^2} + \frac{1}{r}\frac{dW}{dr}\right) \end{aligned}\right\} \qquad (1;52)$$

and the bending stresses are given by

$$\left.\begin{aligned} \sigma_r &= \frac{Ez}{1-\nu^2}\left(\frac{d^2W}{dr^2} + \frac{\nu}{r}\frac{dw}{dr}\right) \\ \sigma_\theta &= \frac{Ez}{1-\nu^2}\left(\nu\frac{d^2W}{dr^2} + \frac{1}{r}\frac{dw}{dr}\right) \end{aligned}\right\} \quad . \tag{1.53}$$

Optimal design is based on the condition

$$\left|\sigma_r - \sigma_\theta\right|_{z=\pm h/2} = \sigma_o \tag{1.54}$$

and on substituting (1.53) in (1.54)

$$hr\frac{d}{dr}\left(\frac{1}{r}\frac{dw}{dr}\right) = \frac{2(1+\nu)}{E}k \tag{1.55}$$

where

$$k = \pm\sigma_o$$

Substituting (1.52) in (1.51) and simplifying

$$r\frac{d}{dr}\left[rh^3\frac{d^2W}{dr^2}\right] + \left(\nu r\frac{dh^3}{dr} - h^3\right)\frac{dw}{dr} = \frac{-12(1-\nu^2)r}{E}\left(\int_a^r rp(r)dr + V(a)\right) \tag{1.56}$$

Equations (1.55, 1.56) constitute a set of nonlinear differential equations for the optimal thickness. Solutions of these equations for particular boundary conditions are given in [61].

An alternative derivation has been given by Huang [62] based on the elastic analogue of equation (1.34):

$$\frac{U}{h} = \text{constant}$$

where U is the strain energy per unit area of the plate given by

$$U = \frac{Eh^3}{12(1-\nu^2)}\left[\left(\frac{d^2W}{dr^2} + \frac{1}{r}\frac{dw}{dr}\right)^2 - \frac{2(1-\nu)}{r}\frac{d^2W}{dr^2}\frac{dw}{dr}\right]$$

From the optimality condition

$$\frac{Eh^2}{12(1 - \nu^2)} \left[\left(\frac{d^2W}{dr^2} + \frac{1}{r}\frac{dw}{dr}\right)^2 - \frac{2(1 - \nu)}{r}\frac{d^2W}{dr^2}\frac{dw}{dr}\right] = C \qquad (1.57)$$

For simplicity, take V(a) = 0 and the pressure p to be uniform. Hence, from the principle of virtual work

$$\begin{aligned} \text{Work done} &= \frac{1}{2}\pi(R^2 - a^2)\, p\bar{W} \\ &= \int_a^R U.(2\pi r\, dr) \\ &= 2\pi C \int_a^R h\, r\, dr \\ &= CV \end{aligned} \qquad (1.58)$$

where

$$R = \text{outer radius}$$

$$V = \text{volume of plate}$$

$$\bar{W} = \frac{2}{R^2 - a^2}\int_a^R Wr\, dr \quad - \quad \text{mean deflection}$$

Eliminating C from (1.57, 1.58) gives the central equation for this formulation. Full details of the approach are given in [62].

For pressure vessels, the equilibrium equations are given by Lakshmikantham and Gerard [64]

$$\left.\begin{aligned} \frac{\sigma_1 h}{R_1} + \frac{\sigma_2 h}{R_2} &= p \\ \sigma_2 &= \frac{pR_1}{2h} \end{aligned}\right\} \qquad (1.59)$$

when σ_1, σ_2 = principal circumferential and meridianal stresses

R_1, R_2 = radii of curvature in the circumferential and meridianal planes

p = internal pressure

h = thickness of the shell

These have been derived on the assumption that the shell thickness is small compared to the radii of curvature and neglecting the effects of gravity.

From (1.59)

$$\sigma_1 = \frac{pR_1}{2h}\left(2 - \frac{R_1}{R_2}\right)$$

The minimum weight analysis is based on the Tresca condition and for purposes of simplicity it is assumed $\sigma_3 = 0$, $\sigma_1 \geq 0$, $\sigma_1 \geq \sigma_2 \geq 0$. Therefore the optimal design lies on the branch EF of the hexagon (Figure 1.1a).

$$\sigma_1 = \sigma_o$$

and the optimal thickness is given by

$$h = \frac{pR_1}{2\sigma_o}\left(2 - \frac{R_1}{R_2}\right) \tag{1.60}$$

Further results on the optimal design of pressure vessels are given in [222]. Schmit et al [65-74] have formulated an automated synthesis capability for the weight minimisation of structures based on the methods of nonlinear programming. The weight is assumed to be a single valued differentiable function $W(x_1, \ldots, x_m)$ in the m design variables which define a point in an m-dimensional design space where each dimension represents a design variable. The weight contours

$W(x_1, \ldots, x_m) = C$ generate a family of hypersurfaces in design space for different values of the parameter C.

The side constraints usually arise from considerations of analysis limitations, compatibility constraints and fabrication limitations and are expressible in the form

$$L_j \leq x_j \leq U_j \qquad \text{for} \quad j = 1, 2, \ldots, m$$

where the bounds L_j, U_j are either constants or functions of the other variables. In vector notation these inequalities become

$$\underline{L} \leq \underline{x} \leq \underline{U} \tag{1.61}$$

where

$$\left.\begin{aligned} \underline{x} &= (x_1, \ldots, x_m) \\ \underline{L} &= (L_1, \ldots, L_m) \\ \underline{U} &= (U_1, \ldots, U_m) \end{aligned}\right\}$$

A design-satisfying condition (1.61) is said to be feasible with respect to the side constraints. The response characteristics of the system are determined by the behaviour variables which relate the design variables and the design requirements to the response of the system. The behaviour variables for a framed structure are typically of the form

$$\underline{B}F(x) = (\sigma_1, \ldots, \sigma_p; \ \delta_1, \ldots, \delta_q)$$

where $\sigma_1, \ldots, \sigma_p$ are the stresses and $\delta_1, \delta_2, \ldots, \delta_q$ the deflections at nodal points of the structure. The behaviour variables for structures subject to multiple load conditions are represented by matrices. For example, the behaviour variables for k load conditions are given by

$$\underline{B}F(x) = \begin{bmatrix} \sigma_1^{(1)}, \ldots\ldots \sigma_p^{(1)}, & \delta_1^{(1)}, \ldots\ldots \delta_q^{(1)} \\ \vdots & \vdots \\ \sigma_1^{(k)}, \ldots\ldots \sigma_p^{(k)}, & \delta_1^{(k)}, \ldots\ldots \delta_q^{(k)} \end{bmatrix}$$

The behaviour constraints can be expressed in the form

$$\underline{L}^* \leq \underline{B}F(x) \leq \underline{U}^* \tag{1.63}$$

and a design satisfying condition (1.63) is said to be feasible with respect to the behaviour constraints.

The weight minimisation problem can therefore be formulated as follows:

Given matrices $\underline{L}$, $\underline{U}$, $\underline{L}^*$, $\underline{U}^*$, determine a design which satisfies the conditions

(a) $\underline{L} \leq \underline{x} \leq \underline{U}$

(b) $\underline{L}^* \leq \underline{B}F(x) \leq \underline{U}^*$

and minimises the weight W(x).

This constitutes a nonlinear programming problem - the minimisation of a general function subject to nonlinear inequality constraints. The behaviour and side constraints are represented by hypersurfaces in design space and the complete set of these individual constraint surfaces considered collectively forms a composite constraint surface dividing the design space into a feasible region and a nonfeasible region. Designs above the composite surface are feasible designs and correspond to designs feasible with respect to both behaviour and side constraints. Designs below this surface are nonfeasible designs and correspond to regions of constraint violation. Designs on the composite surface are said to be boundary designs and correspond to critical designs on the verge of failure. The minimum weight solutions usually, but not necessarily, lie on the composite surface at the intersection of individual contributing constraint surfaces. But it is equally possible for the solutions to lie on the composite surface where the lowest weight contour touches a single contributing surface.

The synthesis starts from an initial feasible design and generates steepest descent motion defined by

$$\underline{x}^{(q+1)} = \underline{x}^{(q)} + t^{(q)} \underline{\psi}^{(q)} \qquad q = 0,1,\ldots \tag{1.64}$$

where

$$\underline{x}^{(q)} = (x_1^{(q)}, \ldots\ldots, x_m^{(q)}) \quad \text{design point at } q^{th} \text{ iteration}$$

$$\underline{\psi}^{(q)} = \frac{-\underline{\nabla} W(x^{(q)})}{|\underline{\nabla} W(x^{(q)})|} \quad \text{normalised steepest descent vector}$$

$$t^{(q)} = \text{step length at } q^{th} \text{ iteration}$$

The step length is defined by

$$t^{(q)} = 2^q \varepsilon; \qquad \varepsilon > 0 \tag{1.65}$$

where ε is a predetermined increment. At each iteration the designs are checked against the behaviour and side constraints and if they are found to be feasible, the step length is doubled and steepest descent motion continues until a constraint is encountered. The distance of travel back to the constraint is calculated by successively halving the step length until the design converges to a point on the constraint (to within a specified tolerance). Steepest descent motion is no longer possible without piercing the constraint surface and an alternative procedure was devised by Schmit whereby the structure is redesigned at constant weight.

This was the method of alternate base planes [70] and was used to generate the directions of search along the constant weight contour through the current boundary point.

The basic steps of the algorithm are:

(a) Set $i = 1$

(b) Generate normalised directions of search

$$\left.\begin{aligned} \psi_j^{(i)} &= R_j \Big/ \left(\sum_{j \neq i}^{m} R_j^2 \right)^{\frac{1}{2}} \quad ; \quad j = 1, \ldots, m; \quad j \neq i \\ &= 0 \qquad\qquad\qquad\quad ; \quad j = i \end{aligned}\right\}$$

where R_j are random numbers

(c) Calculate distances to the side constraints

$$t_j^{(i)} = (L_j - x_j) \Big/ \psi_j^{(i)} \quad ; \quad j = 1, \ldots, m; \quad j \neq i$$

$$t_{m+j}^{(i)} = (U_j - x_j) \Big/ \psi_j^{(i)} \quad ; \quad j = 1, \ldots, m; \quad j \neq i$$

where x_j are coordinates of the boundary point and L_j, U_j are assumed constant.

Define

$$\lambda^{(i)} = \{\min t_j;\ \ t_j > 0,\ \ j = 1, \ldots, 2m,\ \ j \neq i\}$$

$$\mu^{(i)} = \{\min |t_j|;\ t_j < 0,\ \ j = 1, \ldots, 2m,\ \ j \neq i\}$$

(d) Proposed distance of travel in design space is given by

$$\left.\begin{aligned} t_k^{(i)} &= R_k\, \lambda^{(i)}\,; & k &= 1,2,3 \\ &= R_k\, \mu^{(i)}\,; & k &= 4,5,6 \end{aligned}\right\}$$

where R_k is a random number such that $0 < R_k < 1$; $k = 1, \ldots, 6$

(e) Proposed new designs are

$$\underline{x}^{(i,k)} = \left(x_1 + t_k^{(i)}\, \psi_1^{(i)},\ x_2 + t_k^{(i)}\, \psi_2^{(i)},\ \ldots\ldots,\ x_i^{(i,k)},\ \ldots\ldots,\right.$$
$$\left. x_n + t_k^{(i)}\, \psi_n^{(i)}\right);\ \ k = 1, \ldots, 6$$

where $x_i^{(i,k)}$ is calculated from the constant weight condition

$$W(x_1, \ldots, x_n) = W\left(x\ \ + t_k^{(i)}\, \psi_1^{(i)},\ \ x_2 + t_k^{(i)}\, \psi_2^{(i)},\ \ldots,\ x_i^{(i,k)},\right.$$
$$\left.\ldots,\ x_n + t_k^{(i)}\, \psi_n^{(i)}\right);\ \ k = 1, \ldots, 6$$

(f) Check these six designs against the side and behaviour constraints in that order. If any one of $\underline{x}^{(i,k)}$ is feasible steepest descent motion continues as before. Otherwise go to step (g)

(g) Set $i \to i + 1$; go to step (b) and repeat iterations.

Step (g) is equivalent to changing the base plane. If still no feasible designs are forthcoming, the boundary point may be taken as the optimum. This "steepest descent - alternate step" search technique was applied by Schmit et al to the design of trusses and waffle plates, under multiple load conditions. For waffle plates, the behaviour constraints were provided by stability failure modes of gross and local buckling. The side constraints imposed lower and upper bounds on the design variables. This nonlinear programming problem being characterised by (a) multi-dimensional design space, (b) presence of relative minima, (c) nonlinear weight function, (d) nonlinear behaviour constraints, (e) linear side constraints. The design variables for the truss problems were the cross-sectional areas, the weight being linear in the areas. The side constraints ensured non-negative areas. The behaviour constraints imposed limitations on the stresses and deflections and precluded the occurrence of certain buckling modes.

They also consider the problem of a simple shock isolator. A shock isolator being essentially a one-dimensional spring-mass-damper system. The supporting base was subjected to a series of shocks, which were transmitted to the attached mass through the spring-damper combination.

These induced accelerations in the mass which provided a measure of the response to the impulses. The function to be minimised was the maximum value of the accelerations induced by the shocks. The accelerations were functions of the spring stiffness and the damping coefficient which corresponded to the design variables for the problem.

The accelerations had, to some extent, a "black box" representation function, the synthesis being again based on a combination of steepest descent travel in the feasible regions followed by an alternate step which is a move more or less along the constant merit contour. The gradient directions were computed using finite differences. The problem was further complicated by the poor behaviour of the merit contours which gave rise to considerable zig-zagging. This occurs when a ridge is present causing the gradient directions to change sharply from point to point on the merit contour, so that the optimum direction of travel should be along the general direction of the axis of the ridge. Schmit and Fox [73] use a simple procedure for estimating this direction. They consider three consecutive designs $\underline{x}^{(q-2)}$, $\underline{x}^{(q-1)}$, $\underline{x}^{(q)}$ using steepest descent motion (1.64).

Define

$$\left.\begin{aligned} \underline{m}^{(q-1)} &= \underline{x}^{(q-1)} - \underline{x}^{(q-2)} \\ \underline{m}^{(q)} &= \underline{x}^{(q)} - \underline{x}^{(q-1)} \end{aligned}\right\}$$

For zigzag

$$\underline{m}^{(q)} \cdot \underline{m}^{(q-1)} \leq 0$$

and the new direction of travel should be $\left(\underline{x}^{(q)} - \underline{x}^{(q-2)}\right)$. Motion continues along this direction with a step length given by (1.65) until either a constraint is encountered or the merit fails to improve. In the latter case a new steepest descent direction is used to search the feasible regions. Steepest descent procedures break down completely when there are cusps where the gradient is undefined. The cusp "groove" can be estimated using procedures similar to those employed above. When a cusp is encountered, a feasible design was sought in a more or less random manner. Steepest descent motion is initiated from this point until no further progress is possible. This situation corresponds to the vicinity of a second cusp and the line joining the two cusps would define the direction of search in the feasible region. The sense of the vector is from the point of lower merit to that of higher merit. For boundary points, the gradient to the merit contour is estimated using finite differences. This enables the tangent plane to be calculated. Motion along this plane in one direction leads into nonfeasible regions, while in the opposite direction, leads into feasible regions. For concave contours a move in the latter direction would usually lead to designs of improved merit, while for very flat contours, a tangent move usually leads to designs of worse merit. For this case a feasible design is sought which lies inside the merit contour. This is achieved by searching the feasible regions along small steps perpendicular to the tangent plane. Troitskii [126] considers a similar problem using a variational approach. An experimental discussion of the response characteristics of a shock isolator in the absence of side constraints is given in [75].

An alternate approach to the nonlinear programming problem is to use penalty functions to simulate the constraints by unfavourably weighting the merit function in their vicinity. The successive iterations of the problem are forced to lie in the feasible region since the violation of a constraint results in a sudden and rapid deterioration of the objective function. This technique enables the constrained problem to be transformed into a sequence of unconstrained optimization problems, and has recently come into prominence in the structural optimization area [65,76] where penalty functions are introduced through the Heaviside unit function defined by

$$\left.\begin{aligned} H(t) &= 1 \quad \text{for} \quad t < 0 \\ &= 0 \quad \text{for} \quad t \geq 0 \end{aligned}\right\} \tag{1.66}$$

Consider the function

$$\phi(\underline{x}) = \sum_{j=1}^{m} \{(x_j - L_j)^2 H(x_j - L_j) + (U_j - x_j)^2 H(U_j - x_j)\}$$

$$+ \sum_{p,q} \{(BF_{pq} - L^*_{pq})^2 H(BF_{pq} - L^*_{pq}) + (U^*_{pq} - BF_{pq})^2 H(U^*_{pq} - BF_{pq})\} \tag{1.67}$$

For feasible designs

$$\left.\begin{aligned} &L_j \leq x_j \leq U_j \\ &L^*_{pq} \leq BF_{pq}(\underline{x}) \leq U^*_{pq} \end{aligned}\right\} \tag{1.68}$$

Therefore from (1.66, 1.67)

$$\phi(\underline{x}) = 0$$

In general

$$\phi(\underline{x}) \geq 0.$$

Define

$$\psi_s(\underline{x}) = \phi(\underline{x}) + (W - W_s)^2 H(W_s - W); \quad s = 0, 1, \ldots \tag{1.69}$$

where W_o is an initial estimate for the weight satisfying the condition

$$W_o > \min_{\underline{x} \varepsilon R} W(\underline{x})$$

and R is the feasible region defined by (1.68). The parameters W_s are sometimes called the "draw-down" weights.

Hence

$$\left.\begin{aligned} \psi_s &= 0 \quad \text{for } \phi = 0; \quad W \leq W_s \\ &> 0 \quad \text{for } \phi = 0; \quad W > W_s \end{aligned}\right\}$$

Therefore solutions for which $\psi_s \to 0$ are feasible designs of weight less than or equal to W_s. The procedure is made to generate a sequence of feasible designs of decreasing wieght

$$W^1, W^2, \ldots..$$

with corresponding draw-down weights

$$W_o, W_1, \ldots..$$

where

$$W_{s+1} = W_s - \Delta W$$

$$\Delta W = \text{specified weight reduction}$$

This procedure continues until it is not possible to make ψ tend to zero. One of the main advantages of this integrated approach is that only feasible designs which offer a specified weight reduction are examined, thereby eliminating nonfeasible designs. Schmit et al [65,77] have used this formulation to obtain minimum weight solutions to trusses and cylindrical shells [78] in the presence of stress and buckling constraints. Marcal and Gellatly [79] and Felton and Nelson [231]* solved truss problems using a different penalty function transformation based on Carroll's created response surface technique [127] where the modified merit function is given by

$$\psi_s(\underline{x}) = W(\underline{x}) + r_s \sum_i \frac{1}{c_i(x)} \tag{1.70}$$

where the design constraints are represented by $c_i(x) \geq 0$ and r_s is a positive constant which is monotonically decreased to zero. The function (1.70), is minimised for a given $r_s > 0$, and this minima is used as the starting point for the next minimization with a reduced value of r_s. This procedure is repeated with $r_s = 0$. Nonfeasible designs are excluded from the iterations. An efficient strategy for selecting the sequence $\{r_s\}$ is given in [236]. The minima of $\psi_s(\underline{x})$ as $r_s \to 0+$ converge to the constrained minima. The constraints correspond to stress and deflection constraints.† Klein [81] has obtained optimal designs using slack variables to transform inequality constraints into equality constraints. These were incorporated into the weight function using Lagrange multiplier techniques. A detailed discussion of the various penalty function techniques is given in reference [80].

Gellatly and Gallagher [82,83] consider the weight minimisation of a truss system under multiple load conditions with constraints on the

---

* The problem was characterised by thin walled cross-sectional elements with moments of inertia as the design variables.

† Templeman [229] has developed Rosenbrock-type methods for structural optimization problems based on a combination of steepest descent and Fibonacci search procedures.

stress and deflection fields. The design variables were the cross-sectional areas, giving a linear weight function subject to non-linear behaviour constraints. Constant weight redesign was based on a calculation of the normals to the behaviour constraints using the finite element methods of structural analysis. This normal was projected onto the constant weight hyperplane to generate a direction of travel away from the boundary point.

The behaviour variables are given by

$$\underline{BF}(\underline{x}) = (\underline{\sigma};\underline{\delta})$$

where the stress and nodal deflections are given by

$$\left.\begin{aligned} \underline{P} &= \underline{K}_o \cdot \underline{\delta} \\ \underline{\sigma} &= \underline{S} \cdot \underline{\delta} \end{aligned}\right\} \qquad (1.71)$$

and

$\underline{K}_o$ = stiffness matrix

$\underline{S}$ = stress matrix

$\underline{P}$ = load matrix

For a small perturbation in the i^{th} element

$$\left.\begin{aligned} \underline{K}' &= \underline{K}_o + \delta\alpha_i \, \underline{K}_i \\ \underline{\delta}' &= \underline{\delta} + \delta(\underline{\delta}) \\ \underline{\sigma} &= \underline{\sigma} + \delta\underline{\sigma} \end{aligned}\right\} \qquad (1.72)$$

where $\underline{K}_i$ is the stiffness and $\delta\alpha_i$ the fractional increase in the area of the i^{th} element.

From (1.71, 1.72)

$$\left.\begin{aligned}(\underline{K}_o + \delta\alpha_i\ \underline{K}_i)\left(\underline{\delta} + \delta(\underline{\delta})\right) &= \underline{P} \\ \underline{S}(\underline{\delta} + \delta\underline{\delta}) &= \underline{\sigma} + \delta\underline{\sigma}\end{aligned}\right\}$$

Neglecting second order terms

$$\delta\alpha_i\ \underline{K}_i\ \underline{\delta} + \underline{K}_o\delta(\underline{\delta}) = 0$$

$$\underline{S}\ \delta(\underline{\delta}) = \delta\underline{\sigma}$$

This reduces to

$$\left.\begin{aligned}\frac{\partial\underline{\delta}}{\partial\alpha_i} &= -\ \underline{K}_o^{-1}\ \underline{K}_i\ \underline{\delta} \\ \frac{\partial\underline{\sigma}}{\partial\alpha_i} &= S\ \frac{\partial\underline{\delta}}{\partial\alpha_i}\end{aligned}\right\} \qquad (1.73)$$

Equations (1.73) determine the components of the normal to the behaviour constraint surfaces. The direction of travel is obtained by projecting the normals onto the constant weight hyperplane

$$\underline{\psi}_D = \frac{\underline{\psi}_c}{(\underline{\psi}_c\ \psi_W^T)} - \psi_W$$

where

$\underline{\psi}_c$ = normal to the behaviour constraints as defined by (1.73)

$\underline{\psi}_W$ = normal to the weight hyperplanes

A search is made along this direction until the nearest behaviour constraint is encountered. The point midway between the current non-feasible point and theprevious boundary point is taken as the feasible point from which to continue steepest descent motion according to (1.64, 1.65). When a boundary design lies on a side constraint the

the direction of travel was along the direction of constrained steepest descent obtained by projecting the steepest descent vector onto the side constraints, the side constraints being assumed linear.

In most structural problems the constraints of primary importance are the behaviour constraints. A major part of the synthesis has been devoted to developing efficient algorithms for redesign from boundary points on the behaviour constraints. The above problems have been based on an equal weight redesign philosophy.

Best [84] uses a different philosophy by moving along the behaviour constraints instead of moving away from them. As before, the mode of travel in the feasible regions is along the gradient direction but with a step length estimated to the nearest behaviour constraint. The method then moves along the surface in a direction in which the weight decreases most rapidly.

The behaviour variables are given by

$$BF(\underline{x}) = (b_1, b_2, \ldots, b_t) \tag{1.74}$$

The behaviour constraints are given by

$$BF^{(b)} = \left(b_1^{(b)}, b_2^{(b)}, \ldots, b_t^{(b)}\right)$$

The gap vector is defined by

$$\Delta b_i = \varepsilon_1^i\left(b_i^{(b)} - b_i\right)$$

where

$$\left.\begin{aligned} \varepsilon_1^i &= +1 \quad \text{if } b_i^b \text{ is an upper bound} \\ &= -1 \quad \text{if } b_i^b \text{ is a lower bound} \end{aligned}\right\}$$

Therefore a negative gap implies the violation of a constraint.

Equation (1.74) may be written in the form

$$BF(x) = (\underline{\sigma}\,;\,\underline{\delta}) \tag{1.75}$$

where $\underline{\sigma}, \underline{\delta}$ are the element stress and displacement vectors. As before the nodal displacements satisfy the equilibrium equation.

$$\underline{P} = \underline{K}\,\underline{\delta}$$

Therefore, for a small change $\delta\underline{K}$ in $\underline{K}$, comparison with equation (1.72) shows $\delta\underline{K} = \sum \delta\alpha_i K_i$.

$$\underline{P} = (\underline{K} + \delta\underline{K})\underline{\delta}'$$

and

$$\underline{\delta}' = \underline{F}(\underline{P} - \delta\underline{K}\underline{\delta}')$$

where $\underline{F}$ is the flexibility matrix defined by

$$\underline{F} = \underline{K}^{-1}$$

and

$\underline{\delta}'$ was determined from the iterative relations

$$\left.\begin{aligned} \underline{\delta}^{(q+1)} &= \underline{F}(\underline{P} - \delta\underline{K}\,\underline{\delta}^{(q)}) \\ \underline{\delta}^{(0)} &= 0 \end{aligned}\right\} \tag{1.76}$$

The term $-\delta\underline{K}\underline{\delta}^{(q)}$ was treated as an additional load removing the necessity for recomputing the stiffness matrix at each iteration. This enabled the determination of the matrix $\underline{R}$ defined by

$$\underline{R} = \begin{bmatrix} r_{ij} \end{bmatrix}_{t\times m}$$

where

$$r_{ij} = \frac{\partial b_i}{\partial x_j} \qquad i = 1,2,\ldots,t; \quad j = 1,2,\ldots,m;$$

Comparison with (1.72) shows that the design variables x_j correspond to $\delta\alpha_j = \delta x_j / x_j$.

The direction of travel was as follows: consider a boundary design lying at the intersection of r behaviour constraints. The r×m matrix $\underline{C}$ formed from those rows of $\underline{R}$ associated with the closed gaps satisfies the condition

$$\underline{C}\ \underline{u}^T = \underline{0} \tag{1.77}$$

where the direction of travel $\underline{u}$ satisfies the normalisation condition

$$\underline{u}\ \underline{u}^T = 1 \tag{1.78}$$

Consider the function defined by

$$\phi = \frac{d}{d\lambda} W(\underline{x} + \lambda\underline{u}) = \sum_{i=1}^{m} \frac{\partial W}{\partial x_i} u_i = g\ \underline{u}^T \tag{1.79}$$

where

$$g = \underline{\nabla}\ W(\underline{x})$$

The function ϕ measures the rate of change of the weight in the direction $\underline{u}$. The direction $\underline{u}$ is obtained by maximising (1.79) subject to the constraint conditions (1.77, 1.79).

Therefore there exist Lagrange multipliers λ_o, λ_1, ..., λ_r such that

$$-g_j + \sum_{i=1}^{r} \lambda_i\, C_{ij} + 2\lambda_o\, u_j = 0 \qquad j = 1, 2, \ldots, m$$

In matrix notation this becomes

$$-g + \underline{\Lambda}\underline{C} + 2\lambda_o \underline{u} = \underline{0}$$

where

$$\underline{\Lambda} = (\lambda_1, \ldots, \lambda_r)$$

On simplification

$$\underline{u} = -\underline{v}(\underline{v}\ \underline{v}^T)^{\frac{1}{2}} \qquad (1.80)$$

where

$$\underline{v} = -\underline{g} + \underline{g}\ \underline{C}^T(\underline{C}\ \underline{C}^T)^{-1}\ \underline{C}\ .$$

Motion continues along this constrained gradient until the next smallest gap is closed and this is continued until the design lies on as many behaviour constraints as possible. Schmit [125] has pointed out a possible inconsistency in the closed gap assumption, where condition (1.77) is replaced by $\underline{C}\ \underline{u}^T \geq 0$, giving an inequality constrained problem. The distance of travel was estimated from the condition

$$b_j(\underline{x} + \lambda \underline{u}) = b_j^{(b)} \qquad j = 1,2,\ldots,t$$

Taylor series expansion gives

$$b_j(\underline{x}) + \lambda \frac{\partial b_j}{\partial \underline{u}} \approx b_j^{(b)}$$

where

$$\frac{\partial b_j}{\partial \underline{u}} = \sum_{i=1}^{m} u_i \frac{\partial b_j}{\partial x_i}$$

Hence

$$\lambda = \frac{\varepsilon_1^j\ \Delta b_j}{\partial b_j / \partial \underline{u}}$$

The step length is calculated from the condition

$$t = \min_j(\lambda_j,\ \lambda_j > 0) \qquad (1.81)$$

where

$$\lambda_j = \varepsilon_1^j \, \Delta b_j \Bigg/ \left(\frac{\partial b_j}{\partial \underline{u}} \right)$$

These procedures were used to obtain minimum weight solutions to a cantilevered box. A possible disadvantage of the method is that once a constraint is encountered, it is never to be left. In general, there is no guarantee that the optimum will lie on the behaviour constraints when there are side constraints present. This is confirmed by Schmit who has found numerical evidence showing that the fully-stressed design is not always the minimum weight design. The technique used by Best for finding the permissible direction along which the rate of weight decrease is most rapid is essentially a quadratic programming procedure. An earlier version of a synthesis capability proposed by Gellatly et al [97] was based on the derivation of a set of optimum feasible directions. However, there were indications that it was not always possible to obtain such directions. Pope [98] uses an alternate procedure based on Zoutendijk's method of feasible directions [99] for reducing the problem to a series of linear programming problems. Considerable progress has been made by Turner [85,86], Zarghamee [87,88], Rubin [194], McCart et al [195] in applying the finite element methods of structural analysis to optimization problems, in thepresence of dynamic constraints. For example, Zarghamee [87] maximises the lowest natural frequency of vibration of a composite structure subject to a constraint on the total weight. The frequency was calculated from the eigenvalue equation

$$(\underline{K} - \lambda^{(i)}\underline{M})\underline{\delta}^{(i)} = \underline{0} \tag{1.82}$$

where $\underline{K}$, $\underline{M}$ are the stiffness and mass matrices respectively and $\underline{\delta}^{(i)}$ the eigenvector of displacements corresponding to the eigenfrequency $\lambda^{(i)}$. From (1.72)

$$\left.\begin{aligned} \underline{K} &= \underline{K}_o + \sum_j x_j \underline{K}_j \qquad (x_j = \delta\alpha_j) \\ \underline{M} &= \underline{M}_o + \sum_j x_j \underline{M}_j \end{aligned}\right\} \tag{1.83}$$

where x_j correspond to the design variables. Differentiating (1.82) partially with respect to x_j and using (1.83) gives

$$\left(\underline{K}_j - \lambda^{(i)}\underline{M}_j\right)\underline{\delta}^{(i)} - \frac{\partial\lambda^{(i)}}{\partial x_j}\underline{M}\,\underline{\delta}^{(i)} + \left(\underline{K} - \lambda^{(i)}\underline{M}\right)\frac{\partial\underline{\delta}^{(i)}}{\partial x_j} = 0 \tag{1.84}$$

Assume the eigenvectors $\underline{\delta}^{(i)}$ to be normalised with respect to the mass matrix $\underline{M}$ and to form a complete set so that

$$\left.\begin{aligned} \frac{\partial\delta^{(i)}}{\partial x_j} &= \sum_k \beta_k^{(i)}\,\underline{\delta}^{(k)} \\ \underline{\delta}^{(i)^T}\,\underline{M}\,\underline{\delta}^{(j)} &= \delta_{ij} \quad \dagger \end{aligned}\right\} \tag{1.85}$$

From (1.84, 1.85)

$$\frac{\partial\lambda^{(i)}}{\partial x_j} = \underline{\delta}^{(i)^T}\left(\underline{K}_j - \lambda^{(i)}\underline{M}_j\right)\underline{\delta}^{(i)} \tag{1.86}$$

Equation (1.86) measures the rate of change of the eigenfrequency in terms of the corresponding eigenvector. The weight is assumed to be a linear function of the form

....

† This is the kronecker delta defined as $\delta_{ij} = 0$, if $i \neq j$
$= 1$, if $i = j$

$$m(x) = m_o + \sum_j x_j m_j \tag{1.87}$$

where

$$m \leqslant m_o, \quad m_j \text{ constants for all } j.$$

Hence

$$\sum_j x_j m_j \leqslant 0 \tag{1.88}$$

The problem consists in maximising the lowest frequency $\lambda^{(o)} = \lambda^{(o)}(\underline{x})$ subject to condition (1.88) which is linear in $\underline{x}$. This was solved using Rosen's gradient projection method [89] for linear constraints. The gradient direction being given by (1.86). Similar techniques were applied to the minimum weight design of radio-telescope antennae [88]. The optimal frequency problem was studied by Taylor [90] for the special case of a bar using a variational approach based on energy considerations.

The vibration characteristics of a general system are described by the eigenvalue equation (1.82),

$$(\underline{K} - \lambda\underline{M})\underline{\delta} = \underline{0}$$

Substituting (1.83) in the above equation gives

$$\sum_j (\underline{K}_j - \lambda\underline{M}_j)\underline{\delta}x_j = -(\underline{K}_o - \lambda\underline{M}_o)\underline{\delta}$$

Turner [85] considers weight minimization subject to the condition that the natural frequencies of vibration must assume prescribed values. For purposes of simplicity he assumes $\underline{K}_o = \underline{0}$ and $\lambda = \lambda^{(o)}$ corresponding to the lowest frequency. This gives

$$\sum_j \underline{B}_j \underline{\delta} x_j = \lambda^{(o)} \underline{M}_o \underline{\delta}$$

where

$$\underline{B}_j = \underline{K}_j - \lambda^{(o)} \underline{M}_j$$

This equation can be written in the form

$$\underline{D}\,\underline{x} = \lambda^{(o)} \underline{M}_o\,\underline{\delta}$$

where

$$\left.\begin{aligned} \underline{D} &= (\underline{B}_1\,\underline{\delta},\ \underline{B}_2\,\underline{\delta},\ \ldots\ldots) \\ \underline{x} &= (x_1,\ x_2,\ \ldots\ldots)^T \end{aligned}\right\}$$

$$\underline{x} = \lambda^{(o)}\,\underline{D}^{-1}\,\underline{M}_o\,\underline{\delta} \tag{1.89}$$

The weight is a special case of function (1.87) with $m_o = 0$, and $m_j = 1$ for all j.

This implies

$$m = \sum x_j = \lambda^{(o)}(1,\ 1,\ \ldots,1)\underline{D}^{-1}\,\underline{M}_o\,\underline{\delta} \tag{1.90}$$

This result follows from (1.89). The weight minimisation condition is given by

$$\frac{\partial m}{\partial \delta_j} \equiv \lambda^{(o)}(1,1,\ldots,1)\left\{\frac{\partial \underline{D}^{-1}}{\partial \delta_j}\right\}\underline{M}_o\,\underline{\delta} + \lambda^{(o)}(1,1,\ldots,1)\underline{D}^{-1}\left\{\underline{M}_o^{(j)}\right\}$$

$$= 0 \quad \text{for all } j \tag{1.91}$$

where $\{\underline{M}_o^{(j)}\}$ is the j^{th} column of $\underline{M}_o$. But from matrix theory

$$\frac{\partial \underline{D}^{-1}}{\partial \delta_j} = -\,\underline{D}^{-1}\,\frac{\partial \underline{D}}{\partial \delta_j}\,\underline{D}^{-1}$$

Substituting this in (1.91) gives

$$\lambda^{(o)}(1,1,\ldots,1)\underline{D}^{-1}\{\underline{M}_o^{(j)} - \frac{\partial \underline{D}}{\partial \delta_j} \underline{D}^{-1} \underline{M}_o \underline{\delta}\} = 0, \quad \text{for all } j$$

Turner uses this result to show that the minimisation problem is equivalent to optimising the function

$$\phi(\underline{x},\underline{\delta}) \equiv \sum x_j + \underline{\Lambda}\underline{D}\underline{x} - \lambda_o^2 \underline{\Lambda} \underline{M}_o \underline{\delta}$$

This stationary condition is expressed by the system of equations

$$\left.\begin{aligned} \frac{\partial \phi}{\partial \underline{x}} &= 0 \\[2ex] \frac{\partial \phi}{\partial \underline{\delta}} &= 0 \end{aligned}\right\}$$

This gives a system of nonlinear equations which were solved using a modified Newton-Raphson procedure. Applications to more complex aerospace structures* are given by Turner [86], McCart et al [195], and Rudisill and Bhatia [233]. A similar class of problems is discussed by McIntosh and Eastep [93] using the methods of the variational calculus. Other problems of interest include minimum weight problems [96] based on an extension of the fully-stressed design concept to include resonance conditions. Fried [91] has studied the eigenvalue problem (1.82) using Powell's conjugate gradient method of minimisation [92]. Some optimal vibrational problems as applied to beams are given in [94, 95, 111]. Newton and Scholes [128] introduce exponential-type penalty functions to investigate the optimal design of diesel engine pistons. The behaviour characteristics are

---

* Recently Fox and Kapoor [223] have introduced further generalisations based on inequality constraints on the vibrational frequencies. The resulting nonlinear program being solved using Zoutendijk's feasible direction method [99].

represented by the linear equations

$$\underline{K}\,\underline{y} = \underline{B}$$

where

$$\underline{K} = \underline{K}(\underline{x}) \quad \text{is a matrix function of the design variables.}$$

The problem is to minimise the susceptibility to fatigue failure subject to constraints on the piston deflection, weight and design configuration. The fatigue susceptibility criterion is defined by the relation

$$\underline{f} = \underline{K}_2\,\underline{y} = \underline{K}_2\,\underline{K}^{-1}\,\underline{B} \tag{1.92}$$

The deflection vector is given by

$$\left.\begin{aligned} &\underline{\delta} = \underline{K}_1\,\underline{y} = \underline{K}_1\,\underline{K}^{-1}\,\underline{B} \\ \text{where} \qquad &\underline{\delta} \leq \underline{\delta}^{(\max)} \end{aligned}\right\} \tag{1.93}$$

The side constraints are defined by

$$\left.\begin{aligned} &W(\underline{x}) \leq W_o \\ \text{and} \qquad &\underline{L} \leq \underline{x} \leq \underline{U} \end{aligned}\right\} \tag{1.94}$$

where $\underline{L}$, $\underline{U}$, are constant row vectors, and W_o is an upper bound on the total weight. From conditions (1.92 - 1.94) the nonlinear programming problem is defined by

$$\left.\begin{array}{l} \min\limits_{i,j} \max f_{ij}(\underline{x}) \\ \text{subject to the design conditions} \\ \underline{K}_1\ \underline{K}^{-1}(\underline{x})\ \underline{B} \leq \underline{\delta}^{(max)} \\ W(\underline{x}) \leq W_o \\ \underline{L} \leq \underline{x} \leq \underline{U} \end{array}\right\} \tag{1.95}$$

The corresponding unconstrained representation was defined by the modified merit function

$$\text{Min}\left\{\alpha_1 \max_{i,j} f_{ij}(\underline{x}) + \alpha_2\, e^{\beta_1(\underline{K}_1\ \underline{K}^{-1}\ \underline{B} - \underline{\delta}^{max})} + \alpha_3\, e^{\beta_2(W-W_o)}\right\} \tag{1.96}$$

where α_1, α_2, α_3, β_1, β_2 are suitable scale factors. Function (1.96) is essentially a "black box" function, with the penalty terms having an exponential character. This was solved using the methods of Rosenbrock [129] and Nelder and Mead [130]. Available computational experience indicates the simplex method of Nelder and Mead as yielding better results. Kavlie et al [131] studied a class of minimal weight design problems arising in the shipbuilding industry. They used a penalty functions concept based on the sequential unconstrained minimisation technique (SUMT) developed by Fiacco and McCormick [134, 135]. This transformation is similar to Carroll's equation (1.70). The unconstrained problem was solved using the variable metric method of Davidon-Fletcher-Powell [132,133].

This review is concluded by a discussion of some miscellaneous structural optimization problems. Moses [100] obtained minimum weight solutions to a truss using Kelly's cutting plane method [101] to reduce the problem to a series of linear programming problems. Applications to purely linear programming situations are given in [110]. Reinschmidt et al [191], Chern and Prager [232]*, consider some nonlinear programming situations arising from such problems. Some Russian work [102] is available in this area of minimal design using integer and geometric programming procedures [188]. Similar problems have also been investigated by Toakley [105] and Corcoran [190]. Brown and Ang [103] study truss optimal design using Rosen's gradient projection method for nonlinear constraints [104]. Further examples of minimal weight design include cooling towers [114], sandwich panels [193], and shields for nuclear reactors [115]. Other design criteria include optimal strength [112] and deflection [113] problems which were studied using variational techniques. Similar problems are also discussed by Prager and Taylor [119], Prager [192]. Optimal design of torsion springs are studied by Pascual and Ben-Israel [181] using geometric programming techniques whereby the potential energy is minimised subject to stress and side constraints. Razani [116] studied the relationship between the fully-stressed and minimum weight design concepts, and showed that the fully-stressed design does not always converge to the minimum weight design. Criteria are given for the rate of convergence of the iterations in the fully-stressed design procedure and a method based on the Kuhn-Tucker optimality condition of nonlinear programming [120, 123] is presented for determining whether a fully-stressed design is the minimum weight design. If this does not correspond to

* With associated convex programs based on stress and deflection constraints

minimum weight, a procedure is given for detemining the minimum weight design. Kicher [117] studies this relationship using the Lagrange multiplier matrix. The feasibility aspects of the fully stressed design are discussed by Dayaratnam and Patnaik [118]. For a further literature review of some optimal design problems the reader is referred to reference [124].

1.5 SOME LATE ADDITIONS

Since going to press some further additions to the technical literature have appeared. Pappas and Amba-Rao [216] have used penalty function techniques in conjunction with an improved version of the Hooke-Jeeves direct search algorithm [161] for the synthesis of cylindrical shells. A review of some feasible direction methods as applied to structural optimization problems is given by de Silva [217]. A more general class of beam problems is described by Chern [220] using variational techniques. Linear programming type algorithms for the plastic design of frames are given by Charrett and Watson [218]. Reiss and Megarefs [221] consider further extensions of the limit theorems of plastic theory to the design of sandwich plates using variational techniques. Optimal design in rheology is discussed by Zyczlowski [219].

1.6 OPTIMIZATION PROGRAMMING PACKAGES

A comprehensive list of linear and quadratic programs and a class of convex programs written in Algol-Fortran programming languages is given in the book by Künzi et al [168]. Programming packages based on the algorithms of Rosenbrock, Powell, Nelder-Mead, Davidon-Fletcher-Powell are available from the Director, Numerical Optimization Centre, The Hatfield Polytechnic, Hatfield, Herts. These are scheduled to be published shortly by the Centre in book form.

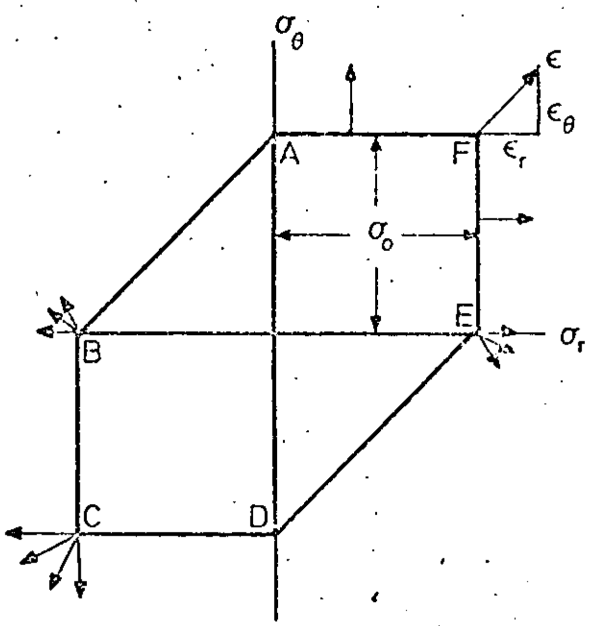

σ_θ
ϵ
ϵ_θ
A
F
ϵ_r
σ_o
B
E
σ_r
C
D

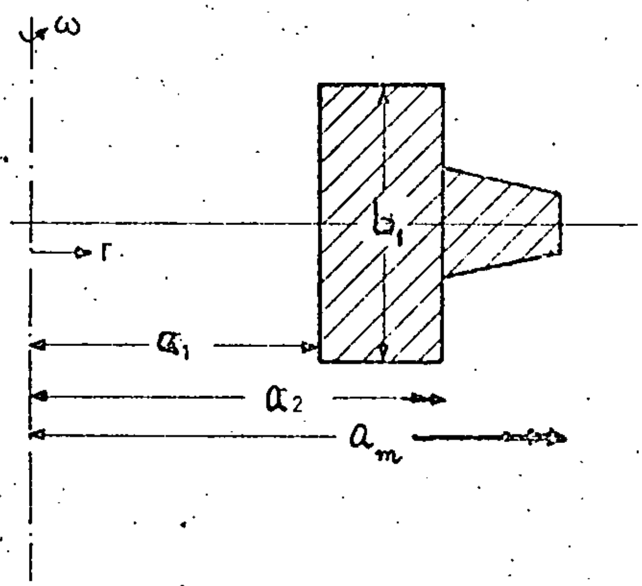

ω
r
b_1
a_1
a_2
a_m

Figs. 1.1a & 1.1b

CHAPTER 2

MINIMUM WEIGHT DESIGN OF DISCS BASED ON A STRESS CONSTRAINT

2.1 DESIGN CONCEPTS

The object of the research described in this chapter is to examine the possibilities of developing an automated synthesis capability for a class of minimum weight design problemsin the presence of non-analytic constraints. The design configuration is completely specified by the design variables which are constrained to vary within a prescribed range, thus making it possible to optimize the system for minimum weight. The side constraints ensure physically reasonable designs and may be expressed in the form

$$S_i(x_1, \ldots\ldots, x_n) \geq 0; \qquad i = 1, \ldots, I, \tag{2.1}$$

where the n real variables $x_1, \ldots, x_n$ correspond to the design variables. For example the condition (2.1) would include as a special case

$$\ell_i \leq x_i \leq u_i, \qquad i = 1, \ldots, n \tag{2.1a}$$

where the bounds ℓ_i, u_i are usually assumed constant. The behaviour or response characteristics of the system are described by the behaviour variables. The behaviour constraints ensure the structural integrity of the system and may be expressed in the form*

$$b_j(x \ , \ldots, x_n) \geq 0; \quad j = 1, \ldots, J \tag{2.2}$$

A special case of this would include constraints of the form

---

* A single load condition has been assumed for simplicity. The extension to multiple load conditions is straightforward.

$$L_j \leq Y_j(x_1, \ldots, x_n) \leq U_j; \quad j = 1, \ldots, m \tag{2.2a}$$

The weight is assumed to be a single-valued differentiable function

$$W = W(x_1, \ldots, x_n)$$

The minimum weight solutions are obtained by minimising $W(x_1, \ldots x_n)$ subject to the constraint conditions (2.1, 2.2, or 2.1a, 2.2a). The functions W, b_j, Y_j are nonlinear in general and the solutions are based on a nonlinear programming formulation. The problems considered are restricted to those for which the behaviour variables cannot be expressed as analytically defined functions of the design variables. The behaviour variables are functions only in the sense that they are computer-oriented rules for determining the behaviour associated with a given design and are not given in a closed analytical form in terms of the design variables. The behaviour variables may be regarded as a "black box" into which are put the design variables representing a given design and out of which comes the corresponding behaviour variables for that design. The box contains such devices as differential equations, matrices, finite difference procedures, a digital computer and so on. This means that the functions b_j, Y_j are essentially numerically defined functions.

These synthesis concepts are illustrated by considering the problem of minimising the weight of a steam turbine disc subject to specified behaviour and side constraints. For purposes of simplicity in this initial investigation the behaviour constraints have been restricted to a consideration that the stresses everywhere whould be below the yield stress. The side constraints on the other hand, impose restrictions on the dimensions and tolerances of the disc. The problem is essentially that of determining the optimal thickness h(r). The stresses are governed by a system of ordinary differential equations containing h(r) and its derivatives. These can be solved only when h(r) is prescribed. The stresses are functionals of h(r) and the problem has essentially a continuous or variational structure. For purposes of numerical computation the problem is discretised and in this representation the stresses correspond to "black box" type variables. The side constraints ensure designs for which h(r) is non-negative. Before a detailed discussion of the problem, some preliminary synthesis concepts are introduced which constitute a framework, within which the problem is formulated.

The design variables define a point in an n-dimensional real Euclidean space E^n called design space

$$\underline{x} = (x_1, \ldots, x_n) \tag{2.3}$$

Consider functions $g_k(\underline{x})$: $k = 1, \ldots, 2(n+m)$ defined by

$$\left.\begin{aligned} g_k(\underline{x}) &= \ell_k - x_k \;; \quad k = 1, \ldots, n \\ &= x_{k-n} - u_{k-n}; \quad k = n+1, \ldots, 2n \\ &= L_{k-2n} - Y_{k-2n}(\underline{x}); \quad k = 2n+1, \ldots, 2n+m \\ &= Y_{k-2n-m}(\underline{x}) - U_{k-2n-m}; \; k = 2n+m+1, \ldots, 2(n+m) \end{aligned}\right\} \quad (2.4$$

From (2.1a, 2.2a)

$$g_k(\underline{x}) \leqslant 0; \qquad k = 1, \ldots, 2(n+m) \tag{2.4a}$$

The feasible region R is a subspace of E^n and consists of points $\underline{x}$ which satisfy the constraint conditions (2.1a, 2.2a, or 2.4a). Therefore

$$R \equiv \{\underline{x} | \underline{x} \in E^n \ ; \ g_k(\underline{x}) \leq 0, \ \forall \ k = 1, \ldots, 2(n+m)\} \tag{2.5}$$

Design points which belong to R are called feasible points. There is associated with each constraint function $g_k(\underline{x})$ a hypersurface defined by

$$G_k \equiv \{\underline{x} | g_k(\underline{x}) = 0\} \ ; \qquad k = 1, \ldots, 2(n+m) \tag{2.5a}$$

The composite constraint surface is defined by

$$G \equiv R \cap G^*$$

where

$$G^* = G_1 \cup G_2 \cup \ldots . \cup G_{2(n+m)}$$

This defines the boundary of R and points which belong to G are called boundary points. The hypersurfaces (2.5a) for the behaviour constraints are nonanalytic and correspond to unknown surfaces in E^n. The weight contours

$$W(\underline{x}) = C$$

define a family of hypersurfaces in E^n for different values of the parameter C. A point $\underline{x} \in R$ is a feasible point while $\underline{x} \notin R$ is a non-feasible point. The synthesis generates a sequence of feasible designs of decreasing weight which converge to the least weight contour in R. An initial design is established and is systematically improved by an alternating iterative process of analysis and design modifications. These redesign cycles correspond to motion in design space along trajectories on which the weight decreases. Therefore the problem consists essentially in the proper selection of the directions and distances of travel.

2.2 STEAM TURBINE DISCS

The steam turbine disc to be optimized is shown in Figure 2.1. The width of the hub and the rim shape have been specified to allow for the attachment of the discs and the spacing of the blades in the turbine, while the depth of the hub is variable to permit adjoining discs to be shrunk on to a common shaft. The thickness distribution for the remainder of the disc is variable but symmetrically distributed about a plane perpendicular to the axis of rotation through the mid-point of the width at the bore.

The overall diameter of steam turbine discs is fixed from considerations of blade strength and steam flow, while the shape of the rim is determined by the aerodynamic and centrifugal loading on the blade. The hub width on discs integral with the shaft are fixed by a combination of the expansion allowances, diaphragm thickness and blade width. However, on shrunk-on discs, the hub width is determined by the stresses at the bore using the Tresca yield condition that the principal shearing stresses at thebore should be below the maximum allowable shear stress. A three-dimensional stress analysis indicates that quite high axial stresses are present at the bore even when the disc is stationary and that these stresses tend to increase with the hub width. Therefore in future work there may be an incentive to reduce the hub width.

The hub depth for shrunk-on discs is determined by the following considerations:

1. It must be the same as that of adjacent discs.
2. It must not be too small as it locates against the face of the shaft during assembly.
3. It must not lie outside the critical radius. The critical radius is defined as the radius such that if further mass is added at a greater radius, the bore stresses will increase, while if further masses are added at a lesser radius, the bore stresses will decrease.

The thickness distribution function describing the disc profile should be a continuous function of the radial distance, with a continuous derivative, and should be blended evenly to the hub and rim to avoid stress concentration effects. This implies that the radius of curvature at any point on the profile would be large compared to the thickness and that there should be no discontinuities in the radius of curvature. If the thickness has a singularity at which there is a discontinuity in derivative then the values of the derivatives on either side are blended to remove the discontinuity. In certain types of steam turbine discs there are balance holes distributed in the circumferential direction to balance the axial steam pressures by reducing the pressure differences on either side of the disc. However, in modern turbines the tendency is for most of the cylinders to be "double flow". The steam enters halfway down the cylinders and splits into two streams which then circulate in opposite directions. The steam pressures are thus self-balancing and no balance holes are needed. The advantages to be gained from balance holes are relatively few, while the increased stresses in their neighbourhood could impose restrictions on the design especially as the allowable stresses are limited by creep; the only cylinders on which balance holes are found in modern turbines are on the single flow intermediate pressure shafts on machines of 350 MW and below.

Creep effects do not usually occur on shrunk-on discs as the temperatures are very low (< 400°F). However on discs integral with the shaft where temperatures of up to 1050°F are encountered, the allowable stresses are limited by creep behaviour of the material.

This means that the strains are calculated in the elastic range. For shrunk-on discs it is necessary to get the maximum possible rim radius and hence high strength steels are used. These do not have a pronounced yield point. For discs designed on a plastic analysis the hoop strains at the bore may be such as to remove the interference between disc and shaft. Therefore the design problem is formulated in the elastic range.

The allowable stresses are governed by the stresses at the bore based on the Tresca yield condition and by the average tangential stresses evaluated at all disc sections from the bore to the rim which should not exceed the ratio of the ultimate tensile strength at the operating temperatures to the bursting factor of safety (= 3.0). However, for practical design purposes the Tresca condition gives a good approximation to the stress limitations throughout the disc.

The stress calculations are based on a two-dimensional analysis on the assumption of radially symmetric plane stress, which means that the axial and shear stresses are neglected compared to the radial and hoop stresses. This implies that the disc should not be too thick. The temperature variations are usually neglected, but the computer program includes the thermal stress calculations as well. The frequency constraint usually adopted in design work is that the ratio of the lowest natural frequency of vibration to the number of nodal diameters should exceed the speed of rotation of the disc. It is generally found that when a curve of frequency against the number of nodal diameters is plotted the minimum occurs at about eight nodal diameters and for this reason in most practical work the constraints are based on eight nodal diameters. However this is not true in general, and sometimes the designs are based on nine nodal diameters. The amplitudes and stresses at resonance decrease as the number of nodal diameters increase rendering resonance less dangerous.

2.3 VARIATIONAL FORMULATION

The weight is given by the functional expression

$$W = \int_{a_1}^{a_m} 2\pi\rho r \; h(r) \; dr \tag{2.6}$$

where a_1, a_m are the inner and outer radii respectively, ρ is the density and $h(r)$ is the thickness at a radial distance r from the axis of rotation. The thickness distribution is defined by Figure 2.1.

$$\left.\begin{aligned} h(r) &= b_1 && \text{for } a_1 \leqslant r \leqslant a_2 \\ &= h(r) && \text{for } a_2 \leqslant r \leqslant a_{m-1} \\ &= b_m && \text{for } a_{m-1} \leqslant r \leqslant a_m \end{aligned}\right\} \tag{2.7}$$

where b_1, b_m, a_1, a_m, a_{m-1} are constants, while $h(r)$, a_2 are variables satisfying the side conditions

$$\left.\begin{aligned} & L \leqslant a_2 \leqslant U \\ & \varepsilon \leqslant h(r) < \infty \ \forall \ r \in [a_2,\ a_{m-1}] \end{aligned}\right\} \tag{2.8}$$

where the bounds L, U, ε are constants determined from design considerations and correspond to constraints on the design configuration of the disc.

From (2.6, 2.7)

$$W = \int_{a_1}^{a_2} 2\pi\rho r b_1 dr + \int_{a_2}^{a_{m-1}} 2\pi\rho r\ h(r)dr + \int_{a_{m-1}}^{a_m} 2\pi\rho r b_m\ dr$$

$$= \pi\rho\left[b_1(a_2^2 - a_1^2) + b_m(a_m^2 - a_{m-1}^2)\right] + 2\pi\rho \int_{a_2}^{a_{m-1}} r\ h(r)\ dr \tag{2.9}$$

The stress distribution is determined on the assumption of radially symmetrical plane stress which means that the axial and shear stresses are neglected compared to the radial and tangential stresses. The physical implications of this assumption is that the disc is not too thick and not too asymmetric about the midplane. Otherwise the assumption that the axial and shear stresses are the same as on the surface (that is, they vanish) is not valid. If the disc were asymmetric shear stresses would be set up. However a small deviation from asymmetry is tolerable.

The equation of dynamic equilibrium is given by [136].

$$\frac{d}{dr}(h\sigma_r) + \frac{h}{r}(\sigma_r - \sigma_\theta) + \rho\omega^2 rh = 0 \tag{2.10}$$

where σ_r, σ_θ are the radial and tangential stresses and ω is the angular velocity of rotation of the disc. (NOTE: This equation is the same as equation (1.6) for the plastic case.)

The material is assumed to obey a yield condition of the form

$$F(\sigma_r, \sigma_\theta) \leq \sigma_o \tag{2.11}$$

where σ_o is the yield stress.

The yield condition used in this investigation is the Tresca maximum shear condition

$$F(\sigma_r, \sigma_\theta) = \max\{|\sigma_r|, |\sigma_\theta|, |\sigma_r - \sigma_\theta|\} \tag{2.12}$$

The stresses are expressed in terms of the radial displacement u(r) by the following compatibility relations

$$\left.\begin{aligned} \sigma_r &= \frac{E}{1 - \nu^2}(e_r + \nu e_\theta) \\ \sigma_\theta &= \frac{E}{1 - \nu^2}(\nu e_r + e_\theta) \\ e_r &= \frac{du}{dr} \\ e_\theta &= \frac{u}{r} \end{aligned}\right\} \tag{2.13}$$

where e_r, e_θ are the radial and tangential strains, E is Young's Modulus and ν is Poisson's ratio.

From (2.10, 2.13)

$$\left.\begin{aligned}\frac{d\sigma_r}{dr} &= -\frac{1}{h}\left[\sigma_r \frac{dh}{dr} + (\sigma_r - \sigma_\theta)\frac{h}{r} + \rho\omega^2 rh\right] \\ \frac{d\sigma_\theta}{dr} &= \frac{(\sigma_r - \sigma_\theta)}{r} - \frac{\nu}{h}\sigma_r \frac{dh}{dr} - \nu\rho\omega^2 r\end{aligned}\right\} \qquad (2.14)$$

The stresses are obtained by solving these differential equations for a given $h = h(r)$, for all $r \varepsilon \left[a_1, a_m\right]$. The boundary conditions on the stresses are given by

$$\left[\sigma_r\right]_{r=a_1} = s_1 \qquad \left[\sigma_r\right]_{r=a_m} = s_m \qquad (2.15)$$

For purposes of simplicity thermal stresses have been neglected. The effect of these is considered later on. The minimisation problem may now be formulated mathematically as follows:

Determine an optimal thickness $h(r)$ and a radius a_2 such that the functional

$$W = \int_{a_1}^{a_m} 2\pi\rho h(r)dr \qquad (2.6)$$

is minimised subject to the constraint conditions:

$$\left.\begin{aligned}\frac{d\sigma_r}{dr} &= -\frac{1}{h}\left[\sigma_r \frac{dh}{dr} + (\sigma_r - \sigma_\theta)\frac{h}{r} + \rho\omega^2 rh\right] \\ \frac{d\sigma_\theta}{dr} &= -\frac{1}{h}\left[\nu\sigma_r \frac{dh}{dr} - (\sigma_r - \sigma_\theta)\frac{h}{r} + \nu\rho\omega^2 rh\right]\end{aligned}\right\} \qquad (2.14)$$

$$F(\sigma_r, \sigma_\theta) - \sigma_o \leqslant 0 \tag{2.11}$$

$$\left.\begin{array}{l} \varepsilon - h \leqslant 0 \\ a_2 \leqslant L \leqslant U \end{array}\right\} \tag{2.8}$$

and the boundary conditions

$$\left.\begin{array}{ll} h(a_1) = b_1, & \sigma_r(a_1) = s_1 \\ h(a_m) = b_m, & \sigma_r(a_m) = s_m \end{array}\right\} \tag{2.7,2.15}$$

This is a very general problem in optimal control theory [139]. The formal solutions are based on the maximum principle of Pontryagin [137] and the optimality principle of Bellman [56,57,140,141]. The former provides the first order necessary conditions for an optimum: Euler-Lagrange equations, transversality conditions and the Weierstrass condition. Gelfand and Fomin [138] give a qualitative illustration of these principles by considering the propagation of a disturbance which can be described in two ways - either in terms of the trajectories along which the disturbance propagates (the 'ray' approach in optics) or in terms of the motion of the wavefront. The wave approach leads to the Hamilton-Jacobi partial differential equation and corresponds to the optimality principle of dynamic programming while the 'ray' approach leads to the classical canonical Euler Lagrange equations which form a system of ordinary differential equations and corresponds to the Pontryagin Principle.

For complex systems, closed analytical solutions are generally impossible to obtain and recourse must be made to numerical procedures.

Computationally, the Bellman formulation is more complex and requires substantial amounts of computer programming and storage facilities, whereas the Pontryagin formulation suffers from all the inherent difficulties of a two-point boundary value problem. Some of the available numerical schemes for solving these boundary value problems include: (a) steepest ascent on the variational Hamiltonian [142-144]. The methods being first order, are relatively simple to implement even for complex problems. Initially when far from the optimum, these methods work well, but as the optimum is approached they tend to exhibit poor convergence properties. Convergence can be accelerated using second order methods such as approximating the Hamiltonian by a quadratic in the neighbourhood of the optimum; (b) quasi-linearisation [145] on the state and adjoint equations in conjunction with a generalised Newton-Raphson method to generate a sequence of approximating functions. For further details on these methods, the reader is referred to [146-148, 139]. More powerful techniques have recently been developed based on a conjugate gradient technique [149-151]. They are based on the condition that at the optimum the Hamiltonian must be maximised with respect to the controls. The basic steps are outlined below:

(a) Set $i = 0$; compute $\underline{g}^{(o)} = \underline{\nabla}u \, H\Big|_{\underline{u}=\underline{u}^{(o)}}$; set $\underline{s}^{(o)} = \underline{g}^{(o)}$

(b) Set $\underline{u}^{(i+1)} = \underline{u}^{(i)} + t^{(i)}\underline{s}^{(i)}$ where $t^{(i)}$ minimises $W(\underline{u}^{(i)}+t^{(i)}\underline{s}^{(i)})$

(c) Compute $\underline{g}^{(i+1)} = \underline{\nabla}u\, H \Big|_{\underline{u}=\underline{u}^{(i+1)}}$

set $\underline{s}^{(i+1)} = \underline{g}^{(i+1)} + \beta^{(i)}\underline{s}^{(i)}$

where

$$\beta^{(i)} = \frac{\left\langle \underline{g}^{(i+1)} \,\middle|\, \underline{g}^{(i+1)} \right\rangle}{\left\langle \underline{g}^{(i)} \,\middle|\, \underline{g}^{(i)} \right\rangle}$$

and

$$\left\langle \underline{g}^{(i)} \,\middle|\, \underline{g}^{(j)} \right\rangle = \int_{a_1}^{a_m} \underline{g}^{(i)}\, \underline{g}^{(j)^T}\, dr$$

(d) Set $i \rightarrow i+1$ go to (b).

The Hamiltonian used in this algorithm is defined by

$$H = -\frac{\lambda_1}{h}\left[\sigma_r \frac{dh}{dr} + (\sigma_r - \sigma_\theta)\frac{h}{r} + \rho\omega^2 rh\right] - \frac{\lambda_2}{h}\left[\nu\sigma_r \frac{dh}{dr} - (\sigma_r - \sigma_\theta)\frac{h}{r} + \nu\rho\omega^2 rh\right] \tag{2.16}$$

where $\lambda_1(r)$, $\lambda_2(r)$, are the adjoint variables satisfying the equations

$$\frac{d}{dr}\begin{pmatrix} \lambda_1 \\ \lambda_2 \end{pmatrix} = -\begin{pmatrix} \dfrac{\partial H}{\partial \sigma_r} \\[2ex] \dfrac{\partial H}{\partial \sigma_\theta} \end{pmatrix} \tag{2.17}$$

In the presence of the inequality constraints (2.8, 2.11) the merit functional W used in step (b) must be replaced by

$$W_k = W + \eta_k \left\{ \int_{a_1}^{a_m} \frac{dr}{\sigma_o - F(\sigma_r, \sigma_\theta)} + \frac{dr}{h - \varepsilon} \right\} \tag{2.18}$$

where $\eta_k \rightarrow 0$ as $k \rightarrow \infty$.

The modified functional (2.18) is essentially an extension of the SUMT procedure of Fiacco and McCormick [134-135]. This can be solved using a penalty function formulation in conjunction with the optimization procedures of Rosenbrock, Powell, Nelder-Mead [129, 130, 92]. An alternate formulation is available when it is possible to parametrise the controls, thereby reducing the problem to a constrained optimization problem. This requires a suitable parametric representation for the controls and could lead to increased computation, especially when the number of parameters involved is large. Due to the formidable computational difficulties associated with the variational formulation, a different mode of solution procedure is proposed.* The problem is discretised using finite difference techniques. The weight integral is replaced by a summation over a discrete set of variables and the stresses correspond to "black box" type functionals, the problem being transformed into a nonlinear programming problem characterised by non-analytic behaviour constraints. This is essentially a form of parametrisation of the control by piecewise linear function.

---

* The optimal control aspects of the problem from an analytical standpoint are discussed in Chapter 5.

2.4 FINITE DIFFERENCE FORMULATION

The disc profile is approximated by a sequence of straight lines (Figures 2.2, 2.3). The interval $[a_2, a_{m-1}]$ is divided into a finite number of subintervals by points $a_2, a_3, \ldots, a_{m-1}$ where

$$a_2 < a_3 < \ldots\ldots < a_{m-1}$$

The thickness $h(r)$ is approximated by a sequence of piecewise linear functions $h_j(r)$ defined as follows:

Let

$$\left.\begin{aligned} h(a_j) &= b_j \\ h_j(r) &= b_{j-1} + \left(\frac{b_j - b_{j-1}}{a_j - a_{j-1}}\right)(r - a_{j-1}) \qquad a_{j-1} \leq r \leq a_j \end{aligned}\right\} \quad (2.19)$$

and

$$h(r) \approx h_j(r) \qquad a_{j-1} \leq r \leq a_j; \quad j = 3, \ldots, (m-1)$$

From (2.9, 2.19)

$$W = \pi\rho b_1(a_2^2 - a_1^2) + \pi\rho b_m(a_m^2 - a_{m-1}^2) + \int_{a_2}^{a_{m-1}} 2\pi\rho r h(r)dr$$

$$= \pi\rho b_1(a_2^2 - a_1^2) + \pi\rho b_m(a_m^2 - a_{m-1}^2) +$$

$$\sum_{j=3}^{m-1} \int_{a_{j-1}}^{a_j} 2\pi\rho r h_j(r)dr \qquad (2.20)$$

The problem has been transformed into a finite difference formulation by approximating $h(r)$ by a series of linear functions $h_j(r)$; $j = 3, \ldots, (m-1)$. This gives a linearised model for the disc. The thickness at radii $a_1, a_2, \ldots, a_m$ are $b_1, b_2, \ldots, b_m$ respectively, and are measured parallel to the axis of rotation.

2.5 SIDE CONSTRAINTS

The constraints on the design configuration are defined by (see equations (2.7, 2.8))

(i) $a_1 < a_2 < \ldots\ldots < a_{m-1} < a_m$

(ii) $b_1 = b_2$ constant

(iii) $b_m = b_{m-1}$ constant

(iv) $a_1, a_3, \ldots, a_{m-1}, a_m$ constants

(v) a_2 variable

(vi) b_j variable $j = 3, \ldots, m-2$

(vii) $b_j \geq \varepsilon$ $j = 3, \ldots, m-2$

(viii) $L \leq a_2 \leq U$

The widths of the hub and rim and rim depth are fixed while the hub depth is variable. Constraints (vii, viii) ensure physically reasonable designs by ensuring that the variable thicknesses b_j are non-negative. The hub radius a_2 is constrained to vary between fixed limits, L, U.

The design variables are given by

$$\underline{x} = (b_3, \ldots, b_{m-2}, a_2) \tag{2.21}$$

This defines a (m-3) dimensional design space. The side constraints are given by

$$\underline{\ell} \leqslant \underline{x} \leqslant \underline{u} \tag{2.22}$$

where the constant row vectors $\underline{\ell}$, $\underline{u}$, are defined by

$$\underline{\ell} = (\varepsilon, \ldots, \varepsilon, L)$$

$$\underline{u} = (\infty, \ldots, \infty, U)$$

They are linear and correspond to hyperplanes in design space.

2.6 BEHAVIOUR CONSTRAINTS

The disc is symmetrical with respect to both its axis of rotation and its midplane and is in dynamic equilibrium under the action of the centrifugal and thermal loading. The stress distribution is determined on the assumption of radially symmetric plane stress. The stress calculations are based on Donaths method [154, 155], which consists essentially in replacing the disc by a series of annular rings of constant width. The stresses at the outer edge of a ring are determined in terms of the stresses at the inner edge. Continuity is ensured by equating the radial displacement and the radial load at the interface of adjacent rings.

The primary goal of this investigation is the study of methods for optimising a class of structural systems in the presence of non-analytic (behaviour) constraints. The analysis phases of the redesign cycle are regarded as a series of "black boxes". The actual mechanisms within the boxes are disregarded. The optimisation procedures are independent of the analysis routines employed and can be used in conjunction with structural analysis programs that are already available. The need for more sophisticated analysis routines for performing more effective redesign cycles may be better assessed after an initial evaluation of the results using existing programs. This is the justification for using the Donath method. It is a relatively simple method and was already available at the commencement of this investigation. The basic equations used are summarised for easy reference. During the stress analysis each of the intervals $[a_{j-1}, a_j]$ for j = 3, ..., (m-1) is further subdivided and the calculations are performed on this subdivided disc. This is to ensure a greater degree of accuracy for the stress computations.

Substituting (2.13) in (2.10) gives

$$\frac{d^2u}{dr^2} + \left(\frac{1}{r} + \frac{1}{h}\frac{dh}{dr}\right)\frac{du}{dr} - \left(\frac{1}{r} - \frac{\nu}{h}\frac{dh}{dr}\right)\frac{u}{r} + \frac{\rho\omega^2(1 - \nu^2)r}{E} = 0 \qquad (2.23)$$

Within each annular ring h(r) is constant and therefore (2.23) reduces to

$$\frac{d^2u}{dr^2} + \frac{1}{r}\frac{du}{dr} - \frac{u}{r^2} + \frac{\rho\omega^2(1 - \nu^2)r}{E} = 0$$

Solving this equation gives

$$u = C_1 r + \frac{C_2}{r} - \frac{\rho}{8}\frac{\omega^2(1 - \nu^2)}{E} r^3$$

where C_1, C_2 are constants of integration.

From (2.13)

$$\left.\begin{aligned}\sigma_r &= \left(\frac{EC_1}{1-\nu}\right) - \left(\frac{EC_2}{1+\nu}\right)\frac{1}{r^2} - \left(\frac{3+\nu}{8}\rho\omega^2\right)r^2 \\ \sigma_\theta &= \left(\frac{EC_1}{1-\nu}\right) + \left(\frac{EC_2}{1+\nu}\right)\frac{1}{r^2} - \left(\frac{1+3\nu}{8}\rho\omega^2\right)r^2\end{aligned}\right\} \quad (2.24)$$

These are the equations describing the rotational stresses within each ring. Similar equations can be formulated for the thermal stresses which are determined from the equation,

$$\frac{d}{dr}(h\sigma_r) + \frac{h}{r}(\sigma_r - \sigma_\theta) = 0 \quad (2.25)$$

where the thermal stresses σ_r, σ_θ are given by

$$\left.\begin{aligned}\sigma_r &= \frac{E}{1-\nu^2}\left[(e_r - \alpha\phi) + \nu(e_\theta - \alpha\phi)\right] \\ \sigma_\theta &= \frac{E}{1-\nu^2}\left[\nu(e_r - \alpha\phi) + (e_\theta - \alpha\phi)\right] \\ e_r &= \frac{du}{dr} \\ e_\theta &= \frac{u}{r}\end{aligned}\right\} \quad (2.26)$$

where α is the coefficient of linear expansion and ϕ is the temperature. Substituting (2.26) in (2.25) gives (with $h(r)$ = constant within each ring)

$$\frac{d^2u}{dr^2} + \frac{1}{r}\frac{du}{dr} - \frac{u}{r^2} - (1+\nu)\alpha\frac{d\phi}{dr} = 0 \quad (2.27)$$

Solving

$$u = C_1 r + \frac{C_2}{r} + (1+\nu)\frac{\alpha}{r}\int^{r} r\phi \, dr$$

where C_1, C_2 are constants of integration.

From (2.26)

$$\sigma_r = \frac{-\alpha E}{r^2}\int^{r} r\phi \, dr + \frac{E}{1-\nu^2}\left[C_1(1+\nu) - \frac{C_2(1-\nu)}{r^2}\right]$$

$$\sigma_\theta = \frac{\alpha E}{r^2}\int^{r} r\phi \, dr - \alpha E\phi + \frac{E}{1-\nu^2}\left[C_1(1+\nu) + \frac{C_2(1-\nu)}{r^2}\right]$$

These determine the thermal stresses within each ring for a prescribed temperature function $\phi(r)$. The resultant stress distribution is given by

$$\left.\begin{aligned} \sigma_r &= \sigma_r^{(rotational)} + \sigma_r^{(thermal)} \\ \sigma_\theta &= \sigma_\theta^{(rotational)} + \sigma_\theta^{(thermal)} \end{aligned}\right\} \qquad (2.28)$$

Although theprogram used includes thermal computations for purposes of simplicity, these are neglected and the results are based entirely on the rotational stresses.

At each stress calculation the computer program subdivides the intervals $[a_{j-1}, a_j]$ for j = 3, ..., (m-1) into further subintervals by points $r_2, \ldots, r_{n-1}$ where

$$\left.\begin{aligned} a_2 &= r_2 < r_3 < \ldots\ldots < r_{n-1} = a_{m-1} \\ &\text{In addition} \\ r_1 &= a_1 \\ r_n &= a_m \end{aligned}\right\} \qquad (2.29)$$

The condition for subdividing the interval $[a_{j-1}, a_j]$ is

$$|b_j - b_{j-1}| > \frac{\delta}{2}(b_j + b_{j-1}) \tag{2.30}$$

where δ is a small positive tolerance. If this condition is satisfied, $[a_{j-1}, a_j]$ is subdivided into u equal subintervals by points $q_o, q_1, \ldots, q_u$ where

$$a_{j-1} = q_o < q_1 < \ldots\ldots < q_u = a_j \tag{2.31}$$

The corresponding thicknesses at these points are given by

$$p_i = h(q_i) \qquad i = 0,1,\ldots,u \; ;$$

and

$$\begin{aligned}
|b_j - b_{j-1}| &= |p_o - p_u| \\
&= |(p_o - p_1) + (p_1 - p_2) + \ldots + \\
&\qquad (p_{u-2} - p_{u-1}) + (p_{u-1} - p_u)| \\
&\leq |p_o - p_1| + |p_1 - p_2| + \ldots + \\
&\qquad |p_{u-2} - p_{u-1}| + |p_{u-1} - p_u| \\
&\leq \frac{\delta}{2}\Big[(p_o + p_1) + (p_1 + p_2) + \ldots + \\
&\qquad (p_{u-2} + p_{u-1}) + (p_{u-1} + p_u)\Big] \\
&\leq \frac{\delta}{2}(2u)K_j
\end{aligned}$$

where $K_j = \max(b_j, b_{j-1})$

Hence,

$$u \geq \frac{1}{\delta K_j} \left| b_j - b_{j-1} \right|$$

or

$$u = 1 + \left\langle \frac{b_j - b_{j-1}}{\delta K_j} \right\rangle \tag{2.32}$$

where <x> denotes the largest integer not exceeding x. The total number of points of subdivision for all the intervals $[a_{j-1}, a_j]$ is n, the points being labelled r_1, r_2, ..., r_n with corresponding thicknesses h_1, h_2, ..., h_n respectively. The reason for this subdivision is to obtain a better estimate for the stress distribution. The number n varies from design to design.

For each design the stresses at these n points are calculated. The principal shearing stresses are then given by [156].

$$\left.\begin{aligned} \tau_1 &= |\sigma_r - \sigma_\theta| \\ \tau_2 &= |\sigma_r| \\ \tau_3 &= |\sigma_\theta| \end{aligned}\right\} \tag{2.33}$$

The stress constraints are defined by the Tresca maximum shear condition

$$\sigma \leq \sigma_o \tag{2.34}$$

where

$$\sigma = \max(\tau_1, \tau_2, \tau_3)$$

σ_o = yield stress for the material.

Therefore the behaviour variables are given by

$$BF(\underline{x}) = (\sigma_{r_1}, \sigma_{r_2}, \ldots, \sigma_{r_n})$$

while the behaviour constraints are defined by

$$\underline{L} \leq \underline{B}F(\underline{x}) \leq \underline{U} \qquad (2.35)$$

where

$$\underline{L} = (0, 0, \ldots, 0)$$

$$\underline{U} = (\sigma_o, \sigma_o, \ldots\ldots, \sigma_o)$$

and

$$n = n(\underline{x})$$

One of the essential features of this investigation is the absence of closed analytical expressions for the stresses in terms of the design variables. The stresses are functions only in the sense that they are computer oriented rules for determining the behaviour associated with a given design. Therefore the stresses may be regarded as a "black box". The contents of the box are ignored. What is essential is the output from the box which enables the stresses to be checked against the yield criterion (2.34). Due to the "black box" nature of the stresses the behaviour constraints correspond to unknown surfaces in design space.

From (2.20) and conditions (ii, iii) of section 2.5, the weight is given by

$$W = \frac{\pi\rho}{3} \sum_{j=3}^{m-2} \left(a_{j+1} - a_{j-1}\right)\left(a_{j+1} + a_j + a_{j-1}\right)b_j + \frac{\pi\rho}{3} b_1\left(-3a_1^2 + a_2^2 + a_3^2 + a_2a_3\right) + \frac{\pi\rho}{3} b_m\left(3a_m^2 - a_{m-1}^2 - a_{m-2}^2 - a_{m-1}a_{m-2}\right) \qquad (2.36)$$

Therefore $W = W(b_3, \ldots, b_{m-2}, a_2)$ is linear in b_j and quadratic in a_2. It is a non-convex function and could give rise to points of relative (local) minima.

2.7 THE NON-LINEAR PROGRAMMING PROBLEM

The problem can be formulated mathematically as a nonlinear programming problem as follows.

Given $\underline{\ell}$, $\underline{u}$, $\underline{L}$, $\underline{U}$, determine a design $\underline{x}$ which satisfies the conditions

(a) $\underline{\ell} \leq \underline{x} \leq \underline{u}$ (2.22)

(b) $\underline{L} \leq \underline{BF}(\underline{x}) \leq \underline{U}$ (2.35)

and minimises

(c) $W(\underline{x})$ (2.36)

The variational structure has been discretised by a nonlinear programming approximation characterised by non-analytic constraints on the behaviour variables. The objective is the development of optimisation procedures applicable to such problems by extending existing methods and formulating new ones. Methods available at the time of this investigation were the "steepest descent - alternate step" mode of travel in design space, developed by Schmit and his associates [64-74] for the automated weight minimisation of trusses and waffle plates with instability constraints. Modifications are introduced to improve their computational efficiency and convergence rates, and generalisations lead to new methods. These are applied to obtain numerical solutions to the disc problem on an English Electric KDF 9 computer. As a preliminary, some of the more commonly used non-linear programming procedures in structural problems are briefly reviewed below.

2.8 NON-LINEAR PROGRAMMING METHODS

Some computational algorithms for minimising a non-linear function subject to a set of inequality constraints are considered. For an unconstrained function with continuous partial derivatives, a minimum occurs at that point where the partial derivatives of the function with respect to its independent variables are zero and its matrix of second partial derivatives is positive definite. These necessary conditions for a minimum correspond to a set of simultaneous equations for which an exact solution is in general impossible, and recourse must be made to approximate or numerical methods. Some commonly used methods for minimisation are based on the method of steepest descent [157-159, 174]. This is an iterative method for determining a good step direction and then minimising the function in this direction. Another group of methods is based on approximating the merit function by the first and second order terms of its Taylor series expansion about a given point [160, 161]. The minimum of the resulting quadratic may be determined exactly and an expansion of the function about this new point obtained. If the third and higher order terms of the series are small the new point will be a better approximation to the solution than the old one, and the closer the point is to the solution, the more negligible will be the effect of the higher order terms. Direct search methods applicable to unconstrained functions include Fibonacci search [162] (this is best suited to one-dimensional unimodal functions); pattern methods [161] based on a combination of local univariate moves followed by pattern moves along the best direction given by the local search; random search methods [163,164] where the independent variables are selected in either a purely random manner or according to some probability distribution function. A detailed discussion of the above methods can be found in the book by Wilde [165]. Recently the techniques of Rosenbrock [129], Powell [92], Nelder-Mead [130] and Davidon-Fletcher-Powell [132,133] have come into prominence in the structural optimization area. These provide very powerful tools for solving unconstrained optimization problems. Future developments in the structural optimization area seem to be centred on these methods, used in conjunction with penalty functions to introduce inequality constraints. A comprehensive description and evaluation of such methods is given in the book by Kowalik and Osborne [80].

The Kuhn-Tucker optimality condition [120-123] establishes conditions for transforming a constrained minimisation problem into an unconstrained problem using Lagrange multipliers and slack variables to convert inequality constraints into equality constraints. The solution to the constrained problem is then given by the saddle point of the Lagrangian formulation. Alternatively, penalty functions may be used to simulate the constraints by unfavourably weighting the merit function in their vicinity [76,80,127,134,135,161]. The successive iterations of the problem are forced to lie in the feasible region, since the violation of the constraint results in a sudden and rapid deterioration of the merit function. Methods for handling the constraints implicitly include: Kelly's cutting plane method [101] for transforming the problem to a series of linear programming problems. The resulting linear programs can be solved using the well-known simplex algorithms of linear programming [166-168]. The book by Kunzi et al [168] contains the actual Algol and Fortran programs for executing these algorithms. Zoutendijk's method of feasible direction [99], gives methods for determining the optimal search vector.

Rosen's gradient projection methods [89,104] can be used for moving on the boundary of a constraint set by projecting the directions of steepest descent onto the tangent planes to the boundary. Alternatively, it is possible to leave the boundary of the feasible region along the constant merit contour [169]. The optimal direction for the "bounce" being given by a quadratic programming problem. A comprehensive list of linear and non-linear programming methods is given in [170-173].

2.9 COMPARISON WITH SCHMIT'S METHOD

Equations (2.13, 2.23, 2.26, 2.27, 2.28) applied to condition (2.34) give a behaviour constraint of the form

$$\sigma[h] \equiv \int_{a_1}^{a_m} \psi\left(r,\ h(r),\ \frac{dh}{dr}\right) dr \leqslant \sigma_o \tag{2.37}$$

The stresses are functionals of the thickness and have a "black box" representation in the discretised non-linear programming formulation. The non-linear programming procedures reviewed in section 2.8 do not apply to constraints of the type (2.37). Methods specifically applicable are those developed by Schmit and his associates [64-74]. Their methods were discussed in Chapter 1. The central theme of this research is to examine the possibilities of improving and extending Schmit's work to problems with constraints of the type (2.37). Their work is discussed in this article in the light of the synthesis procedures developed for the disc optimization.

They start from an initial feasible design and move in the direction of steepest descent to a better design some finite distance away. This procedure is repeated until a constraint is encountered which prevents further moves in the gradient direction. Then an alternate step is taken which is a move along the constant weight contour. After an alternate step, a feasible design should be forthcoming from which a steep descent can be made as before. This process is repeated until no move can be made by either mode at which time an optimum is said to be achieved. The reasoning behind this technique is that since the gradient points in the direction of greatest change it is the best direction to move to move to improve the design. If a move cannot be made in the best direction, then a feasible design is sought which at least does not increase the weight of the design. They use a fixed incremental step length scale in conjunction with steepest descent motion in the feasible region. If the new design is feasible the step length is doubled and this doubling process is continued until a design is reached which violates on a main constraint (side constraints are ignored at this stage). The total distance of travel back to an already feasible design is halved and the direction reversed. In all subsequent iterations, the distance is always halved and the direction reversed after each transition between a feasible and non-feasible design. This doubling and halving technique is thus directed to and converges upon the constraint surface. The method employed here moves in the gradient direction with an accelerated step length directed to the nearest behaviour constraint. This is similar to the step length calculations used by Best [84] (see Chapter 1 for his derivation). The step length decreases as a constraint is approached thus enabling a behaviour constraint to be encountered in a very small number of iterations. Therefore the method is more selective and enables a constraint to be more rapidly encountered than that used by Schmit and his associates. When a design violates a constraint a linear interpolation procedure is used to converge to the composite constraint. The interpolations are always made between a feasible and non-feasible condition. Therefore convergence is more stable and more rapid than a simple halving and doubling process. When a design lies on a constraint it is generally impossible to steep descent without piercing the constraint. An alternate step is then taken such that the weight does not increase (i.e. the point lies on the weight contour through the boundary point). Schmit et al use the method of alternate base planes to generate the directions of search along the weight contour. They obtain a sequence of proposed new designs which are tested in turn against the side and behaviour constraints. If any one of these designs is found to be feasible steepest descent motion is continued as before. The method of alternate base planes was applied to the disc problem and thereafter more selective methods were sought for moving away from the boundary. Initially a direction of search was generated whereby the sections not at yield stress were thinned down in proportion to their relative stress levels while the section at yield was thickened up by a predetermined amount. The distance of bounce was calculated using the constant weight condition. This gave a quadratic equation for the step length. A major disadvantage was the possibility of obtaining complex roots. When real roots were obtained the side (and behaviour) constraints were found to be violated. Thereafter a method was sought which, at least, guaranteed non-violation of the side constraints. The proposed designs then need only be tested against the yield criterion. When yield is violated a simple modification can be introduced to generate a new design, either by reducing the step length which is equivalent to propagating a new direction of search, or by changing the base plane of reference and repeating the process. The satisfaction of the side constraints is ensured by the proper selection of the step length using the linearity condition (2.22) from which the direction of bounce is calculated. The direction is determined by thickening the section of the disc at yield while thinning down the section furthest from yield in such a manner as to leave the weight unchanged. The remaining thickness variables are unaltered. Mathematically this always gives real directions and is more selective than the method of alternate base planes. The physics of the problem being utilised to indicate a direction for bouncing back into the feasible regions. When a design violates the side constraints the boundary nearest to the last feasible point can be easily calculated since the side constraints are linear. Subsequent motion is confined to projected gradient motion.

One of the inherent difficulties of any synthesis is the possibility of obtaining points of relative minima due to non-convexity of W and R. For such cases there is no known method of establishing whether a proposed optimum is, in fact, a global minimum or not. However, it is possible to establish a reasonable degree of confidence in the results obtained by searching a fairly wide region of the feasible domain. It is also possible to select two distinct initial points and run the synthesis along distinct paths. If the final optimum attained is the same (to within a specified tolerance) in the two cases, then it is reasonable to assume that the proposed optimum design is, in fact, an absolute minimum weight design.

Complete details of the analysis and computational procedures are given in de Silva [179, 180, 181]. For purposes of ready reference some of the more important aspects of this investigation are summarised below.

The optimization problem is characterised by

(a) multi-dimensional design space

(b) non-linear weight function

(c) possible relative minima due to non-convex weight function and feasible region

(d) linear side constraints

(e) stresses "black box" type functions.

while the optimization procedure is characterised by (Figure 2.4)

(a) Accelerated steepest descent motion in the feasible region until a constraint is encountered.

(b) constrained steepest descent motion from a side constraint. Since a move in the direction of steepest descent cannot generally be made without piercing the constraint surface, this method moves in the next best direction, the projection of the direction of steepest descent on the constraint surface.

(c) equal weight redesign from a stress constraint surface. Constrained steepest descent motion cannot take place as the surface is unknown. A move is therefore made which, at least, does not increase the weight of the design causing the iterations to diverge away from the minimum weight solutions.

2.10 STEEPEST DESCENT MOTION

The computer program starts from a feasible initial design and generates steepest descent motion defined by the following iterative equation

$$\underline{x}^{(q+1)} = \underline{x}^{(q)} + t^{(q)} \underline{\psi}^{(q)} \tag{2.38}$$

where

$$\left.\begin{aligned}
\underline{x}^{(q)} &= \left(b_3^{(q)},\ \ldots\ldots,\ b_{m-2}^{(q)},\ a_2^{(q)}\right) \\
\underline{\psi}^{(q)} &= -\nabla W\left(\underline{x}^{(q)}\right)\ \left|\nabla W\left(\underline{x}^{(q)}\right)\right| \\
\underline{\nabla} &= \left(\frac{\partial}{\partial b_3},\ \ldots\ldots,\ \frac{\partial}{\partial b_{m-2}},\ \frac{\partial}{\partial a_2}\right)
\end{aligned}\right\} \tag{2.39}$$

$t^{(q)}$ = distance of travel in steepest descent.

From (2.36)

$$\frac{\partial W}{\partial b_j} = \frac{\pi\rho}{3}\left(a_{j+1} - a_{j-1}\right)\left(a_{j+1} + a_j + a_{j-1}\right) \quad \text{for } j = 3, \ldots, (m-2)$$

$$\frac{\partial W}{\partial a_2} = \frac{\pi\rho}{3}\left(2a_2 + a_3\right)\left(b_1 - b_3\right)$$

Therefore using (2.39), equation (2.38) reduces to

$$b_j^{(q+1)} = b_j^{(q)} - \frac{\pi\rho}{3}\left(a_{j+1} - a_{j-1}\right)\left(a_{j+1} + a_j + a_{j-1}\right)t^{(q)} \Big/ N^{(q)}$$

$$\text{for } j = 3, \ldots, (m-2);$$

$$a_2^{(q+1)} = a_2^{(q)} - \frac{\pi\rho}{3}\left(2a_2 + a_3\right)\left(b_1 - b_3\right)t^{(q)} \Big/ N^{(q)}$$

where the normalisation factor $N^{(q)}$ is given by

$$N^{(q)} = \left[\sum_{j=3}^{m-2}\left(\frac{\partial W}{\partial b_j}\right)^2 + \left(\frac{\partial W}{\partial a_2}\right)^2\right]^{\frac{1}{2}}$$

$$= \frac{\pi\rho}{3}\left[\sum_{j=3}^{m-2}\left(a_{j+1} - a_{j-1}\right)^2\left(a_{j+1} + a_j + a_{j-1}\right)^2 + \left(2a_2 + a_3\right)^2\left(b_1 - b_3\right)^2\right]^{\frac{1}{2}}$$

The distance of travel to a stress constraint surface cannot be determined exactly as the surfaces are unknown. Therefore the distance is estimated as follows:

Let

$$h_i^{(q)} \;=\; \text{thickness at } r_i$$

$$\sigma_{r_i}^{(q)} \;=\; \text{maximum shearing stress at } r_i.$$

$$\sigma_o \;=\; \text{yield stress.}$$

For purposes of this estimation, it is assumed that each $h_i^{(q)}$ can be varied independently without affecting the stress distribution elsewhere. Therefore to bring $h_i^{(q)}$ to yield, it must be changed to $\bar{h}_i^{(q)}$ given by

$$\left(2\pi r_i\, \bar{h}_i^{(q)}\right)\sigma_o \;\approx\; \left(2\pi r_i\, h_i^{(q)}\right)\sigma_{r_i}$$

so that

$$\bar{h}_i^{(q)} \;\approx\; \frac{\sigma_{r_i}}{\sigma_o}\, h_i^{(q)}$$

This relation is derived on the assumption that the load remains unchanged, so that the distance $t_i^{(q)}$ to the behaviour constraint surface at r_i is given by

$$\bar{h}_i^{(q)} \;=\; h_i^{(q)} - t_i^{(q)}\,\phi_i^{(q)} \qquad \left(0 \le \phi_i^{(q)} \le 1\right)$$

Hence

$$t_i^{(q)} \;=\; \frac{h_i^{(q)} - \bar{h}_i^{(q)}}{\phi_i^{(q)}}$$

$$\simeq \left(\frac{\sigma_o - \sigma_{r_i}}{\sigma_o}\right) \frac{h_i^{(q)}}{\phi_i^{(q)}}$$

or

$$t_i^{(q)} \geqslant \left(\frac{\sigma_o - \sigma_{r_i}}{\sigma_o}\right) h_i^{(q)}$$

and

$$t^{(q)} = \underset{3 \leqslant i \leqslant (n-2)}{\text{minimum}} \; t_i^{(q)} \tag{2.40}$$

Thus $t^{(q)}$ decreases as the point approaches a behaviour surface. At each iteration the design is checked against the side and stress constraints and, if satisfactory, the corresponding stress distribution is calculated and checked against the yield criterion. If the stresses are below yield stress, a feasible design is obtained, and steepest descent motion continues until a non-feasible design is encountered. A non-feasible design corresponds to a region of constraint violation, i.e. violation of either the side or the behaviour constraints.

2.11 GEOMETRICAL CONSTRAINT VIOLATION

When the design violates the side constraints (2.22), the distances from the last feasible point to the side constraints are calculated and the smallest positive distance is taken, giving a point lying on the nearest side constraint.

2.12 STRESS CONSTRAINT VIOLATION

When a behaviour constraint is violated, a series of linear interpolations are used to converge to a boundary point on a stress constraint surface (to within a given tolerance). Due to their linearity, the side constraints are never violated during the interpolations. The interpolations are always between a feasible and non-feasible design (i.e. a design violating the yield condition).

2.13 BOUNDARY POINT ON A STRESS CONSTRAINT

Suppose the design lies on a behaviour constraint. An alternate step design is sought which preserves the weight constant. Since the synthesis either reduces the weight or holds it constant, it is not possible for the iterations to diverge away from the desired minimum. The direction cosines of the direction of bounce can be determined using either random methods or more selective methods. The random methods are based on the method of alternate base planes described in Chapter 1 and in reference [70]. A random number generator is used to select the directions. The intersection of the directions with the constant weight contour are found and tested as trial designs. If any one of these designs is feasible, steepest descent motion continues as before until a constraint is encountered again. The selective methods utilise the physics of the problem to indicate more systematic directions of search.

Let the current boundary point be given by

$$\underline{x} = (b_3, \ldots, b_{m-2}, a_2) \tag{2.41}$$

and the corresponding behaviour functions by

$$BF(\underline{x}) = (\sigma_{r_1}, \sigma_{r_2}, \ldots\ldots, \sigma_{r_n}) \tag{2.42}$$

where the stresses are evaluated at radii $(r_1, \ldots, r_n)$

The proposed alternate step design is defined by

$$\bar{\underline{x}} = \underline{x} + \Delta\underline{\lambda} \tag{2.43}$$

where

$$\left.\begin{aligned} \underline{\lambda} &= (\lambda_1, \ldots, \lambda_{m-4}, \lambda_{m-3}) \\ \Delta &= \text{step length} \end{aligned}\right\} \tag{2.44}$$

The constant weight condition gives

$$W(\underline{x}) = W(\underline{x} + \Delta\underline{\lambda}) \tag{2.45}$$

From (2.36) condition (2.45) gives, on simplification

$$\lambda_1\lambda_{m-3}^2\,\Delta^3 - \lambda_{m-3}\Big[(b_1-b_3)\lambda_{m-3} - (a_3+2a_2)\lambda_1\Big]\Delta^2 - \Big[\sum_{j=3}^{m-2}(a_{j+1} - a_{j-1})$$

$$\times\,(a_{j+1} + a_j + a_{j-1})\lambda_{j-2} + (b_1-b_3)(a_3+2a_2)\lambda_{m-3}\Big]\Delta = 0$$

There is a common factor of Δ, indicating a zero root. This is reasonable because $\Delta = 0$ corresponds to $\underline{x}$ which is on the constant weight contour. Therefore

$$\lambda_1\lambda_{m-3}^2\ \Delta^2 - \lambda_{m-3}\Big[(b_1-b_3)\lambda_{m-3} - (a_3+2a_2)\lambda_1\Big]\Delta - \Big[\sum_{j=3}^{m-2}(a_{j+1} - a_{j-1})$$

$$\times\ (a_{j+1} + a_j + a_{j-1})\lambda_{j-2} + (b_1-b_3)(a_3+2a_2)\lambda_{m-3}\Big] = 0 \qquad (2.46)$$

2.14 RANDOM SEARCH

This is the method of alternate base planes described in Chapter 1 and [70]. The directions of search are defined by

$$\left.\begin{aligned} \lambda_1 &= 0 \\ \lambda_j &= \frac{R_j}{N} \qquad j = 2, \ldots, (m-3) \end{aligned}\right\} \qquad (2.47)$$

where R_j are random numbers and the normalisation factor N is defined by

$$N = \left(\sum_{j\neq 1} R_j^2\right)^{\frac{1}{2}}$$

Therefore the distances to the side constraints are given by

$$t_j = \frac{b_j - \varepsilon}{-\lambda_{j-2}} \qquad j = 3, \ldots, (m-2)$$

$$t_1 = \frac{(a_2 - L)}{-\lambda_{m-3}}$$

$$t_2 = \frac{(U - a_2)}{\lambda_{m-3}}$$

$$\text{Let} \quad \Delta_1 = \underset{1 \leq j \leq m-2}{\text{minimum}} \, (t_j; \; t_j > 0)$$

$$\Delta_2 = \underset{1 \leq j \leq m-2}{\text{maximum}} \, (t_j; \; t_j < 0)$$

$$\left.\begin{aligned} \text{Define} \quad \Delta_r &= R_r \Delta_1 \qquad & r = 1,2,3 \\ &= R_r \Delta_2 \qquad & r = 4,5,6 \end{aligned}\right\} \tag{2.48}$$

where $0 < R_r < 1$; $\qquad r = 1, \ldots 6$

The constant weight equation (2.46) is used to recalculate λ_1 where $(\lambda_2, \ldots, \lambda_{m-4}, \lambda_{m-3})$ are given by (2.47)

$$\text{Consider} \quad \underline{x}^{(r)} = \underline{x} + \Delta_r \underline{\lambda} \tag{2.49}$$

where

$$\underline{x}^{(r)} = (b_3 + \Delta_r \lambda_1, \; b_4 + \Delta_r \lambda_2, \; \ldots, \; b_{m-2} + \Delta_r \lambda_{m-4}, \; a_2 + \Delta_r \lambda_{m-3})$$

The points (2.49) are tested against the design constraints and if any one of these is feasible steepest descent motion proceeds as before until a constraint is encountered. If none of these six designs is feasible the base plane is changed (i.e. $\lambda_2 = 0$, $\lambda_j = \frac{R_j}{N}$ for $j \neq 2$), and a new set of proposed designs is generated. This process is continued until a feasible design is obtained or the current boundary point is accepted as the proposed optimum.

2.15 SELECTOR METHOD I

This was the first attempt at using the physics of the problem for bouncing back into the feasible regions. For a prescribed set of direction cosines λ_j equation (2.46) is a quadratic for the step length Δ. The direction of bounce, $\underline{\lambda}$, is as follows.

Let

$$\sigma_{r_q} = \sigma_o \qquad q = 2, \ldots, n-1$$

where

$$a_{j-1} \leq r_q \leq a_j \qquad \text{for some } j \in [3, m-1]$$

Define

$$\sigma_{a_\ell} = \max(\sigma_{a_{j-1}}, \sigma_{a_j})$$

The direction ratios are defined by

$$\left.\begin{aligned} \lambda_j &= (\sigma_{a_j} - \sigma_o) \qquad j \neq \ell \\ &= \frac{\partial W}{\partial b_\ell}(x) \Big/ |\nabla W(x)| \qquad j = \ell \\ \text{where} \\ \lambda_\ell &> 0; \quad \lambda_j < 0 \qquad j \neq \ell \end{aligned}\right\}$$

Therefore the direction cosines are given by

$$\left.\begin{aligned} \lambda_j &= (\sigma_{a_j} - \sigma_o) \Big/ N \\ \lambda_\ell &= \frac{\partial W}{\partial_{a_\ell}}(x) \Big/ |\nabla W(x)| \end{aligned}\right\} \qquad (2.50)$$

where the normalisation factor is given by

$$\lambda_\ell^2 + \sum_{j\neq\ell} \left(\frac{\sigma_{a_j} - \sigma_o}{N}\right)^2 = 1$$

$$N^2 = \sum_{j\neq\ell} \left(\sigma_{a_j} - \sigma_o\right)^2 \Big/ \left(1 - \lambda_\ell^2\right)$$

Therefore Δ can now be calculated using equation (2.46). The method of alternate base planes consumed considerable computer time in searching through the random directions to find a feasible point on the weight contour. Selector I reduces the degree of randomness by examining only those directions which on physical considerations tend to move away from a behaviour constraint. The disadvantages of the method are possibilities of (a) complex roots for the quadratic in Δ, (b) negative Δ, (c) violation of side (and behaviour) constraints.

2.16 SELECTOR METHOD II

This is a more selective version designed to overcome the above difficulties. Consider a step length Δ defined by

$$\Delta = \min_i (x_i - \ell_i, u_i - x_i) \tag{2.51}$$

From (2.22) this corresponds to an alternate step within the design variable bounds

$$\underline{\ell} \leqslant \underline{\bar{x}} \leqslant \underline{u} \tag{2.52}$$

For a given step length (2.51) the constant weight equation (2.46) can be viewed as a condition on the direction of bounce $\underline{\lambda}$. This must also satisfy the normalisation condition

$$\sum_{i=1}^{m-3} \lambda_i^2 = 1 \tag{2.53}$$

This gives two equations for (m-3) unknowns giving an infinity of solutions for λ_j. To obtain determinate solutions the number of variables is reduced to two by assigning prescribed values to (m-5) components of $\underline{\lambda}$, these being made zero to obtain real solutions enabling an alternate step to be taken.

The side constraints are linear and it is therefore possible to determine easily a step length Δ which will ensure that the side constraints are never violated. However it is not possible to ensure beforehand that the yield criterion is not violated, as the behaviour surfaces are unknown. Hence an alternate step design can be found which lies on the same weight contour and lying within the design variable bounds. The design is tested against the yield criterion and, if satisfactory, steepest descent motion continues as before. If the design is not satisfactory the step length is progressively reduced by specified amounts, and if no feasible point is forthcoming, a different combination of the direction cosines is set to zero, and hence a different direction of search is propagated. If the yield criterion is still violated, the above method is discontinued and a random search is made to locate possible alternate step designs. In practice, Selector II always worked and therefore there was no necessity to use a random search. Random methods consume computer time in searching through the random directions to find a line which would yield a feasible point on the same weight contour.

However, the method suggested above reduces the degree of randomness and searches only for designs lying within the design variable bounds. Therefore the method is more selective in its directions and was found to be very efficient.

2.17 CONSTRAINED STEEPEST DESCENT MOTION

This corresponds to motion along a side constraint. The boundary iterations are given by a simplified version of Rosen's gradient projection method for linear constraints [89].

2.18 RESULTS AND DISCUSSION

The following problems are considered by way of illustration.

Case (1): A standard turbine disc idealisation characterised by a four-dimensional design space. (m = 7)

Case (2): An arbitrary design configuration to study the possibilities of relative minima due to the absence of convexity conditions. The problem again being characterised by a four-dimensional design space. (m = 7)

Case (3): A standard disc characterised by an eleven-dimensional design space (m = 14). This corresponds to case (1) with a finer grid system to study the stability aspects of the synthesis. This provides a scientific aid for assessing the practical utilisation of the various synthesis capabilities developed here.

Case (4): Synthesis based on the proposed optimal for case (1) with a larger number of grid points. This again corresponds to an eleven-dimensional design space (m = 14).

Cases (1,2,3) are exploited in two sets of subcases labelled (a,b) corresponding to random and Selector II search procedures respectively from a behaviour constraint. Case (4) was run using Selector II only due to time constraints.

The synthesis programs are capable of handling thermal stress computations and multiple load conditions due to centrifugal load factors on the turbine blades. The computations were performed on an English Electric KDF9 computer using Algol. The initial and final designs are shown in Figures (2.5-2.17). Some of the essential features of the synthesis are summarised below. Selector I proved unsuccessful because the quadratic equation for calculating the step length in constant weight bounce gave complex roots. When real roots were forthcoming the synthesis generated designs violating the side constraints. Selector II, however, proved extremely successful. The synthesis starts from afeasible trial design. Initially, the boundary points are not highly constrained. In the initial phases, an alternate step mode of redesign encounters relatively few design constraints in attempting to move from a boundary design. As the synthesis proceeds, the designs become more highly constrained with a correspondingly reduced wedge of acceptability. The average number of redesign attempts associated with each successful redesign tends to increase as the synthesis progresses. However, in the initial stages, Selector I located a feasible design at the first attempt and even in the later stages a successful design was obtained after 1 or 2 attempts. In contrast, the random procedures deteriorated sharply as the synthesis progressed. Both procedures, after a certain stage, gave weight reductions which were negligible in comparison to the time invested. This means that the evaluation of a synthesis capability for large scale systems must be based on effective convergence rather than on total or complete convergence. The results presented here represent a compromise with total convergence.

Selector II exhibited very rapid initial convergence rates and stable characteristics. In contradistinction, random search was less rapid and consumed considerable computer time in searching through the random directions for a feasible point. In addition, the effectiveness of random techniques decrease for high order design spaces.

As regards relative minima, in the absence of convexity conditions there are no known mathematical procedures to provide guidelines. What is possible is to establish a satisfactory degree of confidence in the results using, in part, engineering judgement, experience and intuition. This confidence can be established by subjecting the constant weight contour corresponding to the proposed optimal to close scrutiny. If no feasible designs are forthcoming then, in most cases, the design will be optimal. In practice, such an exhaustive search procedure would be impossible in terms of computer time. An alternate procedure is to run the synthesis from distinct points. If the synthesis converges to designs of similar configuration and weight, confidence is established in the results.

The final designs for case (2) are similar to the designs for cases (1,3,4).

Case (i)	DIMENSION OF DESIGN SPACE (m - 3)	INITIAL WEIGHT (lbs)	FINAL WEIGHT (lbs)		NUMBER OF ITERATIONS		RUN TIME (mins)	
			Case (ia)	Case (ib)	Case (ia)	Case (ib)	Case (ia)	Case (ib)
1	4	3.58934×10^3	1.66187×10^3	2.25877×10^3	62	80	5	7.8
2	4	3.60248×10^3	1.64547×10^3	2.32714×10^3	74	40	5	4.9
3	11	3.58973×10^3	1.61401×10^3	2.14537×10^3	186	408	30	60
4	11	1.65165×10^3	1.03400×10^3	-	188	-	30	-

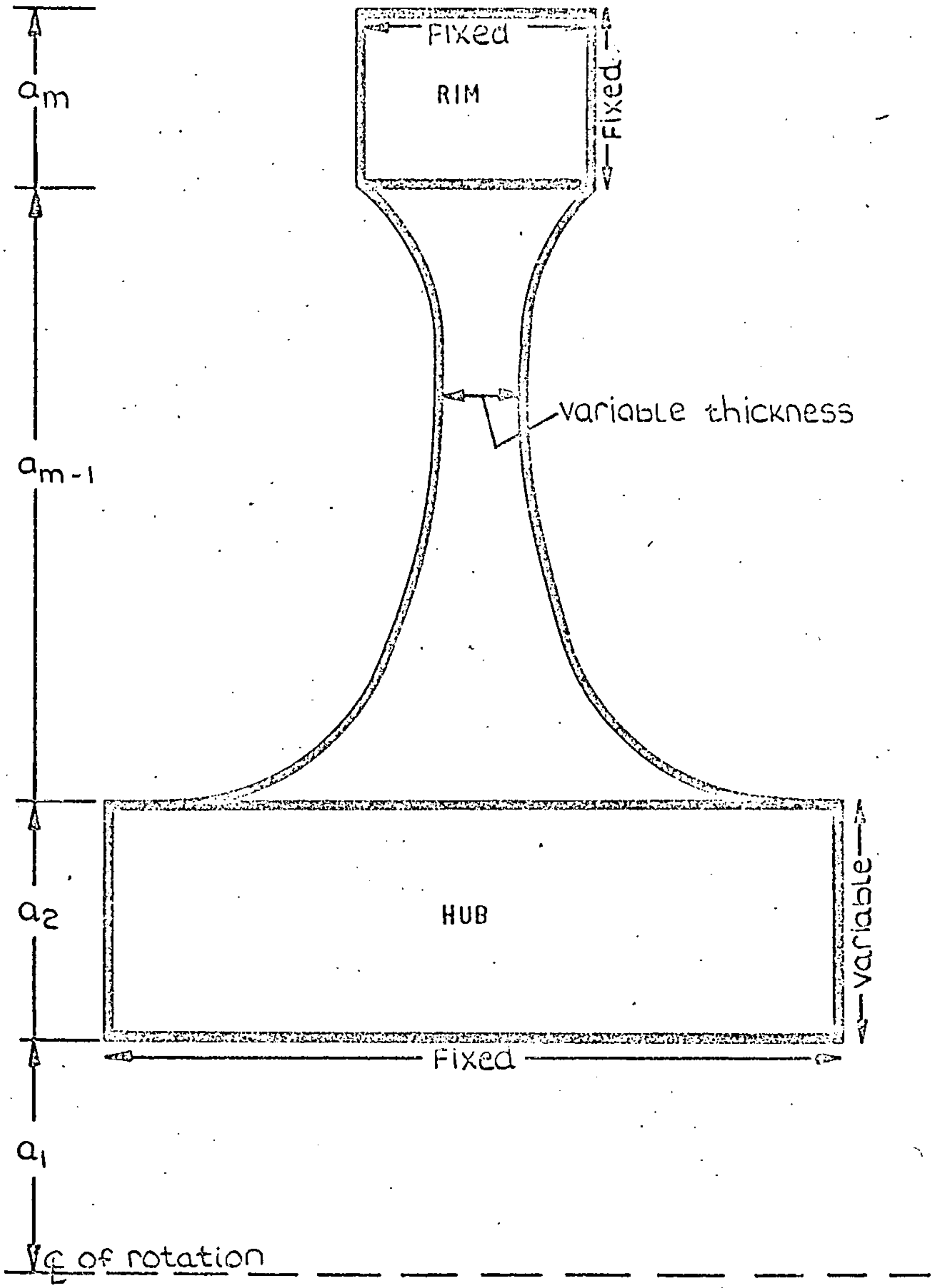

CROSS SECTION OF TYPICAL TURBINE DISC.

FIG. 2.1

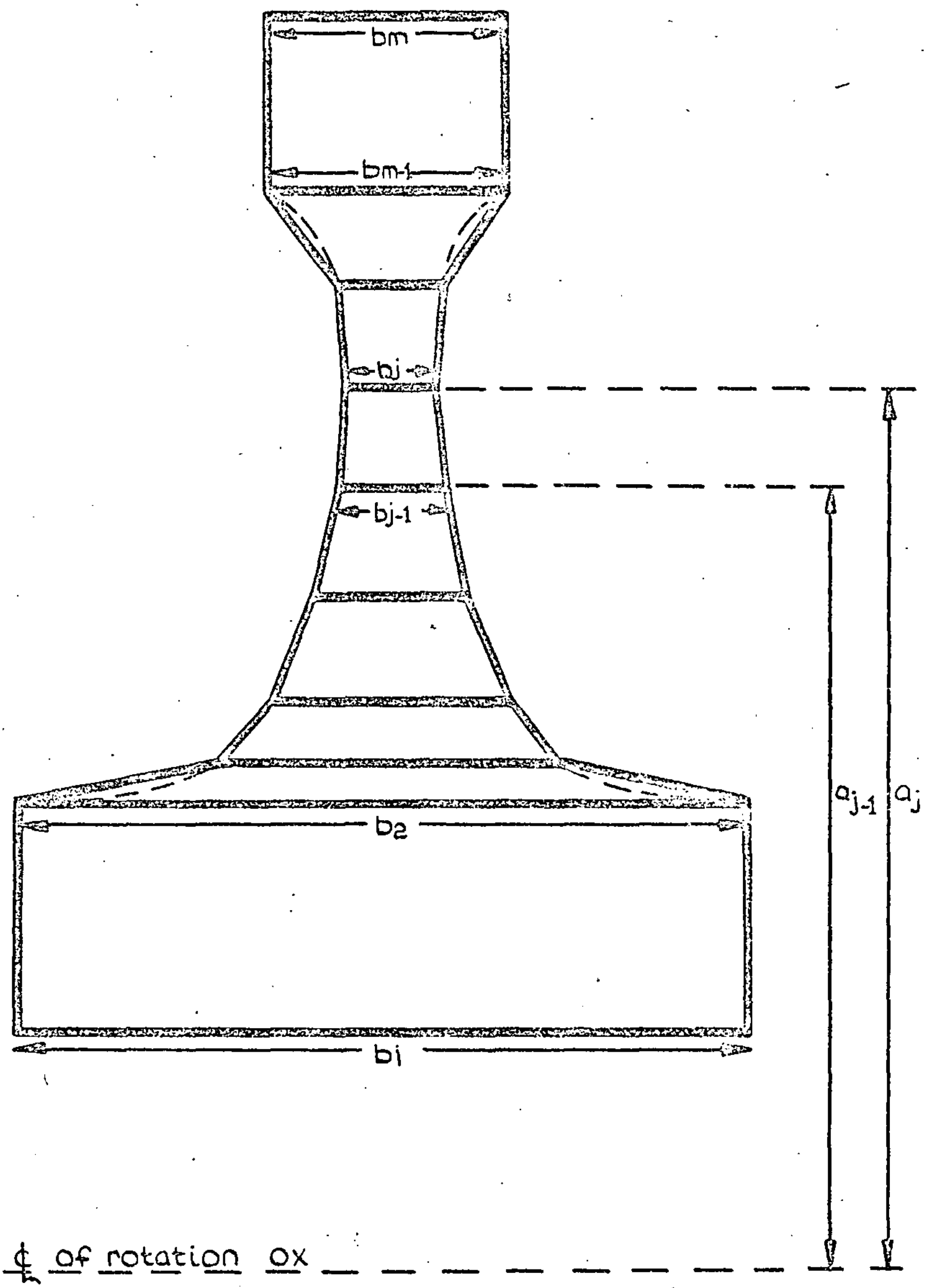

CROSS SECTION OF EQUIVALENT CIRCULAR DISC.

FIG. 2.2

CROSS SECTION OF DISC BOUNDED BY RADII (a_{j-1} a_j)

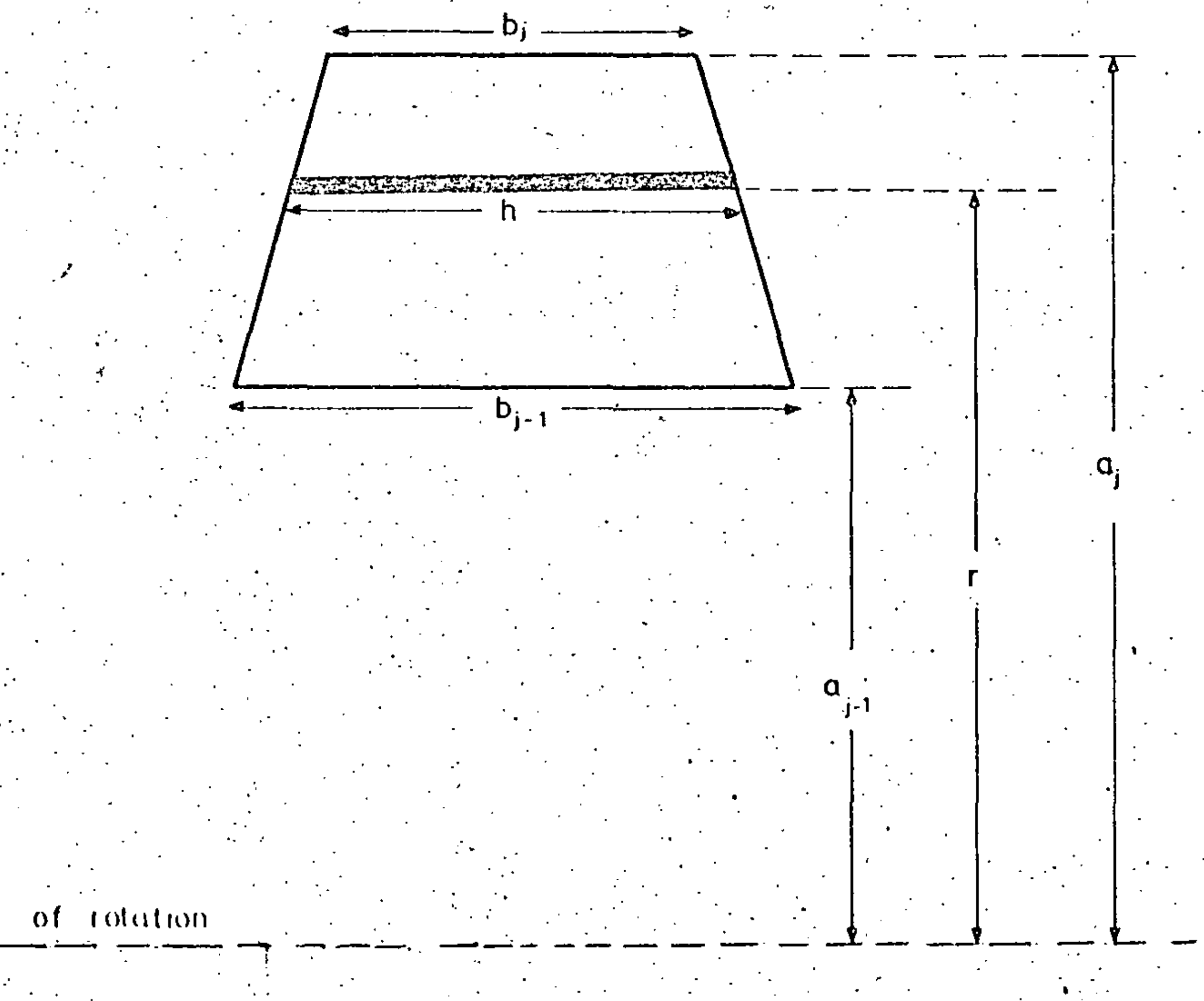

Fig 2.3

FLOW DIAGRAM FOR STRUCTURAL SYNTHESIS BASED ON A STRESS CONSTRAINT

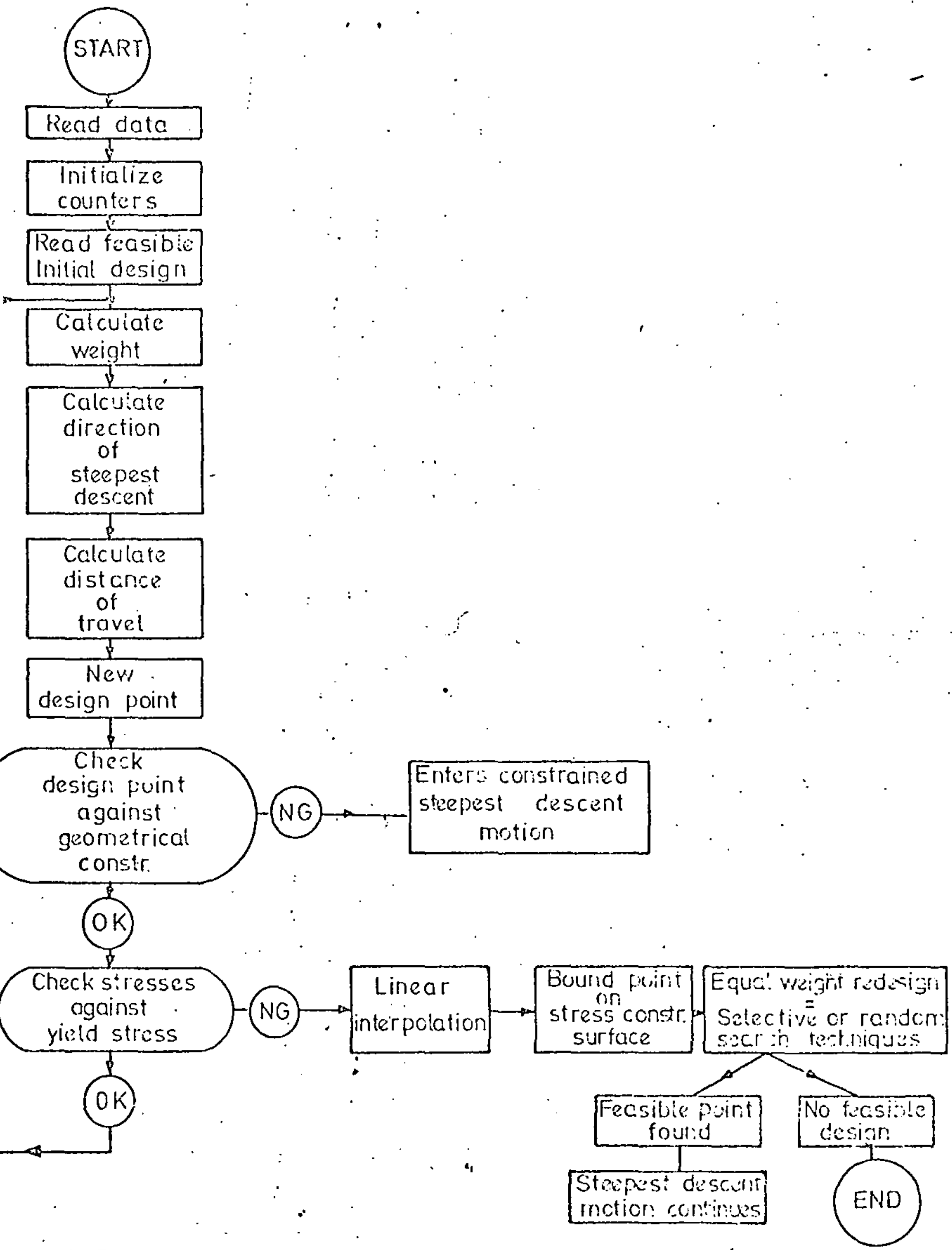

Fig 2.4

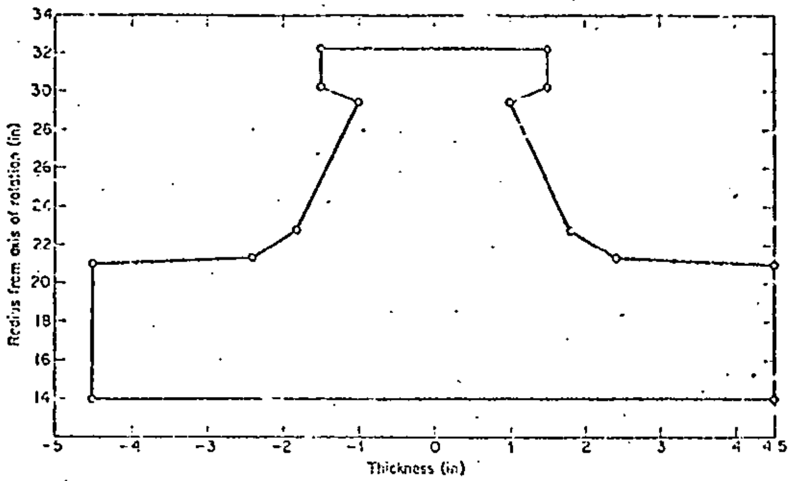

Cases 1a, 1b. Initial design. Weight = $3{\cdot}58934 \times 10^3$ lb.

Fig 2.5

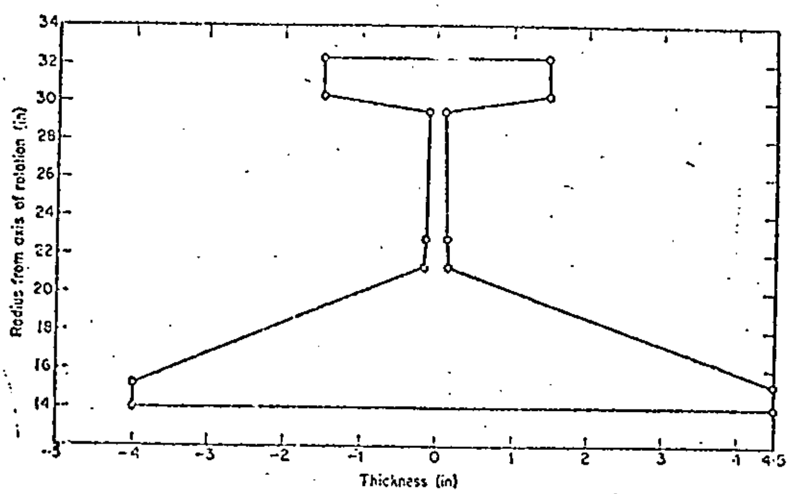

Case 1a; 62 cycles. Final design. Weight = $1{\cdot}66187 \times 10^3$ lb.

Fig 2.6

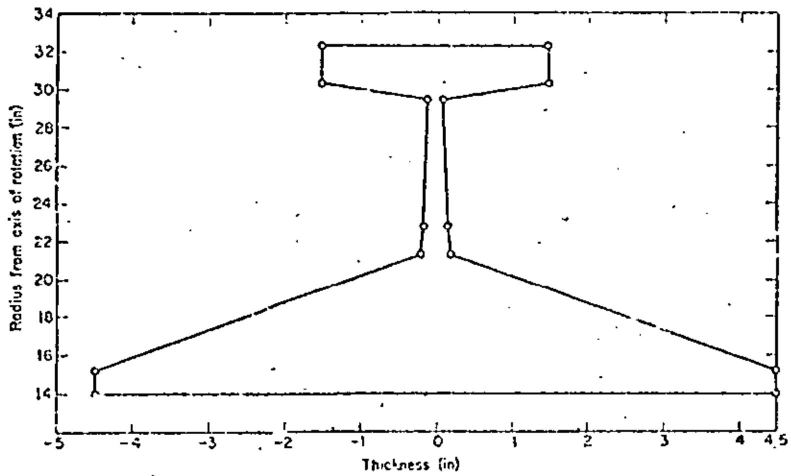

Fig. 2.7

Case 1b; 80 cycles. Final design. Weight = 2·25877×10³ lb.

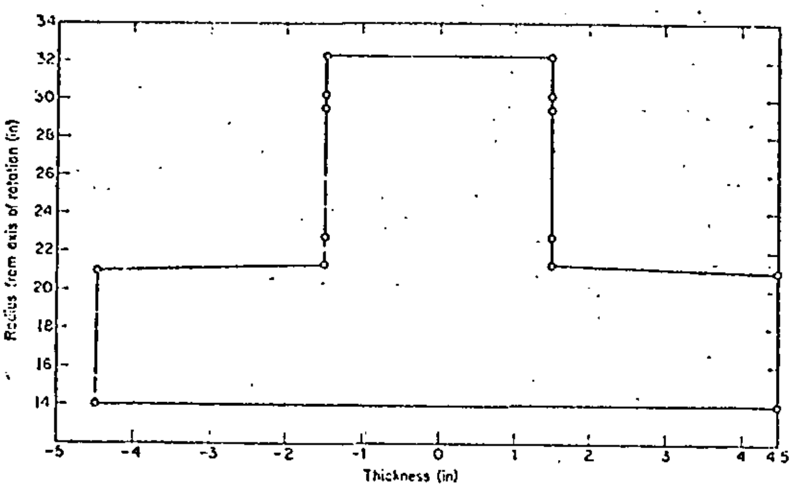

Fig. 2.8

Cases 2a, 2b. Initial design. Weight = 3·60248×10³ lb.

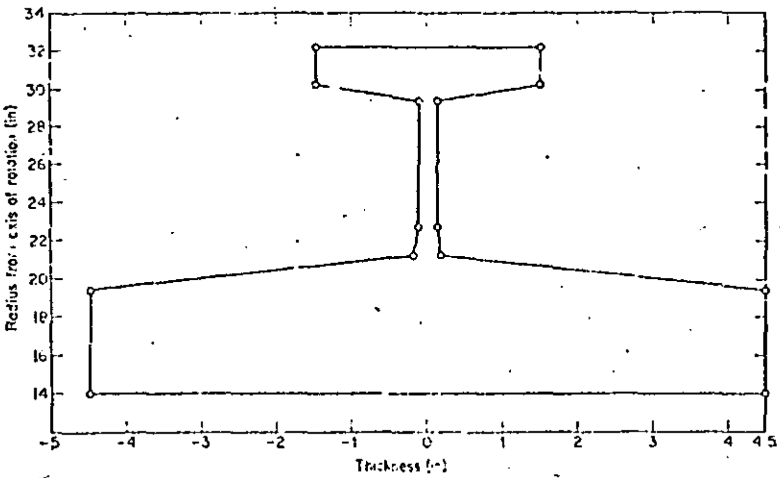

Case 2a: 74 cycles. Final design. Weight = $1{\cdot}64547 \times 10^3$ lb.

Fig. 2.9

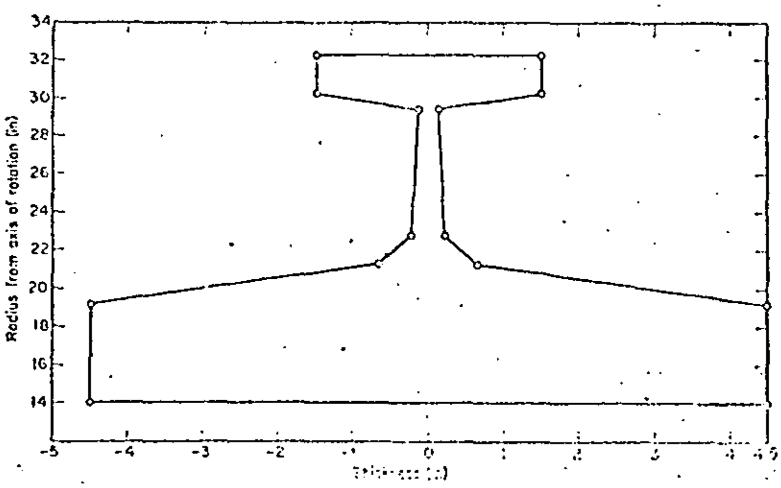

Case 2b: 40 cycles. Final design. Weight = $2{\cdot}32714 \times 10^3$ lb.

Fig. 2.10

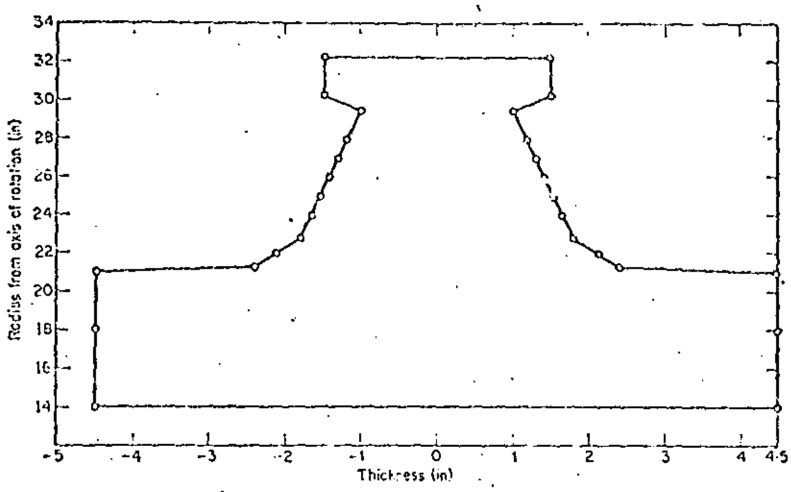

Cases 3a, 3b. Initial design. Weight = 3·58973 × 10³ lb.

Fig. 2.11

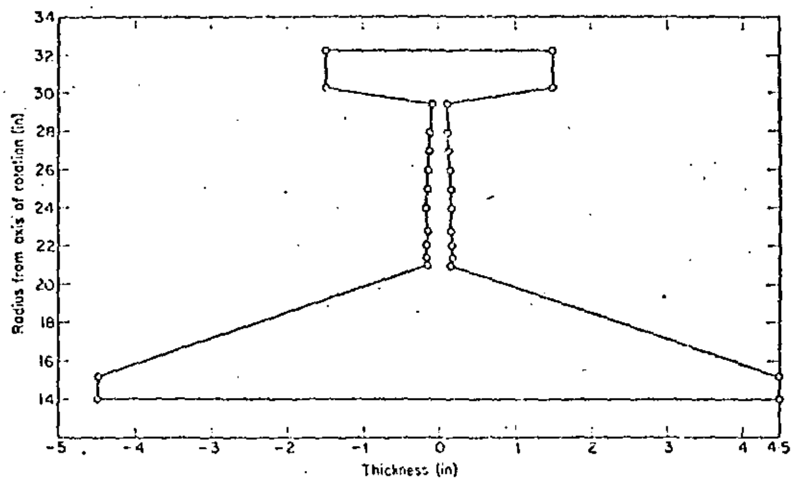

Case 3a; 106 cycles. Final design. Weight = 1·61401 × 10³ lb·

Fig. 2.12

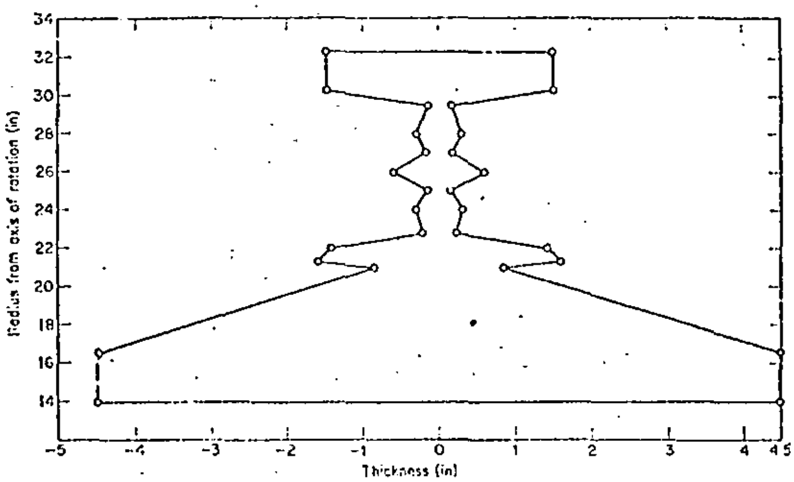

Case 3b. Final design. Weight = $2{\cdot}14537 \times 10^3$ lb.

Fig. 2.13

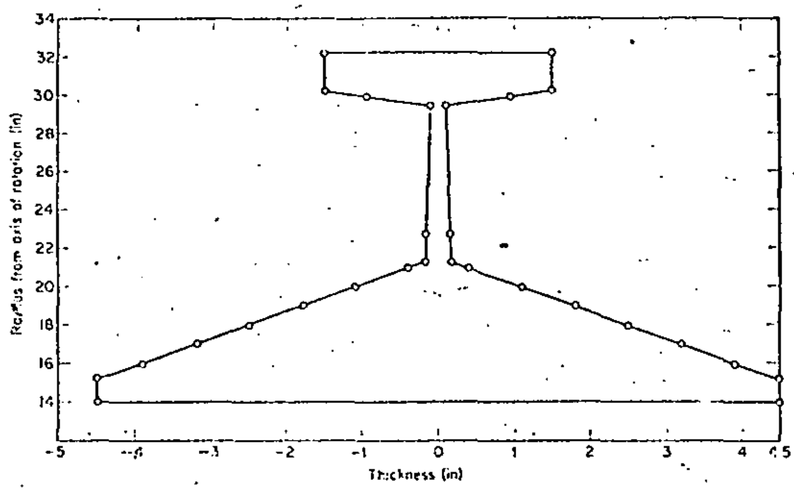

Case 4. Initial design. Weight = $1{\cdot}65165 \times 10^3$ lb.

Fig. 2.14

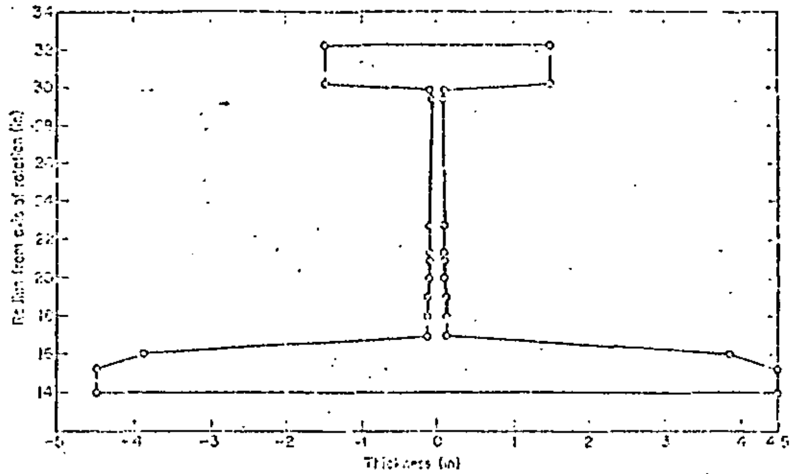

Case 4; 188 cycles. Final design. Weight = 1·03400 × 10³ lb.

Fig. 2.15

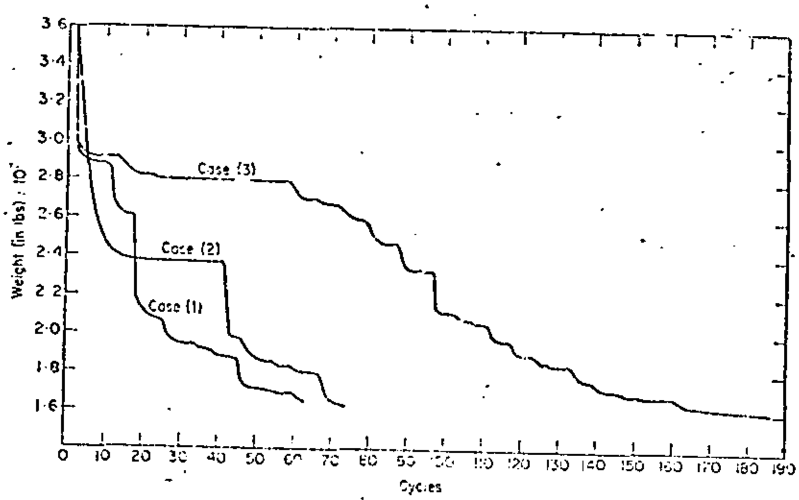

Weight *versus* total redesign attempts. Based on selective search techniques for moving away from a bound point.

Fig. 2.16

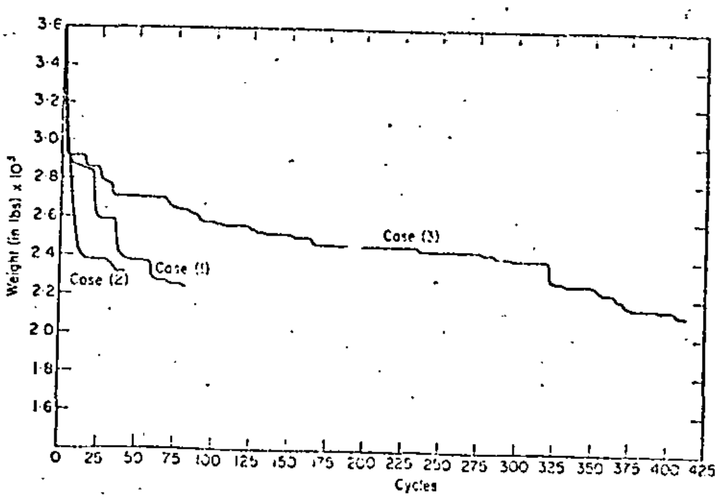

Weight *versus* total redesign attempts. Based on random search.

Fig. 2.17

CHAPTER 3

MINIMUM WEIGHT DESIGN OF DISCS BASED ON A VIBRATION CONSTRAINT

3.1 INTRODUCTION

In Chapter 2, computational procedures based on the methods of non-linear programming were successfully developed for minimising the weight of an axi-symmetric disc of variable thickness subject to specified behaviour and side constraints. For purposes of simplicity in this initial investigation, the behaviour constraints were restricted to a consideration that the stresses should be below the yield stress while the side constraints imposed restrictions on the dimensions and tolerances of the disc. The problem was formulated analytically as a very general optimal control problem. Solutions were obtained by transforming the variational formulation into a non-linear programming formulation by approximating the disc by a discrete model using a piecewise linear representation for the thickness variable. Stability of the solutions was established by subjecting the thickness profile to different representations.

The stresses for the non-linear program were functionals which associated with every point in design space a stress matrix, the columns corresponding to specified loading conditions. The stresses were defined by a set of computer oriented rules which were represented by a "black box" into which were put the design parameters specifying a given design configuration and out of which comes the corresponding stress distributions which were checked against the stress constraints. The associated synthesis procedures were characterised by:

(a) accelerated steepest descent motion in the feasible regions,

(b) constrained steepest descent motion along a known constraint,

(c) constant weight bounce from an unknown constraint.

In the present investigation, these procedures are further generalised and used to synthesise the disc using a dynamics technology in the absence of any statical constraints, whereby the lowest natural frequency of vibration should exceed a specified resonance frequency.

The frequency is again a functional which associates with every point in design space a set of fundamental vibrational frequencies and has a "black box" type representation. The frequency calculations are performed inside the box and the redesign procedures are based entirely on the output - a set of numbers giving the fundamental frequencies at each design iteration. These procedures are independent of the analysis employed and are applicable to problems in conjunction with analysis programs already available. Alternatively, the mechanisms inside the box may be utilised [85,87,93,96] to generate the directions of search in design space. However, the need for refined analysis routines for performing more effective redesign cycles can be more readily assessed after the initial results have been evaluated using existing programs.

The numerical computations were performed on a KDF9 computer giving weight reductions of 56% and 28% for resonance frequencies of 440 and 2000 cycles per second respectively using a turbine disc idealisation. A discussion of these results is included together with a description of some instabilities in the synthesis procedures used arising from the absence of any stress constraints on the problem.

3.2 CONTINUOUS VARIATIONAL FORMULATION

As before the weight is given by

$$W[h] = \int_{a_1}^{a_m} 2\pi\rho r h(r)dr \qquad (3.1)$$

The small deflection motion of a thin disc in polar co-ordinates is given by [175].

$$\left.\begin{aligned}
&\rho h \frac{\partial^2 u}{\partial t^2} - \frac{1}{r}\frac{\partial}{\partial r}(rQ_r) - \frac{1}{r}\frac{\partial Q_\theta}{\partial \theta} = 0 \\
&\frac{1}{r}\frac{\partial}{\partial r}(rM_r) - \frac{M_\theta}{r} - \frac{1}{r}\frac{\partial M_{r\theta}}{\partial \theta} - Q_r = 0 \\
&\frac{1}{r}\frac{\partial M_\theta}{\partial \theta} - \frac{M_{r\theta}}{r} - \frac{1}{r}\frac{\partial}{\partial r}(rM_{r\theta}) - Q_\theta = 0
\end{aligned}\right\} \qquad (3.2)$$

where

$M_r, M_\theta, M_{r\theta}$ = bending moments

Q_r, Q_θ = shear forces

$u(r,\theta,t)$ = axial displacement at time t of section whose initial coordinates are r, θ.

Eliminating Q_r, Q_θ from (3.2)

$$\frac{1}{r}\frac{\partial^2}{\partial r^2}(rM_r) + \left(\frac{1}{r^2}\frac{\partial^2}{\partial \theta^2} - \frac{1}{r}\frac{\partial}{\partial r}\right)M_\theta - \frac{2}{r}\left(\frac{\partial^2}{\partial r\partial\theta} + \frac{1}{r}\frac{\partial}{\partial \theta}\right)M_{r\theta} = \rho h\frac{\partial^2 u}{\partial t^2} \qquad (3.3)$$

where

$$\left.\begin{aligned}
M_r &= -\frac{Eh^3(r)}{12(1-\nu^2)}\left[\frac{\partial^2 u}{\partial r^2} + \nu\left(\frac{1}{r}\frac{\partial u}{\partial r} + \frac{1}{r^2}\frac{\partial^2 u}{\partial \theta^2}\right)\right] \\
M_\theta &= -\frac{Eh^3(r)}{12(1-\nu^2)}\left[\nu\frac{\partial^2 u}{\partial r^2} + \left(\frac{1}{r}\frac{\partial u}{\partial r} + \frac{1}{r^2}\frac{\partial^2 u}{\partial \theta^2}\right)\right] \\
M_{r\theta} &= \frac{Eh^3(r)}{12(1+\nu)}\left[\frac{1}{r}\frac{\partial^2 u}{\partial r \partial \theta} - \frac{1}{r^2}\frac{\partial u}{\partial \theta}\right]
\end{aligned}\right\} \tag{3.4}$$

E is Young's modulus and ν Poisson's ratio for the material.

Consider solutions harmonically dependent on both θ and t

$$u = W(r)\sin(n\theta + pt) \tag{3.5}$$

where

n = number of nodal diameters round the disc

p = frequency of vibration

Substituting (3.4, 3.5) in (3.3) gives on simplification

$$\frac{d^4W}{dr^4} + 2\left(\frac{3}{h}\frac{dh}{dr} + \frac{1}{r}\right)\frac{d^3W}{dr^3} + \left[\frac{3}{h}\frac{d^2h}{dr^2} + \frac{6+3\nu}{hr}\frac{dh}{dr} + \frac{6}{h^2}\left(\frac{dh}{dr}\right)^2 - \frac{2n^2+1}{r^2}\right]\frac{d^2W}{dr^2}$$

$$+ \left[\frac{3\nu}{hr}\frac{d^2h}{dr^2} - \frac{6n^2+3}{hr^2}\frac{dh}{dr} + \frac{6\nu}{h^2 r}\left(\frac{dh}{dr}\right)^2 + \frac{2n^2+1}{r^3}\right]\frac{dW}{dr} - n^2\left[\frac{3\nu}{hr^2}\frac{d^2h}{dr^2} -\right.$$

$$\left.\frac{9}{hr^3}\frac{dh}{dr} + \frac{6\nu}{h^2r^2}\left(\frac{dh}{dr}\right)^2 + \frac{4-n^2}{r^4}\right]W = \frac{12(1-\nu^2)\rho p^2 W}{Eh^2} \tag{3.6}$$

Introducing the transformations

$$\left.\begin{aligned}
x_i &= \frac{d^{(i-1)}W}{dr^{(i-1)}}, \qquad i = 1,2,3,4 \\
x_{i+4} &= \frac{d^{(i-1)}h}{dr^{(i-1)}}, \qquad i = 1,2 \\
u &= \frac{d^2h}{dr^2}
\end{aligned}\right\} \tag{3.7}$$

Equation (3.6) reduces to

$$\left.\begin{aligned}
\frac{dx_i}{dr} &= x_{i+1}, \quad i=1,2,3 \\
\frac{dx_4}{dr} &= \left[\frac{12(1-\nu^2)\rho p^2}{Ex_5^2} + \frac{3n^2\nu}{x_5 r^2}u - \frac{9n^2}{x_5 r^3}x_6 + \frac{6n^2\nu}{x_5^2 r^2}x_6^2 - \frac{n^2(n^2-4)}{r^4}\right]x_1 \\
&\quad - \left[\frac{3\nu}{x_5 r}u - \frac{6n^2+3}{x_5 r^2}x_6 + \frac{6\nu x_6^2}{x_5^2 r} + \frac{2n^2+1}{r^3}\right]x_2 \\
&\quad - \left[\frac{3u}{x_5} + \frac{6+3\nu}{x_5 r}x_6 + \frac{6x_6^2}{x_5^2} - \frac{2n^2+1}{r^2}\right]x_3 - 2\left(\frac{3x_6}{x_5} + \frac{1}{r}\right)x_4 \\
\frac{dx_5}{dr} &= x_6 \\
\frac{dx_6}{dr} &= u
\end{aligned}\right\} \quad (3.8)$$

The inner edge of the disc is clamped while the outer edge is free, so that the associated boundary conditions are given by

$$u = \frac{\partial u}{\partial r} = 0$$

at the clamped edge $r = a_1$ and (with h = constant, see Figure 2.1)

$$\left.\begin{aligned}
M_r &\equiv \frac{\partial^2 u}{\partial r^2} + \nu\left(\frac{1}{r}\frac{\partial u}{\partial r} + \frac{1}{r^2}\frac{\partial^2 u}{\partial \theta}\right) = 0 \\
Q_r - \frac{1}{r}\frac{\partial M_{r\theta}}{\partial \theta} &\equiv \frac{\partial}{\partial r}\left(\frac{\partial^2 u}{\partial r^2} + \frac{1}{r}\frac{\partial u}{\partial r} + \frac{1}{r^2}\frac{\partial^2 u}{\partial \theta^2}\right) + \frac{(1-\nu)}{r^2}\frac{\partial^2}{\partial \theta^2}\left(\frac{\partial u}{\partial r} - \frac{u}{r}\right) = 0
\end{aligned}\right\} \text{at the free edge } r = a_m$$

From (3.2, 3.5, 3.7) these reduce to

$$\left.\begin{aligned}
&x_1(a_1) = x_2(a_1) = 0 \\
&x_3(a_m) + \nu\left[\frac{x_2(a_m)}{a_m} - n^2\,\frac{x_1(a_m)}{a_m^2}\right] = 0 \\
&x_4(a_m) + \frac{x_3(a_m)}{a_m} - \frac{x_2(a_m)}{a_m^2} - \frac{n^2}{a_m^2}\,x_2(a_m) + \frac{2n^2 x_1(a_m)}{a_m^3} + \\
&\qquad + \frac{n^2(1-\nu)}{a_m^2}\left[x_2(a_m) - \frac{x_1(a_m)}{a_m}\right] = 0
\end{aligned}\right\} \qquad (3.9)$$

This problem has been formulated as a problem in optimal control theory where $x_i(r)$, $i = 1,2,\ldots,6$ are the state variables, $u(r)$ is the control variable and p is a control parameter. The optimal control aspects of this problem are discussed further in Chapters 4 and 6.

Therefore the merit functional becomes

$$W = \int_{a_1}^{a_m} 2\pi\rho r x_5(r)\,dr \qquad (3.10)$$

Since from (3.7) $h(r) = x_5(r)$. Conditions (3.9) correspond to the transversality conditions.

3.3 NON-LINEAR PROGRAMMING FORMULATION

For purposes of numerical computations, this continuous formulation is transformed into a discretised non-linear programming approximation using finite differences and is characterised by a "black box" type representation for the frequency.

The weight functional (3.1) is transformed as before [see equation (2.20) of Chapter 2] into a function of the design variables.

$$\left.\begin{array}{l} W[h] \rightarrow W(b_3, \ldots, b_{m-2}, a_2) \\ \text{where} \\ b_j \geq \varepsilon \qquad j = 3, \ldots, (m-2) \\ L \leq a_2 \leq U \\ \text{In addition the frequency satisfies the condition} \\ p \geq p_o \\ \text{where } p_o \text{ is the resonance frequency} \end{array}\right\} \qquad (3.11)$$

The equations of state and transversality (3.8, 3.9) are contained inside the "black box", together with the associated numerical procedures for solving these equations for a prescribed thickness $h(r)$ to determine the vibrational frequencies.

The design parameters representing a given design configuration are put into the "black box", out of which come the corresponding vibrational frequencies which are checked against the vibration constraints (3.11). The mechanisms inside the box include analysis routines for the frequency calculations which are based on an iterative solution of the differential equations of vibrations (3.6) using the Myklestad - Holzer matrix technique [176-178]. This consists essentially in approximating the disc by a series of massless circumferential strips of constant thickness.

Equation (3.6) thus reduces to

$$\frac{d^4W}{dr^4} + \frac{2}{r}\frac{d^3W}{dr^3} - \frac{2n^2+1}{r^2}\frac{d^2W}{dr^2} + \frac{2n^2+1}{r^3}\frac{dW}{dr} + \frac{n^2(n^2-4)}{r^4}W = 0$$

This is a fourth order homogeneous differential equation for which the solution is given by

$$W(r) = A_1r^n + A_2r^{-n} + A_3r^{2+n} + A_4r^{2-n} \qquad n \geq 2$$

where A_1, A_2, A_3, A_4 are constants of integration. These are then eliminated using matrix recurrence relations which enable the consideration of all possible combinations of boundary conditions. The method is relatively simple and was already programmed at the start of this investigation. The contents of the box are disregarded since the purpose of this investigation is to develop computational procedures for describing problems with non-analytic constraints.

Complete details of the analysis are given in de Silva [182,183]. A summarised version of this work is given below.

3.4 SYNTHESIS PROCEDURES

The synthesis procedures in the absence of any stress constraints are characterised by:

(a) steepest descent motion until a vibration constraint is encountered;

(b) constaint weight redesign at the resonance frequency

(c) design parameter bounds never violated.

The computer program (Figure 3.1) consists of moving from an initial feasible design in the direction of the gradient to a better design some finite distance away. This process is repeated until a vibration constraint is encountered which prevents further moves in the gradient direction. Then an alternate step is taken which is a move along the constant weight surface.

The step length in steepest descent mode of travel is determined using a simplified form of Rosen's gradient projection method in conjunction with the linear side constraints. This enables fairly large step lengths to be taken, thereby economising on computer time.

As the designs approach a vibration constraint surface, it is possible that the step lengths used in the steepest descent procedure are too large with the result that the design pierces the constraint surface and moves into a region of constraint violation where the vibrational frequencies of the designs are below the resonance frequency. If this is the case, a quadratic interpolation procedure is used to converge to a design at the resonance frequency by thickening up the variable sections of the disc. This gives a design point on the boundary of the vibration constraint which is a non-analytic surface due to the "black box" nature of the frequency, thereby precluding the use of standard methods of non-linear programming, such as moving along the constraint in a direction in which the weight decreases. Instead, an alternate step is taken along the constant weight surface, where the directions of search are based on either selective methods utilising the physics of the problem or random methods, and are summarised below:

(1) Selector I - Two design parameters are changed leaving the rest unchanged. All possible combinations are considered. (This is identical to Selector II of Chapter 2.)

(2) Selector II - A perturbation method using the Lagrangian energy density vector to estimate the normal to the vibration constraint. The analysis is based on the concept of efficiency coefficients [184, 185] in conjunction with Rayleigh's principle for relating small changes in frequency to small changes in design.

(3) Selector III - Three successive designs are used to estimate a new direction of search. This is used in case there are sharp ridges on the vibration constraint surface. This is essentially an extension of the "zigzag" procedure developed by Schmit and Fox [73].

(4) Random Methods - This is based on the method of alternate base planes described in Chapters 1 and 2.

Since the above search procedures with the exception of Selectors II and III were discussed in Chapter 2, the latter methods only are summarised below.

3.5 SELECTOR II

Rayleigh's principle [184,185] is used to alter the design to achieve changes in frequency. Consider small perturbations about a configuration of stable equilibrium. The kinetic and potential energies are given by [186].

$$\left.\begin{aligned} T &= \frac{1}{2} T_{ij}\, \dot{\eta}_i\, \dot{\eta}_j \\ V &= \frac{1}{2} V_{ij}\, \eta_i\, \eta_j \end{aligned}\right\} \tag{3.12}$$

where

η_i = deviations of the generalised coordinates from equilibrium

T_{ij}, V_{ij} = symmetric constants

The Lagrangian is defined by

$$L = \frac{1}{2}\left(T_{ij}\, \dot{\eta}_i\, \dot{\eta}_j - V_{ij}\, \eta_i\, \eta_j\right) \tag{3.13}$$

Therefore the equations of motion are given by Lagrange's equations

$$T_{ij}\, \ddot{\eta}_j + V_{ij}\, \eta_j = 0 \tag{3.14}$$

Consider the harmonic solutions

$$\eta_i = a_i \sin(pt + \varepsilon) \tag{3.15}$$

Substituting (3.15) in (3.14)

$$- p^2\, T_{ij}\, a_i\, a_j + V_{ij}\, a_i\, a_j = 0 \tag{3.16}$$

Consider small changes in T_{ij}, V_{ij}

$$- p^2 \delta T_{ij} a_i a_j - 2p \delta p T_{ij} a_i a_j + \delta V_{ij} a_i a_j = 0$$

Therefore from (3.12, 3.15, 3.16) this reduces to

$$\frac{\delta p}{p} = - \frac{\Delta T_{max} - \Delta V_{max}}{2V_{max}} \tag{3.17}$$

where

$$T_{max} = \frac{1}{2} p^2 T_{ij} a_i a_j$$

$$V_{max} = \frac{1}{2} V_{ij} a_i a_j$$

Equation (3.17) may be written in the alternative form

$$\delta p = \eta \delta m \tag{3.18}$$

where

δm = change in mass

η = efficiency coefficient.

The efficiency coefficient in turn is defined by

$$\eta = - \frac{p_o \ell}{2\rho V_{max}} \tag{3.19}$$

where

T_{max} = tdV

V_{max} = vdV

ℓ = t − v

t = kinetic energy density

v = potential energy density

ℓ = Lagrangian energy density

In general

$$\delta p = \sum_j \eta_j \delta m_j \tag{3.20}$$

where δm_1, δm_2, ..., are changes in mass at the variable sections of the disc

$$\left.\begin{aligned} \delta m_j &= \left(\frac{\partial W}{\partial b_{j+2}}\right)\Delta b_{j+2}, \qquad j = 1,2,\ldots, m-4 \\ \delta m_{m-3} &= \left(\frac{\partial W}{\partial a_2}\right)\Delta a_2 \end{aligned}\right\} \tag{3.21}$$

substituting (3.21) in (3.20)

$$\delta p = \sum_{j=1}^{m-4} \eta_j \frac{\partial W}{\partial b_{j+2}} \Delta b_{j+2} + \eta_{m-3} \frac{\partial W}{\partial a_2} \Delta a_2$$

$$= t \sum_{j=1}^{m-4} \lambda_j \eta_j \frac{\partial W}{\partial b_{j+2}} + t\lambda_{m-3} \eta_{m-3} \frac{\partial W}{\partial a_2} \tag{3.22}$$

In order to ensure $\delta p > 0$ the direction is defined by

$$\left.\begin{aligned} \lambda_j &= \eta_j \qquad j = 1,\ldots, m-4 \\ \lambda_{m-3} &= \eta_{m-3} \qquad \text{if } \frac{\partial W}{\partial a_2} > 0 \\ &= -\eta_{m-3} \qquad \text{if } \frac{\partial W}{\partial a_2} < 0 \end{aligned}\right\} \tag{3.23}$$

The step length is given by

$$t = \text{Min}\left\{\left[\underset{3 \leq j \leq m-2}{\text{Min}} (b_j - \varepsilon)\right], (a_2 - L), (U - a_2)\right\} \tag{3.24}$$

to ensure designs within the design parameter bounds.

The efficiency coefficients are calculated by considering the bending of the massless elastic circumferential plates of constant thickness used in the frequency calculation.

The strain energy is given by [187].

$$V = \iint \frac{Eh^3}{24(1-\nu^2)} \left\{ \left(\frac{\partial^2 u}{\partial r^2} + \frac{1}{r}\frac{\partial u}{\partial r} + \frac{1}{r^2}\frac{\partial^2 u}{\partial \theta^2} \right)^2 - 2(1-\nu)\left[\frac{\partial^2 u}{\partial r^2}\left(\frac{1}{r}\frac{\partial u}{\partial r} + \frac{1}{r^2}\frac{\partial^2 u}{\partial \theta^2} \right) \right.\right.$$

$$\left.\left. - \left(\frac{\partial}{\partial r}\frac{1}{r}\frac{\partial u}{\partial \theta} \right)^2 \right] \right\} r \, d\theta \, dr + \iint \rho \Omega^2 h r^2 u \frac{\partial u}{\partial r} \, dr \, d\theta \tag{3.25}$$

where

Ω = speed of rotation of the disc.

Substituting (3.5) in (3.25) and averaging over time gives for the strain energy density

$$v = \frac{Eh^2}{24(1-\nu^2)} \left\{ \left(\frac{d^2 W}{dr^2} + \frac{1}{r}\frac{dW}{dr} - \frac{n^2}{r^2} W \right)^2 - 2(1-\nu)\left[\frac{d^2 W}{dr^2}\left(\frac{1}{r}\frac{dW}{dr} - \frac{n^2}{r^2} W \right) \right.\right.$$

$$\left.\left. - \frac{n^2}{r^2}\left(\frac{dW}{dr} - \frac{W}{r} \right)^2 \right] \right\} + \rho \Omega^2 W r \frac{dW}{dr} \tag{3.26}$$

The deflection and slope W, $\frac{dW}{dr}$ respectively are given by the nodal shape matrix from which $\frac{d^2W}{dr^2}$ is calculated using finite differences.

The kinetic energy is given by

$$T = \iint \frac{1}{2} \rho h \left(\frac{\partial u}{\partial t} \right)^2 r \, dr \, d\theta \tag{3.27}$$

Substituting (3.5) in (3.27) and averaging over time gives

$$t = \frac{1}{2} \rho p_o^2 W^2 \tag{3.28}$$

Equations (3.26, 3.28) determine the strain and kinetic energey densities from which the direction ratios (3.23) may be computed. The direction of bounce is then obtained by projecting this direction onto the hyperplane defined by the intersection of

$$\left.\begin{aligned} W(b_3, \ldots, b_{m-2}, a_2) &= \text{constant} \\ a_2 &= \text{constant} \end{aligned}\right\} \qquad (3.29)$$

3.6 SELECTOR III

Consider three successive designs $\underline{x}^{(q-2)}$, $\underline{x}^{(q-1)}$, $\underline{x}^{(q)}$ generated by the constrained steepest descent equation (2.38). The corresponding frequencies are given by

$$p_o = p^{(q)} < p^{(q-1)} < p^{(q-2)} \qquad (3.30)$$

Let $\hat{\underline{x}}$ be the foot of the perpendicular from $\underline{x}^{(q)}$ onto the direction $\underline{\psi}^{(q-2)}$ defined by $\underline{x}^{(q-2)}$, $\underline{x}^{(q-1)}$. The associated frequency p is estimated by linearly interpolating on $\underline{\psi}^{(q-2)}$

$$\hat{p} = \left(1 + \frac{t^{(q-1)}}{t^{(q-2)}} \cdot \cos\theta\right) p^{(q-1)} - \frac{t^{(q-1)}}{t^{(q-2)}} \cos\theta \,.\, p^{(q-2)} \qquad (3.31)$$

where

$$\cos\theta = \underline{\psi}^{(q-1)} \,.\, \underline{\psi}^{(q-2)}$$

The direction ratios are given by

$$\left.\begin{aligned} \underline{\psi} &= \underline{x}^{(q)} - \hat{\underline{x}} && \text{if } \hat{p} \le p_o \\ &= \hat{\underline{x}} - \underline{x}^{(q)} && \text{otherwise} \end{aligned}\right\} \qquad (3.32)$$

The direction of bounce back into the feasible regions is obtained by projecting this direction onto the hyperplane (3.29). The step length is given by (3.24). If the proposed alternate step designs are non-feasible the step length is progressively reduced.

3.7 RESULTS AND DISCUSSION

The numerical work was carried out on an English Electric KDF9 computer using Segmented Algol. The following cases characterised by a four-dimensional design space were considered.

Cases (1,2): a standard turbine disc idealisation using resonance frequencies 440, 2000 cycles per second respectively, (figures 2.5, 3.2, 3.3). The frequency of the initial design, figure 2.5 was 2753·65 cycles per second.

Case (3): an arbitrary design configuration in conjunction with a resonance frequency of 2000 c.p.s. to examine the possibilities of relative minima in the absence of convexity conditions on the weight and feasible regions, (figures 2.8, 3.4-3.6). The frequency of the design of figure 2.8 was 2182·98 c.p.s.

Case (1) using a resonance frequency of 440 c.p.s. gave designs which never encountered a vibration constraint during convergence to the optimum. Therefore an artificial resonance frequency of 2000 cycles per second was introduced to study the interactions of the synthesis with the constraints giving rise to cases (2,3); the initial designs for cases (1,2) being identical.

The programs were run using Selectors I and II in turn for each of the cases (2,3). The results presented here are based on Selector I. Selector II failed to generate a satisfactory direction each time due to the fact that the kinetic energy density at one of the variable sections became very large (of the order of 10^6 in suitable units) in relation to the potential energy densities which were everywhere of the same order of magnitude ($\simeq 10^3$). This part of the investigation consumed comsiderable computer time and it was therefore decided to try Selector III only on the final designs in cases (2,3) to see whether further improvements were possible. Some improvement was obtained but not commensurate with the time consumed. In the initial stages the boundary designs were not highly constrained and a feasible design was obtained at the first attempt using Selector I. Thereafter the designs became more highly constrained with a correspondingly reduced wedge of feasibility requiring a greatly increased number of redesign attempts before a successful design was obtained. This accounts for the shape of the plots of weight versus total redesign attempts (figure 3.6) where its arbitrary nature and the decreasing convergence rate make it impossible to determine when the synthesis is complete. Attempts to consider higher order design spaces proved unsuccessful as the program became too big for the machine.

The final design in case (1) was bounded by all four design parameter constraints, while the final designs in cases (2,3) were bounded to within a reasonable tolerance by the vibration constraint and the design parameter constraint $a_2 = L$. However, this does not necessarily mean that the optimum lies at the intersection of one or more constraint surfaces. The final designs (figures 3.4, 3.5) in cases (2,3), although differing in weight by less than 1%, are radically different in configuration. This may be due to local instabilities or to the presence of pockets of relative minima in the composite constraint surface. Further research is needed to establish this point more conclusively.

3.8 CONCLUSIONS

An automated synthesis capability was developed for discs using a "black box" type representation for the frequency, weight reductions of 56.3%, 28.6% and 29.4% being recorded for the three cases presented here. The frequency calculations used here, though relatively simple from a mathematical standpoint, involve the programming of extremely long and complex routines. This could mean run times of about one hour for comparatively few design cycles, over 98% of the time being consumed in the frequency calculations. The time and the design iterations required to achieve a specified weight reduction increases at an increasing rate with the dimension of the design space, thus precluding any systematic evaluation of such cases. In addition, severe limitations would already be present from storage considerations.

Alternative analysis routines which could be used include an eigenvalue formulation [85,87,93,96] based on the methods of finite elements or finite differences [197]. This approach seems to offer better possibilities for exploiting Selector II, where the Lagrangian energy density vector which determines the normal to the vibration constraint surface could be readily calculated using the member stiffness and mass matrices. A derivation of this normal is given in references [87,194]. The same difficulties regarding storage and time could still be present. In any case, these programs were not available to the author at the start of this investigation. Another possibility is an equivalent reformulation of the problem in which, instead of the weight being minimised, the frequency is maximised with a constraint on the weight $W[h] \leq W_o$, along with the other constraints. These constraints are much easier to handle and enable the more conventional methods of non-linear programming [171] to be better utilised.

The synthesis procedures used here displayed the same general characteristics as those developed in the earlier investigation using a stress constraint. That is to say, rapid initial convergence followed by slow convergence as the designs became more highly constrained with a correspondingly reduced wedge of feasibility. The number of iterations and the time consumed increase very considerably with the dimension of the design space. For instance, cases (1,2), using a stress constraint required 62 iterations with a run time of 5 minutes to achieve a weight reduction of 54%, while the corresponding figures for an eleven-dimensional design space were 186 iterations with a run time of 30 minutes. It is estimated that on the average, the time for a frequency calculation exceeds that for a stress calculation by a factor of over 10:1. It should also be noted that the designs presented here would be substantially modified in the presence of a yield constraint on the stress with a correspondingly reduced weight change.

From a design standpoint, the problem of interest is optimization based on a combined stress and vibration constraint. The program for this investigation is a combination of the separate synthesis programs for stress and vibration constraints. This is primarily an exercise in computer programming and a really effective utilisation requires the development of more automatic software packages for handling such large scale systems.

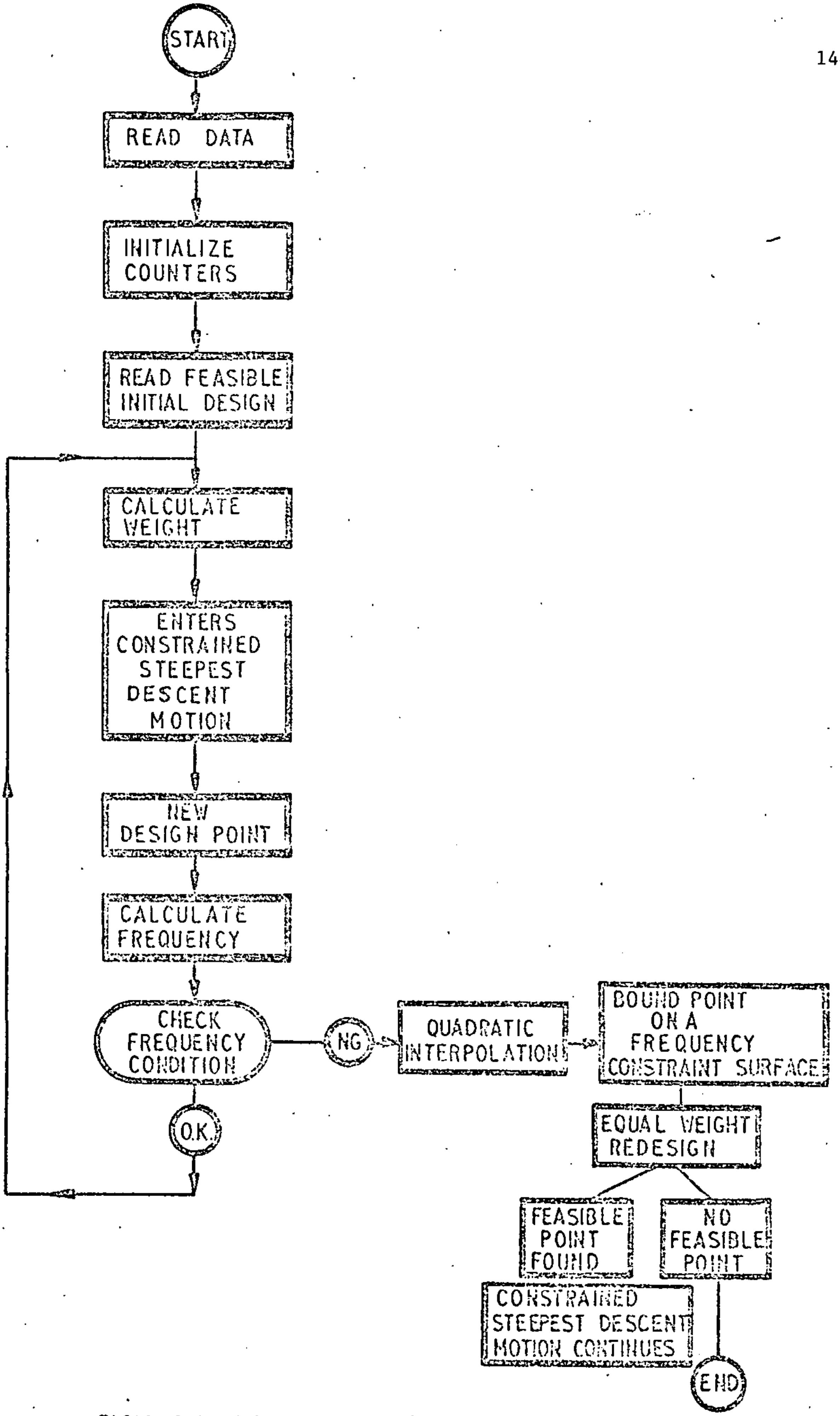

FLOW DIAGRAM FOR STRUCTURAL SYNTHESIS BASED ON A FREQUENCY CONSTRAINT.

FIG. 3.1

FIG. 3.2
WEIGHT = 1·57154 X 10^3 lbs.
FREQUENCY = 1658·85 c.p.s.
REDESIGN ATTEMPTS = 5 ; RUN TIME = 11 MI

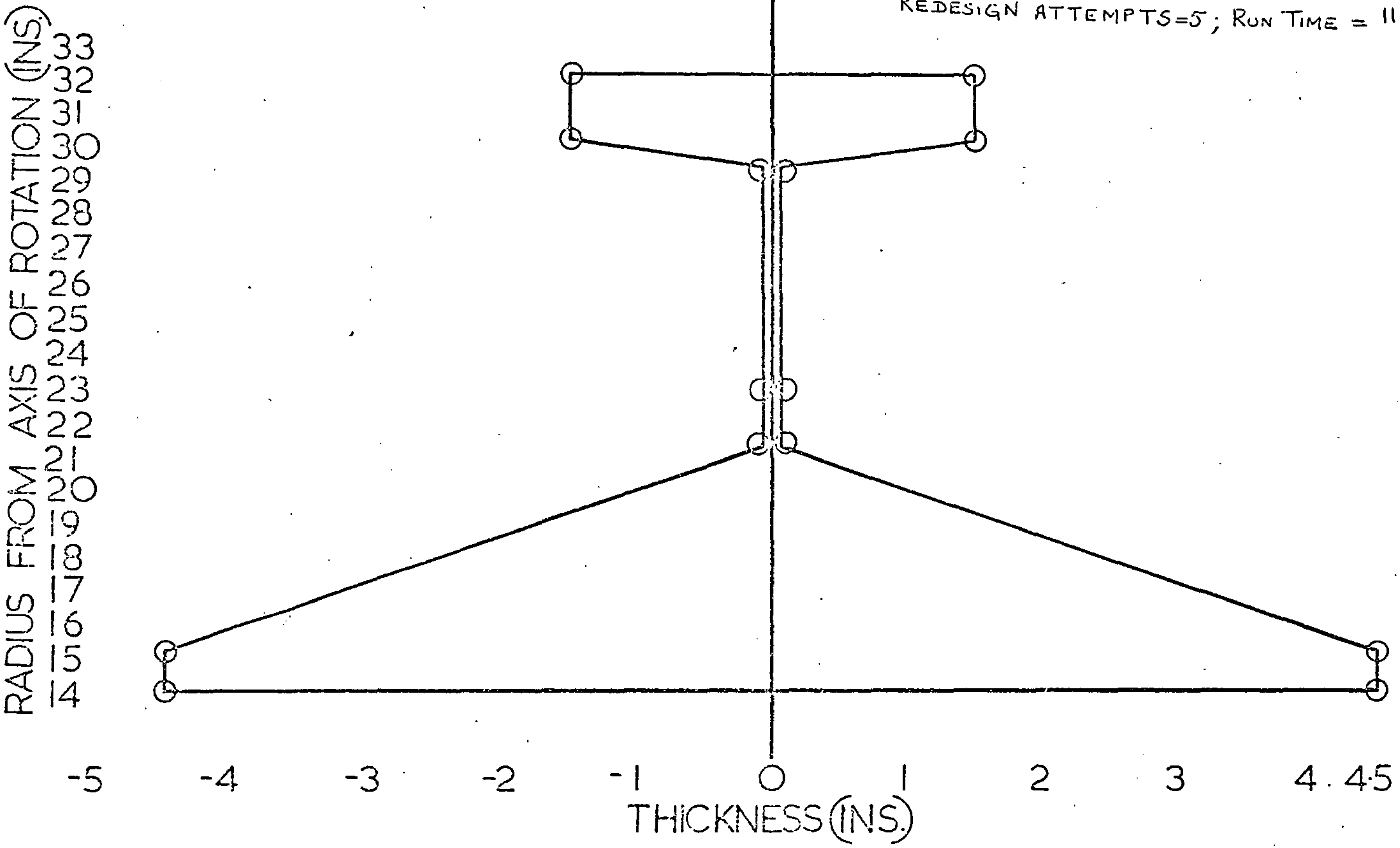

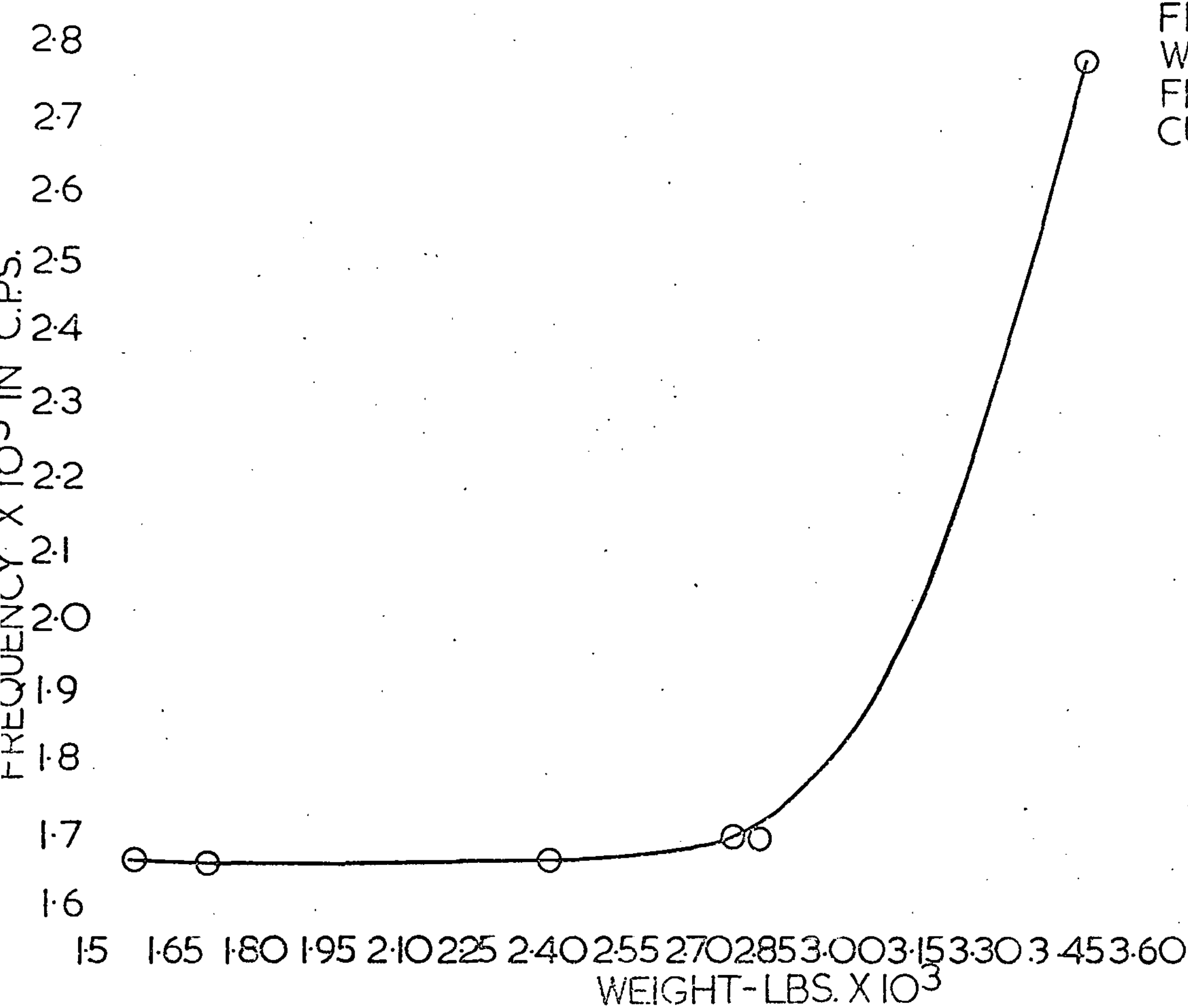

FIG. 3.3
WEIGHT VS
FREQUENCY
CURVE.

WEIGHT=2·56435 X10^3 lbs.
FREQUENCY=2008·62 c.p.s.
REDESIGN ATTEMPTS = 38 ; RUN TIME =53 M

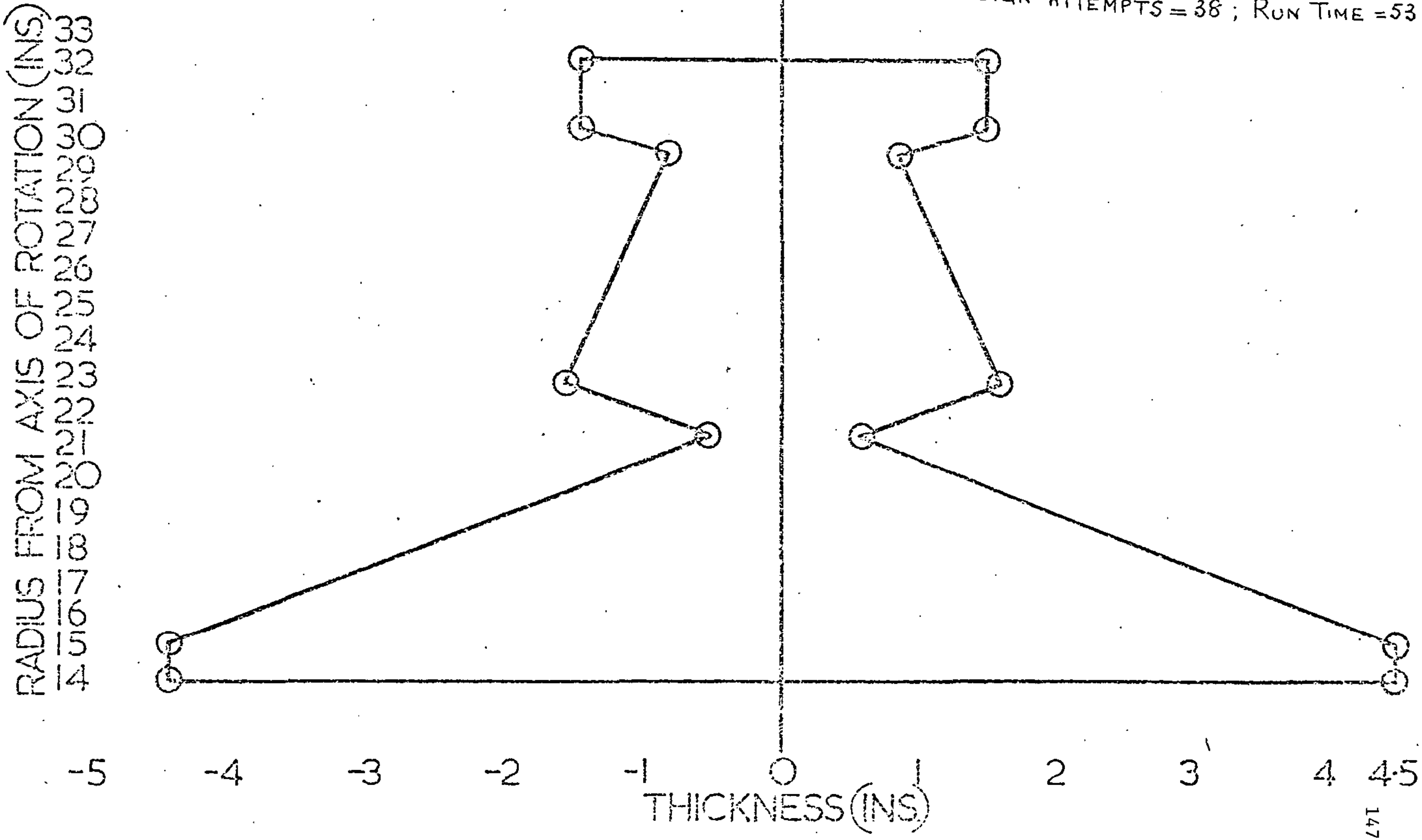

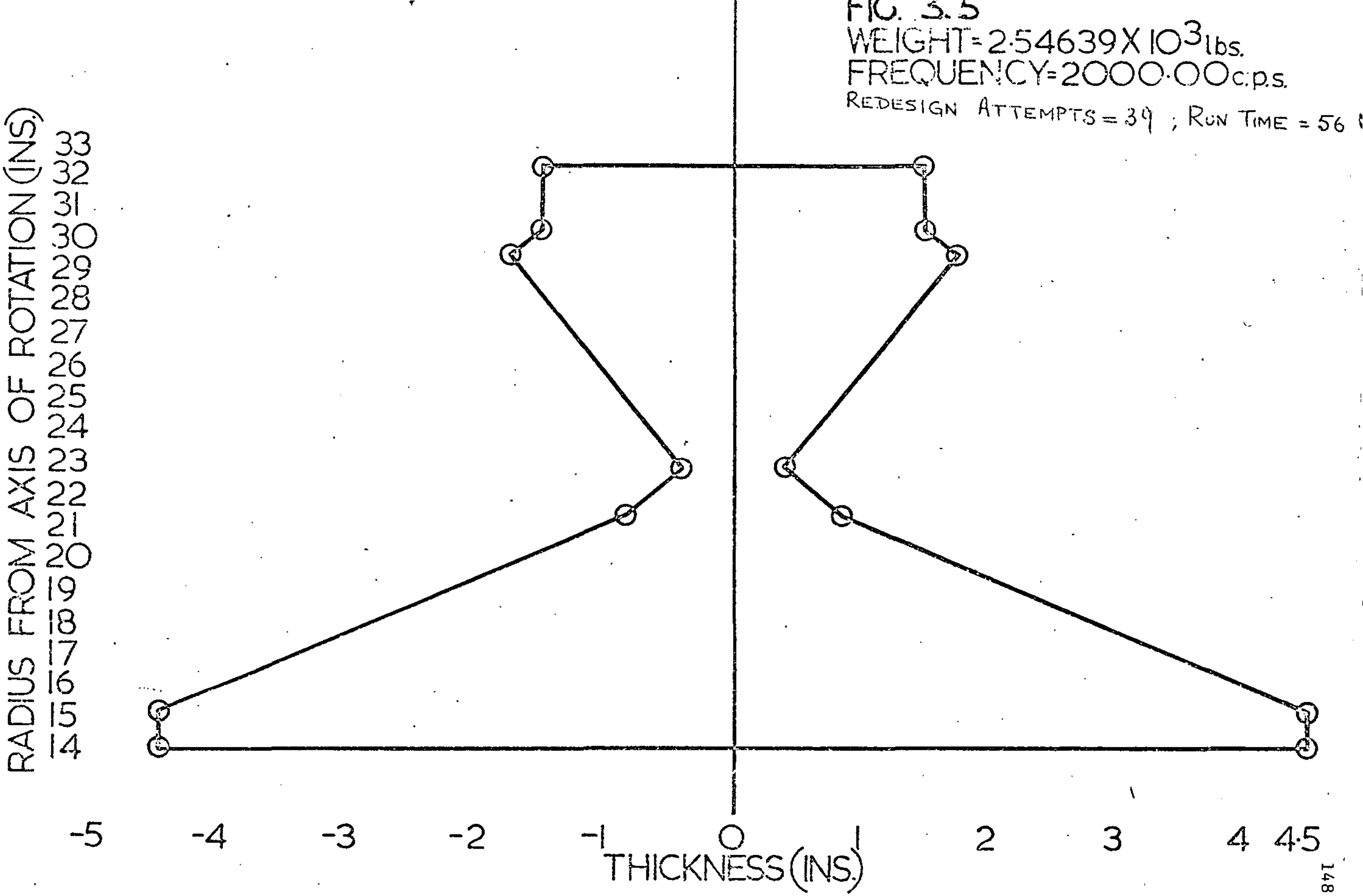
FIG. 3.5
WEIGHT=2·54639 X 10^3 lbs.
FREQUENCY=2000·00 c.p.s.
REDESIGN ATTEMPTS = 39 ; RUN TIME = 56
RADIUS FROM AXIS OF ROTATION (INS.)
33
32
31
30
29
28
27
26
25
24
23
22
21
20
19
18
17
16
15
14
-5
-4
-3
-2
-1
0
1
2
3
4
4·5
THICKNESS (INS.)

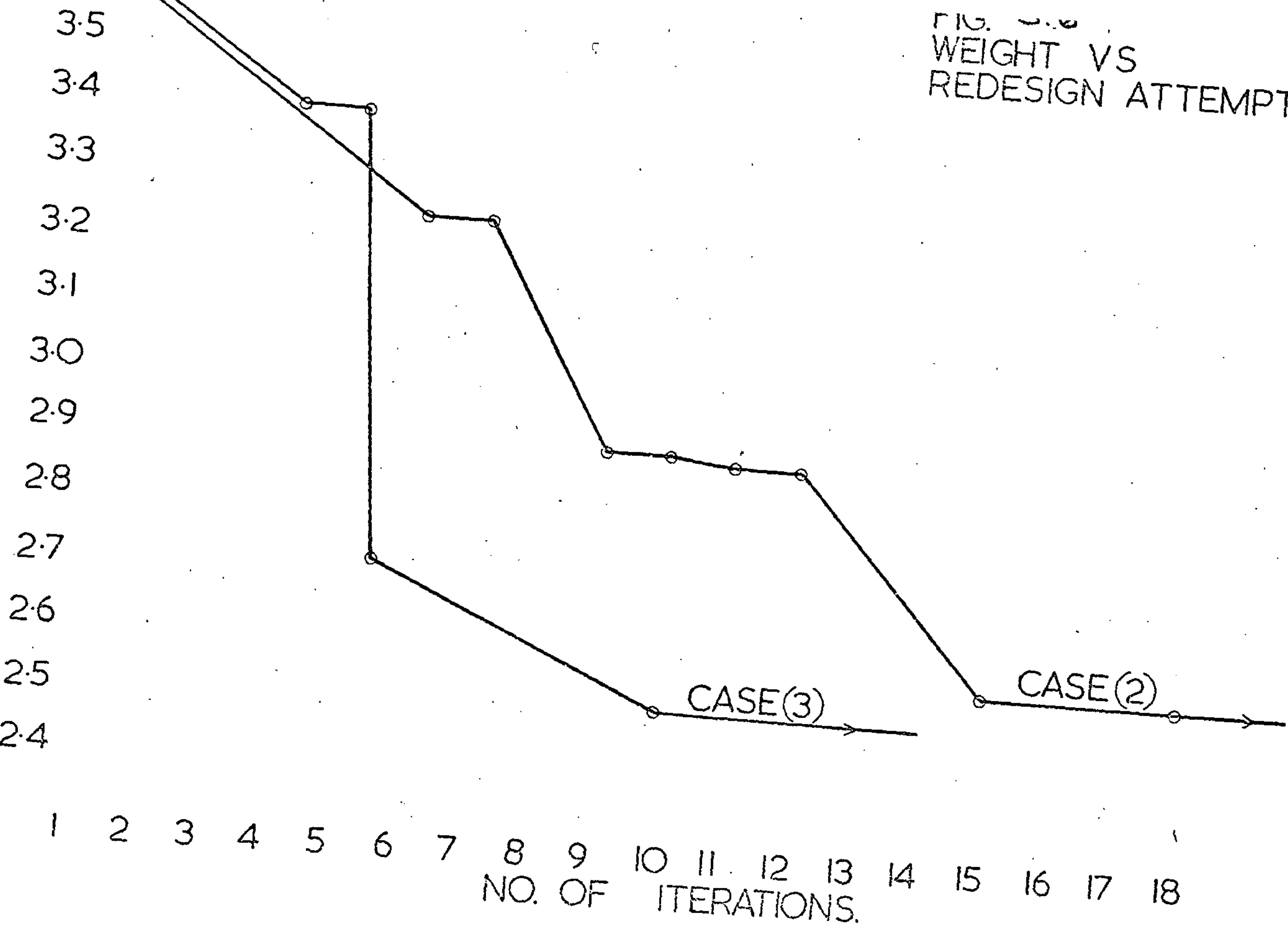

FIG.
WEIGHT VS
REDESIGN ATTEMPTS

Part II - Optimal Control Formulation

CHAPTER 4

PRINCIPLES OF PONTRYAGIN AND BELLMAN

4.1 INTRODUCTION

In Chapters 2 and 3 the problem of minimising the weight of a steam turbine disc subject to specified behaviour and side constraints was considered. The disc was modelled by a piecewise linear function and its design configuration was represented by a discrete set of independent variables which defined a multi-dimensional vector space, called design space. Every design configuration was represented by a unique vector in the space. The side constraints imposed bounds on the design variables to assure physically reasonable designs and corresponded to hyperplanes in design space. The behaviour variables on the other hand were functionals which associated to every vector in the space a uniquely defined vector function - the behaviour constraints corresponding to unknown surfaces in the space. The weight which was a function of the design variables was represented by a family of contours of constant weight. The problem consisted in determining those points on the least weight contour which lie in the feasible region enveloped by the constraint surfaces and was based on a non-linear programming formulation.

This chapter, however, recognises the continuous formulation of the problem [201,202] which is equivalent to a very general optimal control problem with inequality constraints on the behaviour and design variables. The solutions are given by the maximum principle of Pontryagin [137] and the optimality principle of Bellman [140,141]. These represent the first order necessary conditions for an optimal solution: first order conditions meaning those derivable by the use of first variations, namely the Euler-Lagrange equations, the transversality conditions and the Weierstrass condition or their equivalents. Pontryagin's principle is characterised by a system of ordinary differential equations of the Hamiltonian kind, while the dynamic programming formalism of Bellman yields a partial differential equation which is a generalisation of the Hamilton-Jacobi theory of the classical calculus of variations.

These principles have been derived in their full generality using a modified first variation method developed by Breakwell and others [203-206] for introducing inequality constraints into a Lagrange multiplier formulation. The mathematics is comparatively simple and should be more readily acceptable to design engineers than the more sophisticated approach based on set-theoretic considerations [207]. This chapter contains all the main results derived in [207].

4.2 STRUCTURAL OPTIMIZATION PROBLEMS

The systems considered are restricted to structures whose state is governed by a set of ordinary differential equations of the form

$$\frac{d\underline{x}}{dt} = \underline{f}(\underline{x}, \underline{u}, \underline{w}, t); \qquad (4.1)$$

where t is the independent variable, $t_o \leq t \leq t_1$ and $\underline{x}$, $\underline{u}$, $\underline{w}$ are the state, control and control parameter vectors respectively.

$$\underline{x} = \underline{x}(t) = \left(x_1(t), \ldots, x_n(t)\right)$$

$$\underline{u} = \underline{u}(t) = \left(u_1(t), \ldots, u_m(t)\right)$$

$$\underline{w} = (w_1, \ldots, w_\ell)$$

The control parameters correspond to global variables such as the natural frequencies of vibration and total energy, while the state and control vectors correspond roughly to the generalised coordinates and their derivatives. These include behaviour variables such as stresses, deformations and creep strain fields and design variables which specify the design configuration of the structure.

The vectors ($\underline{x}$, $\underline{u}$, $\underline{w}$) are permitted to vary in some prescribed manner so as to optimize a merit criterion of the form

$$I = G(\underline{w}) + \int_{t_o}^{t_1} f_o\left(\underline{x}(t), \underline{u}(t), \underline{w}, t\right)dt \qquad (4.2)$$

This would include as special cases:

(1) the minimum weight or minimum cost design of structures,

(2) selection of some optimal combination of vibrational modes,

(3) efficiency of some engineering component such as minimising the power loss during the transmission of electricity in cables,

(4) maximising the range of a thrust limited rocket.

The constraints on the state and control vectors and parameters are given by inequalities of the form

$$g_k(\underline{x}, \underline{u}, \underline{w}, t) \leqslant 0; \quad k = 1, \ldots, p \qquad (4.3)$$

These correspond to the behaviour and side constraints.

The boundary or end conditions are given by;

$$\left.\begin{aligned}\theta_\rho^{(o)}\left(\underline{x}(t_o),\ \underline{u}(t_o),\ t_o\right) &= 0; \qquad \rho = 1, \ldots, r \leq n+m+1 \\ \theta_\rho^{(1)}\left(\underline{x}(t_1),\ \underline{u}(t_1),\ t_1\right) &= 0; \qquad \rho = 1, \ldots, s \leq n+m+1\end{aligned}\right\} \quad (4.4)$$

and correspond to the external load conditions on the structure.

4.3 OPTIMAL CONTROL PROBLEM

Therefore a very general class of structural optimization problems has been formulated as problems in optimal control theory with the addition of inequality constraints on the state and control vectors and parameters.

Summarising, minimise the functional

$$I = G(\underline{w}) + \int_{t_o}^{t_1} f_o(\underline{x},\ \underline{u},\ \underline{w},\ t)dt$$

in a class of functions and parameters

$$x_i(t),\ u_j(t),\ w_k$$

$$(t_o \leq t < t_1; \qquad i = 1, \ldots, n; \qquad j = 1, \ldots, m; \qquad k = 1, \ldots, \ell)$$

satisfying the differential equations and inequality constraints.

$$\frac{dx_i}{dt} = f_i(\underline{x},\ \underline{u},\ \underline{w},\ t); \qquad i = 1, \ldots, n$$

$$g_k(\underline{x},\ \underline{u},\ \underline{w},\ t) \leq 0 \quad ; \qquad k = 1, \ldots, p$$

and the end conditions

$$\theta_\rho^{(o)}\left[\underline{x}(t_o),\ \underline{u}(t_o),\ t_o\right] = 0; \qquad \rho = 1, \ldots, r \leqslant n+m+1$$

$$\theta_\rho^{(1)}\left[\underline{x}(t_1),\ \underline{u}(t_1),\ t_1\right] = 0; \qquad \rho = 1, \ldots, s \leqslant n+m+1$$

Assumptions

(a) Limits of integration t_o, t_1 are variable

(b) $\underline{u}(t)$ is continuous and piecewise differentiable in $[t_o, t_1]$

(c) f_i, g_k; $i = 1, \ldots, n$; $k = 1, \ldots, p$ are of class C^2.

(d) $\theta_\rho^{(o)}$, $\theta_\rho^{(1)}$ possess first partial derivatives.

The Pontryagin representation of the problem is considered below. The central result of this formulation is the maximisation of the Hamiltonian with respect to the control functions lying in a control set Ω. In the absence of such a constraint set the problem reduces to a general calculus of variations problem.

4.4 METHOD OF SOLUTION

Consider

$$J = \int_{t_o}^{t_1} F dt \tag{4.5}$$

where

$$F(\underline{x}, \dot{\underline{x}}, \underline{u}, \underline{w}, t) = -f_o(\underline{x}, \underline{u}, \underline{w}, t) + \lambda_i(t)\left[f_i(\underline{x}, \underline{u}, \underline{w}, t) - \dot{x}_i\right] - \mu_k(t) g_k(\underline{x}, \underline{u}, \underline{w}, t) \tag{4.6}$$

The summation convention is implied where a repeated suffix denotes summation with respect to that suffix unless otherwise stated or implied. $\lambda_i(t)$, $\mu_k(t)$ have the status of generalised Lagrange multiplier functions.

Define

$$\mu_k(t) = 0 \quad \text{if} \quad g_k(\underline{x}^*, \underline{u}^*, \underline{w}^*, t) < 0 \tag{4.7}$$

where $(\underline{x}^*, \underline{u}^*, \underline{w}^*)$ are the optimal combination of vectors which minimise the functional I.

Consider small perturbations about the optimal combination of vectors, consistent with the constraint conditions (4.1, 4.3, 4.4).

$$\underline{x}(t) = \underline{x}^*(t) + \delta\underline{x}$$

$$\underline{u}(t) = \underline{u}^*(t) + \delta\underline{u}$$

$$\underline{w} = \underline{w}^* + \delta\underline{w}$$

$$I = I^* + \delta I$$

From (4.2, 4.5-4.7)

$$\delta I = \delta G - \delta J - \delta \int_{t_o}^{t_1} \mu_k(t) g_k dt$$

$$= \delta G - \delta J - \Big[\mu_k g_k \delta t\Big]_{t_o}^{t_1} - \int_{t_o}^{t_1} \mu_k \delta g_k dt$$

$$= \delta G - \delta J - \int_{t_o}^{t_1} \mu_k \delta g_k dt \tag{4.8}$$

The only non-zero contribution to the above integral comes from those intervals in which $\mu_k \neq 0$.

This implies

$$\left.\begin{aligned} g_k(\underline{x}^*, \underline{u}^*, \underline{w}^*, t) &= 0 \\ g_k(\underline{x}^*, \underline{u}^*, \underline{w}^*, t) + \delta g_k &< 0 \end{aligned}\right\}$$

i.e.

$$\left.\begin{aligned} \mu_k(t) &\neq 0 \\ \delta g_k &< 0 \end{aligned}\right\} \tag{4.9}$$

The minimising condition

$$\delta I \geq 0 \tag{4.10}$$

for all perturbations consistent with the constraint conditions gives, using (4.7 - 4.9)

$$\left.\begin{aligned} &\mu_k(t) \geq 0; \quad k = 1, \ldots, p; \quad \text{for all} \quad t \in \left[t_o, t_1\right] \\ &\delta G - \delta J = 0 \end{aligned}\right\} \tag{4.11}$$

From (4.5, 4.6)

$$\delta J = \left[F\delta t\right]_{t_o}^{t_1} + \int_{t_o}^{t_1} \delta F(\underline{x}, \dot{\underline{x}}, \underline{u}, \underline{w}, t)dt$$

$$= \left[F\delta t\right]_{t_o}^{t_1} + \int_{t_o}^{t_1} \left(\frac{\partial F}{\partial x_i}\delta x_i + \frac{\partial F}{\partial \dot{x}_i}\delta \dot{x}_i + \frac{\partial F}{\partial u_j}\delta u_j + \frac{\partial F}{\partial w_k}\delta w_k\right)dt \tag{4.12}$$

But

$$\delta \int_{t_o}^{t_1} \dot{x}_i \delta t = \Big[\dot{x}_i \delta t\Big]_{t_o}^{t_1} + \int_{t_o}^{t_1} \delta \dot{x}_i dt$$

Hence,

$$\int_{t_o}^{t_1} \delta \dot{x}_i dt = \delta \int_{t_o}^{t_1} \dot{x}_i dt - \Big[\dot{x}_i \delta t\Big]_{t_o}^{t_1}$$

$$= \Big[\delta x_i - \dot{x}_i \delta t\Big]_{t_o}^{t_1} \tag{4.13}$$

Therefore integrating by parts using (4.6, 4.13)

$$\int_{t_o}^{t_1} \frac{\partial F}{\partial \dot{x}_i} \delta \dot{x}_i dt = \Big[(\delta x_i - \dot{x}_i \delta t)\frac{\partial F}{\partial \dot{x}_i}\Big]_{t_o}^{t_1} - \int_{t_o}^{t_1} \delta x_i \frac{d}{dt}\left(\frac{\partial F}{\partial \dot{x}_i}\right) dt$$

$$= - \Big[(\delta x_i - \dot{x}_i \delta t)\lambda_i(t)\Big]_{t_o}^{t_1} + \int_{t_o}^{t_1} \delta x_i \dot{\lambda}_i(t) dt \tag{4.14}$$

Substituting (4.14) in (4.12)

$$\delta J = \Big[(F + \lambda_i \dot{x}_i)\delta t - \lambda_i \delta x_i\Big]_{t_o}^{t_1} + \int_{t_o}^{t_1} \left\{\left(\dot{\lambda}_i + \frac{\partial F}{\partial x_i}\right)\delta x_i + \frac{\partial F}{\partial u_j}\delta u_j \right.$$

$$\left. + \frac{\partial F}{\partial w_k}\delta w_k\right\} dt \tag{4.15}$$

Define the variational Hamiltonian

$$H(\underline{x}, \underline{u}, \underline{w}, t; \ \underline{\lambda}, \underline{\mu}) = F + \lambda_i \dot{x}_i$$

$$= - f_o(\underline{x}, \underline{u}, \underline{w}, t) + \lambda_i f_i(\underline{x}, \underline{u}, \underline{w}, t) - \mu_k g_k(\underline{x}, \underline{u}, \underline{w}, t)$$

$$\tag{4.16}$$

where

$$\underline{\lambda} = (\lambda_1, \ldots, \lambda_n)$$

$$\underline{\mu} = (\mu_1, \ldots, \mu_p)$$

Substituting (4.16) in (4.15)

$$\delta J = \left[H\delta t - \lambda_i \delta x_i \right]_{t_o}^{t_1} + \int_{t_o}^{t_1} \frac{\partial H}{\partial w_k} \delta w_k dt + \int_{t_o}^{t_1} \left[\left(\dot{\lambda}_i + \frac{\partial H}{\partial x_i} \right) \delta x_i \right.$$

$$\left. + \frac{\partial H}{\partial u_j} \delta u_j \right] dt \qquad (4.17)$$

From (4.11, 4.17)

<u>Adjoint Equations:</u> $\dot{\lambda}_i = -\frac{\partial H}{\partial x_i}$; $i = 1, \ldots, n$ (4.18)

$$\frac{\partial H}{\partial u_j} = 0 \quad ; \quad j = 1, \ldots, m \qquad (4.19)$$

<u>Transversality conditions</u>

$$-\delta G + \left[H\delta t - \lambda_i \delta x_i \right]_{t_o}^{t_1} + \int_{t_o}^{t_1} \frac{\partial H}{\partial w_k} \delta w_k dt = 0 \qquad (4.20)$$

This must be satisfied for all perturbations consistent with (4.4)

From (4.1, 4.16)

$$\dot{x}_i = f_i = \frac{\partial H}{\partial \lambda_i} ; \quad i = 1, \ldots, n \qquad (4.21)$$

Therefore the solutons are characterised by a set of ordinary differential equations of the Hamiltonian kind.

$$\left.\begin{aligned} \frac{d\lambda_i}{dt} &= -\frac{\partial H}{\partial x_i} \quad ; \quad i = 1, \ldots, n \\ \frac{dx_i}{dt} &= \frac{\partial H}{\partial \lambda_i} \quad ; \quad i = 1, \ldots, n \end{aligned}\right\} \tag{4.22}$$

The transversality conditions (4.20) in conjunction with the end conditions (4.4) provide a sufficient set of boundary conditions for solving (4.22).

The following consistency condition can be obtained as a by-product of the analysis

$$\begin{aligned} \frac{dH}{dt} &= \frac{\partial H}{\partial x_i}\dot{x}_i + \frac{\partial H}{\partial u_j}\dot{u}_j + \frac{\partial H}{\partial w_k}\dot{w}_k + \frac{\partial H}{\partial t} + \frac{\partial H}{\partial \lambda_i}\dot{\lambda}_i + \frac{\partial H}{\partial \mu_k}\dot{\mu}_k \\ &= \frac{\partial H}{\partial x_i} f_i + 0 + 0 + \frac{\partial H}{\partial t} - f_i \frac{\partial H}{\partial x_i} - g_k \dot{\mu}_k \\ &= \frac{\partial H}{\partial t} \end{aligned} \tag{4.23}$$

Consider

$$\int_{t_o}^{t_1} \left[H(\underline{x}^*, \underline{u}, \underline{w}^*, t; \ \underline{\lambda}, \underline{0}) - H(\underline{x}^*, \underline{u}^*, \underline{w}^*, t; \ \underline{\lambda}, \underline{0}) \right] dt$$

$$\begin{aligned} &= \int_{t_o}^{t} \left[f_o(\underline{x}^*, \underline{u}^*, \underline{w}^*, t) - f_o(\underline{x}^*, \underline{u}, \underline{w}^*, t) \right] dt \\ &\qquad + \int_{t_o}^{t} \lambda_i(t) \left[f_i(\underline{x}^*, \underline{u}, \underline{w}^*, t) - f_i(\underline{x}^*, \underline{u}^*, \underline{w}^*, t) \right] dt \end{aligned} \tag{4.24}$$

$$= I^* - I \leqslant 0 \tag{4.25}$$

provided

$$g_k(\underline{x}^*, \underline{u}, \underline{w}^*, t) < 0 \tag{4.26}$$

Equation (4.25) must be satisfied by all controls $\underline{u}(t)$ within a sufficiently small neighbourhood of $\underline{u}^*(t)$ and satisfying (4.26). This implies

$$H(\underline{x}^*, \underline{u}, \underline{w}^*, t; \underline{\lambda}, \underline{0}) \leqslant H(\underline{x}^*, \underline{u}^*, \underline{w}^*, t; \underline{\lambda}, \underline{0}) \tag{4.27}$$

provided equation (4.26) is satisfied. This is the Weierstrass condition that the Hamiltonian must be maximised with respect to the controls within the interior of the constraint region bounded by the g_k. (This implies $\mu_k = 0$.) The equations derived in this section are summarised below.

4.5 PONTRYAGIN'S PRINCIPLE

Consider the Hamiltonian

$$H\big(\underline{x}(t), \underline{u}(t), \underline{w}, t; \underline{\lambda}(t), \underline{\mu}(t)\big)$$

$$= -f_o\big(\underline{x}(t), \underline{u}(t), \underline{w}, t\big) + \lambda_i(t)f_i\big(\underline{x}(t), \underline{u}(t), \underline{w}, t\big)$$

$$- \mu_k(t)g_k\big(\underline{x}(t), \underline{u}(t), \underline{w}, t\big) \tag{4.16}$$

where

$$t_o \leqslant t \leqslant t_1; \quad i = 1, \ldots, n; \quad k = 1, \ldots, p$$

For optimal solutions $\big(\underline{x}^*(t), \underline{u}^*(t), \underline{w}^*\big)$ to the problem formulated in section 4.3, the multipliers $\underline{\lambda}(t)$, $\underline{\mu}(t)$ must satisfy the following conditions

$$\text{(a)} \quad \mu_k(t) = 0 \quad \text{if} \quad g_k(\underline{x}^*, \underline{u}^*, \underline{w}^*, t) < 0$$

$$> 0 \quad \text{if} \quad g_k(\underline{x}^*, \underline{u}^*, \underline{w}^*, t) = 0 \qquad (4.11)$$

(b) <u>Adjoint equations</u>

$$\dot{\lambda}_i = -\frac{\partial H}{\partial x_i} \quad ; \quad i = 1, \ldots, n \qquad (4.18)$$

$$\dot{x}_i = \frac{\partial H}{\partial \lambda_i} \quad ; \quad i = 1, \ldots, n \qquad (4.22)$$

$$\frac{\partial H}{\partial u_j} = 0 \quad ; \quad j = 1, \ldots, m \qquad (4.19)$$

This is the equivalent statement of the Weierstrass condition that H must be maximised with respect to the controls within the interior of the constraint region.

(c) <u>Consistency condition</u>

$$\frac{dH}{dt} = \frac{\partial H}{\partial t} \qquad (4.23)$$

(d) <u>Transversality condition</u>

$$-\delta G + \Big[H\delta t - \lambda_i \delta x_i \Big]_{t_o}^{t_1} + \int_{t}^{t_1} \frac{\partial H}{\partial w_k} \delta w_k \, dt = 0 \qquad (4.20)$$

This must be satisfied for perturbations consistent with the end condition (4.4).

(e) Weierstrass condition

$$\left.\begin{array}{l} H(\underline{x}^*, \underline{u}, \underline{w}^*, t; \ \underline{\lambda}, \underline{0}) \leqslant H(\underline{x}^*, \underline{u}^*, \underline{w}^*, t; \ \underline{\lambda}, \underline{0}) \\ \text{provided} \quad g_k(\underline{x}^*, \underline{u}^*, \underline{w}^*, t) < 0; \quad k = 1, \ldots, p \end{array}\right\} \tag{4.27}$$

4.6 RESTRICTED MAXIMUM PRINCIPLE

This corresponds to an arc of the optimal trajectory lying on the boundary of the constraint domain. So that without loss of generality, assume

$$\left.\begin{array}{ll} g_k(\underline{x}^*, \underline{u}^*, \underline{w}^*, t) = 0; & k = 1, \ldots, p' \leqslant p \\ g_k(\underline{x}^*, \underline{u}^*, \underline{w}^*, t) < 0; & k = p'+1, \ldots, p \end{array}\right\} \tag{4.28}$$

where

$$t \in \left[t_e, t_\ell\right]$$

$$t_o \leqslant t_e < t_\ell \leqslant t_1$$

Therefore from the implicit function theorem there exists a neighbourhood of $(\underline{x}^*, \underline{u}^*, \underline{w}^*)$ such that

$$g_k(\underline{x}, \underline{u}, \underline{w}, t) = 0; \quad k = 1, \ldots, p' \tag{4.29}$$

This may be solved uniquely for p' components of $\underline{u}$ as functions of the remaining (m - p') components of $\underline{u}$ and $\underline{x}$, $\underline{w}$, t. Without loss of generality let these p' components be $u_1, u_2, \ldots, u_{p'}$.

Let

$$\underline{u}_c = (u_1, \ldots, u_{p'}) \tag{4.30}$$

where

$$\underline{u}_c = \underline{u}_c\left(u_{p'+1}, \ldots, u_m; \ \underline{x}, \underline{w}, t\right)$$

and

$$\underline{u} = \left(\underline{u}_c; u_{p'+1}, \ldots, u_m\right)$$

From (4.16)

$$H = \hat{H} - \sum_{k=1}^{p} \mu_k g_k \tag{4.31}$$

where

$$\hat{H} = -f_o + \lambda_i f_i$$

This corresponds to the Hamiltonian in the absence of inequality constraints.

From (4.7, 4.18, 4.19, 4.28)

$$\left.\begin{aligned} \frac{d\lambda_i}{dt} &= -\frac{\partial\hat{H}}{\partial x_i} + \sum_{k=1}^{p'} \mu_k(t)\frac{\partial g_k}{\partial x_i}; \qquad i = 1, \ldots, n \\ \frac{\partial H}{\partial u_j} &= \frac{\partial\hat{H}}{\partial u_j} - \sum_{k=1}^{p'} \mu_k(t)\frac{\partial g_k}{\partial u_j} = 0; \quad j = 1, \ldots, p' \end{aligned}\right\} \tag{4.32}$$

These may be written more compactly using matrix algebra as

$$\frac{d\underline{\lambda}}{dt} = -\nabla_x\hat{H} + \hat{\underline{\mu}}\frac{\partial\underline{g}}{\partial\underline{x}} \tag{4.33}$$

$$\nabla_u\hat{H} - \hat{\underline{\mu}}\frac{\partial\underline{g}}{\partial\underline{u}_c} = 0 \tag{4.34}$$

where

$$\hat{\underline{\mu}} = (\mu_1, \ldots, \mu_{p'})$$

$$\nabla_x = \left(\frac{\partial}{\partial x_1}, \ldots, \frac{\partial}{\partial x_n}\right)$$

$$\nabla_u = \left(\frac{\partial}{\partial u_1}, \ldots, \frac{\partial}{\partial u_{p'}}\right)$$

$$\frac{\partial \underline{g}}{\partial \underline{x}} = \begin{bmatrix} \frac{\partial g_1}{\partial x_1} & \cdots\cdots\cdots & \frac{\partial g_1}{\partial x_n} \\ \vdots & & \vdots \\ \frac{\partial g_{p'}}{\partial x_1} & \cdots\cdots\cdots & \frac{\partial g_{p'}}{\partial x_n} \end{bmatrix}_{p' \times n}$$

$$\frac{\partial \underline{g}}{\partial \underline{u}_c} = \begin{bmatrix} \frac{\partial g_1}{\partial u_1} & \cdots\cdots\cdots & \frac{\partial g_1}{\partial u_{p'}} \\ \vdots & & \vdots \\ \frac{\partial g_{p'}}{\partial u_1} & \cdots\cdots\cdots & \frac{\partial g_{p'}}{\partial u_{p'}} \end{bmatrix}_{p' \times p'}$$

Eliminating $\hat{\underline{\mu}}$ from (4.33, 4.34) gives

$$\frac{d\underline{\lambda}}{dt} = -\nabla_x \hat{H} + \nabla_u \hat{H} \left(\frac{\partial \underline{g}}{\partial \underline{u}_c}\right)^{-1} \left(\frac{\partial \underline{g}}{\partial \underline{x}}\right) \tag{4.35}$$

Define

$$p_k(\underline{x}, \underline{u}, \underline{w}, t) = \nabla_x g_k \cdot \underline{f} \; ; \qquad k = 1, \ldots, p'$$

$$= \nabla_x g_k \cdot \frac{d\underline{x}}{dt} \tag{4.36}$$

Suppose the constraints g_k are functions of the state variables only

$$g_k = g_k(\underline{x}); \qquad k = 1, \ldots, p' \tag{4.37}$$

From (4.29, 4.36)

$$p_k = \frac{dg_k}{dt} = 0; \qquad k = 1, \ldots, p' \tag{4.38}$$

Equations (4.35 - 4.38) represent the equations of the restricted maximum principle. The Weierstrass condition corresponds to maximising $\hat{H}$ subject to the constraint (4.38).

4.7 JUMP CONDITION

The condition on the adjoint vector $\underline{\lambda}$ at the entry and leaving points t_e, t_ℓ, defined in (4.28) is considered below.

From (4.33)

$$\lambda(t + h) - \underline{\lambda}(t) = - h\nabla_x\hat{H} + h\hat{\underline{\mu}}\left(\frac{\partial \underline{g}}{\partial \underline{x}}\right) - h\underline{O}(h) \tag{4.39}$$

where

$$\frac{d\underline{\lambda}}{dt} = \frac{\underline{\lambda}(t + h) - \underline{\lambda}(t)}{h} + \underline{O}(h)$$

$$t_o \leqslant t_e \leqslant t < t+h \leqslant t_\ell \leqslant t_1$$

$$\underline{O}(h) \rightarrow 0 \quad \text{as} \quad h \rightarrow 0$$

Let

$$\left.\begin{array}{l} t \rightarrow t_\ell \\ h \rightarrow 0+ \end{array}\right\} \tag{4.40}$$

From (4.39)

$$\underline{\lambda}(t_\ell + 0) - \underline{\lambda}(t_\ell) = + \underline{\nu}(t_\ell)\left(\frac{\partial \underline{g}}{\partial \underline{x}}\right)_{t=t_\ell}$$

i.e.

$$\underline{\lambda}(t_\ell + 0) = \underline{\lambda}(t_\ell) + \underline{\nu}(t_\ell)\left(\frac{\partial \underline{g}}{\partial \underline{x}}\right)_{t=t_\ell} \tag{4.41}$$

where

$$\underline{\hat{\mu}}(t) \longrightarrow \infty$$

such that

$$h\underline{\hat{\mu}}(t) \longrightarrow \text{a finite limit} \equiv \underline{\nu}(t_\ell) \tag{4.42}$$

From (4.11)

$$\underline{\nu}(t_\ell) \geq 0 \tag{4.43}$$

Suppose

$$\left.\begin{array}{l} t < t_e \\ \text{and} \\ g_k < 0; \quad k = 1, \ldots, p' \end{array}\right\} \tag{4.44}$$

This corresponds to approaching the entry point t_e from within the constraint domain.

From (4.11, 4.16, 4.33)

$$\frac{d\underline{\lambda}}{dt} = -\nabla_x \hat{H}$$

$$\underline{\lambda}(t) - \lambda(t - h) = -h\nabla_x \hat{H} - h\underline{O}(h) \tag{4.45}$$

Let

$$t \longrightarrow t_e$$

$$h \longrightarrow 0+$$

then

$$\underline{\lambda}(t_e) - \underline{\lambda}(t_e - 0) = \underline{0}$$

$$\underline{\lambda}(t_e) = \underline{\lambda}(t_e - 0) \tag{4.46}$$

Equations (4.41, 4.43, 4.46) define the jump conditions. $\underline{\lambda}(t)$ is continuous at an entry point but is discontinuous on leaving.

4.8 BELLMAN'S PRINCIPLE

The results of the preceding sections were obtained by minimising G-J from (4.11) with respect to the controls $\underline{u}(t)$ belonging to a control set U defined by (4.3, 4.4). The following minimum cost function is defined corresponding to (4.11)

$$V\left(t,\ \underline{x}(t),\ \underline{\dot{x}}(t),\ \underline{w}\right) = \min_{\substack{\underline{u}(\sigma)\varepsilon U\\ t\leqslant\sigma\leqslant t_1}} \left\{ \int_t^{t_1} -F\left(\underline{x}(\sigma),\ \underline{\dot{x}}(\sigma),\ \underline{u}(\sigma),\ \underline{w},\ \sigma\right)d\sigma + G(\underline{w}) \right\} \tag{4.47}$$

$$= \min_{\substack{\underline{u}(\sigma)\varepsilon U\\ t\leqslant\sigma\leqslant t+h}} \ \min_{\substack{\underline{u}(\sigma)\varepsilon U\\ t+h\leqslant t\leqslant t_1}} \left\{ \int_t^{t+h} -F\left(\underline{x}(\sigma),\ \underline{\dot{x}}(\sigma),\ \underline{u}(\sigma),\ \underline{w},\ \sigma\right)d\sigma + \int_{t+h}^{t_1} -F\left(\underline{x}(\sigma),\ \underline{\dot{x}}(\sigma),\ \underline{u}(\sigma),\ \underline{w},\ \sigma\right)d\sigma + G(\underline{w}) \right\} \tag{4.48}$$

This is obtained by splitting the integral and minimisation operation in (4.47) into two parts: (t, t+h), (t+h, t_1) and in the limit $h \to 0$. The first integral in (4.48) depends only on values of $\sigma\ \varepsilon\ [t,\ t+h]$ and is independent of minimisation for $\sigma > t+h$. Therefore, using mean value theorem for small h

$$\min_{\substack{\underline{u}(\sigma)\varepsilon U\\ t\leqslant\sigma\leqslant t+h}} \ \min_{\substack{\underline{u}(\sigma)\varepsilon U\\ t+h\leqslant\sigma\leqslant t_1}} \left\{ \int_t^{t+h} -F\left(\underline{x}(\sigma),\ \underline{\dot{x}}(\sigma),\ \underline{u}(\sigma),\ \underline{w},\ \sigma\right)d\sigma \right\}$$

$$= \min_{\substack{\underline{u}(\sigma)\varepsilon U\\ t\leqslant\sigma\leqslant t+h}} \left\{ \int_t^{t+h} -F\left(\underline{x}(\sigma),\ \underline{\dot{x}}(\sigma),\ \underline{u}(\sigma),\ \underline{w},\ \sigma\right)d\sigma \right\}$$

$$= \min_{\underline{u}(t)\varepsilon U} \left\{ -hF\left(\underline{x}(t),\ \underline{\dot{x}}(t),\ \underline{u}(t),\ \underline{w},\ t\right) \right\} \tag{4.49}$$

For the remaining term in (4.8) for which σ varies from (t+h) to t_1, the only effect on control applied from (t, t+h) is to determine $(\underline{x}, \dot{\underline{x}})$ at t+h. So that, from the definition (4.47) this term reduces to

$$\underset{t\leq\sigma\leq t+h}{\underset{\underline{u}(\sigma)\varepsilon U}{\text{Min}}}\quad \underset{t+h\leq\sigma\leq t_1}{\underset{\underline{u}(\sigma)\varepsilon U}{\text{Min}}} \left\{ \int_{t+h}^{t_1} -F\left(\underline{x}(\sigma),\ \dot{\underline{x}}(\sigma),\ \underline{u}(\sigma),\ \underline{w},\ \sigma\right)d\sigma \ +\ G(\underline{w}) \right\}$$

$$= \underset{\underline{u}(t)\varepsilon U}{\text{Min}} \left\{ V\left(t+h,\ \underline{x}(t+h),\ \dot{\underline{x}}(t+h),\ \underline{w}\right)\right\} \tag{4.50}$$

Combining (4.47 - 4.50), the following iterative functional equation is obtained.

$$V\left(t,\ \underline{x}(t),\ \dot{\underline{x}}(t),\ \underline{w}\right) = \underset{\underline{u}\varepsilon U}{\text{Min}} \left[-h\hat{F}(\underline{x},\dot{\underline{x}},\underline{u},\underline{w},t) + V\left(t+h,\underline{x}(t+h),\underline{x}(t+h),\underline{w}\right)\right] \tag{4.51}$$

This is the mathematical statement of the optimality principle of dynamic programming [140, 141]. But from Taylor's theorem

$$V\left(t+h,\ \underline{x}(t+h),\ \dot{\underline{x}}(t+h),\ \underline{w}\right) = V(t,\underline{x},\dot{\underline{x}},\underline{w}) + h\,\frac{\partial V}{\partial t} + h\dot{x}_i\,\frac{\partial V}{\partial x_i} + h\ddot{x}_i\,\frac{\partial V}{\partial \dot{x}_i} + O(h^2)$$

Therefore substituting in (4.51) and taking $h \longrightarrow 0$

$$\frac{\partial V}{\partial t} + \underset{\underline{u}\varepsilon U}{\text{Min}} \left[-F + f_i\,\frac{\partial V}{\partial x_i} + \frac{df_i}{dt}\,\frac{\partial V}{\partial \dot{x}_i}\right] = 0$$

On further simplification this becomes

$$\frac{\partial V}{\partial t} + \underset{\underline{u}\varepsilon U}{\text{Min}} \left[f_o + \mu_k g_k + f_i\,\frac{\partial V}{\partial x_i} + \left(\frac{\partial f_i}{\partial x_\ell}\,f_\ell + \frac{\partial f_i}{\partial u_j}\,\dot{u}_j + \frac{\partial f_i}{\partial t}\right)\frac{\partial V}{\partial \dot{x}_i}\right] = 0 \tag{4.52}$$

This equation contains the inequality constraints g_k and corresponds to the generalised Hamilton-Jacobi partial differential equation of dynamic programming. Equations (4.52) can be solved using the method of characteristics to yield the Pontryagin equations of the previous sections. The dynamic programming approach presents considerable storage difficulties for high order systems.

4.9 DISCUSSION

The principles of Pontryagin and Bellman have been derived for a class of structural optimization problems which have been formulated as general optimal control problems. A first variation method was used for introducing the inequality constraints into a generalised Lagrange multiplier formulation. Variations in the functional J defined by (4.5) gave the desired results. One of the difficulties in the simplified approach presented here lies in formulating necessary and sufficient conditions on f_i, g_k, $\theta_\rho^{(o)}$, $\theta_\rho^{(1)}$ for the existence of (4.17) and the derivation of the jump conditions. These difficulties could be resolved using the methods of functional analysis which lie outside the scope of this thesis.

4.10 STRUCTURAL PROBLEMS IN CONTROL FORMULATION

The application of optimal control theory to the structural optimization area is of more recent origin. The formalism is based on the maximum principle of Pontryagin and the optimality principle of Bellman in the theory of dynamic programming. They provide the first order conditions for an optimal: Euler-Lagrange equations, transversality conditions and the Weierstrass condition. These are essentially a systematisation of the variational calculus where an entire function, or functions, is determined to optimise some performance criterion subject to specified constraints. The applications are based on a continuous model and one-dimensional structures [90, 93-95,113,119,126,208-210] have been formulated as optimal control problems with, for example, skin thickness or a beam dimension playing the role of a control function. These are studied in conjunction with static and dynamic technologies. In this connection the work of Haug and Kirmser [208] is of special interest as they consider beam problems in the presence of inequality constraints on the stress and deflection fields using Lagrange multiplier functions.

In Chapters 5 and 6 the scope of optimal control theory is further extended to include more complex structural optimization problems.

CHAPTER 5

OPTIMAL CONTROL FORMULATION OF DISC BASED ON A STRESS CONSTRAINT

5.1 TURBINE DISC PROBLEM

The principles of Pontryagin and Bellman developed in Chapter 4 are applied to the structural optimization problem studied in Chapter 2 where the weight of the turbine disc was minimised in the presence of a stress constraint. The variational formulation was already developed in Chapter 2 and is summarised below for purposes of ready reference.

The weight functional to be minimised is

$$W = \int_{a_1}^{a_m} 2\pi\rho r h(r) dr \tag{5.1}$$

where the thickness distribution is defined by

$$\left.\begin{aligned} h(r) &= b_1 && a_1 \leqslant r \leqslant a_2 \\ &= h(r) && a_2 \leqslant r \leqslant a_{m-1} \\ &= b_m && a_{m-1} \leqslant r \leqslant a_m \end{aligned}\right\} \tag{5.2}$$

The behaviour characteristics are described by the ordinary differential equations

$$\left.\begin{aligned} \frac{d\sigma_r}{dr} &= -\frac{1}{h}\left[\sigma_r \frac{dh}{dr} + \frac{h}{r}(\sigma_r - \sigma_\theta) + \rho\omega^2 rh\right] \\ \frac{d\sigma_\theta}{dr} &= \frac{\sigma_r - \sigma_\theta}{r} - \frac{\nu}{h}\sigma_r \frac{dh}{dr} - \nu\rho\omega^2 r \\ &\text{and} \\ \sigma_r &= s_1 \quad \text{at} \quad r = a_1 \\ \sigma_r &= s_m \quad \text{at} \quad r = a_m \end{aligned}\right\} \tag{5.3}$$

These equations were derived on the assumption of radially symmetric plane stress.

The behaviour and side constraints were defined by

$$\left.\begin{aligned}
&F(\sigma_r, \sigma_\theta) \leqslant \sigma_o \\
&\text{where} \\
&F(\sigma_r, \sigma_\theta) \equiv \max(|\sigma_r|, |\sigma_\theta|, |\sigma_r - \sigma_\theta|) \\
&h(r) \geqslant \varepsilon \qquad \text{for all} \quad r \in [a_2, a_{m-1}] \\
&a_1 < L \leqslant a_2 \leqslant U < a_{m-1}
\end{aligned}\right\} \qquad (5.4)$$

5.2 OPTIMAL CONTROL FORMULATION

The behaviour differential equations (5.3) are transformed into the optimal control formulation by the transformation equations.

$$\left.\begin{aligned}
x_1 &= \sigma_r \\
x_2 &= \sigma_\theta \\
x_3 &= h(r) \\
u &= \frac{dh}{dr}
\end{aligned}\right\} \qquad (5.5)$$

From (5.3, 5.5)

$$\left.\begin{aligned}
\frac{dx_1}{dr} &= -\frac{1}{x_3}\left[x_1 u + \frac{x_3}{r}(x_1 - x_2) + \rho\omega^2 r x_3\right] \\
\frac{dx_2}{dr} &= \frac{x_1 - x_2}{r} - \frac{\nu x_1 u}{x_3} - \nu\rho\omega^2 r \\
\frac{dx_3}{dr} &= u
\end{aligned}\right\} \qquad (5.6)$$

Equations (5.6) correspond to the state equations where

$$\left.\begin{aligned} \text{state vector:} \quad \underline{x} &= (\sigma_r, \sigma_\theta; \; h)_{1\times 3} \\ \text{control vector:} \quad \underline{u} &= \left(\frac{dh}{dr}\right)_{1\times 1} \end{aligned}\right\} \tag{5.7}$$

Therefore the state variables $x_i(r)$ $i = 1,2,3$ correspond to the stresses and disc thickness and the control $u(r)$ is given by the rate of change of thickness.

The constraint conditions (5.4) are given by

$$\left.\begin{aligned} &F(x_1, x_2) \leq \sigma_o \\ &\text{where} \\ &F(x_1, x_2) \equiv \max(|x_1|, |x_2|, |x_1 - x_2|) \\ &x_3 \geq \varepsilon \\ &L \leq a_2 \leq U \end{aligned}\right\} \tag{5.8}$$

The projection of the three-dimensional state space (x_1, x_2, x_3) onto the (x_1, x_2) subspace is given by the Tresca hexagon of figure (1.1a). All admissible states must lie within or on the hexagon. The hub radius a_2 in (5.8) has the status of a control parameter.

The control $u(r)$ is unbounded so that

$$|u(r)| \leq \infty \tag{5.9}$$

The transversality conditions associated with the differential system (5.3) are given by

$$\left.\begin{aligned} \theta^{(1)}: \quad x_1 = s_1, \quad x_3 = b_1 \quad &\text{at} \quad r = a_1 \\ \theta^{(m)}: \quad x_1 = s_m, \quad x_3 = b_m \quad &\text{at} \quad r = a_m \end{aligned}\right\} \tag{5.10}$$

The control $u(r)$ is said to be admissible if it is continuous in

(a_2, a_{m-1}) and satisfies constraint condition (5.9). Therefore for a given admissible control $u(r)$, $a_2 \leqslant r \leqslant a_{m-1}$ the state equations (5.6) in conjunction with the transversality conditions (5.10) possess a unique continuous solution which defines a trajectory in three-dimensional state space $(Ox_1x_2x_3)$ along which the states of the system are transferred between the end manifolds $\theta^{(1)}$, $\theta^{(m)}$. These trajectories are constrained to lie within the region of state space defined by (5.8). The problem is to determine an optimal control which affects such a transfer while minimising the weight integral.

$$W = \int_{a_1}^{a_m} 2\pi\rho r x_3 dr \tag{5.11}$$

The problem has been reduced to a constrained optimal control problem to which the Pontryagin formulation is applicable.

5.3 UNCONSTRAINED PROBLEM

The constraint set (5.8) is a necessary condition for the existence of solutions to the problem. This is proved by considering the one-dimensional unconstrained problem

$$\text{Minimise } W[x_3] = \int_{r_o}^{r_1} 2\pi\rho r x_3 dr; \quad x_3 \in E^1 \tag{5.12}$$

where

$$a_2 \leqslant r_o < r_1 \leqslant a_{m-1}$$

Let $x_3(r) = x_3^*(r)$, $r \varepsilon \left[r_o, r_1\right]$ be the minimising function in class C^2. Then it certainly minimises in the subclass

$$x_3(r) = x_3^*(r) + \varepsilon_o \eta(r); \quad \eta(r) \varepsilon C^2 \tag{5.13}$$

Therefore

$$F(\varepsilon_o) = W\left[x_3\right]$$

$$= W\left[x_3^*\right] + \varepsilon_o \int_{r_o}^{r_1} 2\pi\rho r\eta(r)dr \tag{5.14}$$

But, by definition, $F(\varepsilon_o)$ is a minimum at $\varepsilon_o = 0$.

Therefore

$$F'(0) = 0$$

So that

$$\int_{r_o}^{r_1} 2\pi\rho r\eta(r)dr = 0 \quad \text{for arbitrary } \eta(r) \varepsilon C^2 \tag{5.15}$$

But this is impossible and the problem has no finite solutions for unbounded $x_3(r)$.

5.4 CONSTRAINTS ON THICKNESS $x_3(r)$

Let

$$x_3(r) \geq \varepsilon \qquad \text{for all } r \varepsilon \left[r_o, r_1\right] \tag{5.16}$$

where

$$\left[r_o, r_1\right] \subseteq \left[a_2, a_{m-1}\right]$$

From (5.12)

$$W[x_3] \geq \pi\rho(r_1^2 - r_o^2)\varepsilon \tag{5.17}$$

Hence

$$\left.\begin{aligned} x_3^*(r) &= \varepsilon \quad \text{for all} \quad r \in [r_o, r_1] \\ W[x_3^*] &= \pi\rho(r_1^2 - r_o)^2\varepsilon \end{aligned}\right\} \tag{5.18}$$

Therefore the optimal trajectory lies on the boundary of the state constraint region $x_3 = \varepsilon$.

5.5 CONSTRAINED PROBLEM

Finally, the problem is considered in the presence of the constraint set (5.8).

From (5.1, 5.2, 5.5)

$$W = \pi\rho b_1(a_2^2 - a_1^2) + \pi\rho b_m(a_m^2 - a_{m-1}^2) + \int_{a_2}^{a_{m-1}} 2\pi\rho r x_3 dr \tag{5.19}$$

where

$$W = W(a_2, x_3)$$

W is a minimum when given $a_2 \in [L, U]$

$$x_3^*(r) = \varepsilon \qquad \text{for all} \quad r \in [a_2, a_{m-1}] \tag{5.20}$$

Hence

$$\text{Min} \int_{a_2}^{a_{m-1}} 2\pi\rho r x_3^* dr = \pi\rho(a_{m-1}^2 - a_2^2)\varepsilon \tag{5.21}$$

and

$$W = W(a_2) = \pi\rho b_1(a_2^2 - a_1^2) + \pi\rho b_m(a_m^2 - a_{m-1}^2) + \pi\rho(a_{m-1}^2 - a_2^2)\varepsilon$$

$$= \pi\rho\left[(b_1 - \varepsilon)a_2^2 + b_m(a_m^2 - a_{m-1}^2) + \varepsilon a_{m-1}^2 - b_1 a_1^2\right] \qquad (5.22)$$

This function of a_2 is to be minimised. Solutions exist only for bounded a_2 and are given by

$$\left.\begin{aligned} a_2^* &= L \quad \text{if } b_1 > \varepsilon \\ &= U \quad \text{if } b_1 < \varepsilon \end{aligned}\right\} \qquad (5.23)$$

The optimal control formulation of the problem is now considered.

5.6 MAXIMUM PRINCIPLE

The control characteristics of the structural system are described by the maximum principle of Pontryagin which defines the interaction between optimal control and optimal trajectory in state space.

The unconstrained Hamiltonian $\hat{H}$ is defined by

$$\hat{H}(\lambda_1,\lambda_2,\lambda_3;\, x_1,x_2,x_3,r;\, u) = -2\pi\rho r x_3 - \frac{\lambda_1(r)}{x_3}\left[x_1 u + \frac{x_3}{r}(x_1-x_2) + \rho\omega^2 r x_3\right]$$

$$+ \lambda_2(r)\left\{\frac{x_1 - x_2}{r} - \nu\,\frac{x_1 u}{x_3} - \nu\rho\omega^2 r\right\} + \lambda_3(r)\,.\,u \qquad (5.24)$$

Therefore the adjoint equations are

$$\left.\begin{aligned}
\frac{d\lambda_1}{dr} &\equiv -\frac{\partial\hat{H}}{\partial x_1} = (\lambda_1 + \nu\lambda_2)\frac{u}{x_3} + \frac{\lambda_1 - \lambda_2}{r} \\
\frac{d\lambda_2}{dr} &\equiv -\frac{\partial\hat{H}}{\partial x_2} = -\frac{\lambda_1 - \lambda_2}{r} \\
\frac{d\lambda_3}{dr} &\equiv -\frac{\partial\hat{H}}{\partial x_3} = 2\pi\rho r - (\lambda_1 + \nu\lambda_2)\frac{x_1 u}{x_3^2}
\end{aligned}\right\} \qquad (5.25)$$

These are derived on the assumption that the optimal trajectory lies within the interior of the state constraint domain (5.8)

$$\left.\begin{aligned}
F\big(x_1(r),\ x_2(r)\big) &< \sigma_o \\
x_3 &> \varepsilon
\end{aligned}\right\} \qquad (5.26)$$

The control $u(r)$ is unbounded, hence

$$\frac{\partial\hat{H}}{\partial u} = -(\lambda_1 + \nu\lambda_2)\frac{x_1}{x_3} + \lambda_3 = 0 \qquad (5.27)$$

this being the condition for maximising the Hamiltonian $\hat{H}$. The Hamiltonian (5.24) corresponds to a singular unbounded control. The Hamiltonian is linear in the control so that the optimal control must either lie at a bound or be such that (5.27) is satisfied. There are three possible boundary configurations for the optimal trajectory and are described below.

5.7 RESTRICTED MAXIMUM PRINCIPLE I

Suppose the optimal trajectory belongs to the boundary configuration

$$\left.\begin{array}{lll} F\big(x_1(r),\, x_2(r)\big) < \sigma_o & \text{for all} & r \in \left[r_e,\, r_\ell\right] \\ x_3 = \varepsilon & \text{for all} & r \in \left[r_e,\, r_\ell\right] \end{array}\right\} \tag{5.28}$$

where

$$a_2 \leq r_e < r_\ell \leq a_{m-1} \tag{5.29}$$

From (4.38)

$$\text{Define } p(\underline{x},\, r;\, u) = \nabla_{\underline{x}}(x_3 - \varepsilon) \cdot \frac{d\underline{x}}{dr} \tag{5.30}$$

$$= \frac{dx_3}{dr}$$

$$= u \tag{5.31}$$

From (4.38)

$$u = 0 \tag{5.32}$$

This is expected because $h \equiv x_3 = \varepsilon$ in $\left[r_e,\, r_\ell\right]$ implies $u \equiv \frac{dh}{dr} = 0$

Substituting (5.32) in (5.25) using (4.33)

$$\left.\begin{array}{l} \dfrac{d\lambda_1}{dr} = \dfrac{\lambda_1 - \lambda_2}{r} \\[2ex] \dfrac{d\lambda_2}{dr} = -\dfrac{\lambda_1 - \lambda_2}{r} \\[2ex] \dfrac{d\lambda_3}{dr} = 2\pi\rho r + \hat{\mu} \end{array}\right\} \tag{5.33}$$

Integrating

$$\left.\begin{array}{l} \lambda_1 = A + Br^2 \\ \lambda_2 = A - Br^2 \\ \lambda_3 = \pi\rho r^2 + \int \hat{\mu}(r)dr + C \end{array}\right\} \tag{5.34}$$

where A, B, C are constants of integration. The projection of the adjoint vector $\underline{\lambda}$ on $(\lambda_1,\, \lambda_2)$ subspace is a two-parameter family of parabolas whose foci lie on the axis of rotation.

Substituting (5.32) in state equations (5.6) and simplifying

$$\left.\begin{aligned} \frac{dx_1}{dr} &= -\frac{x_1 - x_2}{r} - \rho\omega^2 r \\ \frac{dx_2}{dr} &= \frac{x_1 - x_2}{r} - \nu\rho\omega^2 r \\ \frac{dx_3}{dr} &= 0 \end{aligned}\right\} \tag{5.35}$$

Integrating

$$\left.\begin{aligned} x_1 &= C_1 - \frac{C_2}{r^2} - \frac{3 + \nu}{8}\rho\omega^2 r^2 \\ x_2 &= C_1 + \frac{C_2}{r^2} - \frac{1 + 3\nu}{8}\rho\omega^2 r^2 \\ x_3 &= \varepsilon \end{aligned}\right\} \tag{5.36}$$

where C_1, C_2 are constants of integration. Eliminating r from (5.36)

$$\begin{aligned} (1 + 3\nu)x_1^2 - (3 + \nu)x_2^2 - 2(1 - \nu)x_1x_2 - 8C_1\nu x_1 + 8C_1x_2 \\ - 4C_1^2(1 - \nu) - 2(1 + \nu)^2 C_2\rho\omega^2 = 0 \end{aligned} \tag{5.37}$$

This defines a family of hyperbolas in (x_1, x_2) subspace whose centres lie on the line

$$\left.\begin{aligned} x_2 &= x_1 \\ x_3 &= \varepsilon \end{aligned}\right\} \tag{5.38}$$

This analysis is applicable to those parts of the optimal trajectory which lie on the boundary $x_3 = \varepsilon$.

5.8 RESTRICTED MAXIMUM PRINCIPLE II

The second possibility is

$$\left.\begin{array}{llll} F\big(x_1(r),\ x_2(r)\big) & = \sigma_o & \text{for all} & r \in [r_e,\ r_\ell] \\ x_3 & > \varepsilon & \text{for all} & r \in [r_e,\ r_\ell] \end{array}\right\} \tag{5.39}$$

where

$$a_2 \leqslant r_e < r_\ell \leqslant a_{m-1}$$

Let

$$\underline{\nabla}_x F = \left(\frac{\partial F}{\partial x_1},\ \frac{\partial F}{\partial x_2},\ 0\right) \tag{5.40}$$

From (4.36)

$$p(\underline{x},r;\ u) = -\frac{1}{x_3}\left[x_1 u + \frac{x_3}{r}(x_1 - x_2) + \rho\omega^2 r x_3\right]\frac{\partial F}{\partial x_1} + \left(\frac{x_1 - x_2}{r} - \frac{\nu x_1 u}{x_3} - \nu\rho\omega^2 r\right)\frac{\partial F}{\partial x_2} \tag{5.41}$$

Since the optimal trajectory lies on the boundary (5.39)

$$p(\underline{x},r;\ u) = 0 \tag{5.42}$$

Hence

$$\frac{u}{x_3} = -\frac{1}{x_1}\left[\left(\frac{x_1 - x_2}{r}\right)\frac{F_{x_1} - F_{x_2}}{F_{x_1} + \nu F_{x_2}} + \rho\omega^2 r\right] \tag{5.43}$$

where F_{x_1}, F_{x_2} denote partial derivatives of F with respect to x_1, x_2 respectively.

From (5.6, 5.43)

$$x_3(r) = x_3^o \exp\left\{-\int \frac{1}{x_1}\left[\left(\frac{x_1 - x_2}{r}\right)\frac{F_{x_1} - F_{x_2}}{F_x + \nu F_x} + \rho\omega^2 r\right]dr\right.$$

$$\text{for all} \quad r \in [r_e,\ r_\ell] \tag{5.44}$$

where x^o is a constant of integration.

Substituting (5.44) in (5.6) and simplifying

$$\left.\begin{aligned}
\frac{dx_1}{dr} &= -\frac{1+\nu}{r}\,\frac{(x_1-x_2)F_{x_2}}{F_{x_1}+\nu F_{x_2}} \\
\frac{dx_2}{dr} &= \frac{1+\nu}{r}\,\frac{(x_1-x_2)F_{x_1}}{F_{x_1}+\nu F_{x_2}} \\
\frac{dx_3}{dr} &= -\frac{x_3}{x_1}\left[\left(\frac{x_1-x_2}{r}\right)\frac{F_{x_1}-F_{x_2}}{F_{x_1}+\nu F_{x_2}} + \rho\omega^2 r\right]
\end{aligned}\right\} \qquad (5.45)$$

This two-parameter family of optimal trajectories is based on the assumption that F has continuous first partial derivatives on the boundary. This is true for most engineering yield conditions, in particular the Tresca yield condition, except at the vertices of the hexagon.

In matrix form the Hamiltonian (5.24) reduces to

$$\hat{H} = -2\pi\rho r x_3 + \underline{\lambda}\ \underline{f} \qquad (5.46)$$

where

$$\underline{\lambda} = (\lambda_1, \lambda_2, \lambda_3)$$

$$\underline{f} = \begin{pmatrix} -\dfrac{1}{x_3}\left[x_1 u + \dfrac{x_3}{r}(x_1-x_2) + \rho\omega^2 r x_3\right] \\[2ex] \dfrac{x_1-x_2}{r} - \dfrac{\nu x_1 u}{x_3} - \nu\rho\omega^2 r \\[2ex] u \end{pmatrix}$$

From (5.41)

$$\nabla_{\mathbf{x}} F \, \underline{f} = 0 \tag{5.47}$$

From the Weierstrass condition the Hamiltonian (5.46) must be maximised with respect to the control u, subject to the constraint condition (5.47).

Using the method of Lagrange multipliers

$$\lambda_i \frac{\partial f_i}{\partial u} + \alpha \frac{\partial F}{\partial x_i} \frac{\partial f_i}{\partial u} = 0$$

Therefore

$$\alpha = -\lambda_i \Big/ \frac{\partial F}{\partial x_i} \tag{5.48}$$

and

$$\frac{\lambda_1}{F_{x_1}} = \frac{\lambda_2}{F_{x_1}} = \frac{\lambda_3}{0}$$

Hence

$$\lambda_3 = 0 \tag{5.49}$$

From (5.46, 5.41)

$$\nabla_{\mathbf{x}} \hat{H} = \underline{\lambda} \begin{pmatrix} -\frac{1}{x_3}\left(u + \frac{x_3}{r}\right), & \frac{1}{r}, & \frac{x_1 u}{x_3^2} \\ \frac{1}{r} - \frac{\nu u}{x_3}, & -\frac{1}{r}, & \nu \frac{x_1 u}{x_3^2} \\ 0, & 0, & 0 \end{pmatrix} + (0, 0, -2\pi\rho r) \tag{5.50}$$

and

$$\nabla_x p = \begin{bmatrix} -\frac{1}{x_3}\left(u + \frac{x_3}{r}\right)F_{x_1} + \left(\frac{1}{r} - \frac{\nu u}{x_3}\right)F_{x_2} + \frac{d}{dr}F_{x_1} \\ \\ \frac{F_{x_1} - F_{x_2}}{r} + \frac{d}{dr}F_{x_2} \\ \\ \frac{x_1 u}{x_3^2}\left(F_{x_1} + \nu F_{x_2}\right) \end{bmatrix}^T \tag{5.51}$$

From (4.35)

$$\frac{d\underline{\lambda}}{dr} = -\nabla_x \hat{H} + \left(\frac{\partial H}{\partial u}\right)\left(\frac{\partial p}{\partial u}\right)^{-1}\nabla_x p \tag{5.52}$$

Substituting (5.24, 5.41, 5.49 - 5.51) in (5.52) and simplifying

$$\left.\begin{aligned} \frac{d\lambda_1}{dr} &= \frac{\lambda_1 - \lambda_2}{r} - \frac{\lambda_1 + \nu\lambda_2}{F_{x_1} + \nu F_{x_2}}\left[\frac{F_{x_1} - F_{x_2}}{r} - \frac{d}{dr}F_{x_1}\right] \\ \\ \frac{d\lambda_2}{dr} &= -\frac{\lambda_1 - \lambda_2}{r} + \frac{\lambda_1 + \nu\lambda_2}{F_{x_1} + F_{x_2}}\left[\frac{F_{x_1} - F_{x_2}}{r} + \frac{d}{dr}F_{x_2}\right] \\ \\ \frac{d\lambda_3}{dr} &= 2\pi\rho r = 0 \,^{\dagger} \end{aligned}\right\} \tag{5.53}$$

The analysis is applicable to a general yield criterion $F = F(x_1, x_2)$. These results are now interpreted for the Tresca yield criterion (5.8).

....

† This means that the axis of rotation $r = 0$ of the disc lies on (λ_1, λ_2) plane.

5.9 TRESCA YIELD CRITERION

On each branch of the Tresca hexagon (figure 1.1a), F_{x_1}, F_{x_2} are constant, therefore

$$\frac{d}{dr} F_{x_1} = \frac{d}{dr} F_{x_2} = 0 \tag{5.54}$$

Substituting (5.54) in (5.53) and simplifying

$$\left.\begin{aligned} \frac{d}{dr}\left(-\lambda_1 F_{x_2} + \lambda_2 F_{x_1}\right) &= (1+\nu)\frac{F_{x_1} + F_{x_2}}{F_{x_1} + \nu F_{x_2}}\left[\frac{-\lambda_1 F_{x_2} + \lambda_2 F_{x_1}}{r}\right] \\ \frac{d}{dr}\left(\lambda_1 + \lambda_2\right) &= 0 \end{aligned}\right\} \tag{5.55}$$

Integrating

$$\left.\begin{aligned} \lambda_1 + \lambda_2 &= D \\ -\lambda_1 F_{x_2} + \lambda_2 F_{x_1} &= Cr^{\alpha} \end{aligned}\right\} \tag{5.56}$$

where

$$\alpha = (1 + \nu)\,\frac{F_{x_1} + F_{x_2}}{F_{x_1} + \nu F_{x_2}}$$

C, D = constants of integration ($C > 0$).

Solving

$$\left.\begin{aligned} \lambda_1 &= \frac{DF_{x_1} - Cr^{\alpha}}{F_{x_1} + F_{x_2}} \\ \lambda_2 &= \frac{DF_{x_2} + Cr^{\alpha}}{F_{x_1} + F_{x_2}} \end{aligned}\right\} \tag{5.57}$$

Substituting (5.43 ,5.57) in (5.24) and simplifying

$$\hat{H} = -2\pi\rho r x_3 + C(1 + \nu)\frac{x_1 - x_2}{F_{x_1} + \nu F_{x_2}}\, r^{\alpha-1} \tag{5.58}$$

On FA, CD (figure 1.1a) the second term on the right of (5.58) is negative, while it is positive on EF, BC, DE, AB. Therefore optimal control must operate along the latter branches of the Tresca hexagon.

Consider states on DE

$$\left.\begin{aligned} x_2 &= x_1 - \sigma_o \\ 0 \leqslant x_1 &\leqslant \sigma_o \\ F_{x_1} &= 1 \\ F_{x_1} &= -1 \end{aligned}\right\} \tag{5.59}$$

Therefore from (5.57, 5.59) for finite λ_1, λ_2

$$C = D = 0 \tag{5.60}$$

Substituting (5.59) in (5.45)

$$\frac{dx_1}{dr} = \frac{1 + \nu}{1 - \nu}\frac{\sigma_o}{r} \tag{5.61}$$

Integrating

$$\left.\begin{aligned} x_1 &= \sigma_o \,\ell n\, a r^{\beta} \qquad a > 0 \\ x_2 &= \sigma_o(\ell n\, a r^{\beta} - 1) \end{aligned}\right\} \tag{5.62}$$

where

$$\beta = \frac{1 + \nu}{1 - \nu} > 1$$

Substituting (5.59, 5.62) in (5.44) and simplifying

$$x_3 = x_3^o \exp\left\{ -\frac{1}{\sigma_o} \int^r \frac{1}{\ell n\ ar^\beta} \left(\frac{2\sigma_o}{(1-\nu)r} + \rho\omega^2 r \right) dr \right. \tag{5.63}$$

$$u = -\frac{x_3^o}{\sigma_o\ \ell n\ ar^\beta} \left[\frac{2\sigma_o}{(1-\nu)r} + \rho\omega^2 r \right] \exp\left\{ -\frac{1}{\sigma_o} \int^r \frac{1}{\ell n\ ar^\beta} \times \left[\frac{2\sigma_o}{(1-\nu)r} + \rho\omega^2 r \right] dr \right\} \tag{5.64}$$

Equations (5.62 - 5.64) determine the state and control vectors on branch DE. From (5.59, 5.62)

$$\frac{1}{a} \leqslant r^\beta \leqslant \frac{e}{a} \tag{5.65}$$

This inequality cannot be satisfied for arbitrary values of the constant of integration a, hence optimal control cannot operate along DE. Similarly it cannot operate along AB either.

Therefore optimal control must operate along BC or EF. Consider states on EF.

$$\left. \begin{aligned} x_1 &= \sigma_o \\ 0 \leqslant x_2 &\leqslant \sigma_o \\ F_{x_1} &= 1 \\ F_{x_2} &= 0 \end{aligned} \right\} \tag{5.66}$$

Substituting (5.66) in (5.45) and simplifying

$$\frac{dx_2}{dr} = \frac{(1 + \nu)}{r}(\sigma_o - x_2)$$

$$\frac{dx_3}{dr} = -\frac{x_3}{\sigma_o}\left(\frac{\sigma_o - x_2}{r} + \rho\omega^2 r\right) \tag{5.67}$$

Integrating,

$$\left.\begin{aligned} x_2 &= \sigma_o - br^{-(1+\nu)}, \qquad b > 0 \\ x_3 &= x_3^o \exp \frac{1}{\sigma_o}\left[\frac{br^{-(1+\nu)}}{1 + \nu} - \frac{\rho\omega^2 r^2}{2}\right] \end{aligned}\right\} \tag{5.68}$$

where b is a constant of integration.

From (5.43, 5.68)

$$u = -\frac{x_3^o}{\sigma_o}\left[br^{-(2+\nu)} + \rho\omega^2 r\right] \exp \frac{1}{\sigma_o}\left[\frac{br^{-(1+\nu)}}{1 + \nu} - \frac{\rho\omega^2 r^2}{2}\right] \tag{5.69}$$

Equations (5.68, 5.69) determine the optimal trajectory and control on the branch EF defined by $x_1 = \sigma_o$. Equation (5.68) defines a monotonic decreasing function of $x_3(r)$ so that from (5.8)

$$x_3^o \geq \varepsilon \exp\left\{-\frac{1}{\sigma_o}\left[\frac{br_\ell^{-(1+\nu)}}{1 + \nu} - \frac{\rho\omega^2 r_\ell^{\,2}}{2}\right]\right\} \tag{5.70}$$

5.10 RESTRICTED MAXIMUM PRINCIPLE III

The final possibility is

$$\left.\begin{aligned} F\big(x_1(r), x_2(r)\big) &= \sigma_o \\ x_3(r) &= \varepsilon \end{aligned}\right\} \tag{5.71}$$

for all $r \in [r_e, r_\ell] \subseteq [a_2, a_{m-1}]$.

From (5.32, 5.43)

$$\frac{x_1 - x_2}{r} \frac{F_{x_1} - F_{x_2}}{F_{x_1} + \nu F_{x_2}} + \rho\omega^2 r = 0 \qquad (5.72)$$

Substituting (5.66) in (5.72)

$$br^{-(2+\nu)} + \rho\omega^2 r = 0 \qquad (5.73)$$

This clearly is inadmissible for all $r \in [r_e, r_\ell]$ and hence (5.71) is not a valid proposition.

5.11 OPTIMAL CONTROL RESULTS

The results derived thus far may be summarised as follows:

(i) $F(x_1(r), x_2(r)) < \sigma_o$ for all $r \in [a_1, a_2]$.

(ii) $F(x_1(r), x_2(r)) < \sigma_o$ for all $r \in [a_{m-1}, a_m]$.

(iii) $F(x_1(r), x_2(r)) = \sigma_o$ for all $r \in [a_2, a_{m-1}]$

(iv) $F(x_1(r), x_2(r)) < \sigma_o$ for all $r \in [r_e, r_\ell]$.

(v) $F(x_1(r), x_2(r)) = \sigma_o$ for all $r \in [r_\ell, a_{m-1}]$

Conditions (iii, v) correspond to $|\sigma_r| = \sigma_o$ with

$$h^*(r) = h_o \exp \frac{1}{\sigma_o} \left\{ \frac{b}{(1 + \nu)} r^{-(1+\nu)} - \frac{\rho\omega^2 r^2}{2} \right\}$$

where the constant h_o satisfies the condition

$$h_o > \varepsilon \exp - \frac{1}{\sigma_o} \left[\frac{b}{(1 + \nu)} r^{-(1+\nu)} - \frac{\rho\omega^2 r_\ell^2}{2}\right]$$

Condition (iv) corresponds to $h^*(r) = \varepsilon$. The analysis given here is essentially a modification of an earlier version proposed by de Silva [212]. This chapter is concluded with a brief description of the jump conditions (see section 4.7) on the adjoint vector. These are the conditions at the entry and leaving points for arcs of the optimal trajectory on the boundary of the state constraint region.

5.12 JUMP CONDITIONS

The adjoint vector is continuous at the entry point $r = r_e$

$$\underline{\lambda}(r_e - 0) = \underline{\lambda}(r_e) \tag{5.74}$$

Therefore from (5.34, 5.57, 5.66)

$$\left.\begin{aligned} A + Br_e^2 &= D - Cr_e^{1+\nu} \\ A - Br_e^2 &= Cr_e^{1+\nu} \end{aligned}\right\} \tag{5.75}$$

But the adjoint vector is discontinuous on leaving (4.41)

$$\underline{\lambda}(r_\ell + 0) = \underline{\lambda}(r_\ell) - \mu(r_\ell)\underline{\nabla}F \tag{5.76}$$

where (see Leitmann [207], Chapter 4) from (5.41)

$$\mu(r) = \underline{\lambda}\left(\frac{\partial \underline{f}}{\partial u}\right)\left(\frac{\partial p}{\partial u}\right)^{-1}$$

$$= \frac{\lambda_1 + \nu\lambda_2}{F_{x_1} + \nu F_{x_2}} \quad \text{for all } r \in \left[r_e, r_\ell\right] \tag{5.77}$$

Substituting (5.66) in (5.57, 5.77)

$$\mu(r) = D - (1 - \nu)Cr^{(1+\nu)}, \quad r_e \leqslant r \leqslant r_\ell \tag{5.78}$$

Substituting (5.78) in (5.76), using (5.34, 5.66)

$$\left.\begin{aligned} A' + B'r_\ell^2 &= D' - C'r_\ell^{(1+\nu)} - D' + (1-\nu)C'r_\ell^{(1+\nu)} \\ &= -\nu C'r_\ell^{(1+\nu)} \\ A' - Br_\ell^2 &= C'r_\ell^{(1+\nu)} \end{aligned}\right\} \tag{5.79}$$

Equations (5.75, 5.79) determine the adjoint vectors on leaving in terms of the hyperbolas on entry. One of the major difficulties lies in determining these entry and leaving points.

CHAPTER 6

OPTIMAL VIBRATION MODES OF DISCS

6.1 INTRODUCTION

This chapter* is essentially a continuation of the research programme described in earlier chapters into analytical and computational procedures based on the methods of mathematical programming for optimising structural systems in the presence of design constraints. As a first step in this direction, the weight of a turbine disc was minimised subject to specified behaviour and side constraints. The behaviour constraints were restricted to a consideration that the stresses should be below the yield stress for the material of the disc while the vibrational frequencies were constrained to be outside given critical resonance bands. The side constraints, on the other hand, imposed restrictions on the dimensions and tolerances of the disc. The problem was formulated as a general problem in optimal control theory with the addition of inequality constraints on the state variables. The state and control variables were given by functions describing the variations in the thickness, stress and deformation fields, with the frequencies corresponding to control parameters.

The continuous formulation was described by the maximum principle of Pontryagin, while for purposes of simplicity, the numerical computations were based on a discretised non-linear programming approximation obtained by using a piecewise linear representation for the thickness variables. The non-linear programming formulation was characterised by non-analytic "black box" type constraints for the behaviour constraints corresponding to functional inequality constraints. These, together with the side constraints, were represented in design

....

* An improved version of this chapter is given in de Silva [239].

space by constraint hypersurfaces which formed a composite constraint surface. The weight was represented by a family of quadratic contours of constant weight and the problem consisted of determining the least weight contour within the feasible region enveloped by the composite constraint surface. The solutions were based on a modified "steepest descent-alternate step" mode of travel in design space developed by Schmit et al [70]: this being one of the most powerful methods available at the time for handling structural optimization problems with non-analytic constraints. This chapter describes further developments in this direction by considering the dual problem of maximising a specified linear combination of the frequencies of vibration of the turbine disc with a constraint on the total weight. The problem is again formulated as a general optimal control problem in the presence of inequality constraints on the state variables. Significant progress has been made in solving the problem using analytical procedures based on the maximum principle of Pontryagin. The adjoint systems of the Pontryagin formulation are solved using perturbation techniques which give rise to fourth order differential equations. These are solved using WKB expansions [213]. These analytical procedures transform the problem into a non-linear programming problem which can then be solved using the Heaviside penalty function transformations [76,80] of non-linear programming in conjunction with Rosenbrock's hill-climbing techniques [129].

This chapter includes a description of the synthesis procedures used to implement the optimized design cycles on an English Electric KDF9 computer together with a preliminary discussion of results.

6.2 OPTIMAL CONTROL FORMULATION

The behaviour analysis for the disc was described in section (3.2). The basic equations are summarised below for purposes of ready reference.

The state equations for the system are given by

$$\left.\begin{aligned}
\frac{dx_i}{dr} &= x_{i+1} \qquad i = 1,2,3 \\
\frac{dx_4}{dr} &= \left[\frac{12(1-\nu^2)\rho p^2}{Ex_5^2} + \frac{3n^2\nu u}{x_5 r^2} - \frac{9n^2 x_6}{x_5 r^3} + \frac{6n^2\nu x_6}{x_5^2 r^2} - \frac{n^2(n^2-4)}{r^4}\right]x_1 \\
&\quad - \left[\frac{3\nu u}{x_5 r} - \frac{6n^2+3}{x_5 r^2}x_6 + \frac{6\nu x_6^2}{x_5^2 r} + \frac{2n^2+1}{r^3}\right]x_2 - \\
&\quad \left[\frac{3u}{x_5} + \frac{6+3\nu}{x_5 r}x_6 + \frac{6x_6^2}{x_5^2} - \frac{2n^2+1}{r^2}\right]x_3 - 2\left(\frac{3x_6}{x_5} + \frac{1}{r}\right)x_4 \\
\frac{dx_5}{dr} &= x_6 \\
\frac{dx_6}{dr} &= u
\end{aligned}\right\} \qquad (6.1)$$

where

$$\left.\begin{aligned}
x_i &= \frac{d^{(i-1)}w}{dr^{(i-1)}} \qquad i = 1,2,3,4 \\
x_{i+4} &= \frac{d^{(i-1)}h}{dr^{(i-1)}} \qquad i = 1,2 \\
u &= \frac{d^2h}{dr^2}
\end{aligned}\right\} \qquad (6.2)$$

The state and control variables and parameters are defined by

state vector: $\underset{\approx}{x} = (x_1, \ldots, x_6) = \left(W, \frac{dW}{dr}, \frac{d^2W}{dr^2}, \frac{d^3W}{dr^3};\ h, \frac{dh}{dr}\right)$

control vector: $u = \frac{d^2h}{dr^2}$

control parameter vector: $\underset{\sim}{p} = (p_1, \ldots, p_\ell\ ; a_2)$

The p_i, $i = 1,2,\ldots,\ell$ are the first ℓ vibrational frequencies of the disc. The transversality conditions at $r = a_1$, a_m are given by

$$\left.\begin{aligned}
&x_1(a_1) = x_2(a_1) = 0 \\
&x_3(a_m) + \nu\left[\frac{x_2(a_m)}{a_m} - \frac{n^2}{a_m^2}\, x_1(a_m)\right] = 0 \\
&x_4(a_m) + \frac{x_3(a_m)}{a_m} - \frac{x_2}{a_m^2}(a_m) - \frac{n^2}{a_m^2}\, x_2(a_m) + \frac{2n^2 x_1(a_m)}{a_m^3} \\
&\qquad + \frac{n^2(1-\nu)}{a_m^2}\left[x_2(a_m) - \frac{x_1(a_m)}{a_m}\right] = 0
\end{aligned}\right\} \tag{6.3}$$

These correspond to the initial and terminal transversality conditions. The state and control inequality constraints are given by

$$\left.\begin{aligned}
&x_5 \geq \varepsilon \qquad \text{for all } r \in \left[a_2, a_{m-1}\right] \\
&L \leq a_2 \leq U \\
&\int_{a_1}^{a_m} 2\pi\rho r x_5\, dr \leq W_o
\end{aligned}\right\} \tag{6.4}$$

where W_o is a given upper bound on the weight.

The merit criterion is defined by a function of the form

$$G(p) = \sum_{i=1}^{\ell} \pm c_i p_i \tag{6.5}$$

where the coefficients c_i are weighting factors based on the Gaussian distribution function

$$\left.\begin{aligned} c_i &= \Phi\left(\frac{p_i - p_1}{p_i}\right) \qquad i = 1,\ldots,\ell \\ \Phi(t) &= \frac{1}{\sqrt{2\pi}} e^{-t^2/2} \end{aligned}\right\} \tag{6.6}$$

so that

$$|c_1| > |c_2| > \ldots\ldots > |c_\ell|$$

The frequencies p_i are assumed to be arranged in ascending order, so that

$$p_1 < p_2 < \ldots\ldots < p_\ell$$

From engineering considerations, the designs must avoid specified frequency bands centred on given resonance frequencies $p_1^o, \ldots, p_\ell^o$.

Then

$$\left.\begin{aligned} a_i &= +\,|c_i| \quad \text{if } p_i > p_i^o \; ; \; i = 1,\ldots,\ell \\ &= -\,|c_i| \quad \text{if } p_i < p_i^o \; ; \; i = 1,\ldots,\ell \end{aligned}\right\} \tag{6.7}$$

where

$$p_1^o < p_2^o < \ldots\ldots < p_\ell^o$$

So that (6.5) gives

$$G(\underline{p}) = \sum_{i=1}^{\ell} a_i p_i \tag{6.8}$$

The initial values for p_i are obtained from experimental data for standard turbine design configurations. When one of these p_i is to the right of the resonance band centred on p_i^o, the frequency must be maximised to move p_i away from p_i^o. Similarly when $p_i < p_o^o$ for some $i \in [1,\ell]$ the corresponding p_i must be minimised to move the optimized designs away from p_i^o. For most design calculations, the lowest frequency p_1 is the most significant, with the others of rapidly decreasing importance. This is ensured by the selection of the c_i according to (6.6). For purposes of simplicity, the c_i are calculated at the standard configurations and are assumed constant during the synthesis.

6.3 THE PONTRYAGIN FORMULATION

The unconstrained Hamiltonian is given by

$$\begin{aligned}\hat{H}(\underline{\lambda};\underline{x};r;u) = \sum_{i=1}^{3} \lambda_i x_{i+1} + \lambda_4 \Bigg[\Bigg(& \frac{12(1-\nu^2)}{Ex_5^2}\rho p^2 + \frac{3n^2\nu u}{x_5 r^2} - \frac{9n^2 x_6}{x_5 r^3} + \\ & \frac{6n^2\nu x_6^2}{x_5^2 r^2} - \frac{n^2(n^2-4)}{r^4}\Bigg) x_1 - \Bigg(\frac{3\nu u}{x_5 r} - \frac{6n^2+3}{x_5 r^2} x_6 + \\ & \frac{6\nu x_6^2}{x_5^2 r} + \frac{2n^2+1}{r^3}\Bigg) x_2 - \Bigg(\frac{3u}{x_5} + \frac{6+3\nu}{x_5 r} x_6 + \frac{6x_6^2}{x_5^2} - \end{aligned}$$

$$\left.\frac{2n^2+1}{r^2}\right)x_3 - 2\left(\frac{3}{x_5}x_6 + \frac{1}{r}\right)x_4\Bigg] + \lambda_5 x_6 + \lambda_6 u \qquad (6.9)$$

where $\lambda_i(r)$; i = 1, ..., 6 are the components of the adjoint vector. Control u(r) is unbounded and continuous in $\left[a_2, a_{m-1}\right]$, so that from the maximum principle

$$\frac{\partial \hat{H}}{\partial u} \equiv \lambda_4\left(\frac{3n^2 \nu x_1}{x_5 r^2} - \frac{3\nu x_2}{x_5 r} - \frac{3x_3}{x_5}\right) + \lambda_6 = 0 \qquad (6.10)$$

The solutions are based on the following representations for the optimal trajectory:

(i) optimal trajectory lies within the interior of the state constraint region $x_5 > \varepsilon$.

(ii) optimal trajectory lies on the boundary $x_5 = \varepsilon$ for which the restricted maximum principle is applicable.

A detailed consideration of these cases is presented below.

6.4 INTERIOR OF CONSTRAINT REGION

For $x_5 > \varepsilon$, the adjoint equations are given by

$$\frac{d\lambda_1}{dr} = -\frac{\partial H}{\partial x_1} = -\lambda_4 A$$

$$\frac{d\lambda_2}{dr} = -\frac{\partial H}{\partial x_2} = -\lambda_1 + \lambda_4 B$$

$$\frac{d\lambda_3}{dr} = -\frac{\partial H}{\partial x_3} = -\lambda_2 + \lambda_4 C$$

$$\frac{d\lambda_4}{dr} = -\frac{\partial H}{\partial x_4} = -\lambda_3 + \lambda_4 D$$

$$\frac{d\lambda_5}{dr} = -\frac{\partial H}{\partial x_5} = -\lambda_4 E$$

$$\frac{d\lambda_6}{dr} = -\frac{\partial H}{\partial x_6} = -\lambda_4 F - \lambda_5 \tag{6.11}$$

where

$$A = \frac{12(1-\nu^2)\rho p^2}{E x_5^2} + \frac{3n^2\nu u}{x_5 r^2} - \frac{9n^2 x_6}{x_5 r^3} + \frac{6n^2\nu x_6^2}{x_5^2 r^2} - \frac{n^2(n^2-4)}{r^4}$$

$$B = \frac{3\nu u}{x_5 r} - \frac{6n^2+3}{x_5 r^2} x_6 + \frac{6\nu x_6^2}{x_5^2 r} + \frac{2n^2+1}{r^3}$$

$$C = \frac{3u}{x_5} + \frac{6+3\nu}{x_5 r} x_6 + \frac{6x_6^2}{x_5^2} - \frac{2n^2+1}{r^2}$$

$$D = 2\left(\frac{3x_6}{x_5} + \frac{1}{r}\right)$$

$$E = \left[-\frac{24(1-\nu^2)\rho p^2}{E x_5^3} - \frac{3n^2\nu u}{x_5^2 r^2} + \frac{9n^2 x_6}{x_5^2 r^3} - \frac{12n^2\nu x_6^2}{x_5^3 r^2}\right] x_1 - \left(-\frac{3\nu u}{x_5^2 r} + \frac{6n^2+3}{x_5^2 r^2} x_6 - \frac{12\nu x_6^2}{x_5^3 r}\right) x_2 - \left(-\frac{3u}{x_5^2} - \frac{6+3\nu}{x_5^2 r} x_6 - \frac{12 x_6^2}{x_5^3}\right) x_3 + \frac{6x_6}{x_5^2} x_4$$

$$F = \left(-\frac{9n^2}{x_5 r^3} + \frac{12n^2 \nu x_6}{x_5^2 r^2}\right) x_1 - \left(-\frac{6n^2+3}{x_5 r^2} + \frac{12\nu x_6}{x_5^2 r}\right) x_2 -$$

$$\left(\frac{6+3\nu}{x_5 r} + \frac{12 x_6}{x_5^2}\right) x_3 - \frac{6x_4}{x_5}$$

Consider the series solutions of the form

$$\lambda_i = \sum_{j=0}^{\infty} \lambda_{ij}\, \eta^j \qquad i = 1,2,\ldots,6 \tag{6.12}$$

where η is a small parameter.

Assume λ_4 small. Substituting (6.12) in (6.10, 6.11) gives

$$\left.\begin{aligned} \lambda_{40} &= \lambda_{50} = \lambda_{60} = 0 \\ \lambda_{10} &= \lambda_1^o \\ \lambda_{20} &= -\lambda_1^o r + \lambda_2^o \\ \lambda_{30} &= \lambda_1^o \frac{r^2}{2} - \lambda_2^o r + \lambda_3^o \end{aligned}\right\} \tag{6.13}$$

Therefore the adjoint vector is given by

$$\left.\begin{aligned} \lambda_1 &= \lambda_1^o + O(\eta) \\ \lambda_2 &= -\lambda_1^o r + \lambda_2^o + O(\eta) \\ \lambda_3 &= \lambda_1^o \frac{r^2}{2} - \lambda_2^o r + \lambda_3^o + O(\eta) \\ \lambda_4 &= O(\eta) \\ \lambda_5 &= O(\eta) \\ \lambda_6 &= O(\eta) \end{aligned}\right\} \tag{6.14}$$

For consistency

$$|D| \longrightarrow \infty \tag{6.15}$$

Therefore,

$$\frac{3}{h}\frac{dh}{dr} + \frac{1}{r} \simeq k ; \tag{6.16}$$

where $|k|$ is a large constant, therefore

$$\left.\begin{aligned} h(r) &\simeq \frac{C}{r^{1/3}} e^{kr/3}; \quad C > 0 \\ &\text{and} \\ h'(r) &\simeq \frac{k}{3} h \\ h''(r) &\simeq \frac{k^2}{9} h \end{aligned}\right\} \tag{6.17}$$

These determine the optimal thickness for subintervals of $[a_2, a_{m-1}]$ for which $h(r) > \varepsilon$. The proof of condition $|k|$ large is given in section 6.6.

Therefore (6.14, 6.17) determine a compatible set of solutions for the adjoint equations (6.11).

Substituting (6.16, 6.17) in (6.1) and simplifying using (6.2)

$$\frac{d^4W}{dr^4} + 2k\frac{d^3W}{dr^3} + k^2\frac{d^2W}{dr^2} + \frac{\nu k^2}{r}\frac{dW}{dr} - \left[\frac{12(1-\nu^2)\rho p^2}{Eh^2} + \frac{n^2\nu k^2}{r^2}\right]W = 0 \tag{6.18}$$

The solutions to this equation are given below.

Case (1a): $k < 0$

Put $x = -k(r - a_2)$, $|k| \longrightarrow \infty$

$$\frac{d^4W}{dx^4} - 2\frac{d^3W}{dx^3} + \frac{d^2W}{dx^2} - \Lambda^4 f(x)W = 0 \tag{6.19}$$

where

$$\left.\begin{aligned} \Lambda^4 &= e^{-2ka_2/3} \quad \text{(large)} \\ f(x) &= \frac{12(1-\nu^2)\rho p^2}{EC^2|k|^{14/3}}\left(-ka_2 + x\right)^{2/3} e^{2/3 x} > 0 \end{aligned}\right\} \tag{6.20}$$

Put

$$W = e^{x/2}\, u(x) \tag{6.21}$$

This gives

$$\frac{d^4u}{dx^4} - \frac{1}{2}\frac{d^2u}{dx^2} + \left[\frac{1}{16} - \Lambda^4 f(x)\right]u = 0 \tag{6.22}$$

Therefore the WKB solutions are given by [213]

$$u(x) = g_o(x)\, e^{\Lambda\phi(x)}\left\{1 + \frac{g_1(x)}{\Lambda} + \frac{g_2(x)}{\Lambda^2} + \cdots\right\} \tag{6.23}$$

Substituting (6.23) in (6.22) and equating to zero coefficients of Λ^4, Λ^3, ..., gives

$$\left.\begin{aligned} \phi_s' &= \{f(x)\}^{1/4}\, e^{is\pi/2} \qquad s = 0,1,2,3 \\ g_o &= \{f(x)\}^{-3/8} \end{aligned}\right\} \tag{6.24}$$

Hence

$$W(x) = \sum_{s=0}^{3} \alpha_s\, e^{x/2}\left[f(x)\right]^{-3/8} \exp\left[\Lambda e^{is\pi/2}\int^{x}\left\{f(x)\right\}^{1/4} dx\right] \times \left(1 + O\left(\frac{1}{\Lambda}\right)\right) \tag{6.25}$$

where α_s, s = 0,1,2,3 are constants of integration.

Case (1b): $k > 0$

Put $x = k(r - a_2)$; $k \longrightarrow \infty$

$$\frac{d^4W}{dx^4} + 2\,\frac{d^3W}{dx^3} + \frac{d^2W}{dx^2} \simeq 0$$

Hence

$$W(r) = \alpha_4 + \alpha_2 r + (\alpha_6 + \alpha_7 r)e^{-kr} \tag{6.26}$$

where α_4, α_5, α_6, α_7 are constants of integration. Equations (6.25, 6.26) determine the solutions to (6.18). The state and control variables are given by (6.2, 6.17, 6.25, 6.26). These equations in conjunction with (6.14) determine the complete representation for the system when the optimal trajectory belongs to the interior of the state constraint region.

The corresponding equations when the optimal trajectory belongs to the boundary are now considered.

6.5 BOUNDARY OF CONSTRAINT REGION

The restricted maximum principle is applied to arcs of the optimal trajectory lying on the state constraint boundary.

$$x_5(r) = \varepsilon \quad \text{for all} \quad r \in \left[r_e, r_\ell\right] \tag{6.27}$$

where

$$a_2 < r_e < r_\ell < a_{m-1}$$

Therefore

$$\nabla \underline{x}(x_5 - \varepsilon) = (0, 0, 0, 0, 1, 0)$$

$p \doteq$ scalar product of $\nabla_x(x_5 - \varepsilon)$ with the right hand side of state equations (6.1)

$= x_6$

Therefore

$$\left.\begin{aligned} x_6 &= 0 \\ u &= 0 \end{aligned}\right\} \tag{6.28}$$

Substituting in state equations (6.1) and simplifying

$$\frac{d^4W}{dr^4} + \frac{2}{r}\frac{d^3W}{dr^3} - \frac{2n^2+1}{r}\frac{d^2W}{dr^2} + \frac{2n^2+1}{r^3}\frac{dW}{dr} + \left[\frac{n^2(n^2-4)}{r^4} - \frac{12(1-\nu^2)\rho p^2}{E\varepsilon^2}\right]W = 0 \tag{6.29}$$

and

$$W(r) = \alpha_8 J_n(\Omega r) + \alpha_9 Y_n(\Omega r) + \alpha_{10} I_n(\Omega r) + \alpha_{11} K_n(\Omega r) \tag{6.30}$$

where

$$\Omega^4 = \frac{12(1-\nu^2)\rho p^2}{E\varepsilon^2}$$

State and control variables are given by (6.2, 6.27, 6.28, 6.30). $J_n(\Omega r)$, $Y_n(\Omega r)$ are Bessel functions and $I_n(\Omega r)$, $K_n(\Omega r)$ are the modified Bessel functions. α_8, α_9, α_{10}, α_{11} are constants of integration.

6.6 OPTIMAL THICKNESS PATTERNS

The optimal thickness is given by figures (6.1, 6.2, 6.3)

$$\left.\begin{aligned} h^*(r) &= h^-(r) && a_2 \leq r \leq r_e \\ &= \varepsilon && r_e \leq r \leq r_\ell \\ &= h^+(r) && r_\ell \leq r \leq a_{m-1} \end{aligned}\right\} \tag{6.31}$$

But from physical continuity conditions

$$\left.\begin{aligned} h^-(a_2) &= b_1; & h^-(r_e) &= \varepsilon \\ h^+(r_\ell) &= \varepsilon\ ; & h^+(a_{m-1}) &= b_m \end{aligned}\right\} \tag{6.32}$$

Therefore from (6.17)

$$b_1 = \frac{C^-}{a_2^{1/3}} \; e^{k^- a_2/3}$$

$$\varepsilon = \frac{C^-}{r_e^{1/3}} \; e^{k^- r_e/3}$$

So that

$$k^- = \frac{3}{a_2 - r_e} \; \ell n \left[\frac{b_1}{\varepsilon} \left(\frac{a_2}{r_e} \right)^{1/3} \right] \tag{6.33}$$

Therefore

$$|k^-| \longrightarrow \infty \quad \text{as} \quad \varepsilon \longrightarrow 0+ \tag{6.34}$$

Again,

$$b_m = \frac{C^+}{a_{m-1}^{1/3}} \; e^{k^+ a_{m-1}/3}$$

$$\varepsilon = \frac{C^+}{r_\ell^{1/3}} \; e^{k^+ r_\ell/3}$$

Therefore

$$k^+ = \frac{3}{a_{m-1} - r_\ell} \ln\left[\frac{b_m}{\varepsilon}\left(\frac{a_{m-1}}{r}\right)^{1/3}\right] \tag{6.35}$$

$$\rightarrow \infty \quad \text{as} \quad \varepsilon \rightarrow 0+ \tag{6.36}$$

Conditions (6.34, 6.35) establish the validity of the result that $|k|$ must be large. Equations (6.32 - 6.36; 6.17) also establish the continuity of $x_5 \equiv h$, $x_6 \equiv \frac{dh}{dr}$ at $r = r_e, r_\ell$, which is a necessary condition for the analysis to be valid. This is demonstrated below:

From (6.33, 6.34, 6.17),

$$h^-(r) = \frac{C^-}{r^{1/3}} e^{k^- r/3}$$

$$= \varepsilon\left(\frac{r_e}{r}\right)^{1/3} e^{-k^-(r_e - r)/3}$$

$$\rightarrow \varepsilon \quad \text{as} \quad r \rightarrow r_e - 0. \tag{6.37}$$

Therefore from (6.31, 6.32, 6.37)

$h^-(r)$ is continuous at $r = r_e$. Similarly $h^+(r)$ is continuous at $r = r_\ell$.

Again, $h'(r) \approx \frac{k}{3} h$, implies the continuity of $h'(r)$ at $r = r_e, r_\ell$.

6.7 SIDE CONSTRAINTS

These represent constraints on the geometrical configuration of of the disc. From figures (6.2, 6.3)

$$r_\ell \geq \frac{1}{k^+} = \frac{a_{m-1} - r_\ell}{3} \left[\ell n \frac{b_m}{\varepsilon} \left(\frac{a_{m-1}}{r_\ell} \right)^{1/3} \right]^{-1}$$

$$r_\ell \geq \frac{a_{m-1}}{3 \ell n \frac{b_m}{\varepsilon} \left(\frac{a_{m-1}}{r_\ell} \right)^{1/3} + 1} \longrightarrow 0 \quad \text{as} \quad \varepsilon \longrightarrow 0+$$

So that

$$0 \leq r_\ell < a_{m-1} \tag{6.38}$$

Again

$$a_2 < r_e < r_\ell \tag{6.39}$$

The weight is given by

$$\int_{a_1}^{a_m} 2\pi\rho r h(r) dr = \int_{a_1}^{a_2} 2\pi\rho r b_1 dr + \int_{a_2}^{r_e} 2\pi\rho r h^-(r) dr + \int_{r_e}^{r_\ell} 2\pi\rho r \varepsilon dr$$

$$+ \int_{r_\ell}^{a_{m-1}} 2\pi\rho r h^+(r) dr + \int_{a_{m-1}}^{a_m} 2\pi\rho r b_m dr$$

$$= \pi\rho b_1 (a_2^2 - a_1^2) + \pi\rho b_m (a_m^2 - a_{m-1}^2) + \pi\rho\varepsilon (r_\ell^2 - r_e^2)$$

$$+ 2\pi\rho \int_{a_2}^{r_e} r h^-(r) dr + 2\pi\rho \int_{r_\ell}^{a_{m-1}} r h^+(r) dr$$

Therefore the constraint on the weight is given by

$$f_1(a_2, r_e, r_\ell) \leq 0 \tag{6.40}$$

where

$$f_1(a_2, r_e, r_\ell) \equiv \pi\rho b_1(a_2^2 - a_1^2) + \pi\rho b_m(a_m^2 - a_{m-1}^2) + \pi\rho\varepsilon(r_\ell^2 - r_e^2)$$

$$+ 2\pi\rho\int_{a_2}^{r_e} rh^-(r)dr + 2\pi\rho\int_{r_\ell}^{a_{m-1}} rh^+(r)dr - W_o$$

These integrals are evaluated using standard numerical integration procedures [214].

The side constraints are given by (6.38 - 6.40) and their two-dimensional representation in the (r_e, r_ℓ) plane is shown in figure (6.4).

6.8 BEHAVIOUR CONSTRAINTS

The radial deformations within the subintervals $[a_1, a_2]$, $[a_{m-1}, a_m]$ are given by

$$\left.\begin{aligned} W(r) &= \alpha_{12}J_n(\Omega r) + \alpha_{13}Y_n(\Omega r) + \alpha_{14}I_n(\Omega r) + \alpha_{15}K_n(\Omega r); \\ &\qquad\qquad a_1 \leqslant r \leqslant a_2 \\ &= \alpha_{16}J_n(\Omega r) + \alpha_{17}Y_n(\Omega r) + \alpha_{18}I_n(\Omega r) + \alpha_{19}K_n(\Omega r); \\ &\qquad\qquad a_{m-1} \leqslant r \leqslant a_m \end{aligned}\right\} \qquad (6.41)$$

where $\alpha_{12}, \ldots, \alpha_{19}$ are constants of integration [see equations 6.25, 6.26, 6.30]. The behaviour requirements are given by eliminating the constants of integration $(\alpha_0, \alpha_1, \ldots, \alpha_{19})$ from equations (6.25, 6.26, 6.30, 6.41). The boundary conditions are obtained from (6.2, 6.3) and the continuity of W, $\frac{dW}{dr}$, $\frac{d^2W}{dr^2}$, $\frac{d^3W}{dr^3}$ at $r = a_2$, r_e, r_ℓ, a_{m-1}. These arise from continuity requirements for the state vector. They are also necessary physical conditions for the continuity of deflection, slope, bending and shear forces. The elimination process gives a (20 × 20) determinantal equation of the form

$$f_2(a_2, r_e, r_\ell, p) \equiv \det \begin{bmatrix} \underline{A}_{11} & \underline{0} & \underline{0} & \underline{A}_{14} & \underline{0} \\ \underline{A}_{21} & \underline{0} & \underline{A}_{23} & \underline{0} & \underline{0} \\ \underline{0} & \underline{A}_{32} & \underline{A}_{33} & \underline{0} & \underline{0} \\ \underline{0} & \underline{A}_{42} & \underline{0} & \underline{0} & \underline{A}_{45} \\ \underline{0} & \underline{0} & \underline{0} & \underline{0} & \underline{B}_1 \\ \underline{0} & \underline{0} & \underline{0} & \underline{B}_2 & \underline{0} \end{bmatrix} = 0 \qquad (6.42)$$

where $\underline{A}_{ij}$ are 4 × 4 submatrices, while $\underline{B}_1$, $\underline{B}_2$ are of order 2 × 4.

The function f_2 is a polynomial in the frequency so that it can be written in the form

$$f_2 \equiv \sum_i \mu_i(a_2, r_e, r_\ell)p^i = 0 \qquad (6.43)$$

Therefore the frequencies correspond to the roots of this polynomial

$$\underline{p} = \underline{p}(a_2, r_e, r_\ell) \qquad (6.44)$$

From (6.5)

$$G(\underline{p}) \rightarrow f_o(a_2, r_e, r_\ell) \qquad (6.45)$$

The vibrational frequencies are introduced into the synthesis procedures through equation (6.42) which is computed numerically using standard triangularisation procedures.

6.9 NONLINEAR PROGRAMMING FORMULATION

The nonlinear programming transformation is given by

$$\text{Maximise } G(\underline{p}) \quad \text{subject to:} \quad \left.\begin{array}{l} f_1(a_2, r_e, r_\ell) \leq 0 \\ L \leq a_2 \leq U \\ a_2 < r_e < r_\ell < a_{m-1} \\ f_2(a_2, r_e, r_\ell, \underline{p}) = 0 \end{array}\right\} \qquad (6.46)$$

This is solved by transforming the problem into a series of unconstrained optimization problems using the Heaviside penalty function transformation [76, 80]. These unconstrained problems are solved using Rosenbrock's method [80, 129].

6.10 RESULTS AND DISCUSSION

The numerical computations were performed on an English Electric KDF9 computer using Algol. The computational effort was characterised by extremely large and complex programming procedures which imposed severe limitations on storage and test facilities. A substantial amount of the time was consumed in the Bessel function calculations [215]. In addition, considerable numerical difficulties arose in the calculation of the determinantal function $f_2(a_2, r_e, r_\ell, p)$ due to the presence of very large numbers, giving rise to local regions of instability in the synthesis.

The programme was initiated by a set of values for a_2, r_e, r_ℓ, p which satisfied the side constraints. However, it was not possible to ensure the vanishing of f_2. This was not a serious disadvantage since the Heaviside penalty function transformation always generates a feasible point as the solution to the equivalent unconstrained problem.

For these reasons, the available computational experience is limited through an examination of the preliminary results indicates that the synthesis is progressing in the right direction. The really effective utilisation of the numerical procedures requires a more powerful range of computers than was available at the time of this investigation.

6.11 CONCLUSION

Powerful synthesis procedures based on the methods of mathematical programming have been developed for solving a highly complex structural optimization problem. Considerable progress has been made in solving the problem using purely analytical techniques based on the maximum principle of Pontryagin which transfcrms the problem into a nonlinear programming problem.

Available computational experience indicates the possibilities of developing a highly systematic synthesis capability when used in conjunction with <u>very</u> large, high speed digital computers. The available evidence appears to warrent further investigation and development in this direction, with particular emphasis on more automatic software packages for handling very large problems.

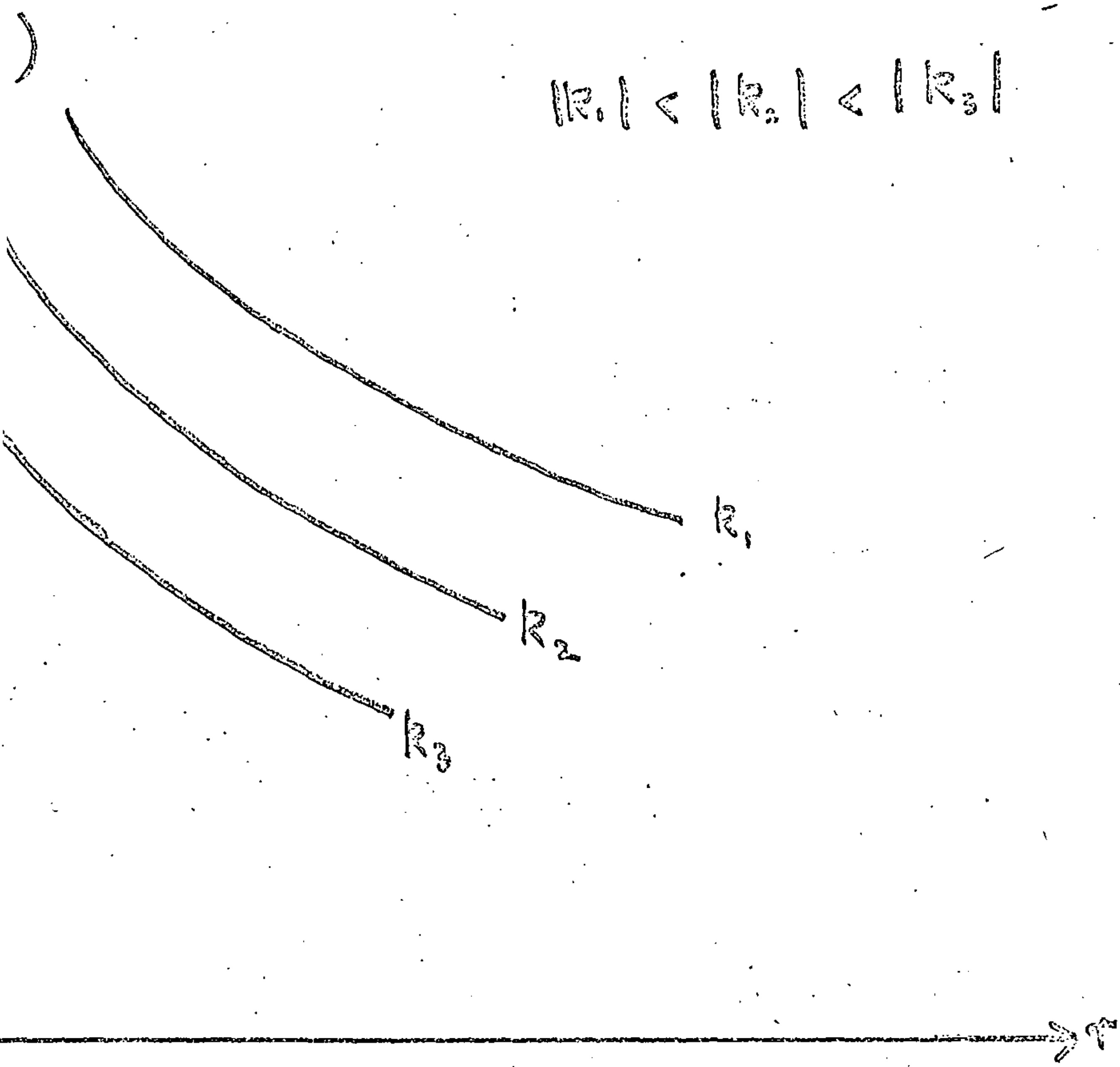

FIG.6.1 Thickness for k < 0

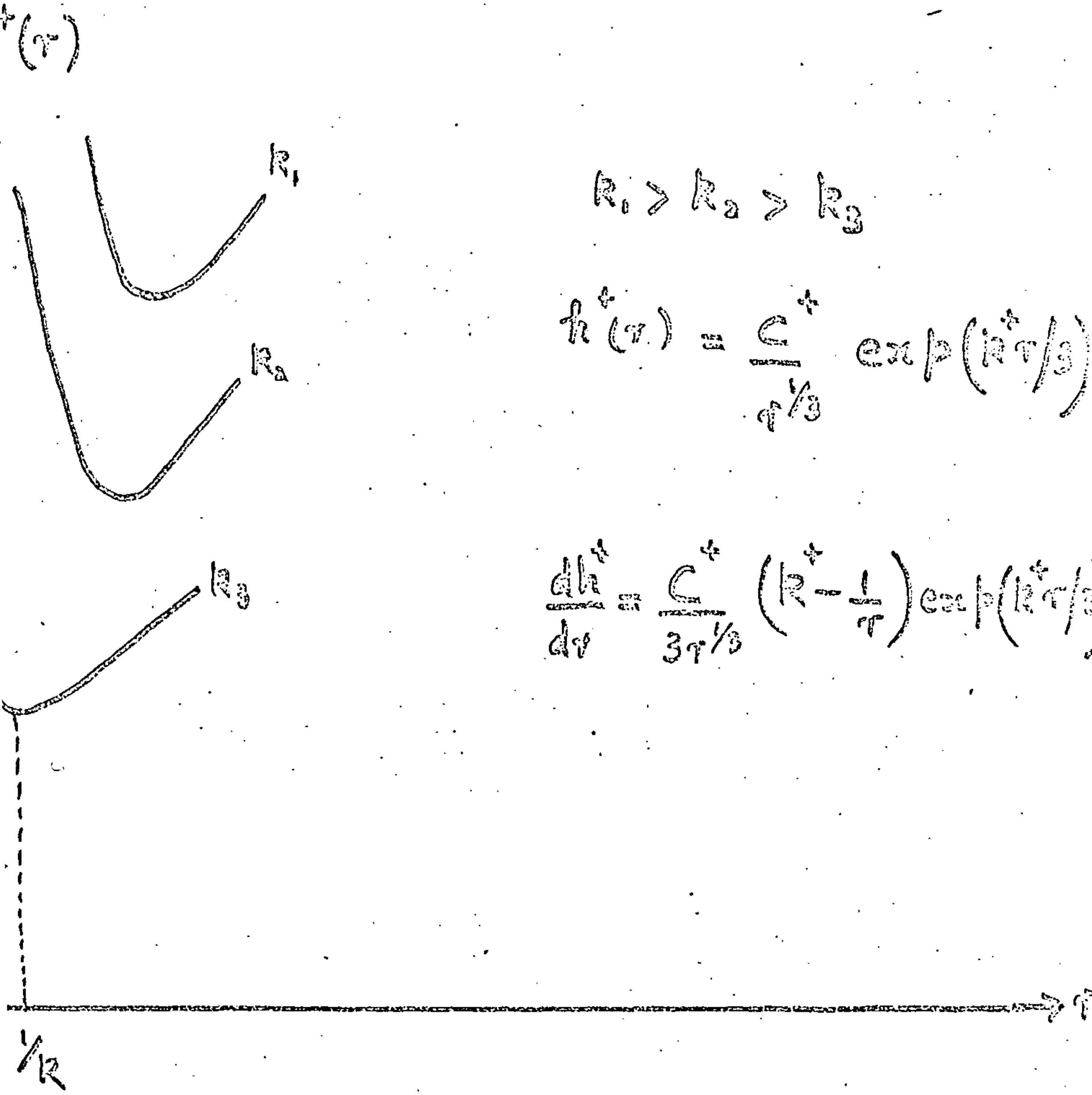

FIG. 6.2 Thickness for $k > 0$

$h^{+}(r) \triangleq h(r)$; $k >$

$h^{-}(r) \triangleq h(r)$; $k <$

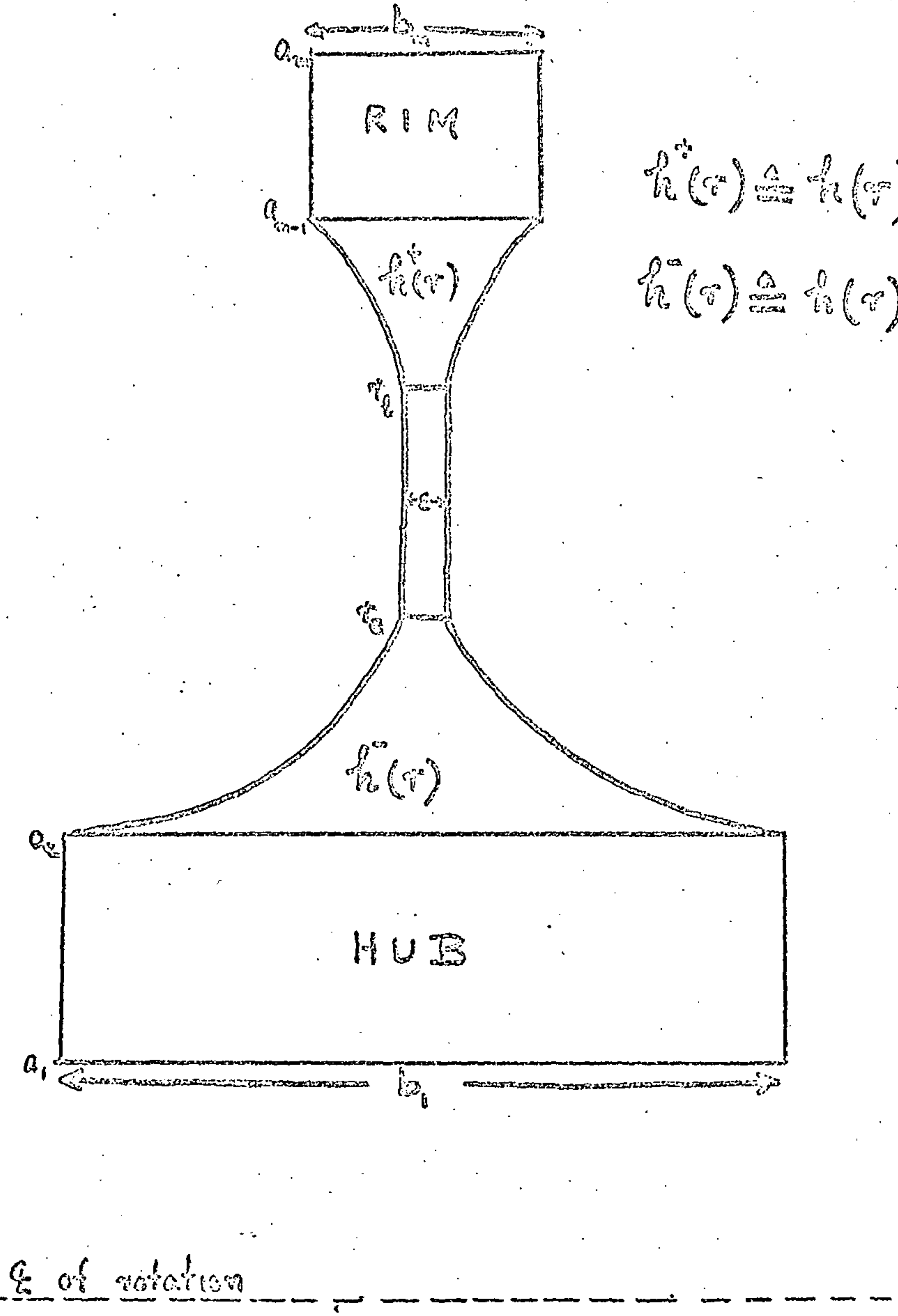

FIG. 6.3 Optimal thickness

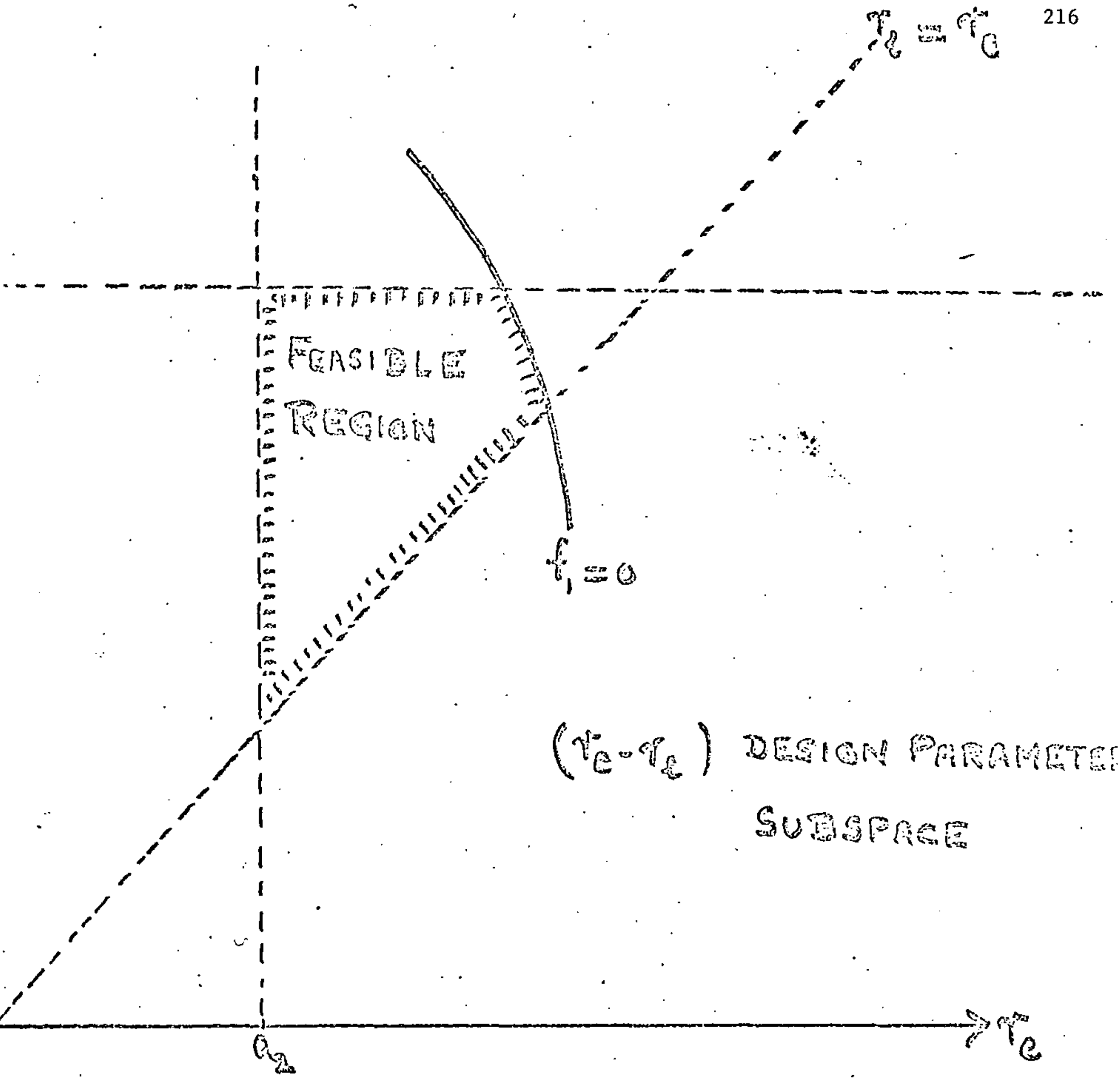

KEY

------ Portions of the boundary on which solutions cannot lie.

——— Portions of the boundary on which solutions can lie.

FIG. 6.4 Optimal Control Problem $\longrightarrow$ Nonlinear Programming Problem

CHAPTER 7

SOME RESEARCH PROBLEMS

NOTES ON SOME RECENT DEVELOPMENTS

This chapter briefly outlines some of the research problems in the structural optimization area which are currently under investigation.

The first problem is essentially a continuation of the research programme described in Chapters 5 and 6 into analytical and computational procedures based on the methods of mathematical programming for optimizing structural systems in the presence of design constraints. The problem considered in Chapters 5 and 6 was that of minimising the weight of a steam turbine disc subject to specified behaviour and side constraints. The behaviour constraints are restricted to a consideration that the stresses everywhere should be below the yield stress and the vibrational frequencies should be outside specified resonance bands. The side constraints, on the other hand, imposed restrictions on the dimensions and tolerances of the disc. The problem was formulated as an optimal control problem in the presence of inequality constraints on the state and control variables. These were described by functions representing the variations in thickness, stress and deformation fields with the frequencies as control parameters. The numerical investigations were based on a discretised nonlinear approximation, while the analytical investigation was based on the Pontryagin principle. In Chapter 6, the (seemingly) dual problem of maximising the vibrational frequencies of the disc subject to a constraint on the total weight was considered. The problem was formulated as an optimal control problem and the analytical procedures included solutions of systems of differential equations using perturbation techniques in conjunction with asymptotic expansions based on WKB procedures.

A heuristic demonstration of the possible relation between problems described in Chapters 3 and 6 is given below. From (3.8, 6.9) it is seen that the Hamiltonian for the problem in Chapter 3 differs from the $\hat{H}$ in (6.9) by the term $-2\pi\rho r x_5$. Consequently the equations (6.11) remain unchanged with the exception of the equation for λ_5 which becomes

$$\frac{d\lambda_5}{dr} = -\frac{\partial \hat{H}}{\partial x_5} = 2\pi\rho r - \lambda_4 E \tag{7.1}$$

But it can be readily shown that $|D| \rightarrow \infty$, implies $E \rightarrow \infty$.

Therefore the analysis developed in Chapter 6 remains virtually unchanged with an associated nonlinear program of the form

$$\text{Min } f_1(a_2,\ r_e,\ r_\ell)$$

subject to constraints of the form

$$\left.\begin{aligned} &\underline{p} \leq \underline{p}_o \\ &L \leq a_2 \leq U \\ &a_2 < r_e < r_\ell < a_{m-1} \\ &f_2(a_2,\ r_e,\ r_\ell,\ \underline{p}) = 0 \end{aligned}\right\} \tag{7.2}$$

The nonlinear programs (6.46, 7.2) exhibit many of the dual characteristics of nonlinear programming. Work is presently under way to re-examine the problems in Chapters 3 and 6, by making a critical study of the necessary and sufficient conditions for the equivalence of minimum weight - maximum frequency design of discs. The problem is again described within the framework of optimal control theory. The equivalence conditions are given by the interactions of the of the optimal control - nonlinear programs for the system. Some powerful techniques for handling such dual systems are described in the book by Canon, Cullum and Polak [224]. This investigation is of considerable industrial interest because:

(a) the application of optimal control theory to complex structural systems such as discs is still in its early stages.

(b) necessary and sufficient conditions have been established on only one-dimensional beam structures. The present investigation would accordingly advance the state of knowledge in this area.

(c) dynamic response constraints are included, thereby increasing the degree of difficulty.

A further development in this direction would be retaining the structural equations of behaviour in the original partial differential form. This would introduce the methods of optimal control for distributed parameter systems [225,228] into the structural optimization area.*

A further problem under investigation is a comparative study of some numerical optimization procedures as applied to structural optimization problems. The problem considered is that proposed by Schmit and Fox [65] where a multi-bar truss system is synthesised

---

* One of the first applications in this area is due to Armand [238] who has considered the minimal weight design of plates subject to a frequency constraint governed by a partial differential equation. Solutions were obtained using a generalised first variation technique.

subject to stress, deflection and buckling constraints. The nonlinear program is transformed into an unconstrained form using the SUMT and Heaviside penalty function techniques [76, 80]. These unconstrained problems are solved using the methods of Rosenbrock, Nelder-Mead, Powell and Davidon-Fletcher-Powell.

FOOTNOTE: Since this thesis was written the problem outlined at the beginning of this chapter is being simultaneously studied using finite element techniques. The method employed is a hybrid method developed by Tong and Pian [240] based on the minimisation of the complementary energy for the system. The elements employed are trapezoidal. The synthesis aspects would be based on the techniques of Gellatly and Gallagher [82] and Fox and Kapoor [223]. The associated computer programs are presently under development.

REFERENCES

1. J.F. Baker — The design of steel frames. Structural Engr., 27 (1949), pp 397-431.
2. H.J. Greenberg & W. Prager — Limit design of beams and frames. Trans.ASCE, 117 (1952), pp 447-484.
3. D.C. Drucker, W. Prager, & H.J. Greenberg — Extended limit design theorems for continuous media. Quart.Appl.Math., 9 (1952), pp 381-389.
4. D.C. Drucker & R.T. Shield — Bounds on minimum weight design. Quart.Appl.Math., 15 (1957), pp 269-281.
5. D.C. Drucker & R.T. Shield — Design for minimum weight. Proc. 9th Inter.Congr.Appl.Mech., Brussels (1956) B.5, pp 212-222.
6. W. Freiberger & B. Tekinalp — Minimum weight design of circular plates. J. Mech.Phy.Solids, 4 (1956), pp 294-299.
7. J. Foulkes — The minimum weight design of structural frames. Proc.Roy.Soc., A223 (1954), pp 482-494.
8. H.G. Hopkins & W. Prager — Limits of economy of material in plates. Trans.ASME, J.Appl.Mech., 22 (1955), pp 372-374.
9. W. Prager — Minimum weight design of plates. Ingenieur, 67 (1955), pp 141-142.
10. H.G. Hopkins & W. Prager — The load-carrying capacities of circular plates. J.Mech.Phys.Solids, 2, (1953), pp 1-13.
11. C.Y. Shen & W. Prager — Optimal plastic design of circular and annular sandwich plates with piecewise constant cross-section. J.Mech.Phys.Solids, 17 (1959), pp 11-16.
12. W. Kozlowski & Z. Mroz — Optimal design of solid plates Int.J.Solids Structures, 5, (1969), pp 781-794.
13. Z. Mroz — On a problem of minimum weight design Quart.Appl.Math., 19 (1961), pp 127-135.

14. R.T. Shield — On the optimum design of shells. Trans.ASME,J.Appl.Mech., 27 (1960), pp 316-322.

15. W. Freiberger — Minimum weight design of cylindrical shells. Trans.ASME J.Appl.Mech., 23 (1956) pp 576-580.

16. W. Freiberger — On the minimum weight design problem for cylindrical sandwich shells. J.Aeron.Sc., 24 (1957), pp 847-848.

17. J. Foulkes — Linear programming and structural design. Proc.2nd Symposium in linear programming, Washington DC (1955), pp 177-184.

18. J. Foulkes — Minimum weight design and the theory of plastic collapse. Quart.Appl.Math., 10 (1953), pp 347-358.

19. B.G. Neal & P.S. Symonds — The calculation of the collapse loads for frames structures. J.Inst.C.E., 35 (1950), pp 21-40.

20. J. Heyman — Plastic design of beams and plane frames for minimum material consumption. Quart.Appl.Math., 8 (1951), pp 373-381.

21. J. Heyman — Plastic design of plane frames for minimum weight. Struct.Engr., 31 (1953), pp 125-129.

22. R.K. Livesley — Optimum design of structural frames for alternative systems of loading. Civil Engr. and Public Works Rev., 54, (1959), pp 738-740.

23. R.K. Livesley — The automatic design of structural frames. Quart.J.Mech.Appl.Math., 9 (1956), pp 257-278.

24. A.R. Toakley — Some computational aspects of optimum rigid plastic design. Int.J.Mech.Sci., 10 (1968), pp 531-537.

25. W. Prager — Mathematical programming and theory of structures. J.SIAM, 13 (1965), pp 312-332.

26. W.R. Spillers — Network techniques applied to structures. Matrix and Tensor Quart., Dec. (1964), pp 31-41.

27. W. Prager — Minimum weight design of a portal frame. J.Eng.Mech.Div., ASCE, 82, (1956), pp 1073(1)-1073(10).

28. A.A. Chires — Some applications of mathematical programming methods in problems of structural mechanics. (Transl.) Bull.Acad.Sc.Ind. Cybernetics (USSR), (1965), pp 110-113.

29. J.F. Brotchie — Direct design of framed structures. J. Struct.Div., ASCE, 90, (1964), pp 243-257.

30. J. Heyman — On the absolute minimum weight design of structures. Quart.J.Mech.Appl.Math., 12 (1959), pp 314-324.

31. R. Mayeda & W. Prager — Minimum weight design of beams for multiple loading. Int.J.Solid Structures, 3, (1967), pp 1001-1011.

32. O. Gross & W. Prager — Minimum weight design ofr moving loads. Proc. 4th U.S. Nat.Cong.Appl.Mech.ASME 2 (1962), pp 1047-1051.

33. W. Prager — Proc.Amer.Concrete Inst., 50.

34. M. Save & W. Prager — Minimum weight design of beams subjected to fixed and moving loads. J.Mech.Phy.Solids, 11, (1963), pp 255-267.

35. M.Z. Cohn — Limit design of reinforced concrete frames. J.Struct.Div.,ASCE, 94, (1968), pp 2467-2483.

36. A.G.M. Michell — The limit of economy of material in frame structures. Phil.Mag. 8, (1904), pp 589-597.

37. W. Prager & P.G. Hodge — Theory of perfectly plastic solids. J. Wiley Press.

38. W.S. Hemp — The theory of structural design. College of Aeronautics Report 115 (1958)-.

39. A.S.L. Chan — The design of Michell optimum structures. College of Aeronautics Report 142 (1960).

40. H.S.Y. Chan — Half-plane slip-line fields and Michell structures. Quart.J.Mech. and Appl.Math., 20 (1967), pp 453-469.

41. H.S.Y. Chan — Minimum volume design of frameworks and discs for alternative loading systems.
Quart.Appl.Maths., 25, (1968), pp 470-473.

42. L.C. Schmidt — Minimum weight layouts of elastic, statically determinate, triangulated frames under alternative load systems.
J.Mech.Phy.Solids, 10 (1962), pp 139-149.

43. H.L. Cox & H.E. Smith — Structures of minimum weight.
Aeron.Res.Comm.Rep.Memo. No. 1923 (1943).

44. H.L. Cox — The theory of design.
Aeron.Res.Council Rept. 19791 Struct. 2037 (1958).

45. H.L. Cox — Structures of minimum weight; the basic theory of design applied to the beam under pure bending.
Aero.Res.Council Rept. 19785, Struct. 2036 (1958).

46. H.L. Cox — The design of structures of least weight.
Pergamon Press (1965).

47. L.C. Schmidt — Fully stressed design of elastic redundant trusses under alternative load systems.
Austr.J.Appl.Sc. 9, (1958), pp 337-348.

48. R.I. Kerr — Optimum structural design based on a stiffness criteria.
B.A.C. Rept. No. S062 (1964).

49. J. Drymael — The design of trusses and its influence on weight and stiffness.
J.Roy.Aeron.Soc. 46 (1942), pp 297-308.

50. G.A. Hegemier & W.Prager — On Michell structures.
Int.J.Mech.Sc. 11 (1969), pp 209-215.

51. G. Gerard — Minimum weight analysis of orthotropic plates under compressive loading.
J.Aerospace Sc., 27 (1960), pp 21-26.

52. E.J. Catchpole — The optimum design of compressive surfaces having unflanged integral stiffeners.
J.Roy.Aeron.Soc. 58 (1954), pp 765-768.

53. H.H. Hilton & M. Feigen Minimum weight analysis based on structural reliability.
J.Aerospace Sc., 27 (1960), pp 641-652.

54. F. Moses & D.E. Kinser Optimum structural design with failure probability constraints.
J.AIAA, 5 (1967), pp 1152-1158.

55. R. Kalaba Design of minimal weight structures for given reliability and cost.
J.Aerospace Sc., 29 (1962), pp 355-356.

56. R. Bellman Dynamic programming.
Oxford University press, (1957).

57. R. Bellman & S.E. Dreyfus Applied Dynamic programming.
Oxford University Press (1962).

58. R.F.D. Porter Goff Decision theory and the shape of structures.
J.Roy.Aeron.Soc., 70 (1966), pp 448-452.

59. A.C. Palmer Optimal structure design by dynamic programming.
J.Struct.Div.ASCE 94 (1968), pp 1887-1906.

60. E.H. Salmon Materials and structures.
Longmans, Vol I, pp 374-375.

61. I.G. Tadjbakhsh Elastic optimum design of circular plates.
Proc.7th Midwestern Mechanics Conf. (1961), pp 216-222.

62. N.C. Huang Optimal design of elastic structures for maximum stiffness.
Int.J.Solids Structures, 4 (1968), pp 689-700.

63. M.A. Ranta On the optimum shape of a rotating disc of any isotropic material.
Int.J.Solids Structures 5, (1969), pp 1247-1257.

64. G. Gerard & C. Lakshmikantham Optimum thin wall pressure vessels of anistropic material.
Trans.ASME J.Appl.Mech. 33 (1966), pp 623-628.

65. L.A. Schmidt & R.L. Fox An integrated approach to structural synthesis and analysis.
J.AIAA 3, (1965), pp 1104-1112.

66. L.A. Schmit Structural design by systematic synthesis. Proc.2nd.Nat.Conf.Electronic Computation, Struct.Div., ASCE (1960), pp 105-132.

67. L.A. Schmit & T.P. Kicher Synthesis of material and configuration selection. J.Struct.Div.,ASCE, 88 (1962), pp 79-102.

68. L.A. Schmit & W.M. Morrow Structural synthesis with buckling constraints. J.Struct.Div. ASCE 89 (1963), pp 107-126.

69. L.A. Schmit & R.H. Mallet Design synthesis in a multi-dimensional design space with automated material selection. Eng.Design Center Rept. 2-62-2, Case Inst.Tech. (1962).

70. L.A. Schmit, T.P. Kicher & W.M. Morrow Structural synthesis capability for integrally stiffened waffle plates. J.AIAA 1 (1963), pp 2820-2836.

71. L.A. Schmit & T.P. Kicher Structural synthesis of symmetric waffle plates. NASA Tech. Note D-1691 (1962).

72. L.A. Schmit & T.P. Kicher Structural synthesis of symmetric waffle plates with integral orthogonal stiffeners. Eng.Design. Center, Rept. 2-61-1, Case Inst.Tech. October (1961).

73. L.A. Schmit & R.L. Fox Synthesis of a simple shock isolator. NASA CR55, Washington DC (1964).

74. L.A. Schmit Automated redesign. Int.Sc. and Technol. Jnl. June (1966), pp 63-78.

75. K.C. Falcon et al. Optimization of vibration absorbers: a graphical method for use on idealised systems with restricted damping. J.Mech.Eng.Sci., 9 (1967), pp 374-381.

76. J. Kowalik Non-linear programming procedures and design optimization. Acta.Polytech.Scandinavia, Math.Comp.Mach.Ser. 13 (1966).

77. L.A. Schmit, W.M. Morrow & T.P. Kicher Structural synthesis capability for integrally stiffened cylindrical shells.
Proc.AIAA/ASME 9th Structures, Structural Dynamics and Materials Conference, Paper 68-327 (1968).

78. W.J. Stroud & N.P. Sykes Minimum weight stiffened shells with slight meridianal curvature designed to support axial compressive loads.
J.AIAA, 7 (1969), pp 1599-1601.

79. P.V. Marcal & R.A. Gellatly Application of the created response surface technique to structural optimization.
Proc.2nd Conf on Matrix Methods in structural mechanics, AFFDL-TR-68-150, Wright Patterson AFB Ohio (1968), pp 83-110.

80. J. Kowalik & M.R. Osborne Methods for unconstrained optimization problems.
Elsevier (1968).

81. B. Klein Direct use of extremal principles in solving certain types of optimization problems involving inequalities.
J.ORSA, 3, (1955), pp 168-175.

82. R.A. Gellatly & R.H. Gallagher A procedure for automated minimum weight structural design, Part I.
Aeron.Quart. 17 (1966), pp 216-230.

83. R.A. Gellatly & R.H. Gallagher A procedure for automated minimum weight structural design, Part II.
Aeron.Quart. 17 (1966), pp 332-342.

84. G.C. Best Completely automatic weight minimization method for high speed digital computers.
J.Aircraft 1 (1964), pp 129-133.

85. M.J. Turner Design of minimum mass structures with specified natural frequencies.
J.AIAA 5, (1967), pp 406-412.

86. M.J. Turner — Optimization of structures to satisfy flutter requirements.
J.AIAA, 7 (1969), pp 945-951.

87. M.S. Zarghamee — Optimum frequency of structures.
J.AIAA, 6 (1968), pp 749-750.

88. M.S. Zarghamee — Minimum weight design of enclosed antennas.
J.Struct.Div., ASCE, 95 (1969), pp 1139-1152.

89. J.B. Rosen — The gradient projection method, Part I.
J.SIAM, 8, (1960), pp 181-217.

90. J.E. Taylor — Minimum mass bar for axial vibration at specified natural frequency.
J.AIAA, 5, (1967), pp 1911-1913.

91. I. Fried — Gradient methods for finite element eigen problems.
J.AIAA, 7, (1969), pp 739-741.

92. M.J.D. Powell — An efficient method for finding the minimum of a function of several variables without calculating derivatives.
Computer J., 7, (1964), pp 155-164.

93. S.C. McIntosh & F.E. Eastep — Design of minimum mass structures with specified stiffness properties.
J.AIAA, 6, (1968), pp 962-964.

94. C.Y. Shen — Elastic minimum weight design for specified fundamental frequency.
Int.J. Solids Structures, 4 (1968), pp 953-958.

95. L.J. Icerman — Optimal structural design for given dynamic deflection.
Int.J. Solids Structures, 5 (1969), pp 473-490.

96. J.W. Young & H.N. Christiansen — Synthesis of a space truss based on dynamic criteria.
J.Struct.Div., ASCE, 92, (1966), pp 425-442.

97. R.A. Gellatly & R.H. Gallagher — Instability effects in automated minimum weight design.
Paper presented at symposium on Structural Stability and Optimization (1967), Loughborough University of Technology.

98. G.G. Pope — The design of optimum structures of specified basic configuration.
Int.J.Mech.Sci., 10, (1968), pp 251-263.

99. G. Zoutendijk — Methods of feasible directions.
Elsevier, Amsterdam, (1960).

100. F. Moses — Optimum structural design using linear programming.
J.Struct.Div., ASCE, 90, (1964), pp 89-104.

101. J.E. Kelley — The cutting plane method for solving convex programs.
J.SIAM, 8, (1960), pp 703-712.

102. D.A. Matsyulyavichus — On the question of the synthesis of configuration of rod-shaped statically determinate structures of minimum weight.
Izv.Akad.Nauk.USSR., Technicheskaya Kibernetika No. 1, (1965), pp 114-117. (Transl. No. 1272, English Electric Co.).

103. D.M. Brown & A.H.S. Ang — Structural optimization by nonlinear programming.
J.Struct.Div., ASCE, 92 (1966), pp 319-340.

104. J.B. Rosen — The gradient projection method for nonlinear programming, Part II.
J.SIAM, 9 (1961), pp 514-532.

105. A.R. Toakley — Optimum design using available sections.
J.Struct.Div., ASCE, 94, (1968), pp 1219-1241.

106. G.J. Megarefs — Method for minimal design of axisymmetric plates.
J.Eng.Mech.Div., ASCE, 92, (1966), pp 79-99.

107. G.J. Megarefs — Minimal design of sandwich axisymmetric plates I.
J.Eng.Mech.Div., ASCE, 93, (1967), pp 245-269.

108. G.J. Megarefs — Minimal design of sandwich axisymmetric plates II.
J.Eng.Mech.Div., ASCE, 94, (1968), pp 177-198.

109. G.J. Megarefs & H.S. Sidhu — Simplifications in minimal design of frames.
J.Struct.Div., ASCE, 94, (1968), pp 2985-2998.

110. K.M. Romstad & C.K. Wang — Optimum design of framed structures.
J.Struct.Div., ASCE, 94, (1968), pp 2817-2845.

111. R.M. Brach — Optimum design of beams for sudden loading.
J.Eng.Mech.Div., ASCE, 94, (1968), pp 1395-1407.

112. J.E. Taylor — Maximum strength elastic structural design.
J.Eng.Mech.Div., ASCE, 95, (1969), pp 653-663.

113. I. Tadjbakhsh — An optimum design problem for the nonlinear elastica.
SIAM J.Appl.Math., 16, (1968), pp 964-972.

114. P.L. Gould — Minimum weight design of hyperbolic cooling towers.
J.Struct.Div., ASCE, 95, (1969), pp 203-208.

115. S. Sasse — Method for weight optimization of a two material shield for reactor radiation.
Nucl.Struct.Eng. 2, (1965), pp 327-334.

116. R. Razani — Behaviour of fully stressed design of structures and its relationship to minimum weight design.
J.AIAA, 3, (1965), pp 2262-2268.

117. T.P. Kicher — Optimum design, minimum weight versus fully stressed.
J.Struct.Div., ASCE, 92, (1969), pp 773-774.

118. P. Dayarathnam & S. Patnaik — Feasibility of full stress design.
J.AIAA, 7, (1969), pp 773-774.

119. W. Prager & J.E. Taylor — Problems of optimal structural design.
Trans.ASME, J.Appl.Mech., 35, (1968), pp 102-106.

120. H.W. Kuhn & A.W. Tucker — Nonlinear programming.
Proc. 2nd Berkeley symposium on Math.Statistics and Probability.
Edited by J. Neumann, Univ. of Calif. Press, Berkeley, (1951), pp 481-492.

121. B. Bernholtz — A new derivation of the Kuhn-Tucker conditions.
J.ORSA 12, (1964), pp 295-299.

122. D.J. Wilde — Differential calculus in nonlinear programming.
J.ORSA 10, (1962), pp 764-773.

123. A.W. Tucker — Linear and nonlinear programming.
Symposium on modern techniques for extremum problems.
7th National meeting of the ORSA, (1965), pp 244-257.

124. Z. Wasiutynski & A. Brandt The present state of knowledge in the field of optimum design of structures. Appl.Mech.Rev., 16, (1963), pp 341-350.

125. L.A. Schmit Comment on "Completely automatic weight minimization method for high speed digital computers." J.Aircraft, 1, (1964), pp 375-376.

126. V.A. Troitskii On the synthesis of optimal dampers. PMM, 31, (1967), pp 649-654.

127. C.W. Carroll The created response surface technique for optimizing nonlinear restrained systems. J.ORSA, 9, (1961), pp 169-184.

128. D.A. Newton & A. Scholes An investigation into computer aided optimal piston design. English Electric Co., Report No. W/M(1A), (1968), p 1458.

129. H.H. Rosenbrock An automatic method for finding the greatest or least value of a function. Computer J., 3, (1960), pp 175-184.

130. J.A. Nelder & R.A. Mead A simplex method for function minimisation. Computer J., 7, (1965), pp 308-313.

131. J. Bracken & G.P. McCormick Selected applications of nonlinear programming. John Wiley, (1968), ch. 6.

132. W.C. Davidon Variable metric method for minimisation. Research Development Report, ANL-5990 (Rev.), U.S. Atomic Energy Commission, (1959).

133. R. Fletcher & M.J.D. Powell A rapidly convergent descent method for minimization. Computer J., 6, (1963), pp 163-168.

134. A.V. Fiacco & G.P. McCormick The sequential unconstrained minimization technique for nonlinear programming, a primal-dual method. Mang.Sci., 10, (1964), pp 360-366.

135. A.V. Fiacco & G.P. McCormick Computational algorithms for the sequential unconstrained minimization technique for nonlinear programming.
Manag. Sci., 10, (1964), pp 601-617.

136. L. Cavallaro Stress analysis of rotating discs.
Nucl.Struct.Eng. 2, (1965), pp 271-281.

137. L.S. Pontryagin et al Mathematical theory of optimal control processes.
Interscience Press, (1962).

138. I.M. Gelfand & F.V. Fomin Calculus of variations.
Prentice Hall, (1963), pp 208-226.

139. M.R. Hestenes Variational theory and optimal control theory.
Computing methods in Optimization Problems, (editors, A.V. Balakrishnan & L.W. Neustadt)
Academic Press, (1964), pp 1-22.

140. S.E. Dreyfus Dynamic programming and the calculus of variations.
Academic Press, (1965), Ch. 5.

141. S.E. Dreyfus Variational problems with inequality constraints.
J.Math.Anal.Appl., 4, (1962), pp 297-308.

142. H.J. Kelley Method of gradients.
Optimization techniques (editor G. Leitmann),
Academic Press (1962), pp 205-254.

143. A.E. Bryson & W.F. Denham A steepest descent method for solving optimum programming problems.
Trans. ASME, J. Appl.Mech., 29, (1962), pp 247-257.

144. R.G. Gottlieb Rapid convergence to optimum solutions using a min-H strategy.
J.AIAA, 5, (1967), pp 322-329.

145. E.S. Lee Quasi-linearization in optimization: A numerical study.
J.AIChE, 13, (1967), pp 1043-1051.

146. B.D. Tapley & J.M. Lewallen Comparison of several numerical optimization methods.
Jnl. of Opt. Theory & Applic., 1, (1967), pp 1-32.

147. J.N. Hanson Comparison of two optimizations of a nonlinear boundary value problem.
J.AIAA, 6, (1968), pp 1979-1985.

148. J.L. Speyer & A.E. Bryson Optimal programming problems with a bounded state space.
J.AIAA, 6, (1968), pp 1488-1491.

149. L.S. Lasdon, S.K. Mitter & A.D. Warren The conjugate gradient method for optimal control problems.
Trans.IEEE, AC-12, (1967), pp 132-138.

150. L.S. Lasdon, A.D. Warren & R.K. Rice An interior penalty method for inequality constrained optimal control problems.
Trans.IEEE AC-12, (1967), pp 388-395.

151. G.N. Saridis & Z.V. Rekasius Design of approximately optimal feedback controllers for systems with bounded states.
Trans.IEEE AC-12, (1967), pp 373-379.

152. C. Lakshmikantham & G. Gerard Minimum weight design of stiffened cylinders.
Aeron.Quart., (1970), pp 49-68.

153. G. Gerard Optimum structural design concepts for aerospace vehicles.
J.Spacecraft, 3, (1966), pp 5-18.

154. E. D'Sylva Disc stresses.
English Electric Co.Ltd., Report No. W/M(4A) (1961), p 88.

155. L.G. Roberts Amendments to program 00011 which calculates disc stresses.
English Electric Co. Ltd., Report No. W/M(6A) p 1010.

156. I.S. Sokolnikoff Mathematical theory of elasticity.
McGraw Hill (1956), pp 49-51.

157. A.D. Booth An application of the method of steepest descent to the solution of systems of nonlinear simultaneous equations.
Quart.J.Mech.Appld.Math. 2, (1949), pp 460-480.

158. C.G. Broyden A class of methods for solving nonlinear simultaneous equations. J.Math.Comp., (1965), pp 577-593.

159. D.P. Feder Automatic lens design with a high speed computer. J.Optical Soc.Am., 52, (1962), pp 177-183.

160. P.F. Davis An interim report on a new method of finding the optimum design of a reactor. English Electric Co. Ltd., Report No. W/AT 336.

161. R. Hooke & F.A. Jeeves Direct search solution of numerical and statistical problems. J.ACM, 8, (1961), pp 212-229.

162. D.J. Wilde Optimization Methods. Adv.Chem.Engr., 3, (1962), pp 273-331.

163. S.H. Brooks A comparison of maximum seeking methods. J.ORSA, 7, (1959), pp 430-457.

164. S.H. Brooks A discussion of random methods for seeking maxima. J.ORSA, 6, (1958), pp 244-251.

165. D.J. Wilde Optimum seeking methods. Prentic Hall, (1964).

166. A. Charnes, W.W. Cooper & A. Henderson An introduction to linear programming. J. Wiley & Sons, (1953).

167. C.G. Broyden An alternative derivation of the simplex method. J.IMA, 2, (1966), pp 40-54.

168. H.P. Künzi, H.G. Tzschach & C.A. Zehnder Numerical methods of mathematical optimization (with Algol and Fortran programs), Academic Press, (1968).

169. J.L. Greenstadt A ricocheting gradient method for nonlinear programming. J.SIAM 14, (1966), pp 429-445.

170. H.A. Spang A review of minimization techniques for nonlinear functions. Rev.SIAM, 4, (1962), pp 343-365.

171. T.L. Saaty & J. Bram Nonlinear Mathematics.
J. Wiley & Sons, (1964), Ch 3.

172. C.G. Broyden Optimization Studies.
English Electric Co. Ltd., Report No. W/AT 1086.

173. H.P. Künzi & W. Krelle Nonlinear programming.
Blaisdell (1966).

174. J.B. Crockett & H. Chernoff Gradient methods of maximization.
Pacific J. Maths. 5, (1955), pp 33-50.

175. S. Timoshenko Theory of plates and shells.
McGraw Hill (1940).

176. F.F. Ehrich A matrix solution for vibration of modes of non-uniform discs.
Trans. ASME, J. Appl.Mech., 23, (1956), pp 109-115.

177. P.S. Brass Disc and blade vibrations.
English Electric Co., Report No. W/M(6B), (1965), p 1022.

178. P.S. Brass The calculation of the natural frequencies of turbine discs.
English Electric Co., Report No. W/M(4B), u 142.

179. B.M.E. de Silva The application of nonlinear programming to the automated minimum weight design of rotating discs.
Optimization (ed. R. Fletcher) Academic Press (1969), pp 115-150.

180. B.M.E. de Silva Minimum weight design of steam turbine discs.
English Electric Co., Report No. W/M(4B), (1967), p 1323.

181. B.M.E. de Silva On the application of nonlinear programming to the automatic structural synthesis of turbine discs.
English Electric Co. Report No W/M(6B), (1965), p 1126.

182. B.M.E. de Silva Minimum weight design of discs using a frequency constraint.
Trans.ASME. J.Eng.Ind., 91, (1969), pp 1091-1099.

183. B.M.E. de Silva Automated weight minimization based on a frequency constraint.
English Electric Co., Report No. W/M(4B), (1968), p 1452.

184. K. Fullard Frequency tuning of compressor rotor blades.
Symposium on numerical methods in vibration problems.
Institute of Sound and Vibration Research, University of Southampton, (1966).

185. B. Irons Differential applications of Rayleigh's Principle.
Rolls Royce Aero Div., Stress Memo, ASM 588.

186. H. Goldstein Classical Mechanics.
Addison-Wesley Publ. Co. (1959), Ch. 10.

187. H.L. Langhaar Energy methods in applied mechanics.
J. Wiley Co. (1962), Ch. 5 (see also reference 175).

188. R.J. Duffin, E.L. Peterson & C. Zener Geometric programming.
John Wiley (1967).

189. L.D. Pascual & A. Ben-Israel On the solution of maximization problems of optimal design by geometric programming.
J.Eng.Maths. 4, (1970), pp 349-360.

190. P.J. Corcoran Configurational optimization of structures.
Int.J.Mech.Sci., 12, (1970), pp 459-462.

191. K.F. Reinschmidt, A. Cornell & J.F. Brotchie Iterative design and structural optimization.
J.Struct.Div., ASCE 92, (1966), pp 281-318.

192. W. Prager Optimal thermo-elastic design for given deflection.
Int.J.Mech.Sci., 12, (1970), pp 705-709.

193. C.P. Smolenski & E.M. Krokosky Optimal multifactor design procedure for sandwich panels.
J.Struct.Div., ASCE, 96, (1970), pp 823-837.

194. C.P. Rubin Minimum weight design of complex structures subject to a frequency constraint.
J.AIAA, 8, (1970), pp 923-927.

195. B.R. McCart, E.J. Haug & T.D. Streeter Optimal design of structures with constraints on natural frequency.
J.AIAA, 8, (1970), pp 1012-1019.

196. Z. Mroz Optimal design of structures of composite materials.
Int.J.Solids Struct. 6, (1970), pp 859-870.

197. B.M.E. de Silva An eigenvalue analysis for calculating the vibrational modes of steam turbine discs.
Int.J.Math.Educ.Sci.Technol. 2, (1971), pp 171-181.

198. H.S.Y. Chan On Foulkes Mechanism in portal frame design for alternate loads.
Trans. ASME, Jnl.Appl.Mech. 36, (1969), pp 73-75.

199. H.S.Y. Chan Mathematical porgramming in optimal plastic design.
Int.J.Solids Structures 4, (1968), pp 885-895.

200. W.S. Hemp & H.S.Y. Chan Optimum design of pin-jointed frameworks.
R & M No. 3632, Min.Tech., Her Majesty's Stationary Office, (1966).

201. B.M.E. de Silva Non-classical variational problems in minimum weight structural optimization problems.
English Electric Co. Rept. No. W/M(4B) p 1382 (1968).

202. B.M.E. de Silva Variational methods in minimum weight design problems.
English Electric Co. Report No. W/M(4B), (1968), p 1442.

203. J.V. Breakwell Optimization of trajectories.
J.SIAM 7, (1959), pp 215-247.

204. B. Garfinkel Minimal problems in airplane performance.
Q.Appl.Math. 9 (1951), pp 149-162.

205. L.D. Berkovitz Variational methods in problems of control and programming.
J.Math.Anal.Applic. 3 (1961), pp 145-169.

206. R. Timman Optimization theory for ordinary differential equations.
J.Eng.Math. 1, (1967), pp 159-185.

207. G. Leitmann Introduction to optimal control.
McGraw-Hill (1966).

208. E.J. Haug & P.G. Kirmser Minimum weight design of beams with inequality constraints on stress and deflection. Trans.ASME.J.Appl.Mech. 34, (1967), pp 999-1004.

209. L.C.W. Dixon Further comments on Pontryagin's maximum principle applied to the profile of a beam. J.Roy.Aeron.Soc. 72, (1968), pp 518-519.

210. N.W. Bellamy & M.J. West Methods of profile optimization by iterative analogue computation. Computer J. 12, (1969), pp 132-138.

211. G. Gerard Minimum weight analysis of compression structures. N.Y. University Press, New York, (1956).

212. B.M.E. de Silva The application of Pontryagin's Principle to a minimum weight design problem. Trans. ASME, J. Basic Eng. 92, (1970), pp 245-250.

213. H. Jeffreys & B. Jeffreys Methods of Mathematical Physics Cambridge University Press, (1956), pp 522-525.

214. Modern Computing Methods - Notes on Applied Science, No. 16, DSIR, Ch. 7.

215. D.F. Barnard A Whetsone Algol program to calculate Bessel functions of real argument and integral order. English Electric Co., Tech.Memo W/M, (1967), u 9076.

216. M. Pappas & C.L. Amba-Rao A direct search algorithm for automated optimum structural design. J.AIAA 9, (1971), pp 387-393.

217. B.M.E. de Silva Feasible direction methods in structural optimization: optimum structural design. In Theory and Application (R.H. Gallagher & O.C. Zienkiewicz, eds.), John Wiley (1972), Chapter 8 (to appear). 10-14.

218. D.E. Charrett & G.D. Wilson A mathematical programming method for design and analysis of structures. Proc. 2nd Australasian Conf. on Mech. of Struct. (1971), pp 10.1-10.22.

219. M. Zyczkowski Optimal structural design in Rheology.
Trans.ASME J.Appl.Mech 38, (1971), pp 39-46.

220. J.M. Chern Optimal structural design for given deflection in presence of body forces.
Int.J.Solids Struct. 7, (1971), pp 373-382.

221. R. Reiss & G.J. Megarefs Minimal design of sandwich axisymmetric plates obeying Mises criterion.
Int.J.Solids Struct. 7, (1971), pp 603-623.

222. A.C. Pipkin & R.S. Rivlin Minimum weight design for pressure vessels reinforced with inextensible fibres.
Trans. ASME, J.Appl.Mech., 30, (1963), pp 103-108.

223. R.L. Fox & M.P. Kapoor Structural optimization in the dynamics response regime, a computational approach.
J.AIAA, 8, (1970), pp 1798-1804.

224. M.D. Cannon, C.D. Cullum & E. Polak Theory of optimal control and mathematical programming.
McGraw-Hill (1970).

225. A.G. Butkovskiy Distributed Control Systems
Elsevier (1969).

226. W. Kozlowski & Z. Mroz Optimal design of disks subject to geometric constraints.
Int.J.Mech.Sci., 12, (1970), pp 1077-1021.

227. E. Heer & J.N. Yang Optimization of structures based on fracture mechanics and reliability criteria.
J.AIAA 9, (1971), pp 621-628.

228. A.C. Robinson A survey of optimal control of distributed parameter systems.
Automatica 7, (1971), pp 371-388.

229. A.B. Templeman A steepest gradient method for optimum structural design.
Int.J.Num.Meth.Eng. 3, (1971), pp 249-259.

230. A. Gjelsvik Minimum weight design of continuous beams.
Int.J.Solids, Struct. 7, (1971), pp 1411-1425.

231. L.P. Felton & R.B. Nelson Optimized components in frame synthesis. J.AIAA 9 (1971), pp 1027-1031.

232. J.M. Chern & W. Prager Minimum weight design of statically determinate trusses subject to multiple constraints. Int.J.Solids Struct. 7, (1971), pp 931-940.

233. C.S. Rudisill & K.G. Bhatia Optimization of complex structures to satisfy flutter requirements.

234. W. Johnson et al The displacement field and its significance for certain minimum weight two-dimensional frames using the analogy with perfectly plastic flow in metal working. Int.J.Mech.Sci. 13, (1971), pp 547-561.

235. B.M.E. de Silva Application of optimal control theory to some structural optimization problems. Vibrations and International Design Automation Conference, Sept 8-10, (1971), Canada, ASME paper 71, Vibr.66.

236. I.C.I. Monograph No. 5 Nonlinear optimization techniques, Oliver & Boyd, (1969), Ch. 5.

237. R.L. Fox Optimization methods for engineering design. Addison-Wesley, (1971).

238. J.L. Armand Minimum design of plate structures for specified fundamental frequency. J.AIAA, 9, (1971), pp 1739-1745.

239. B.M.E. de Silva Optimal vibrational modes of a disc. Journal of Sound and Vibration, 2, (1972), pp 19-34

240. P. Tong and T.H.H. Pian A variational principle and the convergence of a finite element method based on assumed stress distribution. Int. J. Solids Struct. 5, (1969), pp 463-472.

APPENDIX: RESEARCH PAPERS BY THE AUTHOR

This Appendix contains the following research papers by the author (listed as references 179, 182, 212, 239, 197, 217 respectively) in support of this thesis application.

1. B.M.E. de Silva — The application of nonlinear programming to the automated minimum weight design of rotating discs.
   Optimization (R. Fletcher, ed.) Academic Press, London, (1969), pp 115-150.
2. B.M.E. de Silva — Minimum weight design of discs using a frequency constraint.
   Transactions of the American Society of Mechanical Engineers, Journal of Engineering for Industry, 91, (1969), pp 1091-1099.
3. B.M.E. de Silva — Application of Pontryagin's Principle to a minimum weight design problem.
   Transactions of the American Society of Mechanical Engineers, Journal of Basic Engineering, 92, (1970), pp 245-250.
4. B.M.E. de Silva — Optimal vibrational modes of a disc.
   Journal of Sound and Vibration, 21, (1972), pp 19-34.

5. B.M.E. de Silva An eigenvalue analysis for calculating the vibrational modes of steam turbine discs. International Journal of Mathematical Education in Science and Technology, 2, (1971), pp 171-181.

6. B.M.E. de Silva Feasible direction methods in structural optimization. Optimum Structural Design: In Theory and Application (R.H. Gallagher & O.C. Zienkiewicz, eds.) John Wiley (1972), Chapter 8 (to appear).

9. The Application of Nonlinear Programming to the Automated Minimum Weight Design of Rotating Discs

B. M. E. DE SILVA
Mechanical Engineering Laboratory, English Electric Company, Leicester, England

1. Introduction

The object of the research described in this paper is to investigate the feasibility of using nonlinear programming procedures to solve a class of minimum weight structural optimization problems with nonanalytic constraints. The structural configuration of the system is completely specified by the design parameters of which some are fixed and others are permitted to vary within a prescribed range, thus making it possible to optimize the system for minimum weight. The constraints on the design variables ensure physically reasonable designs and may be expressed in the form

$$l_i \leqslant x_i \leqslant u_i \quad \text{for } i = 1, \ldots, n \tag{1}$$

where the n real variables $x_1, \ldots, x_n$ are the design variables for the system. The bounds l_i, u_i are constants or functions of the other design variables.

The behaviour or response of the system is governed by the behaviour variables (that is stresses, deflection, vibrational frequencies, and so on), which are also constrained to vary within a prescribed range to prevent failure of the system under the design loads. For instance, the behavioural constraints may include statical constraints which prevent the stresses exceeding the yield stress, instability constraints which prevent failure of the structure by buckling, dynamical constraints which restrict the natural frequencies of vibration to lie within prescribed frequency bands, and so on. The behavioural constraints may therefore be expressed in the form

$$L_j \leqslant y_j(x_1, \ldots, x_n) \leqslant U_j \quad \text{for } j = 1, \ldots, m. \tag{2}$$

The weight of the structure is assumed to be a single valued differentiable function of the design variables

$$W = W(x_1, \ldots, x_n). \tag{3}$$

The minimum weight solutions are obtained by minimizing Eqn (3) subject to the constraint conditions (1), (2). The functions W, y_j in general are nonlinear and the solutions are given by a nonlinear programming formulation.

The minimum weight problems considered in this paper are restricted to problems for which the behaviour variables cannot be expressed analytically as functions of the design variables. Therefore it is not possible to use closed form analytical procedures for determining the minimum weight solutions and recourse must be made to approximate or numerical procedures. The behaviour variables are functions only in the sense that they are computer oriented rules for determining the behaviour associated with a given design and are not given in a closed analytical form in terms of the design variables. Thus the behaviour variables may be regarded as a "black box" into which are put the design variables representing a given design and out of which comes the behaviour variables for that design. The box contains such devices as differential equations, finite difference procedures, a digital computer, and so on.

Consider for instance the problem of minimizing the weight of a steam turbine disc subject to specified geometrical and behavioural constraints. For purposes of simplicity, the turbine disc is idealized as a rotating circular disc (Fig. 1) of variable thickness. The behavioural constraints have been restricted to a consideration that the stresses in the disc should be below the yield stress, while the geometrical constraints impose restrictions on the dimensions and tolerances of the disc.

The weight is given by the functional expression

$$W[h] = \int_{a_1}^{a_m} 2\pi\rho r h(r) dr \tag{4}$$

where a_1, a_m are the inner and outer radii respectively, ρ is the density and $h(r)$ is the thickness at a radial distance r from the axis of rotation, $h(r)$ being measured parallel to the axis of rotation. The equilibrium equation for the disc is given by [1]

$$\frac{d}{dr}(h\sigma_r) + \frac{h}{r}(\sigma_r - \sigma_\theta) + \rho\omega^2 r h = 0 \tag{5}$$

where σ_r, σ_θ are the radial and tangential stresses respectively and ω is the angular velocity of rotation of the disc. This equation has been derived on the assumption of radially symmetric plane stress. The stresses may be expressed in terms of the radial displacement $u(r)$ by the following compatibility relations

$$\sigma_r = \frac{E}{1-\nu^2}(e_r + \nu e_\theta), \qquad \sigma_\theta = \frac{E}{1-\nu^2}(\nu e_r + e_\theta), \tag{5a}$$

$$e_r = \frac{du}{dr}, \qquad e_\theta = \frac{u}{r}, \tag{5b}$$

where e_r, e_θ are the radial and tangential strains, E is Young's modulus and ν is Poisson's ratio.

Therefore substituting Eqns (5a), (5b) in (5) gives the following differential equation for $u(r)$

$$\frac{d^2u}{dr^2} + \left(\frac{1}{r} + \frac{1}{h}\frac{dh}{dr}\right)\frac{du}{dr} - \left(\frac{1}{r} - \frac{\nu}{h}\frac{dh}{dr}\right)\frac{u}{r} + \frac{\rho\omega^2(1-\nu^2)}{E} r = 0. \tag{6}$$

Therefore in order to determine $u(r)$ explicitly it is necessary to specify

$$h = h(r) \qquad (a_1 \leqslant r \leqslant a_m) \tag{6a}$$

as a function of r. Then for prescribed boundary conditions on σ_r, σ_θ given by

$$[\sigma_r]_{r=a_1} = s_1; \qquad [\sigma_r]_{r=a_m} = s_m \tag{6b}$$

Eqn (6) uniquely determines $u(r)$ as a function of r. Therefore from Eqns (5a), (5b) the stresses σ_r, σ_θ may be determined as functions of r. The stresses are functionals of $h(r)$ and correspond to black box type behaviour variables.

The material of the disc is assumed to obey a yield condition of the form

$$F(\sigma_r, \sigma_\theta) \leqslant \sigma_0 \tag{7}$$

where σ_0 is the yield stress. The yield condition used in this investigation is the yield condition of Tresca defined by [2]

$$F(\sigma_r, \sigma_\theta) \equiv \max\left\{\tfrac{1}{2}|\sigma_r - \sigma_\theta|, \tfrac{1}{2}|\sigma_r|, \tfrac{1}{2}|\sigma_\theta|\right\}. \tag{7a}$$

The variation of $h(r)$ is defined by

$$h(r) \geqslant \varepsilon \tag{8}$$

where ε is a specified tolerance which ensures that $h(r)$ is never negative. The problem then consists of determining an optimal $h(r)$ which minimizes Eqn (4) subject to the constraint conditions (6)–(8) and is essentially a Bolza type problem in the calculus of variations [3] for which the discretized nonlinear programming approximation is characterized by nonanalytic constraints on the behaviour variables.

This paper includes: (1) reformulating the disc problem as a problem in nonlinear programming, and (2) developing minimization procedures for solving problems with nonanalytic constraints by extending existing methods and formulating new ones. Methods currently applicable are the "steepest descent–alternate step" mode of travel in design space proposed by Schmit *et al.* [4]–[12] for the automated weight minimization of trusses and waffle plates with instability constraints. Modifications are introduced to improve their computational efficiency and convergence rates. Generalizations lead to new methods; (3) applying these methods to obtain numerical solutions to the disc problem on an English Electric KDF9 computer for purposes of comparative evaluation.

Before discussing these topics, some preliminary design concepts are introduced which contain the framework for formulating the minimization problem.

2. Design Concepts

The design variables define a point

$$x = (x_1, \ldots, x_n) \tag{9}$$

in an n-dimensional real euclidean space E_n, called the design space. Consider the functions $g_k(x)$ for $k = 1, \ldots, 2(n+m)$ defined by

$$\begin{aligned} g_k(x) &= l_k - x_k && \text{for } k = 1, \ldots, n \\ &= x_{k-n} - u_{k-n} && \text{for } k = n+1, \ldots, 2n \\ &= L_{k-2n} - y_{k-2n}(x) && \text{for } k = 2n+1, \ldots, 2n+m \\ &= y_{k-2n-m}(x) - U_{k-2n-m} && \text{for } k = 2n+m+1, \ldots, 2(n+m). \end{aligned} \tag{10}$$

Therefore the constraint conditions (1), (2) become

$$g_k(x) \leqslant 0 \text{ for } k = 1, \ldots, 2(n+m). \tag{11}$$

The feasible region R is a subspace of E_n and consists of points $x \in E_n$ which satisfy the constraint conditions (1), (2) or (11), so that

$$R \equiv \left\{x;\ g_k(x) \leqslant 0 \ \text{ for } k = 1, \ldots, 2(n+m)\right\}. \tag{11a}$$

Design points which belong to R are called feasible points.

There is associated with each constraint function $g_k(x)$ a hyper-surface defined by

$$G_k \equiv \left\{x;\ g_k(x) = 0 \ \text{ for } k = 1, \ldots, 2(n+m)\right\}. \tag{11b}$$

The hypersurfaces for nonanalytic functions correspond to unknown surfaces in E_n.

The composite constraint surface is given by

$$G \equiv R \cap (G_1 \cup G_2 \ldots, \cup G_{2(n+m)}) \tag{11c}$$

and defines the boundary of R and points which belong to G are called boundary points. The weight contours

$$W(x) = c \tag{11d}$$

define a family of hypersurfaces in E_n. The minimization procedures generate a sequence of feasible designs of decreasing weight which converge to the least weight contour in R. A feasible initial design is established and is systematically improved by an alternating iterative process of analysis and design modifications. These automated design cycles correspond to motion in the design space along paths which the weight decreases. Therefore the minimization process consists in the proper selection of the directions and distances of travel in design space.

3. Illustrative Problem

The steam turbine disc to be optimized is shown in Fig. 1. The width of the hub and the rim shape have been specified to allow for the attachment of the discs and the spacing of the blades in the turbine while the depth of the hub is variable to permit adjoining discs to be shrunk onto a common shaft. The thickness distribution for the remainder of the disc is variable but symmetrically distributed about the midplane. The thickness $h(r)$ is defined by

$$\begin{aligned} h(r) &= b_1 && \text{for } a_1 \leqslant r \leqslant a_2 \\ &= h(r) && \text{for } a_2 \leqslant r \leqslant a_{m-1} \\ &= b_m && \text{for } a_{m-1} \leqslant r \leqslant a_m \end{aligned}$$

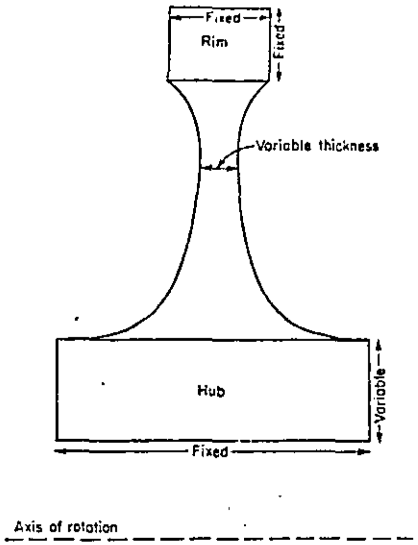

FIG. 1. Cross section of typical turbine disc.

where b_1 = width of hub (fixed), b_m = width of rim (fixed), and a_1, a_m, a_{m-1} are fixed radii while a_2 is variable. Therefore Eqn (4) becomes

$$W = \pi\rho b_1 (a_2^2 - a_1^2) + \pi\rho b_m (a_m^2 - a_{m-1}^2) + \int_{a_2}^{a_{m-1}} 2\pi\rho r h(r) dr$$

$$= \pi\rho b_1 (a_2^2 - a_1^2) + \pi\rho b_m (a_m^2 - a_{m-1}) + 2\pi\rho \sum_{j=3}^{m-1} \int_{a_{j-1}}^{a_j} r h(r) dr \quad (12)$$

where $a_1 < a_2 < a_3 < \ldots < a_{m-2} < a_{m-1} < a_m$. The function $h(r)$ is approximated by a sequence of linear functions $h_j(r)$ for $j = 3, \ldots, (m-1)$ defined by (Fig. 2).

$$h(r) \simeq h_j(r) \quad \text{for } a_{j-1} \leqslant r \leqslant a_j;\ j = 3, \ldots, (m-1) \quad (12a)$$

where

$$h_j(r) = b_{j-1} + \left(\frac{b_j - b_{j-1}}{a_j - a_{j-1}}\right)(r - a_{j-1}) \quad \text{for } a_{j-1} \leqslant r \leqslant a_j;\quad j = 3, \ldots, (m-1) \quad (12b)$$

$$h(a_j) = b_j \quad \text{for } j = 1, \ldots, m. \quad (12c)$$

Therefore Eqn (12) gives

$$W \simeq \pi\rho b_1 (a_2^2 - a_1^2) + \pi\rho b_m (a_m^2 - a_{m-1}^2) + 2\pi\rho \sum_{j=3}^{m-1} \int_{a_{j-1}}^{a_j} r h_j(r) dr$$

$$= \tfrac{1}{3}\pi\rho \sum_{j=3}^{m-2} (a_{j+1} - a_{j-1})(a_{j+1} + a_j + a_{j-1}) b_j$$

$$+ \tfrac{1}{3}\pi\rho\, b_1(-3a_1^2 + a_2^2 + a_3^2 + a_2 a_3)$$

$$+ \tfrac{1}{3}\pi\rho\, b_m(3a_m^2 - a_{m-1}^2 - a_{m-2}^2 - a_{m-1} a_{m-2}). \quad (12d)$$

The integral formulation (4) has been transformed into a finite difference form (12d) by linearizing the disc. $b_1, \ldots, b_m$ are the thicknesses parallel to

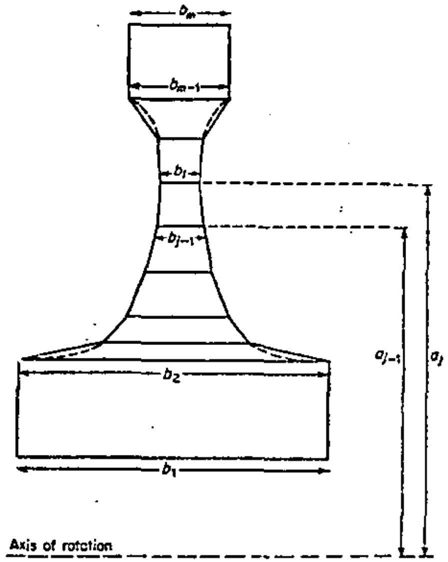

FIG. 2. Discretized nonlinear programming model.

the axis of rotation at specified radii $a_1, \ldots, a_m$ respectively. The disc profile is then obtained by joining adjacent thicknesses $\{b_{j-1}, b_j$ for $j = 2, \ldots, m\}$ by straight lines.

4. Geometrical Constraints

The following geometrical constraints are imposed on the disc dimensions

(1) $a_1 < a_2 < a_3 < \ldots < a_{m-2} < a_{m-1} < a_m$

(2) $b_1 = b_2$ (fixed)

(3) $b_m = b_{m-1}$ (fixed)

(4) $a_1, a_3, \ldots, a_{m-1}, a_m$ are all fixed

(5) a_2 is variable

(6) b_j is variable for $j = 3, \ldots, (m-2)$

(7) $b_j \geqslant \varepsilon_1$ for $j = 3, \ldots, (m-2)$

(8) $a_1 + \varepsilon_3 \leqslant a_2 \leqslant a_3 - \varepsilon_2$

where $\varepsilon_1, \varepsilon_2, \varepsilon_3$ = tolerances on the design variables. Conditions (2), (3) mean that the width of the hub and rim are fixed while (4), (5) mean that the depth of the rim is fixed but the depth of the hub is variable. The tolerance ε_1 ensures non-negative b_j, while $\varepsilon_2, \varepsilon_3$ restrict a_2 to lie within specified tolerances of a_1, a_3.

Therefore the design variables for the problem are given by

$$x = (b_3, \ldots, b_{m-2}, a_2). \tag{13}$$

This corresponds to an $(m-3)$ dimensional design space. The geometrical constraints are given by

$$l \leqslant x \leqslant u \tag{13a}$$

where

$$l = (\varepsilon_1, \ldots, \varepsilon_1, a_1 + \varepsilon_3), \quad u = (\infty, \ldots, \infty, a_3 - \varepsilon_2). \tag{13b}$$

These are linear constraints and correspond to hyperplanes parallel to the coordinate planes.

5. Behavioural Constraints

The disc is symmetrical with respect to both its axis of rotation and its midplane and is in dynamic equilibrium under the action of the centrifugal and thermal loadings. The stress calculations are based on Donath's method [13, 14] which consists essentially in replacing the disc by a series of annular rings of constant width. The stresses at the outer edge of a ring are determined in terms of the stresses at the inner edge. Continuity is ensured by equating the radial displacement and the radial load at the interface of adjacent rings. The stress equations are summarized below for ready reference.

Within each ring the thickness $h(r)$ is constant so that Eqn (6) reduces to

$$\frac{d^2u}{dr^2} + \frac{1}{r}\frac{du}{dr} - \frac{u}{r^2} + \frac{\rho\omega^2(1-\nu^2)}{E} r = 0, \tag{14}$$

that is

$$u = C_1 r + \frac{C_2}{r} - \frac{\rho\omega^2(1-\nu^2)}{8E}, \tag{14a}$$

where C_1, C_2 are constants of integration. Therefore from Eqns (5a), (5b) the rotational stresses are given by

$$\left.\begin{aligned} \sigma_r &= \alpha - \frac{\beta}{r^2} - \frac{\rho\omega^2(3+\nu)}{8} r^2 \\ \sigma_\theta &= \alpha + \frac{\beta}{r^2} - \frac{\rho\omega^2(1+3\nu)}{8} r^2 \end{aligned}\right\} \tag{14b}$$

where α, β are constants within each ring.

Similarly the thermal stresses are given by

$$\frac{d}{dr}(h\sigma_r) + \frac{h}{r}(\sigma_r - \sigma_\theta) = 0, \tag{14c}$$

where

$$\left.\begin{aligned} \sigma_r &= \frac{E}{1-\nu^2}[(e_r - \alpha\phi) + (e_\theta - \alpha\phi)] \\ \sigma_\theta &= \frac{E}{1-\nu^2}[\nu(e_r - \alpha\phi) + (e_\theta - \alpha\phi)] \end{aligned}\right\} \tag{14d}$$

α is the coefficient of linear expansion and ϕ is the temperature. Substituting (5b), (14d) in (14c) gives

$$\frac{d^2u}{dr^2}+\left(\frac{1}{r}+\frac{1}{h}\frac{dh}{dr}\right)\frac{du}{dr}-\left(\frac{1}{r}-\frac{\nu}{h}\frac{dh}{dr}\right)\frac{u}{r}$$

$$-(1+\nu)\left(\frac{1}{h}\frac{dh}{dr}+\frac{d\phi}{dr}\right)=0. \tag{14e}$$

Therefore within each ring

$$\frac{d^2u}{dr^2}+\frac{1}{r}\frac{du}{dr}-\frac{u}{r^2}-(1+\nu)\alpha\frac{d\phi}{dr}=0$$

that is
$$u=A_1r+\frac{A_2}{r}+(1+\nu)\frac{\alpha}{r}\int^r r\phi dr$$

where A_1, A_2 are constants of integration. Thus the thermal stresses are given by (14d), (5b).

$$\left.\begin{aligned}\sigma_r &= -\frac{\alpha E}{r^2}\int r\phi dr+\gamma-\frac{\sigma}{r^2}\\ \sigma_\theta &= \frac{\alpha E}{r^2}\int r\phi dr-\alpha E\phi+\gamma+\frac{\delta}{r^2}\end{aligned}\right\} \tag{14f}$$

where γ, δ are constants. The temperature $\phi(r)$ is a prescribed function of r.

The resultant stresses are then given by

$$\left.\begin{aligned}\sigma_r &= \sigma_r\,(\text{rot})+\sigma_r\,(\text{thermal})\\ \sigma_\theta &= \sigma_\theta\,(\text{rot})+\sigma_\theta\,(\text{thermal})\end{aligned}\right\} \tag{14g}$$

In general, the analysis phase of the redesign cycles consists of a series of black boxes into which are fed the design variables and out of which comes the behaviour variables. The contents of the boxes which include structural models and mathematical procedures for determining the behaviour variables do not play a significant role in the subsequent design modification iterations

and may be ignored. So that what is essential is the output from the black boxes which enables the behaviour variables to be checked against the behavioural constraints to ensure designs that do not violate the behavioural requirements for the problem. A more sophisticated analysis procedure merely means more accurate values for the behaviour variables associated with a given design and does not necessarily provide any new information on the minimization procedures. Therefore from this standpoint, Donath's method is a very acceptable form of analysis. It is relatively simple and was already available at the time this investigation was started.

At each stress calculation the computer program subdivides the intervals $[a_{j-1}, a_j]$ for $j = 3, \ldots, (m-1)$ into further subintervals by points $r_2, r_3, \ldots, r_{n-1}$ where

$$\left.\begin{aligned}&a_2 = r_2 < r_3 < \ldots < r_{n-1} - a_m\\ \text{In addition}\quad &r_1 = a_1;\quad r_n = a_m.\end{aligned}\right\} \tag{15}$$

The criterion for subdividing the interval $[a_{j-1}, a_j]$ is

$$|b_{j-1}-b_j| > \tfrac{1}{2}\varepsilon\,(b_{j-1}+b_j) \tag{15a}$$

where ε is a positive tolerance. If this criterion is satisfied $[a_{j-1}, a_j]$ is subdivided into u equal parts by points $q_0, q_1, \ldots, q_u$

$$a_{j-1} = q_0 < q_1 < \ldots < q_u = a_j. \tag{15b}$$

The corresponding thicknesses at these points are given by

$$p_i = h(q_i)\quad \text{for } i = 0, \ldots, u \tag{15c}$$

so that

$$\begin{aligned}|b_j-b_{j-1}| &= |p_u-p_0|\\ &= |(p_u-p_{u-1})+(p_{u-1}-p_{u-2})+\ldots+(p_2-p_1)+(p_1-p_0)|\\ &\leqslant \tfrac{1}{2}\varepsilon[(p_u-p_{u-1})+(p_{u-1}+p_{u-2})+\ldots+(p_2+p_1)+(p_1+p_0)]\\ &\leqslant \varepsilon u K_j\end{aligned}$$

where
$$K_j = \max\,(b_j, b_{j-1})$$

so that
$$u = 1+\left\langle\frac{|b_j-b_{j-1}|}{K_j}\right\rangle \tag{15d}$$

where $\langle x \rangle$ is the largest integer not exceeding x. The total number of points of subdivision for each of the intervals $[a_{j-1}, a_j]$ is n, the points being labelled $r_1, r_2, \ldots, r_n$ with thickness $h_1, h_2, \ldots h_n$ respectively. The reason for this subdivision is to obtain a better estimate for the stress distribution. The number n varies from design to design.

For each design the stresses σ_r, σ_θ at $r_1, \ldots, r_n$ are calculated. Therefore the principal shearing stresses at these radii are given by [2]

$$\tau_1 = \tfrac{1}{2}|\sigma_r - \sigma_\theta|, \quad \tau_2 = \tfrac{1}{2}|\sigma_r|, \quad \tau_3 = \tfrac{1}{2}|\sigma_\theta|. \tag{16}$$

The stress constraints are defined by the Tresca yield condition

$$\tau \leqslant \tau_0 \tag{16a}$$

where τ_0 is the critical stress and τ is the maximum principal shearing stress.

$$\tau = \max(\tau_1, \tau_2, \tau_3). \tag{16b}$$

Therefore the behaviour variables are given by

$$y(x) = (\tau_{r_1}, \tau_{r_2}, \ldots, \tau_{r_n}) \tag{17}$$

while the behavioural constraints are given by

$$L \leqslant y(x) \leqslant U \tag{17a}$$

where

$$L = (0, 0, \ldots, 0), \qquad U = (\tau_0, \tau_0, \ldots, \tau_0). \tag{17b}$$

Due to the black box nature of the stresses the behavicural constraints correspond to unknown surfaces in design space.

6. Weight Function

The weight $W = W(b_3, \ldots, b_{m-2}, a_2)$ given by Eqn (12d) is a quadratic in a_2 but linear in b_j. The function W and the feasible region R are in general nonconvex and the problem may possess relative minima.

7. Nonlinear Programming Formulation

The disc problem may be formulated mathematically as a nonlinear programming problem as follows.

Given l, u, L, U determine a design x which satisfies the conditions

(1) $l \leqslant x \leqslant u$

(2) $L \leqslant y(x) \leqslant U$

and minimizes the weight $W(x)$.

8. Nonlinear Programming Procedures

Nonlinear programming procedures applicable to structural problems with analytic constraints include:

(1) Cutting plane method [15, 16] for transforming a nonlinear problem to a series of linear programming problems.
(2) Rosen's gradient projection method [17–19].
(3) Penalty function methods for transforming a constrained problem to a series of unconstrained minimization problems [20–22] each of which can be solved using any of several well-known methods on unconstrained minimization [23–25].
(4) Lagrangian methods [26, 27] using the properties of the saddle point of the Lagrangian function.
(5) Methods for leaving the boundary of the feasible region along the constant weight surface [28], the direction for the "bounce" being given by a quadratic programming problem.
(6) Steepest descent procedures [29–31] for automated weight minimization using matrix methods of structural analysis.

Equations (6), (14e), (14g) applied to (16a) may be written in the form

$$\tau[h] \equiv \int^{r} \phi\left(r, h(r), \frac{d}{dr} h(r)\right) dr \leqslant \tau_0. \tag{18}$$

The above methods do not apply to constraints of the type (18). A "steepest descent–alternate step" procedure developed by Schmit *et al.* [4–12] may however be readily adapted to describe these problems; they started from an initial feasible point and moved in the direction of steepest descent to a better design some finite distance away. This procedure is repeated until a constraint is encountered which prevents further moves in the gradient direction. Then an alternate step is taken which is a move along the constant weight surface. After the alternate step a feasible point should have been obtained from which a steep descent can be made. The process is continued until no move can be made by either mode—at which time an optimum is said to be achieved. The reasoning behind this technique is that since the gradient direction points in the direction of greatest change it is the best direction to move in to improve the design. If a move cannot be made in the best direction, then a move is made which at least does not increase the weight of the design.

A fixed incremental step length is used in conjunction with steepest descent motion, the step length being doubled at each feasible iteration. This doubling process is repeated until a design is reached which violates on a main constraint (geometrical constraints are ignored at this stage); the total distance of travel back to an already feasible point is then halved, and the direction reversed. In all subsequent iterations, the distance is always halved and the direction reversed after each transition between a violated and non-violated condition. Thus, this halving and doubling process is directed to and converges upon the constraint surface. A random number generator was then used to propagate the directions of search along the constant weight surface. A sequence of proposed new designs was generated which was tested in turn against the geometrical and behavioural constraints. If any one of these designs was found to be feasible steepest-descent motion was continued as before. This method for leaving the boundary of R is called the method of alternate base planes [8] and will be described in the following section. The methods described in this paper use an accelerated steepest-descent mode of travel in the feasible region, the step length being estimated to the nearest constraint. The step length decreases as a constraint is approached and this enables a constraint to be encountered more rapidly than a straightforward doubling process. When a design violates a constraint, a linear interpolation technique is used to converge to the constraint surface, the interpolations being always between a violated and non-violated design. In general, this ensures a better convergence rate than a doubling and halving process.

The method of alternate base planes was applied to the disc problem and thereafter more selective methods were sought for leaving the boundary of R. A direction of search was generated whereby the sections of the disc not at yield stress were thinned in proportion to their stress levels relative to the yield stress, while the section at yield was thickened by a predetermined factor. The step length was then calculated using the equal weight condition, which gave a quadratic equation for the step length. A major difficulty was the possibility of obtaining complex roots and even if real roots were forthcoming there was no guarantee that the geometrical and behavioural constraints were not violated. Therefore a method was devised which always guaranteed non-violation of the geometrical constraints.

In this method the proposed design need only be tested against the yield criterion. The linearity of the geometrical constraints enables a step length

to be easily calculated which ensures an alternate step within the design variable bounds. The direction is then determined from the conditions of equal weight and normalization. To obtain real determinate solutions the number of unknowns is reduced to two by assigning zero values to the remaining variables. This corresponds to changing two design variables and leaving the rest unaltered. The section at yield stress is thickened, while the section furthest from yield is thinned so as to leave the weight unchanged. If the design violates the yield criterion the step length is progressively halved a specified number of times, and if no feasible design is forthcoming a different combination of direction cosines is set to zero, generating a different direction of search. If the yield condition is still violated this method is scrapped and the random method is used to determine an alternate step design.

The nonconvexity of W and R in general gives rise to pockets of relative minima. There is no known method yet of establishing whether a proposed solution is in fact a global solution or not. However, it is possible to establish a reasonable degree of confidence by searching a fairly wide region of design space. It is also possible to select two different initial points and run the minimization procedures along distinct paths. If the solution is the same (to within a reasonable tolerance) in the two cases, it is reasonable to assume that the proposed solution is a global one.

9. Minimization Procedures

The disc optimization problem [32, 33] is characterized by:

(1) Multi-dimensional design space
(2) Nonlinear weight function
(3) Relative minima
(4) Linear geometrical constraints
(5) Stresses "black box" type functions

while the optimization procedure is characterized by (Fig. 3):

(1) Accelerated steepest descent motion in the feasible region until a constraint is encountered.
(2) Constrained steepest descent motion from a geometrical constraint. Since a move in the direction of steepest descent cannot generally be made without piercing through the constraint, the method moves in the next best direction, the projection of the direction of steepest descent on the constraint surface.
(3) Equal weight redesign from a behavioural constraint surface. Constrained steepest descent motion cannot take place as the surfaces are unknown. A move is therefore made which at least does not increase the weight of the design.

10. Steepest Descent Motion

The computer program starts from an initial feasible design and enters steepest motion defined by the following iterative equation

$$x^{(q+1)} = x^{(q)} + t^{(q)}\psi^{(q)} \tag{19}$$

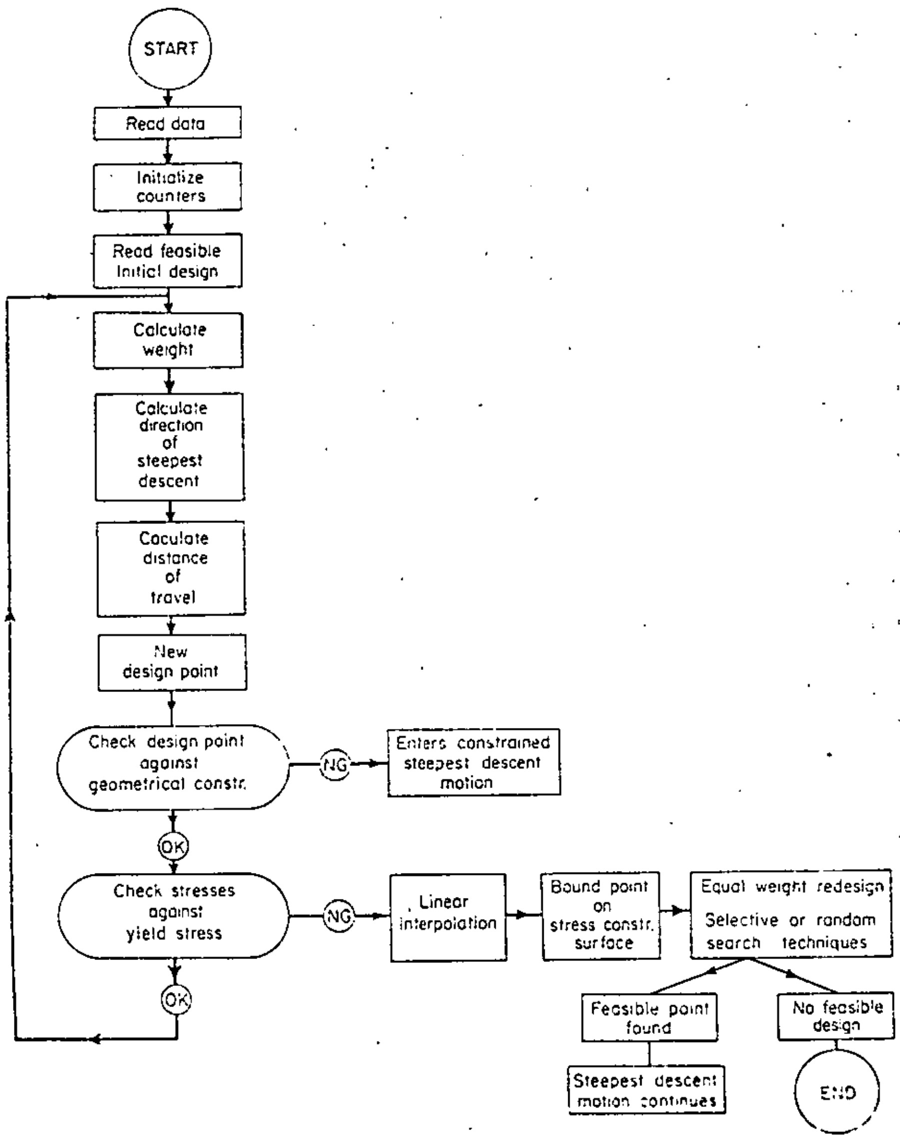

FIG. 3. Flow diagram for structural synthesis based on a stress constant.

where

$$\left.\begin{aligned} &x^{(q)} = (b_3^{(q)}, \ldots, b_{m-2}^{(q)}, a_2^{(q)}), \quad \psi^{(q)} = -\nabla W(x^{(q)})/|\nabla W(x^{(q)})|, \\ &\nabla = \left(\frac{\partial}{\partial b_3}, \ldots, \frac{\partial}{\partial b_{m-2}}, \frac{\partial}{\partial a_2}\right), \\ &t^{(q)} = \text{step length}, \\ &q = \text{design cycle counter.} \end{aligned}\right\} \tag{19a}$$

Therefore from Eqn (12d)

$$\left.\begin{aligned} \frac{\partial W}{\partial b_j} &= \frac{\pi\rho}{3}(a_{j+1}-a_{j-1})(a_{j+1}+a_j+a_{j-1}) \text{ for } j = 3, \ldots, (m-2) \\ \frac{\partial W}{\partial a_2} &= \frac{\pi\rho}{3}(2a_2+a_3)(b_1-b_3). \end{aligned}\right\} \tag{19b}$$

Equation (19) therefore reduces to

$$\left.\begin{aligned} b_j^{(q+1)} &= b_j^{(q)} - \frac{\pi\rho}{3}(a_{j+1}-a_{j-1})(a_{j+1}+a_j+a_{j-1})t^{(q)}/N^{(q)} \\ &\quad \text{for } j = 3, \ldots, (m-2) \\ a_2^{(q+1)} &= a_2^{(q)} - \frac{\pi\rho}{3}(2a_2+a_3)(b_1-b_3)t^{(q)}/N^{(q)} \end{aligned}\right\} \tag{19c}$$

where the normalization factor $N^{(q)}$ is given by

$$N^{(q)} = \frac{\pi\rho}{3}\left[\sum_{j=3}^{m-2}(a_{j+1}-a_{j-1})^2(a_{j+1}+a_j+a_{j-1})^2 + (2a_2+a_3)^2(b_1-b_3)^2\right]^{\frac{1}{2}}. \tag{19d}$$

The distance to a behavioural constraint cannot be determined exactly as the surfaces are unknown. Therefore the step length is estimated as follows. Let

$h_i^{(q)}$ = thickness at radius r_i;

$\tau_{r_i}^{(q)}$ = maximum principal shearing stress at r_i.

For purposes of this calculation, it is assumed that each $h_i^{(q)}$ can be changed independently without affecting the stress distribution elsewhere. Therefore to bring $h_i^{(q)}$ to yield stress it must be changed to $\bar{h}_i^{(q)}$ given by

$$(2\pi r_i \bar{h}_i^{(q)})\tau_0 \simeq (2\pi r_i h_i^{(q)})\tau_{r_i}$$

$$\bar{h}_i^{(q)} \simeq \frac{\tau_{r_i}}{\tau_0} h_i^{(q)}. \tag{20}$$

This relation is derived on the assumption that the load remains unchanged. Therefore the distance $t_i^{(q)}$ to the constraint surface at r_i is given by

$$\bar{h}_i^{(q)} = h_i^{(q)} - t_i^{(q)}\phi_i^{(q)} \qquad (0 \leqslant \phi_i \leqslant 1)$$

so that
$$t_i^{(q)} = \left(\frac{\tau_0 - \tau_{r_i}}{\tau_0}\right)\frac{h_i^{(q)}}{\phi_i^{(q)}}$$

where

$$\left.\begin{aligned} \phi_i^{(q)} &= \frac{\psi_j^{(q)}(r_i - a_{j-1}) + \psi_{j-1}^{(q)}(a_j - r_i)}{a_j - a_{j-1}} \\ \text{and} \quad & a_{j-1} \leqslant r_i \leqslant a_j \quad \text{for } j = 3, \ldots, (m-2) \end{aligned}\right\} \tag{20a}$$

then
$$t^{(q)} = \min_{3 \leqslant i \leqslant n-2} t_i^{(q)}. \tag{20b}$$

Thus $t^{(q)}$ decreases as a behavioural constraint surface is approached. At each iteration the design is checked against the geometrical and behavioural constraints. The design is first checked against the geometrical constraints and if the geometrical constraints are not violated, the corresponding stress distribution is calculated and then checked against the yield criterion. If the stresses are below the yield stress, the design is feasible and steepest descent motion continues until a non-feasible design is encountered. A non-feasible design corresponds to a region of constraint violation, that is violation of either the geometrical or the stress constraints.

11. Geometrical Constraint Violation

The design lies outside the geometrical bounds. The distances from the last feasible design to the geometrical constraints are calculated and the least positive distance is taken, giving a point lying on the nearest constraint. Let $x^{(q+1)}$, $x^{(q)}$ be the non-feasible and feasible designs respectively. Therefore

from Eqns (19c), (13a), (13b), the distances to the geometrical constraints are given by

$$\left.\begin{aligned} t_j &= \frac{3(b_j^{(q)} - \varepsilon_1)N^{(q)}}{\pi\rho(a_{j+1} - a_{j-1})(a_{j+1} + a_j + a_{j-1})} \quad \text{for } j = 3, \ldots, (m-2) \\ t_1 &= \frac{3(a_2^{(q)} - a_1 - \varepsilon_3)N^{(q)}}{\pi\rho(2a_2 + a_3)(b_1 - b_3)} \\ t_2 &= \frac{3(a_3 - \varepsilon_2 - a_2^{(q)})N^{(q)}}{-\pi\rho(2a_2 + a_3)(b_1 - b_3)}. \end{aligned}\right\} \tag{21}$$

Therefore the required design is given by

$$x^* = x^{(q)} + t^*\psi^{(q)} \tag{21a}$$

where
$$t^* = \min_{1 \leqslant j \leqslant m-2} (t_j;\, t_j > 0). \tag{21b}$$

The point x^* is checked against the behavioural constraints and, if satisfactory, the program enters constrained steepest descent motion.

12. Behavioural Constraint Violation

A linear interpolation procedure is used to converge to a boundary point on a behaviour constraint (to within a specified tolerance). Due to their linearity the geometrical constraints are never violated during the subsequent interpolations, which are always between a feasible and non-feasible design (violating the yield criterion). Let $x^{(q+1)}$, $x^{(q)}$ be the non-feasible and feasible designs respectively. The corresponding behaviour functions are given by

$$\left.\begin{aligned} y(x^{(q+1)}) &= (\tau_{r_1}^{(q+1)}, \ldots, \tau_{r_n}^{(q+1)}) \\ y(x^{(q)}) &= (\tau_{R_1}^{(q)}, \ldots, \tau_{R_N}^{(q)}) \end{aligned}\right\} \tag{22}$$

where the stresses are evaluated at radii $(r_1, \ldots, r_n)$ $(R_1, \ldots, R_N)$ respectively. Suppose the yield stress is exceeded at a section of the disc at a radial distance r_k.

Let $\tau_v = \tau_{r_k}^{(q+1)} > \tau_0 \qquad (1 \leqslant k \leqslant n)$

$$\tau_f = (\tau^{(q)})_{r=r_k}$$

$$= \frac{\tau_{R_{t+1}}^{(q)}(r_k - R_t) + \tau_{R_t}^{(q)}(R_{t+1} - r_k)}{(R_{t+1} - R_t)} < \tau_0 \tag{22a}$$

where $R_t \leqslant r_k \leqslant R_{t+1} \qquad (1 \leqslant t \leqslant N-1).$

τ_f is the corresponding mean stress at r_k in the feasible design $x^{(q)}$. Therefore the linear interpolations are defined by

$$\hat{x}^{(1)} = x^{(q)} \qquad \Delta^{(1)} = x^{(q)}$$

$$\bar{x}^{(r)} = \hat{x}^{(r)} + \delta^{(r)}\psi^{(q)} \qquad \text{for } r = 1, 2, \ldots$$

$$\delta^{(r)} = \frac{\tau_0 - \tau_f}{\tau_r - \tau_f}\Delta^{(r)}$$

$$\Delta^{(r+1)} = \Delta^{(r)} - \delta^{(r)} \qquad \text{if } \hat{x}^{(r)} \text{ is feasible}$$

$$= \delta^{(r)} \qquad \text{otherwise}$$

where $\delta^{(r)}$ = step length at rth interpolation; $\Delta^{(r)}$ = distance between current feasible and non-feasible designs; $\hat{x}^{(r)}$ = current feasible design, when yield criterion is violated at several radial points r_s

$$\delta^{(r)} = \min_s \delta s^{(r)}.$$

These interpolations continue until $x^{(r)}$ converge to a constraint surface (that is when the design lies on the constraint surface to within 99·2 per cent yield stress or when the incremental distance $\Delta^{(r)} \leqslant 0{\cdot}01$).

13. Equal Weight Redesign

Let x = boundary point on a behavioural constraint surface, $\bar{x}$ = proposed alternate step design, that is

$$\bar{x} = x + t\lambda$$

where $\lambda = (\lambda_1, \ldots, \lambda_{m-3})$; $\quad t$ = step length.

The proposed new design lies on the constant weight surface, so that

$$W(x) = W(x + t\lambda). \tag{23}$$

Substituting Eqn (23) in Eqn (12d) and simplifying

$$\lambda_1\lambda_{m-3}^2 t^3 - \lambda_{m-3}[(b_1 - b_3)\lambda_{m-3} - (a_3 + 2a_2)\lambda_1]t^2$$
$$- \left[\sum_{j=3}^{m-2}(a_{j+1} - a_{j-1})(a_{j+1} + a_j + a_{j-1})\lambda_{j-2} + (b_1 - b_3)(a_3 + 2a_2)\lambda_{m-3}\right]t = 0.$$

There is a common factor of t, indicating a zero root, which is to be expected since $t = 0$ satisfies Eqn (23). Therefore

$$\lambda_1\lambda_{m-3}^2 t^2 - \lambda_{m-3}[(b_1 - b_3)\lambda_{m-3} - (a_3 + 2a_2)\lambda_1]t - \left[\sum_{j=3}^{m-2}(a_{j+1} - a_{j-1})\right.$$
$$\left.\times (a_{j+1} + a_j + a_{j-1})\lambda_{j-2} + (b_1 - b_3)(a_3 + 2a_2)\right] = 0. \tag{23a}$$

14. Method of Alternate Base Planes

The direction of search [8] is defined by

$$\lambda_i^{(i)} = 0 \qquad \text{for } i = 1, \ldots, (m-3) \tag{24}$$

$$\lambda_j^{(i)} = \frac{R_j}{N} \qquad \text{for } j = 1, \ldots, (m-3); j \neq i \tag{24a}$$

where R_j are random numbers and N is the normalization factor defined by

$$N = \left(\sum_{j=1}^{m-3} R_j\right)^{\frac{1}{2}}.$$

Therefore the distances to the geometrical constraints are given by

$$t_j^{(i)} = \frac{b_j - \varepsilon_1}{-\lambda_{j-2}^{(i)}} \qquad \text{for } j = 3, \ldots, (m-2)$$

$$t_1^{(i)} = \frac{a_2 - a_1 - \varepsilon_3}{-\lambda_{m-3}^{(i)}}; \qquad t_2^{(i)} = \frac{a_3 - \varepsilon_2 - a_2}{\lambda_{m-3}^{(i)}}.$$

Let

$$\Delta_1^{(i)} = \min_{1 \leqslant j \leqslant m-2} (t_j;\, t_j > 0)$$

$$\Delta_2^{(i)} = \max_{1 \leqslant j \leqslant m-2} (t_j;\, t_j < 0).$$

Define

$$\left.\begin{aligned} \Delta_r^{(i)} &= R_r\, \Delta_1^{(i)} \qquad \text{for } r = 1, 2, 3 \\ &= R_r\, \Delta_2^{(i)} \qquad \text{for } r = 4, 5, 6 \end{aligned}\right\} \tag{24b}$$

where $\quad 0 < R_r < 1 \quad$ for $r = 1, \ldots, 6$.

Therefore the step length for equal weight redesign is given by

$$t = \Delta_r^{(i)} \tag{25}$$

and Eqn (23a) becomes

$$\lambda_1 \lambda_{m-3}^2\, \Delta_r^{(i)2} - \lambda_{m-3}\left[(b_1 - b_3)\lambda_{m-3} - (a_3 + 2a_2)\lambda_1\right] \Delta_r^{(i)}$$

$$- \left[\sum_{j=3}^{m-2} (a_{j+1} - a_{j-1})\,(a_{j+1} + a_j + a_{j-1})\lambda_{j-2} + (b_1 - b_3)\,(a_3 + 2a_2)\right] = 0.$$

This equation is used to redetermine $\lambda_i^{(i)}$ where $\lambda_j^{(i)}$ for $j \neq i$ are given by Eqn (24a) and $\Delta_r^{(i)}$ by Eqn (24b).

Consider the designs

$$\bar{x}_i^{(r)} = x + \Delta_r^{(i)}\lambda \qquad \text{for } r = 1, \ldots, 6 \tag{25a}$$

where $\quad W(b_3, \ldots, b_i, \ldots, b_{m-2}, a_2)$

$$= W(b_3 + \Delta_r^{(i)}\lambda_1, \ldots, \bar{b}_i^{(r)}, \ldots, b_{m-2} + \Delta_r^{(i)}\lambda_{m-4}, a_2 + \Delta_r^{(i)}\lambda_{m-3}).$$

The designs are tested against the design requirements and if any one of these is feasible, steepest descent motion proceeds until a constraint is encountered. If none of these designs is feasible, the base plane is changed $(i \to i+1)$ and a new set of proposed designs is generated. This process is continued until a feasible design is obtained or the current boundary design is accepted as the proposed optimum.

15. Selective I

This was the first attempt at using the physics of the problem to move away from a behavioural constraint. For a given direction λ, Eqn (23a) is a quadratic in the step length. Let the behaviour variables for the boundary point be given by

$$y(x) = (\tau_{r_1}, \ldots, \tau_{r_n})$$

where $\quad \tau_{r_q} = \tau_0, \quad$ for $a_{l-1} \leqslant r_q \leqslant a_l;\quad 1 \leqslant q \leqslant n;\quad 2 \leqslant l \leqslant m.$

Define $\quad \tau_{a_k} = \max(\tau_{a_{l-1}}, \tau_{a_l})$

where $\quad k = (l-1)$ or 1. $\qquad$ (26)

Therefore the direction of search is given by

$$\begin{aligned} \lambda_j &= (\tau_{a_j} - \tau_o)/N < 0 \qquad &&\text{for } j \neq k \\ &= \frac{\partial W}{\partial b_k}(x^{(q)})/|\nabla W(x^{(q)})| > 0 \qquad &&\text{for } j = k \end{aligned} \tag{26a}$$

where the normalization factor N is given by

$$N^2 = \left(\sum_{j \neq k} (\tau_{a_j} - \tau_0)^2\right) \Big/ (1 - \lambda_k^2).$$

The method of alternate base planes consumed computer time in searching through the random directions to find a line which would give a feasible point on the same weight contour. Selective I reduces the degree of randomness by examining only those directions which on physical considerations move away from a behavioural constraint. The disadvantages are, (1) possibility of complex roots, (2) even if real roots are forthcoming, the step length may be negative, and (3) geometrical constraints may be violated.

16. Selective II

This is a more intelligent version designed to overcome the above difficulties. From Eqns (13a), (13b) a step length defined by

$$t = \min_i (x_i - l_i,\, u_i - x_i) \tag{27}$$

gives an alternate step within the design variable bounds. Therefore

$$l \leqslant \bar{x} \leqslant u. \tag{27a}$$

The direction is then determined from the equal weight condition (23a) and the normalization condition

$$\sum_{i=1}^{m-3} \lambda_i^2 = 1. \tag{27b}$$

Equations (23a), (27b) are indeterminate. To obtain determinate solutions the number of unknowns is reduced to two by assigning predetermined values to $(m-5)$ cosines. These are made zero to obtain real solutions. The following designs are considered:

$$\bar{x}^{(r)} = x + (t/2^r)\lambda^{(r)} \qquad \text{for } r = 0, \ldots, 3 \tag{28}$$

The designs are tested against the behavioural constraints and if any one of these is feasible, steepest descent motion continues as before. If no feasible design is forthcoming, a different direction of search is generated corresponding to a different combination of direction cosines being assigned the value zero.

Define $$\tau_{a_s} = \min_{2 \leqslant j \leqslant (m-2)} \tau_{a_j}.$$

The following cases are considered

Case 1. $s \neq 2$.

$$\begin{aligned} \bar{b}_s &= b_s + t\lambda_s, & \lambda_s &< 0 \\ \bar{b}_k &= b_k + t\lambda_k, & \lambda_k &> 0 \\ \bar{b}_j &= b_j & &\text{for } j = 3, \ldots, (m-2);\ j \neq k, s \\ \bar{a}_2 &= a_2 & t &= b_s - \varepsilon_1 \end{aligned}$$

Therefore from Eqns (23a), (27b)

$$\lambda_s = -\frac{\mu}{\sqrt{(1+\mu^2)}}, \quad \lambda_k = \frac{1}{\sqrt{(1+\mu^2)}} \tag{29}$$

where $$\mu = \frac{(a_{k+1}-a_{k-1})(a_{k+1}+a_k+a_{k-1})}{(a_{l+1}-a_{l-1})(a_{l+1}+a_{l-1})} > 0.$$

Case 2. $s = 2$, $k \neq 3$.

$$\begin{aligned} \bar{b}_k &= b_k + t\lambda_k, & \lambda_k &> 0 \\ \bar{b}_j &= b_j & &\text{for } j = 3, \ldots, (m-2);\ j \neq k \\ \bar{a}_2 &= a_2 + t\lambda_{m-3}, & \lambda_{m-3} &< 0 \\ t &= a_2 - (a_1 + \varepsilon_3). \end{aligned}$$

Therefore from Eqns (23a), (27b)

$$\alpha t^2 \lambda_{m-3}^4 + 2\alpha(a_3 + 2a_2)t\lambda_{m-3}^3 + [1 + \alpha(a_3 + 2a_2)^2]\lambda_{m-3}^2 - 1 = 0 \tag{29a}$$

where $$\alpha = \frac{(b_1 - b_3)^2}{(a_{k+1}-a_{k-1})^2(a_{k+1}+a_k+a_{k-1})^2}.$$

Equation (29a) has a real root in $[1, 0]$ and is determined using linear interpolations being always between function values of opposite sign. Therefore from (27b), λ_k is given by, $\lambda_k = \sqrt{(1 - \lambda_{m-3}^2)}$.

Case 3. $s = 2$, $k = 3$.

$$\begin{aligned} \bar{b}_3 &= b_3 + t\lambda_1 & \lambda_1 &> 0 \\ \bar{b}_j &= b_j & j &= 4, \ldots, (m-2); \\ \bar{a}_2 &= a_2 + t\lambda_{m-3} & \lambda_{m-3} &< 0 \\ t &= a_2 - (a_1 + \varepsilon_3). \end{aligned}$$

Equations (23a), (27b) reduce to

$$\begin{aligned} t^4\lambda_{m-3}^6 + 2\gamma t^3 \lambda_{m-3}^5 + (\gamma^2 - 2\beta^2 + \alpha^2 - t^2)t^2\lambda_{m-3}^4 + 2(\alpha^2 - \beta^2 - t^2)\gamma t_{m-3}^3 \\ + (\beta^4 + \alpha^2\gamma^2 - \gamma^2 t^2 + 2\beta^2 t^2)\lambda_{m-3}^2 + 2\beta^2\gamma t\lambda_{m-3} - \beta^4 = 0. \end{aligned} \tag{29b}$$

when

$$\alpha = (b_1 - b_3), \qquad \beta^2 = (a_4 - a_2)(a_4 + a_3 + a_2), \qquad \gamma = (a_3 + 2a_2).$$

As before Eqn (29b) has a real root in $[-1, 0]$.

17. Constrained Steepest Descent Motion

Constrained steepest descent motion is defined by

$$x^{(q+1)} = x^{(q)} + t^{(q)}\psi^{(q)} \tag{30}$$

where $t^{(q)}$ is given by Eqn (20b) and $\psi^{(q)}$ is determined as follows.

Case 1. $x^{(q)}$ lies on $b_k = \varepsilon_1$, $3 \leqslant k \leqslant (m-2)$.

Then

$$\begin{aligned}\psi_j^{(q)} &= -\frac{1}{N}\left(\frac{\partial W}{\partial b_{j+2}}\right) && \text{for } j = 1, \dots, (m-4);\ j \neq k \\ &= 0 && \text{for } j = k \\ &= -\frac{1}{N}\left(\frac{\partial W}{\partial a_2}\right) && \text{for } j = (m-3)\end{aligned}$$

where

$$N = \left[\sum_{j \neq k}\left(\frac{\partial W}{\partial b_{j+2}}\right)^2 + \left(\frac{\partial W}{\partial a_2}\right)^2\right]^{\frac{1}{2}}.$$

Case 2. $x^{(q)}$ lies on $a_2 = a_1 + \varepsilon_3$ or $a_2 = a_3 - \varepsilon_2$.

Then

$$\begin{aligned}\psi_j^{(q)} &= -\frac{1}{N}\left(\frac{\partial W}{\partial b_{j+2}}\right) && \text{for } j = 1, \dots, (m-4) \\ &= 0 && \text{for } j = (m-3)\end{aligned}$$

where

$$N = \left[\sum_{j=1}^{m-4}\left(\frac{\partial W}{\partial b_{j+2}}\right)^2\right]^{\frac{1}{2}}.$$

This is a simplified form of Rosen's gradient projection method for linear constraints.

18. Numerical Results

The following cases were considered.

Case 1. A standard steam turbine disc with seven points of division.

Case 2. An arbitrary shaped disc with the same number of divisions.

TABLE I

Case	Dimension of design space $(m-3)$	Initial weight (lbs)	Final Weight (lb) Case (a)	Final Weight (lb) Case (b)	Number of iterations Case (a)	Number of iterations Case (b)	Run time (mins) Case (a)	Run time (mins) Case (b)
1	4	$3{\cdot}58934 \times 10^3$	$1{\cdot}66187 \times 10^3$	$2{\cdot}25877 \times 10^3$	62	80	5	7.833
2	4	$3{\cdot}60248 \times 10^3$	$1{\cdot}64547 \times 10^3$	$2{\cdot}32714 \times 10^3$	74	40	5	4·9
3	11	$3{\cdot}58973 \times 10^3$	$1{\cdot}61401 \times 10^3$	$2{\cdot}4537 \times 10^3$	186	408	30	60
4	11	$1{\cdot}65165 \times 10^3$	$1{\cdot}03400 \times 10^3$	—	188	—	30	—

Case 3. A standard disc with fourteen points of division.

Case 4. Final design for case (1) but with a finer division.

These cases were run using the Selective II and the method of alternate base planes in turn and are labelled cases (a), (b), respectively. They are shown in Figs 4–14, and are also summarized in Table I above for ready reference.

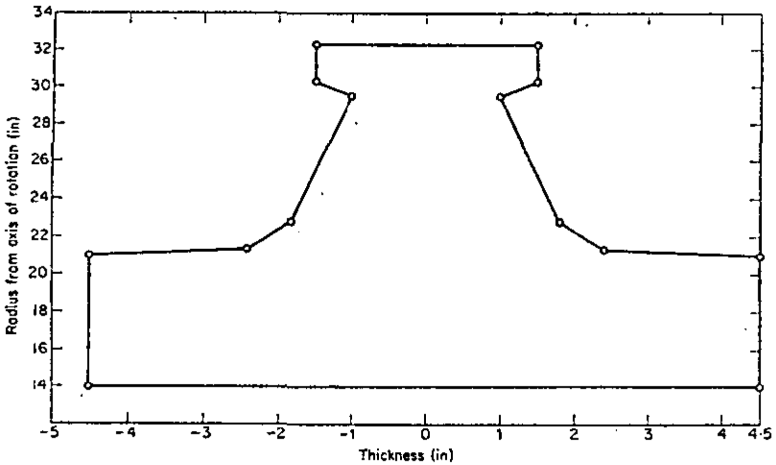

FIG. 4. Cases 1a, 1b. Initial design. Weight = $3{\cdot}58934\times10^3$ lb.

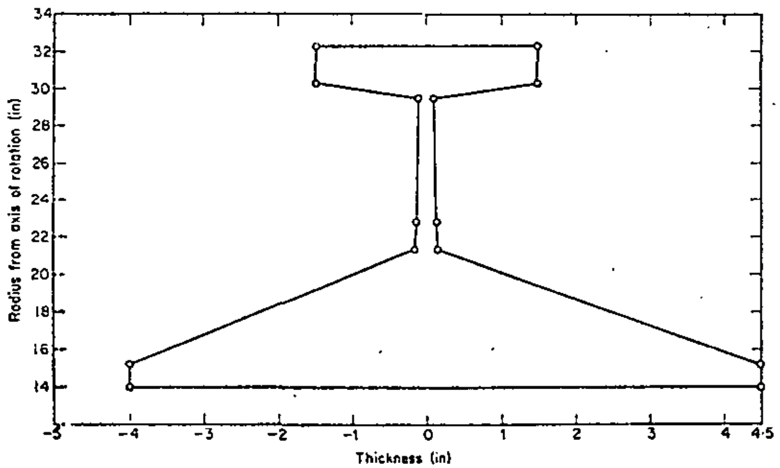

FIG. 5. Case 1a; 62 cycles. Final design. Weight = $1{\cdot}66187\times10^3$ lb.

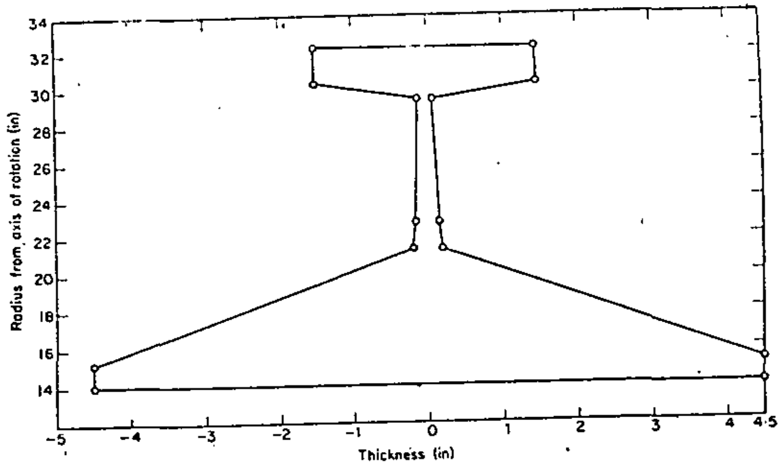

FIG. 6. Case 1b; 80 cycles. Final design. Weight = $2{\cdot}25877\times10^3$ lb.

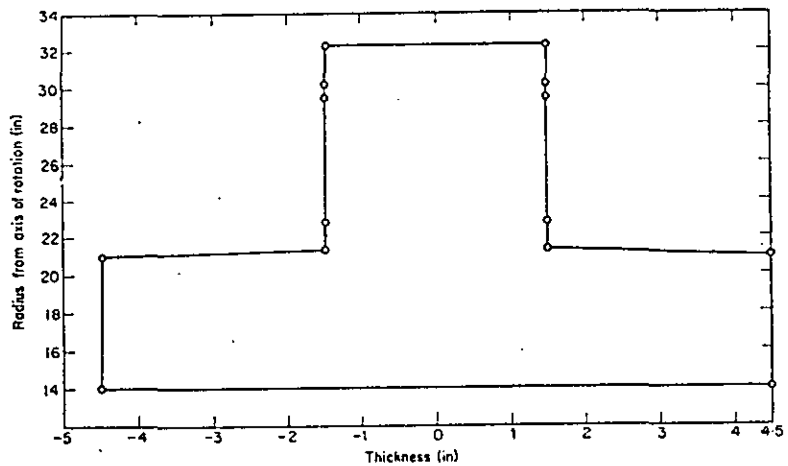

FIG. 7. Cases 2a, 2b. Initial design. Weight = $3{\cdot}60248\times10^3$ lb.

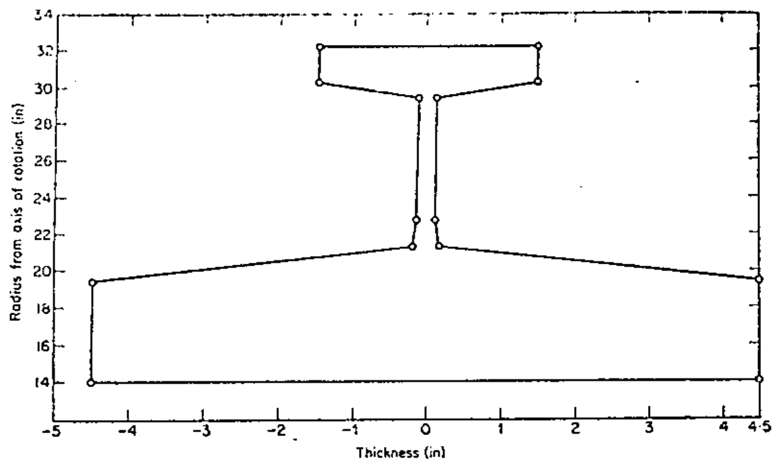

FIG. 8. Case 2a; 74 cycles. Final design. Weight = $1{\cdot}64547 \times 10^3$ lb.

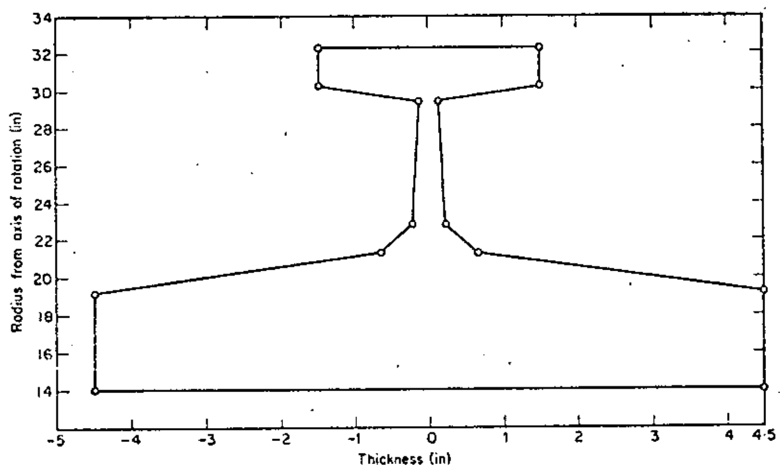

FIG. 9. Case 2b; 40 cycles. Final design. Weight = $2{\cdot}32714 \times 10^3$ lb.

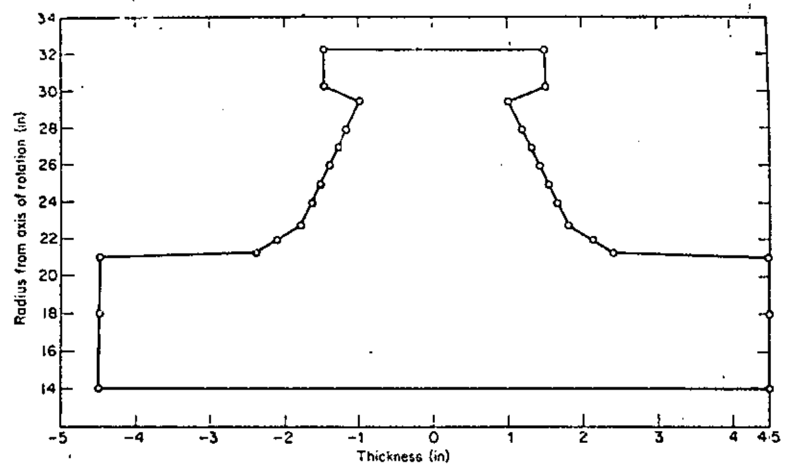

FIG. 10. Cases 3a, 3b. Initial design. Weight = $3{\cdot}58973 \times 10^3$ lb.

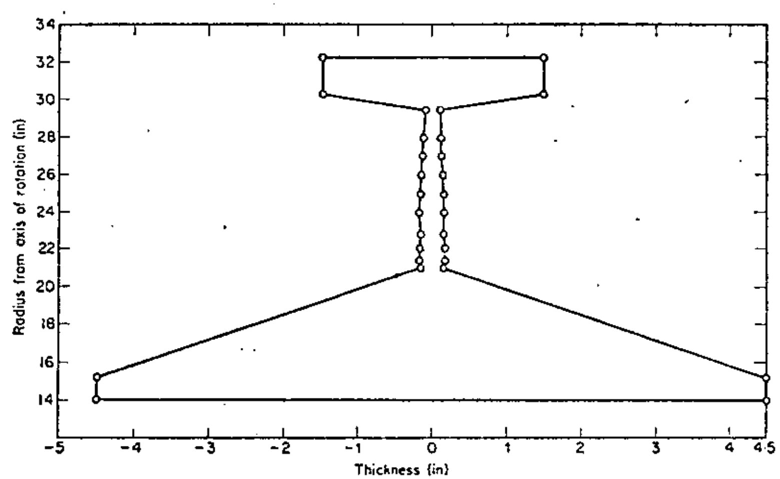

FIG. 11. Case 3a; 186 cycles. Final design. Weight = $1{\cdot}61401 \times 10^3$ lb.

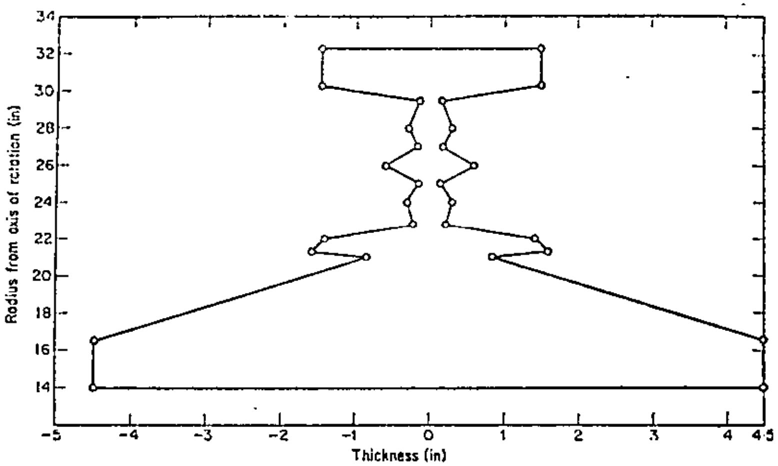

FIG. 12. Case 3b. Final design. Weight = $2{\cdot}14537 \times 10^3$ lb.

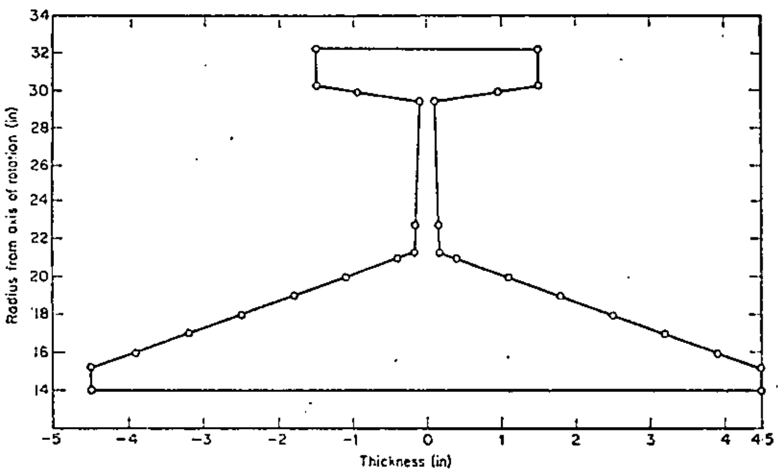

FIG. 13. Case 4. Initial design. Weight = $1{\cdot}65165 \times 10^3$ lb.

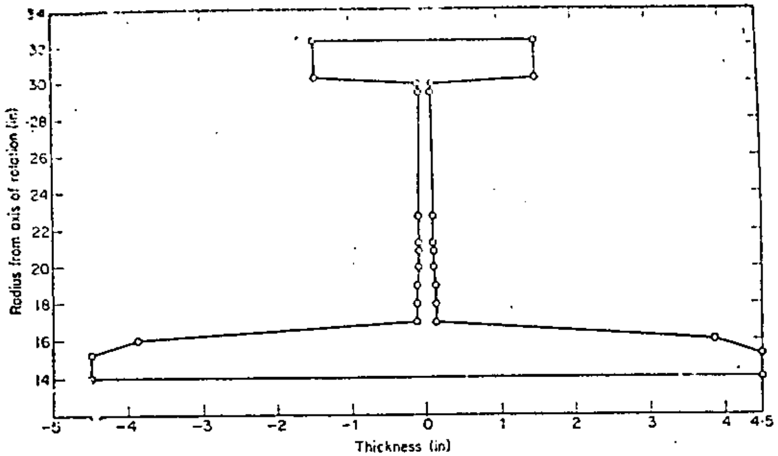

FIG. 14. Case 4; 188 cycles. Final design. Weight = $1{\cdot}03400 \times 10^3$ lb.

The discs were made of mild steel for which the density and elastic properties were assumed constant. The numerical work was carried out on an English Electric KDF9 computer using Algol compiler language.

19. Discussion

Although the initial designs for cases (1), (2) differ in weight by less than 0·005 per cent they are radically different in configuration; but the resulting designs tend to have approximately the same weight and configuration. Case (2) was run primarily to test for relative minima to establish whether the starting design influenced the final outcome. Cases (3), (4) were run to investigate the stability of the minimization paths. Initially the weight reductions were relatively rapid (Figs 15–16) but tended to slow down as the optimum was reached. As the iteration progressed equal weight redesign tended to give design points lying close to the behavioural constraints thereby slowing down the weight reductions. The random method consumed considerable computer time in searching through the random directions to locate a feasible design. However, Selective II was always able to locate a feasible design after one or two trials. Selective I never worked since almost always complex roots were generated for the quadratic equation for determining the step length; in the few occasions when real roots were forthcoming, the geometrical constraints were violated giving negative thicknesses. The number of iterations to obtain a specified weight reduction depends primarily on the dimension of the design space.

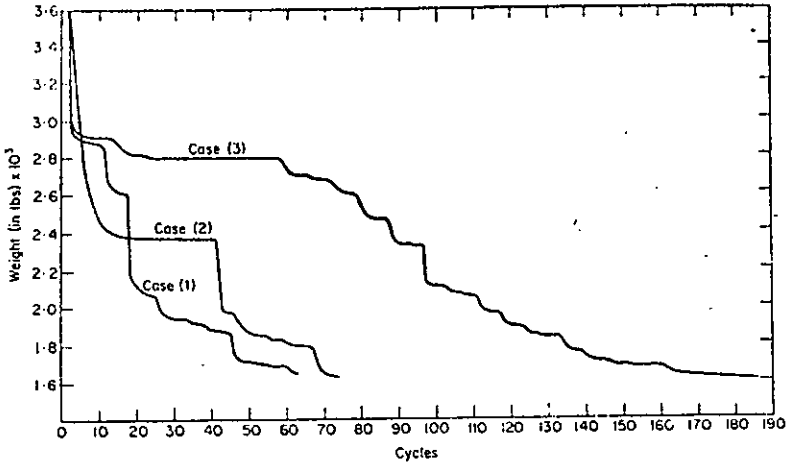

FIG. 15. Weight *versus* total redesign attempts. Based on selective search techniques for moving away from a bound point.

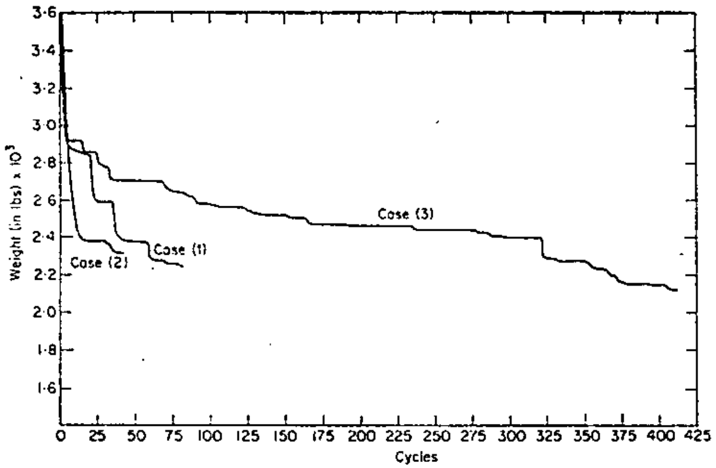

FIG. 16. Weight *versus* total redesign attempts. Based on random search.

The estimated step length used in the steepest descent mode of travel enabled a behavioural constraint to be encountered after about two or three iterations and thereafter the linear interpolation technique gave rapid convergence onto the constraint.

Acknowledgements

The research described in this paper was sponsored and supported by the Mechanical Engineering Laboratories of the English Electric Company, by whose permission this paper is published. Acknowledgement is also made to Dr W. A. Green of the Department of Theoretical Mechanics, University of Nottingham, for many valuable suggestions and discussions.

References

1. L. Cavallaro (1965). Stress analysis of rotating discs. *Nucl. Struct. Engng*, **2**, 271-281.
2. W. Prager and P. G. Hodge. "Theory of Perfectly Plastic Solids", Chapter 1. John Wiley, New York.
3. B. M. E. de Silva (1968). "Non-classical variational Problems in Minimum Weight Structural Optimization Theory". English Electric Company. Rpt. No. W/M(4B)p.1382.
4. L. A. Schmit (1960). "Structual Design by Systematic Synthesis". Proceedings of the 2nd National Conference of Electronic Computation, Structural Division A.S.C.E., 105-132.
5. L. A. Schmit and T. P. Kicher (1962). "Synthesis of Material and Configuration Selection". Structural Division, A.S.C.E., **88**, No. ST3, 79-102.
6. L. A. Schmit and W. M. Morrow (1963). "Structural Synthesis with Buckling Constraints". Structural Division, A.S.C.E., **89**, No. ST2, 107-126.
7. L. A. Schmit and R. H. Mallett (1962). "Design Synthesis in a Multi-dimensional Design Space with Automated Material Selection". E.D.C. Rpt. 2-62-2, Case Inst. Tech.
8. L. A. Schmit, T. P. Kicher and W. M. Morrow (1963). "Structural Synthesis Capability for Integrally Stiffened Waffle Plates". A.I.A.A., **1**, No. 12, 2820-2836.
9. L. A. Schmit and T. P. Kicher (1962). "Structural Synthesis of Symmetric Waffle Plates". N.A.S.A. Tech. Note D-1691.
10. L. A. Schmit and T. P. Kicher (1961). "Structural Synthesis of Symmetric Waffle Plates with Integral Orthogonal Stiffeners". E.D.C. Rpt. 2-61-1, Case Inst. Tech.
11. L. A. Schmit and R. L. Fox (1963). "Synthesis of a Simple Shock Isolator". E.D.C. Rpt. 2-63-4, Case Inst. Tech.
12. L. A. Schmit (1966). "Automated Redesign". International Scientific Tech. 63-78.
13. E. D'Sylva. "Disc Stresses". English Electric Company Rpt. W/M(4A) p.88.
14. L. G. Roberts. "Amendments to Program 00011 which Calculates Disc Stresses". English Electric Company Rpt. No. W/M(6A).1010.
15. J. E. Kelley Jr. (1960). The cutting plane method for solving convex programs. *J. Soc. ind. appl. Math.*, **8**, (4) 703-712.
16. F. Moses (1964). "Optimum Structural Design using Linear Programming". Structural Division, A.S.C.E., **90**, No. ST6, 89-104.
17. J. B. Rosen (1960). The gradient projection method, Part I. *J. Soc. ind. appl. Math.*, **8**, (1) 181-217.

18. J. B. Rosen (1961). The gradient projection method for nonlinear programming, Part II. *J. Soc. ind. appl. Math.*, 9, (4), 514-532.
19. D. M. Brown and A. Ang. (1965). "A Nonlinear Programming Approach to the Elastic Minimum Weight Design of Steel Structures". University of Illinois, Urbana, Illinois.
20. A.V. Fiacco and G. P. McCormick (1964). The sequential unconstrained minimization technique for nonlinear programming; a primal-dual method. *Mgmt. Sci.*, **10**, (2), 360-365.
21. L. A. Schmit and R. L. Fox (1964). An integrated approach to structural synthesis and analysis. *Am. Inst. Aerom. Aseran.*, 3, (6), 1104-1112.
22. L. A. Schmit and R. L. Fox (1964). An Integrated Approach to Structural Synthesis and Analysis. 5th Annual Conference on Structural Materials. New York, 294-315.
23. J. B. Crockett and H. Chernoff (1955). Gradient methods of maximization. *Pacif. J. Math.*, **5**, (1), 33-50.
24. D. J. Wilde (1964). "Optimum Seeking Methods". Prentice-Hall Englewood, New Jersey.
25. J. Kowalik (1966). Nonlinear programming procedures and design optimization. *Acta. polytech. scand.*, series d, **13**,.
26. B. Klein (1955). Direct uses of extremal principles in solving certain types of optimization problems involving inequalities. *J. Ops. Res.*, **3**, (2), 168-175.
27. H. W. Kuhn and A. W. Tucker (1951). "Nonlinear Programming". Proceedings 2nd Berkeley Symposium on Mathematical Statistics and Probability. (J. Neumann, ed.), pp. 481-492. University California Press, Berkeley.
28. J. L. Greenstadt (1966). A ricocheting gradient method for nonlinear programming. *Soc. ind. appl. Math.*, **14**, (3), 429-445.
29. R. A. Gellatly and R. H. Gallagher (1966). A procedure for automated minimum weight structural design—Part I. *Aeronaut. Q.*, **17**, (3), 216-230.
30. R. A. Gellatly and R. H. Gallagher (1966). A procedure for minimum weight structural design—Part II. *Aeronaut. Q.*, **17**, (4), 332-342.
31. G. C. Best (1964). Completely automatic weight minimization method for high speed digital computers. *J. Aircraft*, **1**, (3), 129-133.
32. B. M. E. de Silva (1965). "On the Application of Nonlinear Programming to the Automatic Structural Synthesis of Turbine Discs". English Electric Company, Rpt. No. W/M(6B) 1022.
33. B. M. E. de Silva (1967). "The Minimum Weight Design of Steam Turbine Discs". English Electric Company, Rpt. No. W/M(4B) 1323.

B. M. E. DE SILVA
Mathematician,
Mechanical Engineering Laboratory,
English Electric Company Ltd.,
Whetstone, Near Leicester, England

Minimum Weight Design of Disks Using a Frequency Constraint

The problem considered is that of minimizing the weight of a circular disk subject to specified behavioral and side constraints. The behavioral constraints have been restricted to a consideration that the lowest natural frequency of vibration should exceed a specified resonance frequency while the side constraints impose restrictions on the dimensions and tolerances of the disk. The problem has been formulated as a nonlinear programming problem characterized by a "black box" type representation for the frequency calculations. This paper includes a description of the synthesis procedures used together with a discussion of results.

1 Introduction

In a previous investigation [1–3][1] computational procedures based on the methods of nonlinear programming were successfully developed for minimizing the weight of an axisymmetric disk of variable thickness subject to specified behavior and side constraints. For purposes of simplicity in this initial investigation, the behavioral constraints were restricted to a consideration that the stresses should be below the yield stress while the side constraints imposed restrictions on the dimensions and tolerances of the disk. The problem was formulated analytically [4–5] as a very general problem in the calculus of variations with the addition of state and control inequality constraints, the control and state variables being given by the thickness and stress distribution functions, respectively. Solutions were obtained by transforming the variational formulation into a nonlinear programming formulation by approximating the disk by a discrete model using a piecewise linear representation for the control variable. Stability of the solutions was established by subjecting the control to different representations.

The nonlinear programming formulation was characterized by:

(*a*) multidimensional design space
(*b*) design parameter bounds to ensure physically reasonable designs
(*c*) quadratic weight function
(*d*) pockets of relative minima
(*e*) the stresses were functionals which associated to every point in design space a stress matrix, the columns corresponding to specified loading conditions. The stresses were defined by a set of computer oriented rules which were represented by a "black box" into which were put the design parameters specifying a given design configuration and out of which comes the corresponding stress distributions which were checked against the stress constraints. The associated synthesis procedures were characterized by:

(*a*) accelerated steepest descent motion in the feasible regions,
(*b*) constrained steepest descent motion along a known constraint,
(*c*) constant weight bounce from an unknown constraint.

In the present investigation, these procedures are further generalized and used to synthesize the disk using a dynamics technology in the absence of any statical constraints, whereby the lowest natural frequency of vibration should exceed a specified resonance frequency. The frequency is again a functional which associates to every point in design space a set of fundamental vibrational frequencies and has a "black box" type representation. The frequency calculations are performed inside the box and the redesign procedures are based entirely on the output—a set of numbers giving the fundamental frequencies at each design iteration. These procedures are independent of the analysis employed and are applicable to problems in conjunction with analysis programs already available. Alternatively, the mechanisms inside the box may be utilized [6–10] to generate the directions of search in design space. However, the need for refined analysis routines for performing more effective redesign cycles can be more readily assessed after the initial results have been evaluated using existing programs.

The numerical computations were performed on a KDF9 computer giving weight reductions of 56 percent and 28 percent for

[1] Numbers in brackets designate References at end of paper.

Contributed by the Vibrations Research Committee and presented at the Vibrations Conference, Philadelphia, Pa., March 30–April 2, 1969, of The American Society of Mechanical Engineers. Manuscript received at ASME Headquarters November, 22, 1968. Paper No. 69-Vibr-1.

Nomenclature

a_1 = inner radius of disk
a_m = outer radius of disk
r = radial distance
$h(r)$ = thickness at a radial distance r
ρ = density of material
$W[h]$ = weight functional
b_1 = width of hub (fixed)
b_m = width of rim (fixed)
a_{m-1} = inner radius of rim
a_2 = hub radius (variable)
b_j = thickness at radius a_j
L = lower bound on a_2
U = upper bound on a_2
ϵ = positive tolerance on the thickness
p = vibrational frequency
p_0 = resonance frequency
$\mathbf{x}$ = $(b_3, \ldots, b_{m-2}, a_2)$ is the vector of design parameters
q = design cycle counter
ψ = $(\lambda_1, \ldots, \lambda_{m-4}, \lambda_{m-3})$, direction of search
t = step length in design space
W = weight function
δM_j = change in mass at variable sections a_j
δp = frequency change
η_j = efficiency coefficient at radius a_j
k = kinetic energy density
v = potential energy density
V = maximum potential energy
E = Young's modulus
ν = Poisson's ratio
u = axial displacement
W = radial component of axial displacement
Ω = angular velocity of rotation
n = number of nodal diameters
θ = angle between consecutive steepest descent vectors

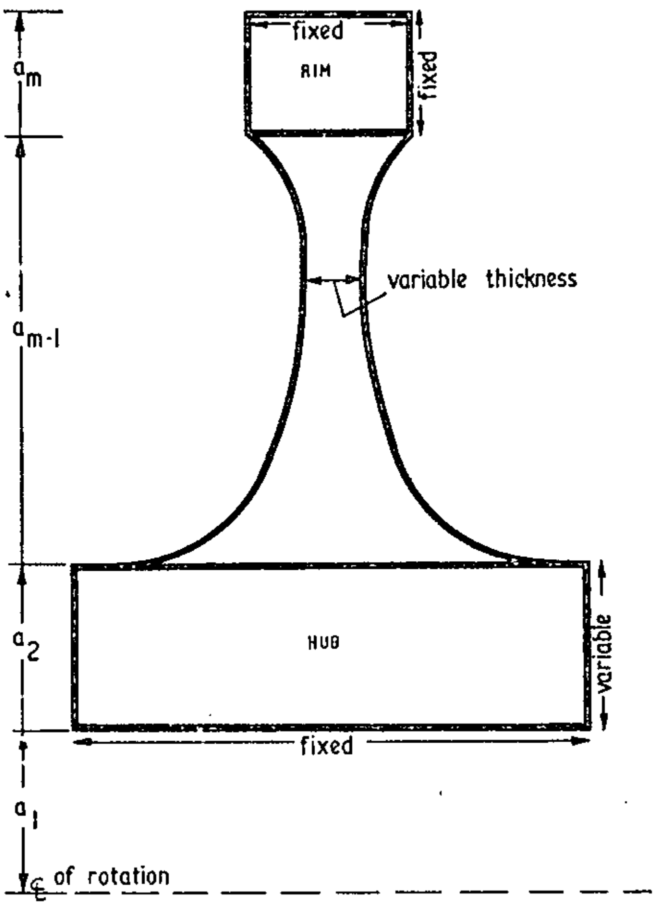

Fig. 1 Cross section of typical turbine disk

resonance frequencies of 440 and 2000 cycles per second, respectively, using a turbine disk idealization. A discussion of these results is included together with a description of some instabilities in the synthesis procedures used arising from the absence of any stress constraints on the problem.

2 Nonlinear Programming Formulation

It is possible to formulate the problem analytically as a very general problem in the calculus of variations [11] in which the weight functional to be minimized is given by

$$W[h] = \int_{a_1}^{a_m} 2\pi\rho r h(r) dr \tag{1}$$

where a_1, a_m are the inner and outer radii, respectively, $h(r)$ is the thickness at a radial distance r and ρ is the density of material. For purposes of numerical computations, the variational formulation is transformed into a discrete nonlinear programming formulation using finite differences and is characterized by a "black box" type representation for the frequency.

Consider a thickness distribution of the form (Fig. 1).

$$\left.\begin{aligned} h(r) &= b_1 & a_1 \le r \le a_2 \\ &= h(r) & a_2 \le r \le a_{m-1} \\ &= b_m & a_{m-1} \le r \le a_m \end{aligned}\right\} \tag{2}$$

where b_1, b_m, a_1, a_m, a_{m-1} are constants while a_2 is a variable satisfying the condition

$$L \le a_2 \le U \tag{3}$$

where L, U are constants.

In addition

$$h(r) \ge \epsilon, \qquad a \le r \le a_{m-1} \tag{3a}$$

where ϵ = positive tolerance to ensure nonnegative thickness. The disk is essentially an idealization of a turbine disk for which the width of the hub and the rim shape is fixed to allow for the attachment of the disks and the spacing of the blades in the turbine while the depth of the hub is variable to permit adjoining disks to be shrunk onto a common shaft. The thickness distribution for the remainder of the disk is variable but symmetrically distributed about the midplane.

Consider any partition of the interval $[a_2, a_{m-1}]$ defined by

$$a_2 < a_3 < a_4 \ldots . a_{m-3} < a_{m-2} < a_{m-1}$$

In each subinterval $[a_{j-1}, a_j]$, the thickness $h(r)$ is approximated by a linear function $h_j(r)$ defined by (Fig. 2).

$$h_j(r) = b_{j-1} + \left(\frac{b_j - b_{j-1}}{a_j - a_{j-1}}\right)(r - a_{j-1}) \tag{4}$$

where

$$h(a_j) = b_j, \qquad j = 1, 2, \ldots, m$$

substituting (2), (4) in (1)

$$\begin{aligned} W[h] &= \pi\rho b_1(a_2^2 - a_1^2) + \pi\rho b_m(a_m^2 - a_{m-1}^2) \\ &+ \int_{a_2}^{a_{m-1}} 2\pi\rho r h(r) dr \approx \pi\rho b_1(a_2^2 - a_1^2) + \pi\rho b_m(a_m^2 - a_{m-1}^2) \\ &+ \sum_{j=3}^{m-2} \int_{a_{j-1}}^{a_j} 2\pi\rho r h_j(r) dr = \frac{\pi\rho}{3} \sum_{j=3}^{m-2} (a_{j+1} - a_{j-1}) \\ &\times (a_{j+1} + a_j + a_{j-1}) + \frac{\pi\rho b_1}{3}(-3a_1^2 + a_2^2 + a_3^2 + a_2 a_3) \\ &+ \frac{\pi\rho}{3} b_m(3a_m^2 - a_{m-1}^2 - a_{m-2}^2 - a_{m-1}a_{m-2}) \end{aligned} \tag{5}$$

Therefore the weight functional has been reduced to a function of the design parameters

$$\left.\begin{aligned} &W[h] \rightarrow W(b_3, \ldots, b_{m-2}, a_2) \text{ defined by (5)} \\ &\text{where} \\ &b_j \ge \epsilon, \qquad j = 3, \ldots, m-2 \\ &L \le a_2 \le U \\ &\text{In addition, the frequency satisfies the condition} \\ &p \ge p_0 \end{aligned}\right\} \tag{6}$$

where p_0 = resonance frequency.

The design parameters representing a given design configuration are put into the "black box," out of which come the corresponding vibrational frequencies which are checked against the vibration constraints (6). The mechanisms inside the box include analysis routines for the frequency calculations which are based on an iterative solution of the differential equations of vibrations using the Myklesford-Holzer matrix technique [12–14]. The method is relatively simple and was already programmed at the start of this investigation. The contents of the box are disregarded since the purpose of this investigation is to develop computational procedures for describing problems with nonanalytic constraints.

The nonlinear programming formulation (6) is characterized by:

(*a*) multidimensional design space
(*b*) quadratic weight function
(*c*) relative minima in the absence of convexity conditions
(*d*) linear constraints on the design parameters giving hyper/planes in design space

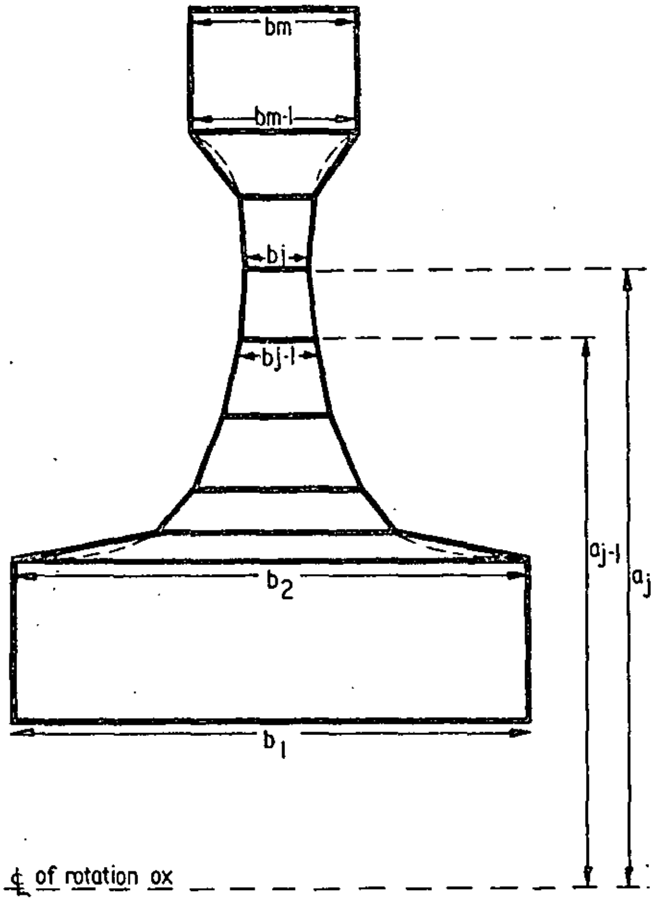

Fig. 2 Cross section of equivalent discretized disk

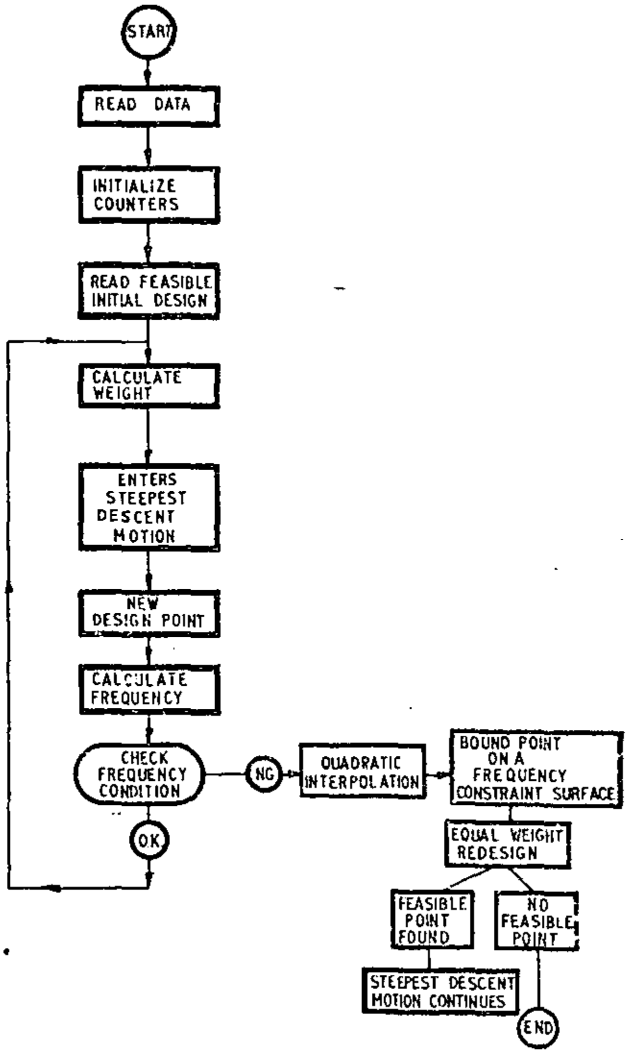

Fig. 3 Structural synthesis flow diagram

(*c*) frequency is a functional with a "black box" representation giving an unknown constraint hyper/surface.

3 Synthesis Procedures

The synthesis procedures in the absence of any stress constraints are characterized by:

(*a*) steepest descent motion until a vibration constraint is encountered,

(*b*) constant weight redesign at the resonance frequency,

(*c*) design parameter bounds never violated.

The computer program (Fig. 3) consists of moving from an initial feasible design in the direction of the gradient to a better design some finite distance away. This process is repeated until a vibration constraint is encountered which prevents further moves in the gradient direction. Then an alternate step is taken which is a move along the constant weight surface. After the alternate step a feasible design should have been obtained from which a steepest descent can be made. The process is continued until no move can be made by either mode, at which time an optimum is said to be achieved. The reasoning behind this procedure is that since the gradient points in the direction of greatest change, it is the best direction to move to improve the design. If a move cannot be made in the best direction then a move is made which at least does not increase the weight of the design. The steepest descent mode of travel is defined by the iterative equation

$$\mathbf{x}^{(q+1)} = \mathbf{x}^{(q)} + t^{(q)}\boldsymbol{\psi}^{(q)} \qquad q = 0, 1, 2, \ldots \qquad (7)$$

where $\boldsymbol{\psi}^{(q)}$ is the normalized direction of steepest descent and $t^{(q)}$ is the step length which is determined using a simplified form of Rosen's gradient projection method [15] in conjunction with the side constraints. This enables fairly large step lengths to be taken, thereby economizing on computer time.

As the designs approach a vibration constraint surface, it is possible that the step lengths used in the steepest descent procedure are too large, with the result that the design pierces through the constraint surface and moves into a region of constraint violation where the vibrational frequencies of the designs are below the resonance frequency. If this is the case, a quadratic interpolation procedure is used to converge to a design at the resonance frequency by thickening up the variable sections of the disk. This gives a design point on the boundary of the vibration constraint which is a nonanalytic surface due to the "black box" nature of the frequency, thereby precluding the use of standard methods of nonlinear programming such as moving along the constraint in a direction in which the weight decreases. Instead, an alternate step is taken along the constant weight surface, where the directions of search are based on either selective methods utilizing the physics of the problem or random methods, and are summarized below.

1 Selector I—Two design parameters are changed leaving the rest unchanged. All possible combinations are considered.

2 Selector II—A perturbation method using the Lagrangian energy density vector to estimate the normal to the vibration constraint.

3 Selector III—Three successive designs are used to estimate a new direction of search. This is used in case there are sharp ridges on the vibration constraint surface.

4 Random methods where a random number generator is

used to generate the directions. The intersection of these random directions with the constant weight contour are found and tested as trial designs. A modified version proposed by Schmit et al [16], is used, called the method of alternate base planes. A summary of these programs is given below.

4 Selector I

The constant weight redesign condition at the resonance frequency is given by

$$W(\mathbf{x}) = W(\mathbf{x} + t\psi) \tag{8}$$

where

$\mathbf{x}$ = current design at critical frequency

t = step length

ψ = direction of search

Substituting (8) in (5)

$$\lambda_1\lambda^2_{m-3}t^2 - \lambda_{m-3}[(b_1 - b_3)\lambda_{m-3} - (a_3 + 2a_2)]t - \left[\sum_{j=3}^{m-2} (a_{j+1} - a_{j-1})(a_{j+1} + a_j + a_{j-1})\lambda_{j-2} + (b_1 - b_3)(a_3 + 2a_2)\lambda_{m-3}\right] = 0 \tag{9}$$

where λ_j for $j = 1, \ldots, m - 3$ are the components of ψ. This gives a quadratic equation for determining the step length when the direction is specified. Alternatively, this is a condition on the direction when the step length is specified. The latter viewpoint is adopted here, the step length being selected to ensure designs within the design parameter bounds so that the proposed alternate step designs need be checked against the vibration constraint only. The random methods are less selective and consume considerable computer time in searching through the random directions for designs that are acceptable with respect to both the design parameter bounds and the vibration constraints.

The direction cosines of the direction for bouncing back into the feasible regions must satisfy condition (9) and the normalization condition

$$\sum_{j=1}^{m-3} \lambda_j^2 = 1 \tag{10}$$

In general, these define an indeterminate system of equations which are reduced to a determinate form by specifying (m-5) of the components in some way and then calculating the remaining two components using equations (9), (10). It was found convenient to make these (m-5) direction cosines zero to ensure real solutions.

The sections of greatest and least thickness are altered leaving the rest unchanged. If no feasible design is forthcoming, the step length is progressively reduced or a new direction is generated corresponding to a different combination of design parameters that are altered. Full details of the analysis are given in references [2, 3] to which the reader is referred to for more extensive details.

5 Selector II

Rayleigh's principle [17] based on the properties of the efficiency coefficients [18] was used to relate small changes in frequency to small changes in design

$$\delta p = \Sigma \eta_j \delta M_j \tag{11}$$

where δM_1, δM_2, . . . are changes in the mass at the variable sections and

$$\eta_j = -\frac{p_0(k - v)}{2pV} \tag{12}$$

where k, v are the kinetic and potential energy densities respectively and V is the maximum potential energy. From (5), (8)

$$\left.\begin{aligned} \delta M_j &= \left(\frac{\partial W}{\partial b_{j+2}}\right) \Delta b_{j+2}; \quad j = 1, \ldots, m - 4 \\ &= \left(\frac{\partial W}{\partial a_2}\right) \Delta a_2; \quad j = m - 3 \end{aligned}\right\} \tag{13}$$

Substituting (13) in (11)

$$\delta p = \sum_{j=1}^{m-4} \eta_j \frac{\partial W}{\partial b_{j+2}} \Delta b_{j+2} + \eta_{m-3} \frac{\partial W}{\partial a_2} \Delta a_2 = t \sum_{j=1}^{m-4} \lambda_j \eta_j \frac{\partial W}{\partial b_{j+2}} + t\lambda_{m-3}\eta_{m-3} \frac{\partial W}{\partial a_2} \tag{14}$$

The bounce back condition is characterized by $\delta p > 0$, which is satisfied by

$$\left.\begin{aligned} \lambda_j &= \eta_j, \quad j = 1, \ldots, m - 4 \\ \lambda_{m-3} &= \eta_{m-3} \quad \text{if} \quad \frac{\partial W}{\partial a_2} > 0 \\ &= -\eta_{m-3} \quad \text{if} \quad \frac{\partial W}{\partial a_2} < 0 \end{aligned}\right\} \tag{15}$$

The step length is given by

$$t = \text{Min}\left\{\min_{3 \leq j \leq m-2} (b_j - \epsilon), (a_2 - L), (U - a_2)\right\} \tag{16}$$

to ensure designs within the design parameter bounds. The strain energy is given by [19]

$$V = \iint \frac{Eh^3(r)}{24(1 - \nu^2)} \left\{\left(\frac{\partial^2 u}{\partial r^2} + \frac{1}{r}\frac{\partial u}{\partial r} + \frac{1}{r^2}\frac{\partial^2 u}{\partial \theta^2}\right)^2 - 2(1 - \nu) \times \left[\frac{\partial^2 u}{\partial r^2}\left(\frac{1}{r}\frac{\partial u}{\partial r} + \frac{1}{r^2}\frac{\partial^2 u}{\partial \theta^2}\right) - \left(\frac{\partial}{\partial r}\frac{1}{r}\frac{\partial u}{\partial \theta}\right)^2\right]\right\} rd\theta dr + \iint \rho\Omega^2 h r^2 u \frac{\partial u}{\partial r}\, dr d\theta \tag{17}$$

where

Ω = speed of rotation of the disk

E = Young's modulus

ν = Poisson's ratio

$u(r, \theta, t)$ = axial displacement at time t of section whose initial coordinates are r, θ.

Consider solutions harmonically dependent on both θ and t

$$u = \hat{W}(r) \sin (n\theta + pt) \tag{18}$$

where n is the number of nodal diameters. Substituting (18) in (17) gives

$$v = \frac{Eh^2}{24(1 - \nu^2)} \left\{\left(\frac{d^2\hat{W}}{dr^2} + \frac{1}{r}\frac{d\hat{W}}{dr} - \frac{n^2}{r^2}\hat{W}\right)^2 - 2(1 - \nu)\left[\frac{d^2\hat{W}}{dr^2}\left(\frac{1}{r}\frac{d\hat{W}}{dr} - \frac{n^2}{r^2}\hat{W}\right) - \frac{n^2}{r^2}\left(\frac{d\hat{W}}{dr} - \frac{\hat{W}}{r}\right)^2\right] + \rho\Omega^2\hat{W}r\frac{d\hat{W}}{dr}\right\} \tag{19}$$

The deflection and slope $\hat{W}$, $d\hat{W}/dr$ respectively are given by the model shape matrix from which $\dfrac{d^2\hat{W}}{dr^2}$ is calculated using finite differences. The kinetic energy is given by

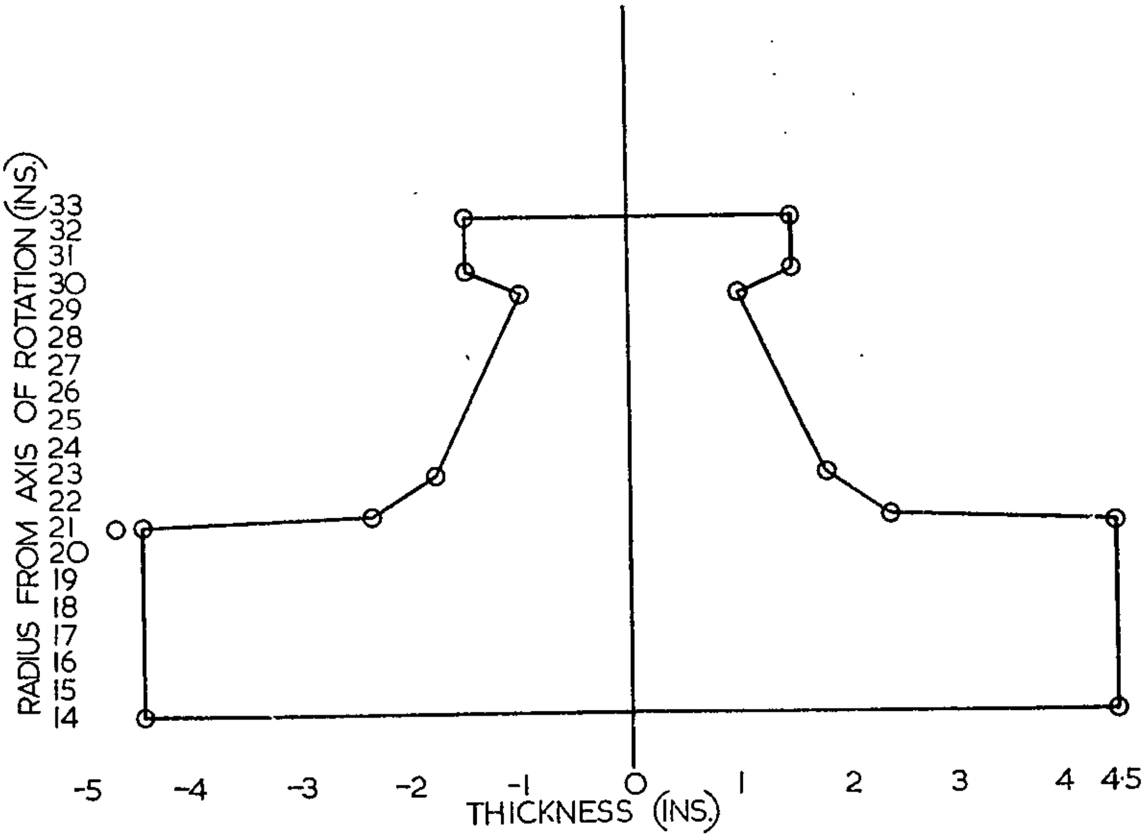

Fig. 4 Case (1): initial design, weight = 3.59 × 10³ lbs, frequency = 2755.65 cps

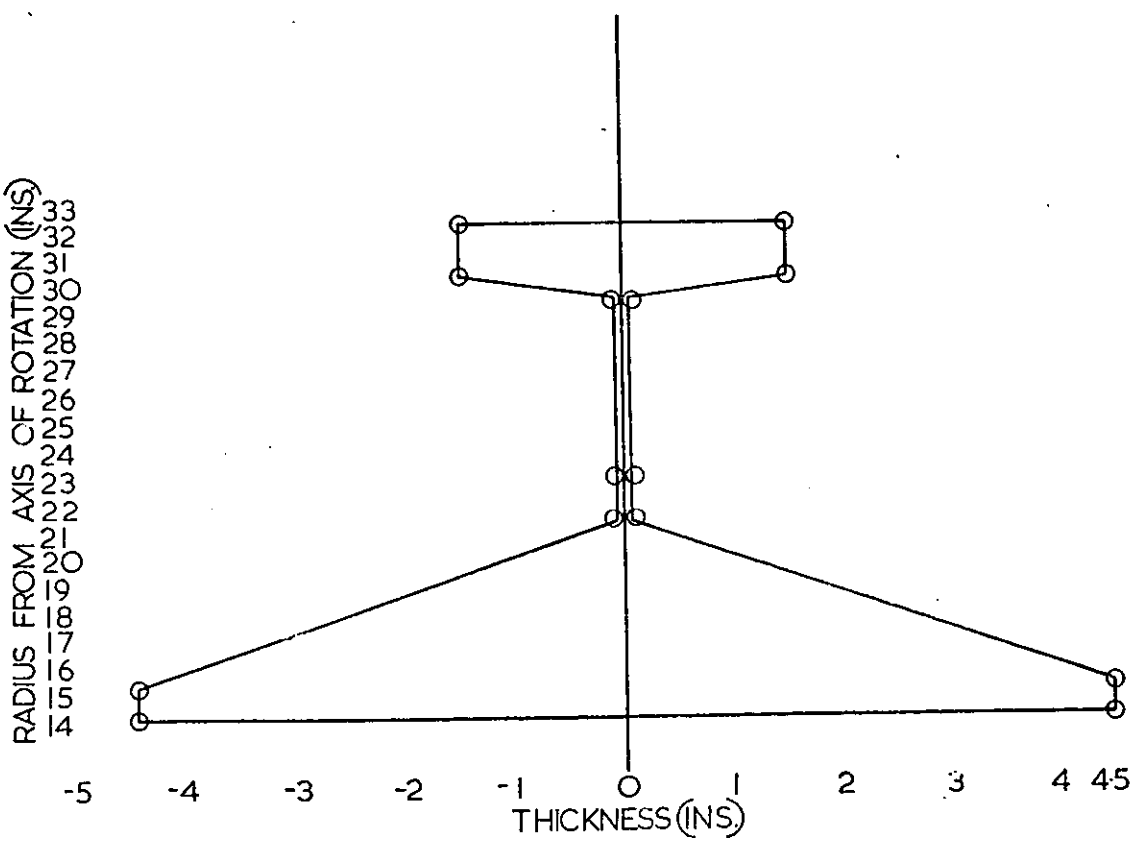

Fig. 5 Case (1): final design, weight = 1.57 × 10³ lbs, frequency = 1658.85 cps, redesign attempts = 5, run time = 11 min

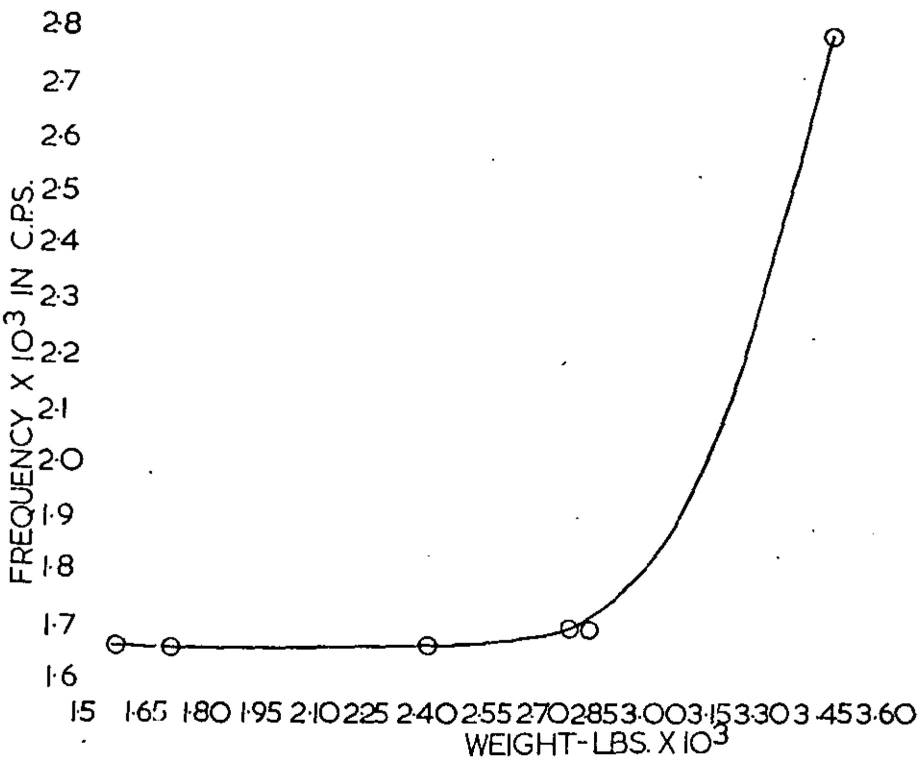

Fig. 6 Case (1): weight versus frequency curve for Case (1)

$$T = \iint \frac{1}{2} \rho h \left(\frac{\partial u}{\partial t}\right)^2 r dr d\theta \tag{20}$$

Substituting (18) in (20) gives

$$k = \frac{1}{2} \rho p_0^2 \hat{W}^2 \tag{21}$$

Equations (19) and (21) determine the strain and kinetic energy densities from which the direction ratios (15) may be computed. The direction of bounce is then obtained by projecting this direction onto the hyperplane defined by the intersection of

$$\left.\begin{aligned} W(b_3, \ldots, b_{m-2}, a_2) &= \text{constant} \\ a_2 &= \text{constant} \end{aligned}\right\} \tag{22}$$

6 Selector III

Consider three successive designs $\mathbf{x}^{(q-2)}$, $\mathbf{x}^{(q-1)}$, $\mathbf{x}^{(q)}$ generated by the steepest descent equation (7). The corresponding frequencies are given by

$$p_0 = p^{(q)} < p^{(q-1)} < p^{(q-2)} \tag{23}$$

Let $\mathbf{x}$ be the foot of the perpendicular from $\mathbf{x}^{(q)}$ onto the direction $\psi^{(q-2)}$ defined by $\mathbf{x}^{(q-2)}$, $\mathbf{x}^{(q-1)}$. The associated frequency p is estimated by linearly interpolating on $\psi^{(q-2)}$

$$p = \left(1 - \frac{l^{(q-1)}}{l^{(q-2)}} \cos\theta\right) p^{(q-2)} + \frac{l^{(q-1)}}{l^{(q-2)}} \cos\theta \, p^{(q-1)} \tag{24}$$

where

$$\cos\theta = \psi^{(q-1)} \cdot \psi^{(q-2)}$$

The direction ratios are given by

$$\left.\begin{aligned} \psi &= \mathbf{x}^{(q)} - \mathbf{x} \quad \text{if} \quad p < p_0 \\ &= \mathbf{x} - \mathbf{x}^{(q)} \qquad \text{otherwise} \end{aligned}\right\} \tag{25}$$

The direction of bounce back into the feasible regions is obtaine by projecting this direction onto the hyperplane (22). The ste length is given by (16). If the proposed alternate step desigr are nonfeasible the step length is progressively reduced.

7 Results and Discussion

The numerical work was carried out on an English Electri KDF9 computer using Segmented Algol. The following case characterized by a four dimensional design space were considered

Case (1, 2)—a standard turbine disk idealization using reso nance frequencies 440, 2000 cycles per second, respectively, (Figs 4–6).

Case (3)—an arbitrary design configuration in conjunction with a resonance frequency of 2000 cps to examine the possibilities of relative minima in the absence of convexity conditions on the weight and feasible regions Figs. (7–10).

Case (1) using a resonance frequency of 440 cps gave designs which never encountered a vibration constraint during convergence to the optimum. Therefore an artificial resonance frequency of 2000 cps was introduced to study the interactions of the synthesis with the constraints giving rise to Cases (2, 3), the initial designs for Cases (1, 2) being identical.

The programs were run using Selector I and II in turn for each of the cases (2, 3). The results presented here are based on Selector I. Selector II failed to generate a satisfactory direction each time, due to the fact that the kinetic energy density at one of the variable sections became very large (of the order of 10^5 in suitable units) in relation to the potential energy densities which were everywhere of the same order of magnitude ($\approx 10^3$). This part of the investigation was very heavy on computer time and it was therefore decided to try Selector III only on the final designs in Cases (2, 3) to see whether further improvements were possible. Some improvement was obtained but was not commensurate with the time consumed. In the initial stages, the boundary designs were not highly constrained and a feasible design was obtained at the first attempt using Selector I. Thereafter, the designs became

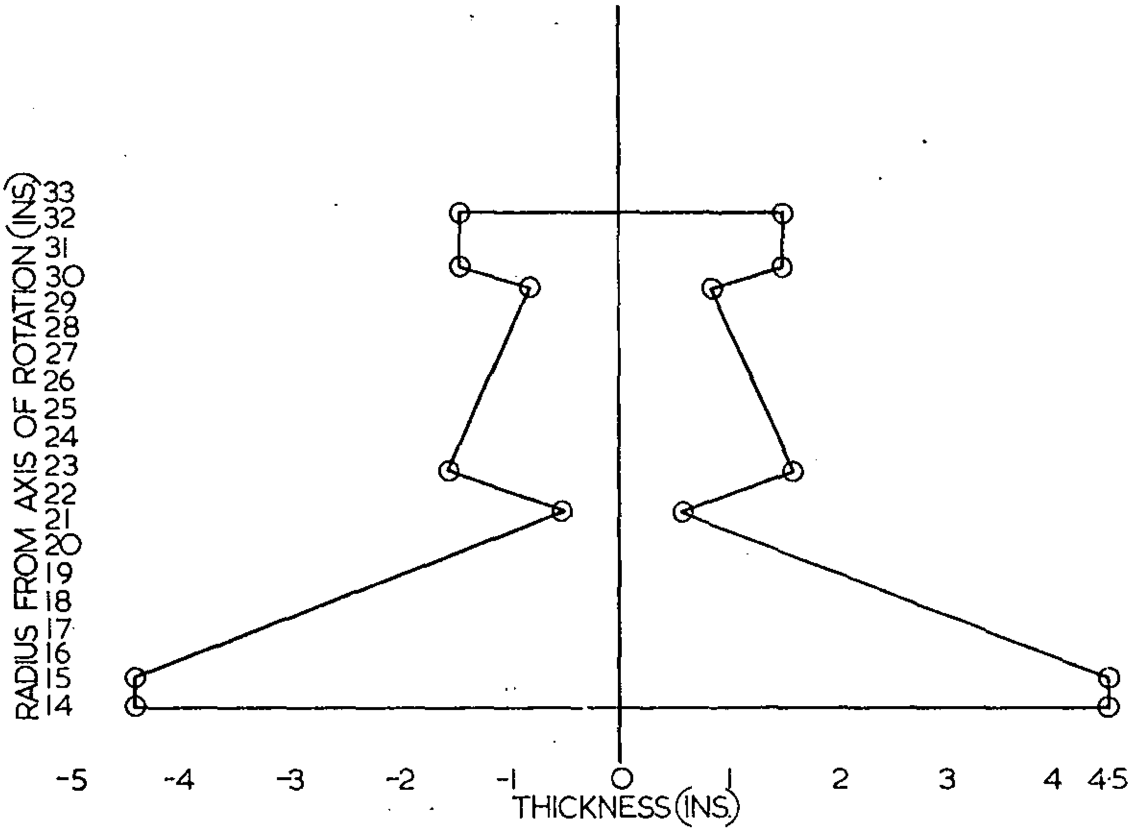

Fig. 7 Case (2): final design, weight = 2.56 = 10^3 lb, frequency = 2008.62 cps, redesign attempts = 38, run time = 53 min

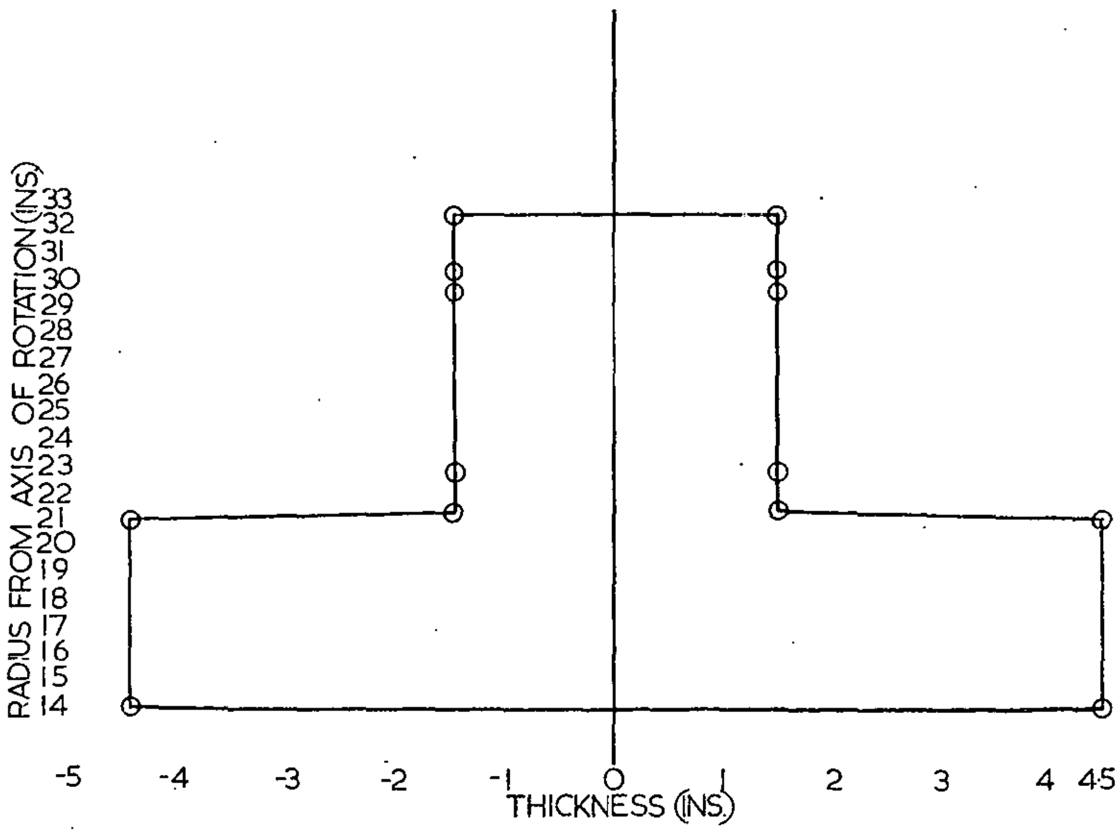

Fig. 8 Case (3): initial design, weight = 3.60 $\times$ 10^3 lb, frequency = 2182.93 cps

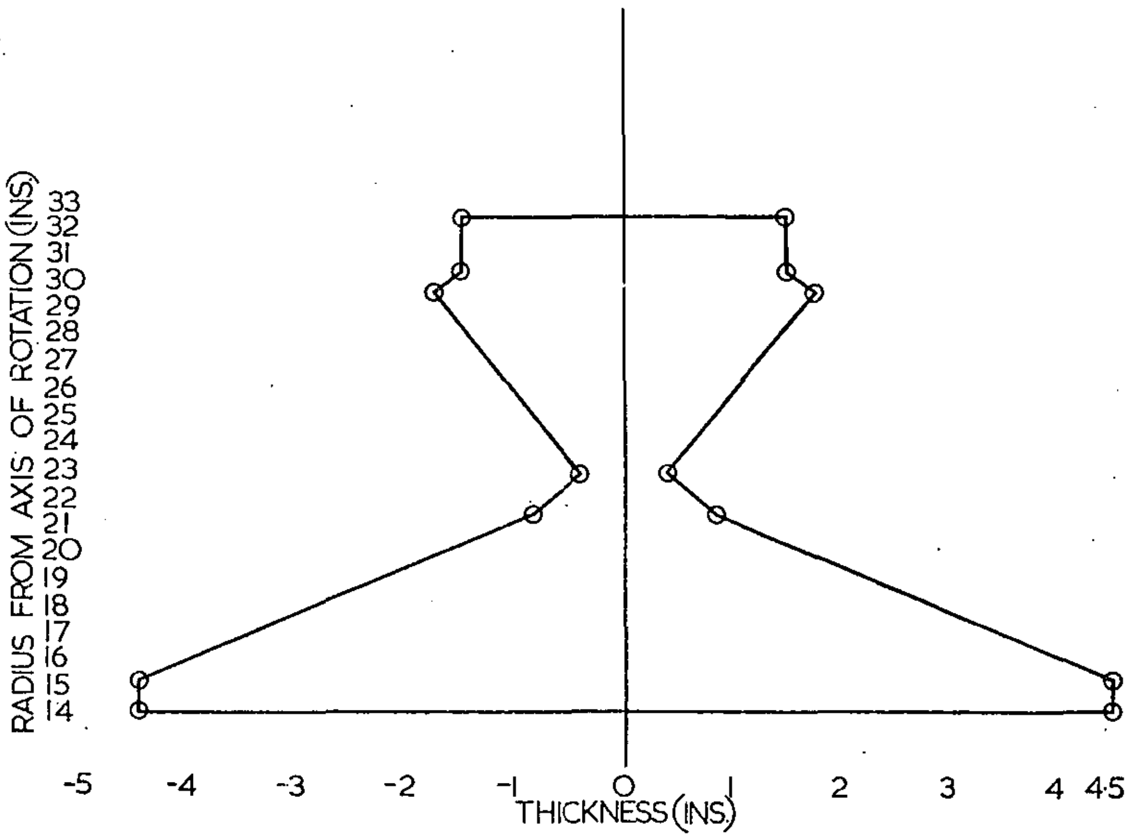

Fig. 9 Case (3): final design, weight = 2.55 × 10^3, frequency = 2000.00 cps, redesign attempts = 39, run time = 56 min

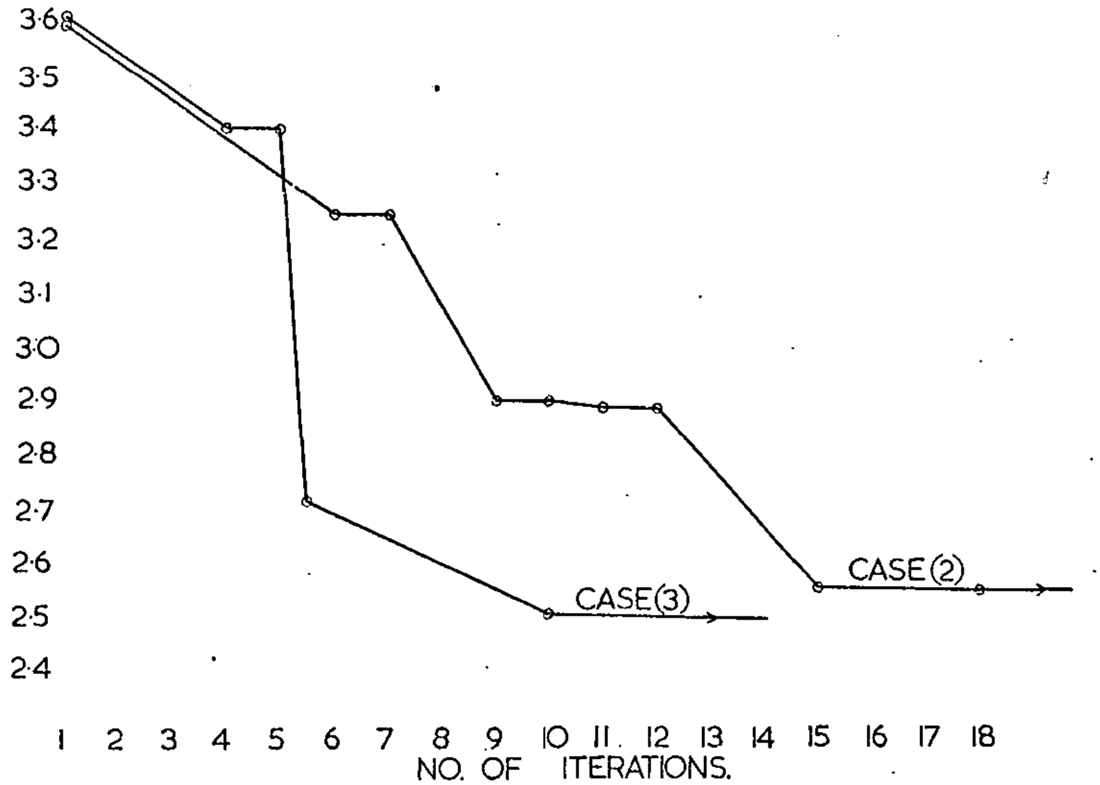

Fig. 10 Weight versus redesign attempts for Cases (2, 3)

more highly constrained with a correspondingly reduced wedge of feasibility requiring a greatly increased number of redesign attempts before a successful design was obtained. This accounts for the shape of the plots of weight versus total redesign attempts (Fig. 10) where its arbitrary nature and the decreasing convergence rate make it impossible to determine when the synthesis is complete. Attempts to consider higher order design spaces proved unsuccessful as the program became too big for the machine.

The final design in Case (1) was bounded by all four design parameter constraints while the final designs in Cases (2, 3) were bounded to within a reasonable tolerance by the vibration constraint and the design parameter constraint $a_2 = L$. However, this does not necessarily mean that the optimum lies at the intersection of one or more constraint surfaces. The final designs (Figs. 7, 9) in Cases (2, 3), although differing in weight by less than 1 percent, are radically different in configuration. This may be due to the local instabilities or to the presence of pockets of relative minima in the composite constraint surface. Further research is needed to establish this point more conclusively.

8 Conclusions

An automated synthesis capability was developed for disks using a "black box" type representation for the frequency, weight reductions of 56.3 percent, 28.6 percent, 29.4 percent being recorded for the three cases presented here. The frequency calculations used here, though relatively simple from a mathematical standpoint, involve the programming of extremely long and complex routines. This could mean run times of about 1 hour for comparatively few design cycles, over 98 percent of the time being consumed in the frequency calculations. The time and the design iterations required to achieve a specified weight reduction increases at an increasing rate with the dimension of the design space, thus precluding any systematic evaluation of such cases. In addition, severe limitations would already be present from storage considerations.

Alternative analysis routines which could be used include an eigenvalue formulation [6–10] based on the method of finite elements. This approach seems to offer better possibilities for exploiting Selector II, where the Lagrangian energy density vector, which determines the normal to the vibration constraint surface, could be readily calculated using the member stiffness and mass matrices. A derivation of this normal is given in reference [9]. The same difficulties regarding storage and time could still be present. In any case, these programs were not available to the author at the start of this investigation. Another possibility is an equivalent reformulation of the problem in which instead of the weight being minimized, the frequency is maximized with a constraint on the weight $W[h] \leq W_0$, along with the other constraints. These constraints are much easier to handle and enable the more conventional methods of nonlinear programming [20] to be better utilized.

The synthesis procedures used here displayed the same general characteristics as those developed in the earlier investigations [1–3] using a stress constraint. That is to say, rapid initial convergence followed by slow convergence as the designs became more highly constrained with a correspondingly reduced wedge of feasibility. The number of iterations and the time consumed increase very considerably with the dimensions of the design space. For instance, Cases (1, 2) using a stress constraint required 62 iterations with a run time of 5 minutes to achieve a weight reduction of 54 percent while the corresponding figures for an eleven-dimensional design space were 186 iterations with a run time of 30 minutes. It is estimated that on the average, the time for a frequency calculation exceeds that for a stress calculation by a factor of over 10:1. It should also be noted that the designs presented here would be substantially modified in the presence of a yield constraint on the stress with a correspondingly reduced weight change.

9 Acknowledgments

This research was sponsored and supported by the Mechanical Engineering Laboratories of the Company by whose permission this paper is published.

Acknowledgment is also made to Drs. A. H. England and T. G. Rogers of the Department of Theoretical Mechanics, University of Nottingham, England, for many valuable discussions during the course of this investigation. Also to Mr. G. A. Pennington for assistance in developing the segmented computer programs.

References

1 de Silva, B. M. E., "On the Application of Nonlinear Programming to the Automatic Structural Synthesis of Turbine Discs," English Electric Co. Report No. W/M(6B), 1965, p. 1126.

2 de Silva, B. M. E., "Minimum Weight Design of Steam Turbine Discs," English Electric Co., Report No. W/M(4B), 1967, p. 1323.

3 de Silva, B. M. E., "The Application of Nonlinear Programming to the Automated Minimum Weight Design of Rotating Discs," to appear in *Proceedings of Conference on Optimisation*, University of Keele, March 25th–28th 1968.

4 de Silva, B. M. E., "Nonclassical Variational Problems in Minimum Weight Structural Optimisation Theory," English Electric Co. Report No. W/M(4B), 1968, p. 1382.

5 de Silva, B. M. E., "Variational Methods in Minimum Weight Design Problems," *English Electric Co. Report No. W/M (4B)*, 1968, p. 1442.

6 Taylor, J. E., "Minimum Mass Bar for Axial Vibration at Specific Natural Frequency," *Journal of American Institute of Aeronautics and Astronautics*, Vol. 5, No. 5, 1967, pp. 1911–1913.

7 Turner, M. J., "Design of Minimum Mass Structures With Specific Natural Frequencies," *Journal of American Institute of Aeronautics and Astronautics*, Vol. 5, No. 3, 1967, pp. 406–412.

8 Young, J. W., and Christiansen, H. N., "Synthesis of a Space Truss Based on Dynamic Criteria," *Journal of the Structural Division*, American Society of Civil Engineers, Vol. 92, No. ST6, 1966, pp. 425–442.

9 Zarghamee, M. S., "Optimum Design of Structures," *Journal of American Institute of Aeronautics and Astronautics*, Vol. 6, No. 4, 1968, pp. 749–750.

10 McIntosh, S. C., and Eastep, F. E., "Design of Minimum Mass Structures With Specified Stiffness Properties," *Journal of American Institute of Aeronautics and Astronautics*, Vol. 6, No. 5, 1968, pp. 962–964.

11 Leitmann, G., *Introduction to Optimal Control*, McGraw-Hill, New York, 1966, chapter 4.

12 Ehrich, F. F., "A Matrix Solution for the Vibration of Modes of Nonuniform Disks," *Journal of Applied Mechanics*, Trans. ASME, Vol. 23, No. 1, 1956, pp. 109–115.

13 Brass, P. S., "Disc and Blade Vibrations," English Electric Co. Report No. W/M(6B), 1965, p. 1022.

14 Brass, P. S., "The Calculation of the Natural Frequencies of Turbine Discs," English Electric Co. Report No. W/M(6B)u. p. 142.

15 Rosen, J. B., "The Gradient Projection Method Part I," *Journal of Society of Industrial and Applied Mathematics*, Vol. 8, No. 1, 1960, pp. 181–217.

16 Schmit, L. A., Kicher, T. P., and Morrow, W. M., "Structural Synthesis Capability for Integrally Stiffened Waffle Plates," *Journal of American Institute of Aeronautics and Astronautics*, Vol. 1, No. 12, 1963, pp. 2820–2836.

17 Fullard, K., "Frequency Tuning of Compressor Rotor Blades," Symposium on Numerical Methods for Vibration Problems, Institute of Sound and Vibration Research, University of Southampton, 1966.

18 Irons, B., "Differential Applications of Rayleigh's Principle," Rolls-Royce Aero Division, Stress memorandum ASM 588.

19 Timoshenko, S., *Theory of Plates and Shells*, McGraw-Hill, New York, 1st ed., 1940, pp. 50–51.

20 Saaty, T. L., and Bram, J., *Nonlinear Mathematics*, McGraw-Hill, New York, 1st ed., 1964, pp. 93–174.

B. M. E. de SILVA
Numerical Analysis Section,
Mechanical Engineering Laboratory,
English Electric Co. Ltd.,
Cambridge Road,
Whetstone Leicester, England;
Presently, Lecturer,
Mathematics Department,
University of Technology,
Loughborough, Leics., England

Application of Pontryagin's Principle to a Minimum Weight Design Problem

A minimum weight design problem has been formulated as a general problem in optimal-control theory with the addition of state and control inequality constraints. Complete analytical solutions have been derived using the maximum principle of Pontryagin.

Introduction

This investigation is part of a research program into computational procedures based on the methods of mathematical programming for optimizing structural systems in the presence of constraints. As a first step in this direction, the weight of a disk was minimized [1–5][1] subject to specified behavioral and side constraints. The behavioral constraints were restricted to a consideration that the stresses should be everywhere below the yield stress and the natural frequencies of vibration should lie within specified resonance bands. The side constraints on the other hand imposed restrictions on the dimensions and tolerances of the disk. The problem was formulated analytically [6–7] as a Bolza problem of the calculus of variations with the frequencies as control parameters. The design requirements were represented by state and control inequality constraints, the control and state variables being given by functions describing the variations in thickness, stress, and deflection fields.

For purposes of numerical computations, the variational formulation was transformed into a discrete nonlinear programming formulation which was characterized by a "black-box-type" representation for the behavioral variables, giving rise to functional inequality constraints. These, together with the side constraints, were represented in design space by hypersurfaces which formed a composite constraint surface. The weight was represented by a family of contours of constant weight and the problem consisted of determining the least weight contour within the feasible region enveloped by the composite constraint surface. The solutions were based on a modified "steepest-descent—alternate step" mode of travel in design space.

This investigation considers the continuous formulation of the problem in the absence of a dynamic constraint. Analytical solutions based on the maximum principle of Pontryagin are given for the resulting variational formulation. These represent the first-order necessary conditions for an optimal solution thus enabling the analytic characteristics of the problem to be compared with the numerical results obtained previously.

Statement of Problem

The variational formulation is obtained by idealizing the turbine disk as a rotating circular disk of variable thickness. The weight is given by the functional expression, Fig. 1,

$$W[h] = \int_{a_i}^{a_m} 2\pi\rho r h(r) dr \tag{1}$$

where

a_i = inner radius
a_m = outer radius
$h(r)$ = thickness at a radial distance r
ρ = density of material assumed constant

The radial distance is measured from the axis of rotation along the normal direction, while $h(r)$ is measured parallel to the axis of rotation. The behavior of the disk is governed by the differential equations [2, 3]

$$\begin{aligned} \frac{d\sigma_r}{dr} &= -\frac{1}{h}\left[\sigma_r \frac{dh}{dr} + \frac{h}{r}(\sigma_r - \sigma_\theta) + \rho\omega^2 r h\right] \\ \frac{d\sigma_\theta}{dr} &= \frac{\sigma_r - \sigma_\theta}{r} - \frac{\nu}{h}\sigma_r \frac{dh}{dr} - \nu\rho\omega^2 r \end{aligned} \tag{2}$$

where σ_r, σ_θ are the radial and tangential stresses, respectively, ν is Poisson's ratio, and ω the angular velocity of rotation. These have been derived on the assumption of radially symmetric plane stress. The case of plane stress involving an additional component $\sigma_{r\theta}$ can be handled using an analysis similar to that presented here. The state variables are the stresses which satisfy the transversality conditions

[1] Numbers in brackets designate References at end of paper.

Contributed by the Automatic Control Division and presented at the Winter Annual Meeting, Los Angeles, Calif., November 16–20, 1969, of The American Society of Mechanical Engineers. Manuscript received at ASME Headquarters, July 29, 1969. Paper No. 69-WA/Aut-1.

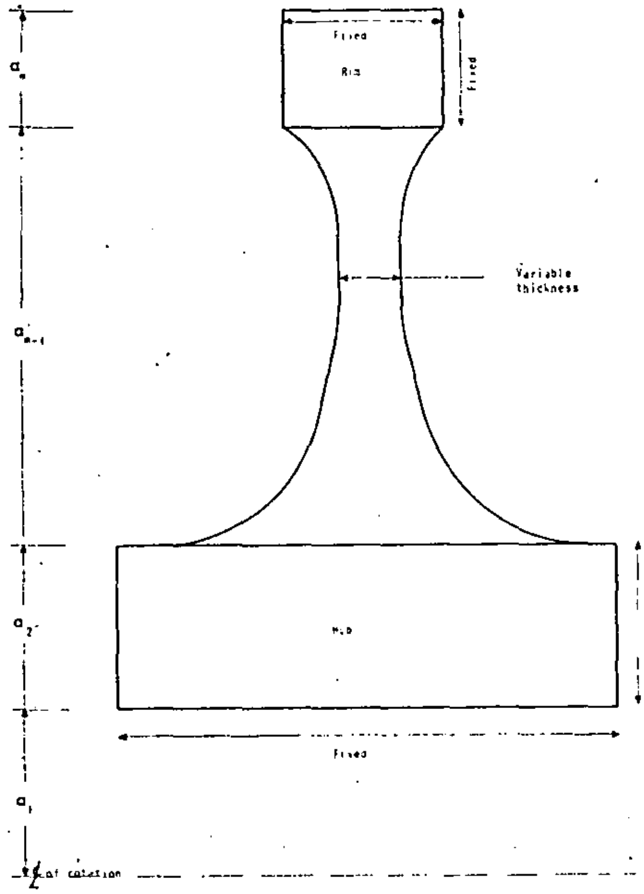

Fig. 1 Cross section of disk

$$\begin{aligned} \theta^{(1)}: \quad \sigma_r &= s_1 \qquad \text{at } r = a_1 \\ \theta^{(m)}: \quad \sigma_r &= s_m \qquad \text{at } r = a_m \end{aligned} \tag{3}$$

where s_1, s_m are constants.

The material of the disk is assumed to obey the Tresca yield condition

$$F(\sigma_r, \sigma_\theta) \leq \sigma_0 \tag{4}$$

where

$$F(\sigma_r, \sigma_\theta) = \max(|\sigma_r|, |\sigma_\theta|, |\sigma_r - \sigma_\theta|)$$

This state constraint region is illustrated in Fig. 2.

Consider a thickness distribution of the form

$$\begin{aligned} h(r) &= b_1 \qquad a_1 \leq r \leq a_2 \\ &= h(r) \qquad a_2 \leq r \leq a_{m-1} \\ &= b_m \qquad a_{m-1} \leq r \leq a_m \end{aligned} \tag{5}$$

where b_1, b_m, a_1, a_m, a_{m-1} are constants while $h(r)$, a_2 are variables satisfying the constraint conditions

$$\begin{aligned} a_1 < L \leq a_2 \leq U < a_{m-1} \\ h(r) \geq \epsilon > 0 \ \forall \ r \in [a_2, a_{m-1}] \end{aligned} \tag{6}$$

where L, U, ϵ are positive constraints.

The controls $h(r)$, $\dot{h}(r)$[2] are said to be admissible if

1 They are continuous in a_1, a_m.

2 The function $h(r)$ belongs to the constant control set U defined by (5) and (6).

For given admissible controls $h(r)$, $\dot{h}(r)$, $a_1 \leq r \leq a_m$, the state equations (2) in conjunction with the transversality conditions (3) possess a unique continuous solution which defines a trajectory in state space along which the states of the system are transferred between the end manifolds $\theta^{(1)}$, $\theta^{(m)}$. These trajectories are constrained to lie within the interior of the region of state space defined by (4). It is required to determine the optimal control $h^*(r)$, $\dot{h}^*(r)$, $a_1 \leq r \leq a_m$ which effects such a transfer while minimizing the weight (1).

As shown next, the constraints (6) provide necessary conditions for the existence of solutions.

Unconstrained Problem

Consider the optimal control problem in the absence of constraints on the control variables. Minimize

$$M[h] \doteq \int_{r_0}^{r_1} 2\pi\rho r h(r) dr, \qquad h \in E' \tag{7}$$

where

$$a_2 \leq r_0 < r_1 \leq {}_{m-1}$$

Let $h = h^*(r) \ \forall \ r \in [r_0, r_1]$ be the minimizing function in class C^2 (i.e., $\ddot{h}^*(r)$ exists and is continuous). Then it is minimizing in the subclass

$$h(r) = h^*(r) + \epsilon_0\eta(r); \qquad \eta(r) \in C^2 \tag{8}$$

where ϵ_0 is a small parameter.

Let

$$\begin{aligned} F(\epsilon_0) &= M[h] \\ &= \int_{r_0}^{r_1} 2\pi\rho r[h^*(r) + \epsilon_0\eta(r)]dr \\ &= \int_{r_0}^{r_1} 2\pi\rho r h^*(r)dr + \epsilon_0 \int_{r_0}^{r_1} 2\pi\rho r\eta(r)dr \\ &= M[h^*] + \epsilon_0 \int_{r_0}^{r_1} 2\pi\rho r\eta(r)dr \end{aligned} \tag{9}$$

But $F(\epsilon_0)$ is a minimum at $\epsilon_0 = 0$

$$F'(0) = 0$$

that is,

$$\int_{r_0}^{r_1} 2\pi\rho r\eta(r)dr = 0$$

for arbitrary $\eta(r)$.

But this is impossible and therefore the problem has no finite solutions over the entire function space and solutions exist only for bounded $h(r)$.

Constraints on h(r)

Consider the problem in the presence of the control constraint

$$h(r) \geq \epsilon \ \forall \ r \in [r_0, r_1] \tag{10}$$

From (7)

$$M[h] \geq \pi\rho(r_1^2 - r_0^2)\epsilon \tag{11}$$

$$\begin{aligned} \therefore h^*(r) &= \epsilon \ \forall \ r \in [r_0, r_1] \\ M^* \doteq M[h^*] &= \pi\rho(r_1^2 - r_0^2)\epsilon \end{aligned} \tag{12}$$

---

[2] $\dot{(\ )} = \dfrac{d}{dr}(\ )$.

Therefore optimal control is bang-bang in $[r_0, r_1]$.

Presence of Control Set U

Therefore, the solutions in the presence of the control set U are obtained in the following way. From (1) and (5)

$$W[h;\, a_2] = \pi\rho b_1(a_2^2 - a_1^2) + \pi\rho b_m(a_m^2 - a_{m-1}^2) + \int_{a_2}^{a_{m-1}} 2\pi\rho r h(r)dr \quad (13)$$

The minimum of the integral in equation (13) is given by

$$a_2^* = a_{m-1}$$

or from (12) (14)

$$h^*(r) = \epsilon \ \forall\ r \in [a_2, a_{m-1}]$$

But the first possibility is excluded by the constraint condition (6). Therefore the optimal solution is given by

$$h^*(r) = \epsilon \ \forall\ r \in [a_2, a_{m-1}]$$

$$\min \int_{a_2}^{a_{m-1}} 2\pi\rho r h(r)dr = \pi\rho(a_{m-1}^2 - a_2^2)\epsilon \quad (14a)$$

$$\therefore W[h^*;\, a_2]$$

$$= \pi\rho b_1(a_2^2 - a_1^2) + \pi\rho b_m(a_m^2 - a_{m-1}^2) + \pi\rho(a_{m-1}^2 - a_2^2)\epsilon$$

$$= \pi\rho[(b_1 - \epsilon)a_2^2 + b_m(a_m^2 - a_{m-1}^2) + \epsilon a_{m-1}^2 - b_1 a_1^2] \quad (15)$$

This may be regarded as a function of the control parameter a_2 and is to be minimized. Solutions exist only for bounded a_2 and are given by

$$a_2^* = L \quad \text{if } b_1 > \epsilon$$
$$= U \quad \text{if } b_1 < \epsilon \quad (16)$$

$$\therefore W^* \doteq W[h^*;\, a_2^*]$$

$$= \pi\rho \min\,[(b_1 - \epsilon)L^2, (b_1 - \epsilon)U^2] + b_m(a_m^2 - a_{m-1}^2) + \epsilon a_{m-1}^2 - b_1 a_1^2 \quad (16a)$$

Optimal control is continuous and bang-bang in $[a_2, a_{m-1}]$. Solutions exist only for bounded $h(r)$, a_2.

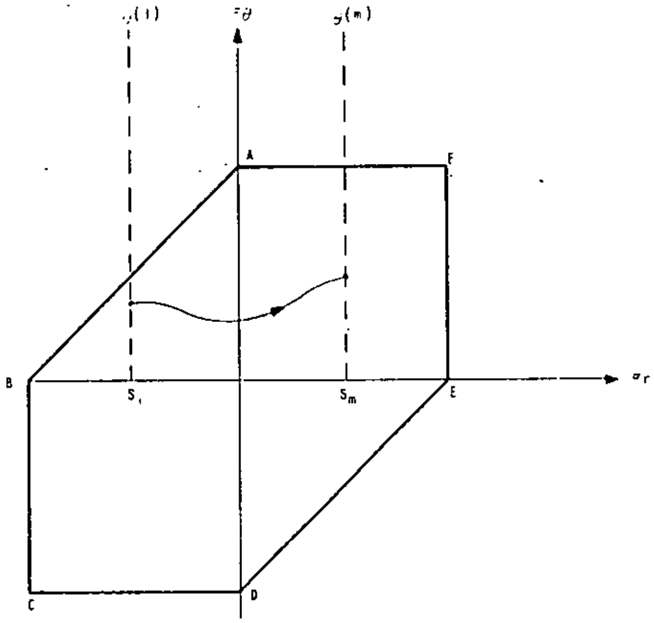

Fig. 2 Tresca Yield condition—two dimension state constraint region

Maximum Principle

The maximum principle of Pontryagin and the associated Hamiltonian formulation is used to introduce the state variables into the problem.

$$H(\lambda_0, \lambda_1, \lambda_2;\, \sigma_r, \sigma_\theta, r;\, h, \dot h)$$
$$\doteq 2\pi\rho r h\lambda_0(r) - \frac{\lambda_1(r)}{h}\left[\sigma_r \dot h + \frac{h}{r}(\sigma_r - \sigma_\theta) + \rho\omega^2 r h\right] + \lambda_2(r)\left[\frac{\sigma_r - \sigma_\theta}{r} - \frac{\nu}{h}\sigma_r \dot h - \nu\rho\omega^2 r\right] \quad (17)$$

It is known from the maximum principle that λ_0 is a nonpositive constant

$$\lambda_0(r) = \text{const} \leq 0 \quad (18)$$

The associated adjoint equations are given by

$$\frac{d\lambda_1}{dr} = -\frac{\partial H}{d\sigma_r} = \frac{\lambda_1 - \lambda_2}{r} + (\lambda_1 + \nu\lambda_2)\frac{\dot h}{h}$$
$$\frac{d\lambda_2}{dr} = -\frac{\partial H}{\partial\sigma_\theta} = -\frac{\lambda_1 - \lambda_2}{r} \quad (19)$$

In addition to the state and adjoint equations (2) and (19), it is assumed that the yield condition satisfies

$$F(\sigma_r(r), \sigma_\theta(r)) < \sigma_0 \quad (20)$$

The control $\dot h(r)$ is unconstrained and continuous

$$\therefore \frac{\partial H}{\partial \dot h} \equiv \lambda_1 + \nu\lambda_2 = 0 \quad (21)$$

Therefore (17) reduces to

$$H = 2\pi\rho r h\lambda_0 - \left(\frac{\lambda_1 - \lambda_2}{r}\right)(\sigma_r - \sigma_\theta) \quad (22)$$

Maximizing H with respect to $h(r)\epsilon U$ gives

$$\lambda_0 = \text{const} < 0$$
$$h(r) = \epsilon \quad (23)$$

The state equations reduce to

$$\frac{d\sigma_r}{dr} = -\frac{\sigma_r - \sigma_\theta}{r} - \rho\omega^2 r$$
$$\frac{d\sigma_\theta}{dr} = \frac{\sigma_r - \sigma_\theta}{r} - \nu\rho\omega^2 r \quad (24)$$

$$\therefore \sigma_r = C_1 - \frac{C_2}{r^2} - \frac{3 + \nu}{8}\rho\omega^2 r^2$$
$$\sigma_\theta = C_1 + \frac{C_2}{r^2} - \frac{1 + 3\nu}{8}\rho\omega^2 r^2 \quad (25)$$

where C_1, C_2 are constants of integration. Eliminating r from (25),

$$(1 + 3\nu)\sigma_r^2 - (3 + \nu)\sigma_\theta^2 - 2(1 - \nu)\sigma_r\sigma_\theta - 8C_1\sigma_r + 8C_1\sigma_\theta - 4C_1^2(1 - \nu) - 2(1 + \nu)^2 C_2\rho\omega^2 = 0 \quad (26)$$

This defines a family of hyperbolas in state space whose centers lie on the line

$$\sigma_\theta = \nu\sigma_r \quad (27)$$

From (23) and (21)

$$\frac{d\lambda_1}{dr} = \frac{\lambda_1 - \lambda_2}{r}$$
$$\frac{d\lambda_2}{dr} = -\frac{\lambda_1 - \lambda_2}{r} \tag{28}$$

Therefore the adjoint equations are given by

$$\lambda_1(r) = A + Br^2$$
$$\lambda_2(r) = A - Br^2 \tag{29}$$

where A, B are constants of integration and correspond to a two parameter family of parabolas whose foci lie on the axis of rotation. The problem corresponds to a nonautonomous system with fixed end points a_1, a_m. The optimal control (23) is obtained by maximizing the Hamiltonian (17) with respect to the controls. The maximum principle used is applicable to points within the interior of the constraint region (20). A modified analysis applicable to points belonging to the boundary of this region is given next.

Restricted Maximum Principle

Consider an optimal trajectory such that

$$F(\sigma_r(r), \sigma_\theta(r)) = \sigma_0 \;\forall\; r \in [r_e, r_l] \tag{30}$$

where

$$a_1 \leq r_e < r_l \leq a_m \tag{30}$$

Let

$$\nabla F \doteq \left(\frac{\partial F}{\partial \sigma_r}, \frac{\partial F}{\partial \sigma_\theta}\right) \tag{31}$$

$$p(\sigma_r, \sigma_\theta, r; h, \dot{h}) \doteq -\frac{1}{h}\left[\sigma_r \dot{h} + \frac{h}{r}(\sigma_r - \sigma_\theta) + \rho\omega^2 rh\right]\frac{\partial F}{\partial \sigma_r} + \left[\frac{\sigma_r - \sigma_\theta}{r} - \frac{\nu}{h}\sigma_r \dot{h} - \nu\rho\omega^2 r\right]\frac{\partial F}{\partial \sigma_\theta} \tag{32}$$

Since the optimal trajectory defined by equation (2) belongs to the boundary of the constraint region (30)

$$p(\sigma_r, \sigma_\theta, r; h, \dot{h}) = 0 \tag{33}$$

$$\therefore h(r) = h_0 \exp - \left\{\int^r \frac{1}{\sigma_r}\left[\left(\frac{\sigma_r - \sigma_\theta}{r}\right)\frac{F\sigma_r - F\sigma_\theta}{F\sigma_r + rF\sigma_\theta} + \rho\omega^2 r\right]\frac{dr}{r}\right\} \quad \forall\; r \in [r_e, r_l] \tag{34}$$

where $F\sigma_r$, $F\sigma_\theta$ denotes partial derivatives with respect to σ_r, σ_θ, respectively.

Substituting (34) into (2)

$$\frac{d\sigma_r}{dr} = -\frac{1+\nu}{r}\frac{(\sigma_r - \sigma_\theta)F\sigma_\theta}{F\sigma_r + \nu F\sigma_\theta}$$
$$\frac{d\sigma_\theta}{dr} = \frac{1+\nu}{r}\frac{(\sigma_r - \sigma_\theta)F\sigma_r}{F\sigma_r + \nu F\sigma_\theta} \tag{35}$$

This defines a two parameter family of trajectories in state space. These equations have been derived on the assumption that F possesses continuous second partial derivatives along the boundary. This condition is satisfied for the Tresca yield surface (4) everywhere except at the vertices. However, the stress states are uniquely determined at the vertices and the corresponding optimal control is obtained by direct substitution in the first of equations (2).

Let

$$A \doteq \begin{bmatrix} \frac{\partial}{\partial \sigma_r}\left(\frac{d\sigma_r}{dr}\right), \frac{\partial}{\partial \sigma_\theta}\left(\frac{d\sigma_r}{dr}\right) \\ \frac{\partial}{\partial \sigma_r}\left(\frac{d\sigma_\theta}{dr}\right), \frac{\partial}{\partial \sigma_\theta}\left(\frac{d\sigma_\theta}{dr}\right)\end{bmatrix} = \begin{bmatrix} -\frac{1}{h}\left(\dot{h} + \frac{h}{r}\right), \frac{1}{r} \\ \frac{1}{r} - \nu\frac{\dot{h}}{h}, -\frac{1}{r}\end{bmatrix} \tag{36}$$

$$B \doteq \begin{bmatrix} \frac{\partial}{\partial \dot{h}}\left(\frac{d\sigma_r}{dr}\right) \\ \frac{\partial}{\partial \dot{h}}\left(\frac{d\sigma_\theta}{dr}\right)\end{bmatrix} = \begin{bmatrix} -\frac{\sigma_r}{h} \\ -\nu\frac{\sigma_r}{h}\end{bmatrix} \tag{37}$$

Therefore the adjoint equations are given by

$$\frac{d\boldsymbol{\lambda}}{dr} = -\boldsymbol{\lambda}\mathbf{A} + \boldsymbol{\lambda}\mathbf{B}\left(\frac{\partial p}{\partial \dot{h}}\right)^{-1}\nabla p \tag{38}$$

where

$$\boldsymbol{\lambda} = (\lambda_1(r), \lambda_2(r))$$

These equations have been derived using Chapter 4 of reference [8] in which

$$\mathbf{R} = p;\; \mathbf{u}^c = \dot{h};\; \frac{\partial \mathbf{f}}{\partial \mathbf{u}^c} = \mathbf{B};\; \frac{\partial \mathbf{f}}{\partial \mathbf{x}} = \mathbf{A};\; \mathbf{x} = (\sigma_r, \sigma_\theta, r);\; \frac{\partial \mathbf{R}}{\partial \mathbf{x}} = \nabla_x p$$

Substituting (36) and (37) into (38)

$$\frac{d\lambda_1}{dr} = \frac{\lambda_1 - \lambda_2}{r} - \frac{\lambda_1 + \nu\lambda_2}{F\sigma_r + \nu F\sigma_\theta}\left(\frac{F\sigma_r - F\sigma_\theta}{r} - \dot{F}\sigma_r\right)$$
$$\frac{d\lambda_2}{dr} = -\frac{\lambda_1 - \lambda_2}{r} + \frac{\lambda_1 + \nu\lambda_2}{F\sigma_r + \nu F\sigma_\theta}\left(\frac{F\sigma_r - F\sigma_\theta}{r} + \dot{F}\sigma_\theta\right) \tag{39}$$

Tresca Yield Condition

The results obtained thus far are applicable to a general yield surface F. Consider the form of these equations when applied to the Tresca condition (4) except at the vertices, where the solutions are uniquely determined by the state variables.

Therefore $F\sigma_r$, $F\sigma_\theta$, are constants

$$\dot{F}\sigma_r = \dot{F}\sigma_\theta = 0 \tag{40}$$

From (39), (40)

$$\frac{d}{dr}(-\lambda_1 F\sigma_\theta + \lambda_2 F\sigma_r) = \frac{(1+\nu)(F\sigma_r + F\sigma_\theta)}{F\sigma_r + \nu F\sigma_\theta}\left[-\frac{\lambda_1 F\sigma_\theta + \lambda_2 F\sigma_r}{r}\right] \tag{41}$$

Therefore integrating

$$-\lambda_1 F\sigma_\theta + \lambda_2 F\sigma_r = Cr^\alpha \tag{42}$$

where

$$\alpha = (1+\nu)\frac{F\sigma_r + F\sigma_\theta}{F\sigma_r + \nu F\sigma_\theta}$$

$$C = \text{positive constant}$$

Substituting (34) and (42) into (17) gives

$$H = 2\pi\rho rh\lambda_0 + C(1+\nu)\frac{\sigma_r - \sigma_\theta}{F\sigma_r + \nu F\sigma_\theta}r^{\alpha-1} \tag{43}$$

It is required to determine an optimal control $h^*(r) \in U$ which maximizes (43). It can easily be verified that for parts along AF or CD, Fig. 2, the second term on the right-hand side of (43) is negative while parts along FE, BC, ED, and BA give positive values. Therefore the optimal solutions lie on the latter branches of the yield surface.

Consider points along ED

$$\begin{aligned} \sigma_\theta &= \sigma_r - \sigma_0 \\ F\sigma_r &= 1 \\ F\sigma_\theta &= -1 \end{aligned} \tag{44}$$

Substituting (44) into (35) gives

$$\frac{d\sigma_r}{dr} = \frac{1+\nu}{1-\nu}\frac{\sigma_0}{r} \tag{45}$$

$$\therefore \sigma_r = \ln ar^{\beta} \qquad (a > 0) \tag{46}$$

where

$$\beta = \frac{1+\nu}{1-\nu}\sigma_0 > 0$$

Under the influence of this trajectory the state of the system would eventually leave the branch ED and move into the nonfeasible region of state space. Therefore optimal control must operate along FE or CB. Consider points along FE

$$\begin{aligned} \sigma_r = \sigma_0; &\qquad 0 \leq \sigma_\theta \leq \sigma_0 \\ F\sigma_r = 1; &\qquad F\sigma_\theta = 0 \end{aligned} \tag{47}$$

Substituting (47) in (35) gives

$$\frac{d\sigma_\theta}{dr} = (1+\nu)\frac{\sigma_0 - \sigma_\theta}{r} \tag{48}$$

$$\therefore \sigma_\theta = \sigma_0 - br^{-(1+\nu)} \tag{49}$$

where b is a positive constant of integration. The optimal control is obtained by substituting (47) into (34):

$$h(r) = h_0 \exp\left[\frac{b}{(1+\nu)\sigma_0} r^{-(1+\nu)} - \frac{\rho\omega^2 r^2}{2\sigma_0}\right] \tag{50}$$

This is a monotonic decreasing function of r. Therefore the second of the constraint conditions (6) are satisfied by selecting the constant h_0 such that

$$h_0 > \epsilon \exp - \left[\frac{b}{(1+\nu)\sigma_0} r_l^{-(1+\nu)} - \frac{\rho\omega^2 r_l^2}{2\sigma_0}\right].$$

The adjoint equations are obtained in the following way. From (39) and (40)

$$\frac{d\lambda_1}{dr} + \frac{d\lambda_2}{dr} = 0 \tag{51}$$

$$\therefore \lambda_1(r) + \lambda_2(r) = D \tag{52}$$

From (42), (52)

$$\begin{aligned} \lambda_1(r) &= \frac{DF\sigma_r - Cr^{\alpha}}{F\sigma_r + F\sigma_\theta} \\ \lambda_2(r) &= \frac{DF\sigma_\theta + Cr^{\alpha}}{F\sigma_r + F\sigma_\theta} \end{aligned} \tag{53}$$

Substituting (47) into (53) gives

$$\begin{aligned} \lambda_1(r) &= D - Cr^{(1+\nu)} \;\forall\; r \in [r_e, r_l] \\ \lambda_2(r) &= Cr^{(1+\nu)} \;\forall\; r \in [r_e, r_l] \end{aligned} \tag{54}$$

The major results established in this section are that the optimal control (50) must operate along the optimal trajectory $|\sigma_r| = \sigma_0$ with adjoint equations (54). This result is confirmed by numerical results obtained previously [2, 3].

Jump Condition

The adjoint vector is continuous at the entry point $r = r_e$

$$\lambda(r_e - 0) = \lambda(r_e) \tag{55}$$

This implies from (29) and (54)

$$\begin{aligned} A + Br_e^2 &= D - Cr_e^{1+\nu} \\ A - Br_e^2 &= Cr_e^{1+\nu} \end{aligned} \tag{56}$$

This adjoint vector is discontinuous on leaving

$$\lambda(r_l + 0) = \lambda(r_l) - \mu(r_l)\nabla F \tag{57}$$

where

$$\begin{aligned} \mu(r) &= \lambda B \left(\frac{\partial p}{\partial h}\right)^{-1} \\ &= \frac{\lambda_1 + \nu\lambda_2}{F\sigma_r + \nu F\sigma_\theta} \;\forall\; r \in [r_e, r_l] \end{aligned} \tag{58}$$

Substituting (47) into (58) gives

$$\mu(r) = B - (1-\nu)Ar^{\alpha}, \qquad r_e \leq r \leq r_l \tag{59}$$

Substituting (59) into (57) using (29) and (47) gives

$$\begin{aligned} A^1 + B^1 r_l^2 &= D - Cr_l^{(1+\nu)} - B + (1-\nu)Ar_l^{1+\nu} \\ A^1 - B^1 r_l^2 &= Cr_l^{1+\nu} \end{aligned} \tag{60}$$

From (56) and (60), the adjoint vectors on leaving may be determined in terms of the hyperbolas on entry.

Conclusions

Complete analytical solutions have been obtained using the Pontryagin formulation and are characterized by

1 $F(\sigma_r(r), \sigma_\theta(r)) < \sigma_0 \;\forall\; r \in [a_1, a_2]$

2 $F(\sigma_r(r), \sigma_\theta(r)) < \sigma_0 \;\forall\; r \in [a_{m-1}, a_m]$

3 $F(\sigma_r(r), \sigma_\theta(r)) < \sigma_0$ for $r \in [a_2, a_{m-1}]$ implies $h^*(r) = \epsilon$

4 $F(\sigma_r(r), \sigma_\theta(r)) = \sigma_0 \;\forall\; r \in [r_e, r_l] \in [a_2, a_{m-1}]$ implies $h^*(r) = h_0 \exp\left\{\frac{b}{(1+\nu)\sigma_0} r^{-(1+\nu)} - \frac{\rho\omega^2 r^2}{2\sigma_0}\right\} > \epsilon$ the optimal trajectory corresponding to $|\sigma_r| = \sigma_0$.

5 Optimal state and control vectors uniquely determined at the vertices of the Tresca hexagon by the state equations.

6 The control parameter a_2 attains its limiting values.

Conditions (1) and (2) have been derived using the transversality conditions (3) and the state equations (25). A detailed analysis at the vertices of the Tresca hexagon is given in reference [2].

Acknowledgment

Acknowledgment is made to Prof. T. V. Davies, Professor of Mathematics, University of Leicester, for many valuable discussions and suggestions in the course of this investigation. This paper has been written as part of the research program of the Mechanical Engineering Laboratory of the English Electric Company Ltd. and is published by permission of the English Electric Co. Ltd.

References

1 de Silva, B. M. E., "On the Application of Nonlinear Programming to the Automatic Structural Synthesis of Turbine Disks," English Electric Co. Report No. W/M(6B) 1965, p. 1126.

2 de Silva, B. M. E., "Minimum Weight Design of Steam Turbine Disks," English Electric Co. Report No. W/M(4B) 1967, p. 1323.

3 de Silva, B. M. E., "The Application of Nonlinear Programming to the Automated Minimum Weight Design of Rotating Disks," *Optimization*, ed. by Fletcher, R., Academic Press, 1969, pp. 115–150.

4 de Silva, B. M. E., "Automated Weight Minimization Based on a Frequency Constraint," English Electric Co. Report No. W/M-(4B) 1968, p. 1452.

5 de Silva, B. M. E., "Minimum Weight Design of Disks Using a Frequency Constraint," *Journal of Engineering for Industry*, TRANS. ASME, Series, B, Vol. 91, No. 4, Nov. 1969, pp. 1091–1099.

6 de Silva B. M. E., "Nonclassical Variational Problems in Minimum Weight Structural Optimization Theory," English Electric Co. Report No. W/M(4B) 1968, p. 1382.

7 de Silva, B. M. E., "Variational Methods in Minimum Weight Design Problems," English Electric Company Report No. W/M(4B) July 1968, p. 1442.

8 Leitmann, G., *Introduction to Optimal Control*, McGraw-Hill, 1st ed., 1966, Chapter 4.

Journal of Sound and Vibration (1972) **21** (1), 19–34

OPTIMAL VIBRATIONAL MODES OF A DISC

B. M. E. DE SILVA

Department of Mathematics,
University of Technology, Loughborough LE11 3TU, England

(*Received* 13 *September* 1971 *and in revised form* 20 *December* 1971)

The problem considered is that of maximizing a linear combination of the natural frequencies of vibration of a turbine disc idealization of variable thickness. The problem is formulated as a general problem in optimal control theory with the addition of inequality constraints on the state variables. Significant progress has been made in solving the problem by using purely analytical techniques based on the maximum principle of Pontryagin. These transform the problem into a nonlinear programming problem which is solved numerically by using the Heaviside penalty function transformation in conjunction with Rosenbrock's hill-climbing techniques.

Available computational experience indicates that these procedures provide powerful tools for handling complex structural optimization problems.

1. INTRODUCTION

This investigation is a continuation of a research programme into analytical and computational procedures based on the methods of mathematical programming for optimizing structural systems in the presence of design constraints. Initially mathematical programming procedures were successfully developed for obtaining minimum weight solutions to a turbine disc of variable thickness in the presence of constraints on the stresses and the frequencies of vibration [1–5]. The stresses were required to be below the yield stress for the material of the disc while the vibrational frequencies were constrained to be outside given critical frequency bands. The problem was formulated as a general problem in optimal control theory with the addition of inequality constraints on the state and control variables. These variables were given by functions describing the variations in the thickness stress and deformation fields, with the frequencies corresponding to control parameters.

The continuous formulation [6–8] was described by the maximum principle of Pontryagin, while the numerical computations were based on a discretized non-linear programming formulation obtained by using a piecewise linear representation for the control variables. The non-linear programming formulation was characterized by non-analytic "black box" type constraints for the behavioural constraints, and the solutions were based on a generalized "steepest descent–alternate step" mode of travel in configuration space developed by Schmit *et al.* [9]: this being one of the most powerful methods available at the time for solving structural optimization problems with non-analytic constraints.

The work described here is an investigation of the dual problem of maximizing some linear combination of the frequencies of vibration of the turbine disc with a constraint on the total weight. The problem is again formulated as a general optimal control problem in the presence of inequality constraints on the state and control variables. Significant progress has been made in solving the problem by using analytical procedures based on the (restricted) maximum principle of Pontryagin [10]. The adjoint systems of the Pontryagin formulation are solved by using perturbation techniques which give rise to fourth-order differential equations.

These are solved by using WKB expansions [11]. These analytical procedures transform the problem into a nonlinear programming problem, which is then solved by using the Heaviside penalty function transformations [12, 13] of non-linear programming in conjunction with Rosenbrock's hill-climbing techniques [14].

This paper includes a description of the synthesis procedures used to implement the optimized design cycles on an English Electric KDF9 computer together with a discussion of results.

2. DISC CONFIGURATION

The thickness distribution of the disc is assumed to be of the form (Figure 1)

$$\begin{aligned} h(r) &= b_1 \qquad & a_1 \leqslant r \leqslant a_2, \\ &= h(r) & a_2 \leqslant r \leqslant a_{m-1}, \\ &= b_m, & a_{m-1} \leqslant r \leqslant a_m, \end{aligned} \tag{1}$$

where b_1, b_m, a_1, a_m and a_{m-1} are constants while $h(r)$ and a_2 are variables satisfying the conditions

$$\begin{gathered} a_1 \leqslant L \leqslant a_2 \leqslant U < a_{m-1}, \\ h(r) \geqslant \epsilon > 0, \qquad \forall r \in [a_2, a_{m-1}], \end{gathered} \tag{2}$$

where L and U are bounds on the hub radius while ϵ is a small positive tolerance to ensure non-negative thicknesses. $h(r)$ is the thickness at a radial distance r, $h(r)$ being measured parallel to the axis of the disc. a_1, a_m are the inner and outer radii, respectively, while b_1, b_m are the widths of the hub and rim respectively.

The constraint on the total weight is

$$\int_{a_1}^{a_m} 2\pi\rho r h(r)\, dr \leqslant W_0 \tag{3}$$

where ρ is the density of material, assumed to be constant and W_0 is a positive constant.

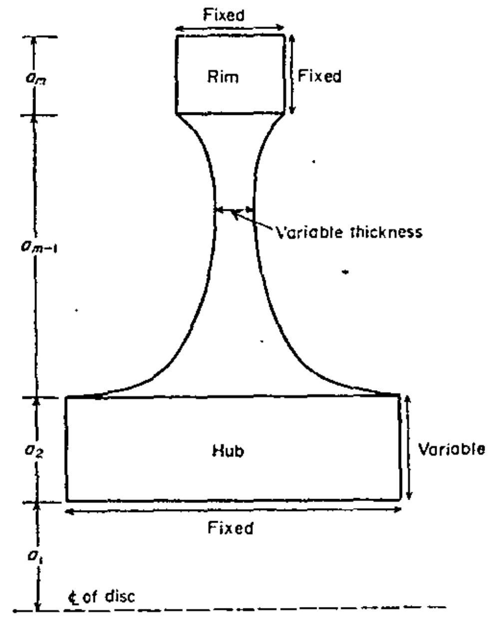

Figure 1. Cross section of typical turbine disc.

For purposes of simplicity, the disc, which is essentially an idealization of a turbine disc, is studied in the absence of the blades. The width of the hub and the rim shape are fixed to allow for the attachment of the discs and the spacing of the blades in the turbine while the depth of the hub is variable to permit adjoining discs to be shrunk onto a common shaft. The thickness distribution for the remainder of the disc is variable but symmetrically distributed about the midplane.

Conditions (2) and (3) determine the side constraints for the problem. The vibration aspects are discussed below.

3. BEHAVIOURAL EQUATIONS

The small deflection motion of a thin disc in polar coordinates is given by [15]

$$\rho h\frac{\partial^2 u}{\partial t^2}-\frac{1}{r}\frac{\partial}{\partial r}(rQ_r)-\frac{1}{r}\frac{\partial Q_\theta}{\partial \theta}=0,$$

$$\frac{1}{r}\frac{\partial}{\partial r}(rM_r)-\frac{M_\theta}{r}-\frac{1}{r}\frac{\partial M_{r\theta}}{\partial \theta}-Q_r=0,$$

$$\frac{1}{r}\frac{\partial M_\theta}{\partial \theta}-\frac{M_{r\theta}}{r}-\frac{1}{r}\frac{\partial}{\partial r}(rM_{r\theta})-Q_\theta=0, \tag{4}$$

where M_r, M_θ, $M_{r\theta}$ are the bending and twisting moments, Q_r, Q_θ are the shear forces and $u(r,\theta,t)$ is the axial displacement at time t of the section whose initial coordinates are (r,θ).

A cylindrical coordinate system $O(r,\theta,z)$ is used, where Oz is along the axis of the disc, r is the radial distance from Oz, and θ is the angular coordinate about Oz. Eliminating Q_r, Q_θ from equations (4) gives

$$\frac{1}{r}\frac{\partial^2}{\partial r^2}(rM_r)+\left(\frac{1}{r^2}\frac{\partial^2}{\partial \theta^2}-\frac{1}{r}\frac{\partial}{\partial r}\right)M_\theta-\frac{2}{r}\left(\frac{\partial^2}{\partial r\,\partial \theta}+\frac{1}{r}\frac{\partial}{\partial \theta}\right)M_{r\theta}=\rho h\frac{\partial^2 u}{\partial t^2}, \tag{5}$$

where

$$M_r=-\frac{Eh^3}{12(1-\nu^2)}\left[\frac{\partial^2 u}{\partial r^2}+\nu\left(\frac{1}{r}\frac{\partial u}{\partial r}+\frac{1}{r^2}\frac{\partial^2 u}{\partial \theta^2}\right)\right],$$

$$M_\theta=-\frac{Eh^3}{12(1-\nu^2)}\left[\nu\frac{\partial^2 u}{\partial r^2}+\left(\frac{1}{r}\frac{\partial u}{\partial r}+\frac{1}{r^2}\frac{\partial^2 u}{\partial \theta^2}\right)\right],$$

$$M_{r\theta}=\frac{Eh^3}{12(1+\nu)}\left[\frac{1}{r}\frac{\partial^2 u}{\partial r\,\partial \theta}-\frac{1}{r^2}\frac{\partial u}{\partial \theta}\right]. \tag{6}$$

E is Young's modulus and ν is Poisson's ratio for the material, both assumed to be constant.

Consider solutions harmonically dependent on both θ and t:

$$u(r,\theta,t)=W(r)\sin(n\theta+pt), \tag{7}$$

where n is the number of nodal diameters round the disc and p is the natural frequency of vibration. $W(r)$ is the radial form of the function which describes the axial displacement. Substituting equations (6) and (7) into equation (5) gives

$$\frac{d^4 W}{dr^4}+2\left(\frac{3}{h}\frac{dh}{dr}+\frac{1}{r}\right)\frac{d^3 W}{dr^3}+\left[\frac{3}{h}\frac{d^2 h}{dr^2}+\frac{6+3\nu}{hr}\frac{dh}{dr}+\frac{6}{h^2}\left(\frac{dh}{dr}\right)^2-\frac{2n^2+1}{r^2}\right]\frac{d^2 W}{dr^2}$$
$$+\left[\frac{3}{hr}\frac{d^2 h}{dr^2}-\frac{6n^2+3}{hr^2}\frac{dh}{dr}+\frac{6\nu}{h^2 r}\left(\frac{dh}{dr}\right)^2+\frac{2n^2+1}{r^3}\right]\frac{dW}{dr}$$
$$-n^2\left[\frac{3\nu}{hr^2}\frac{d^2 h}{dr^2}-\frac{9}{hr^3}\frac{dh}{dr}+\frac{6\nu}{h^2 r^2}\left(\frac{dh}{dr}\right)^2+\frac{4-n^2}{r^4}\right]W=\frac{12(1-\nu^2)}{Eh^2}\rho p^2 W. \tag{8}$$

This is the basic equation describing the behaviour of the disc, in flexural motion only. In order that Pontryagin's Principle be applied, this is reduced to a system of four equations of the first order.

The transversality conditions are provided by the boundary conditions at the edges of the disc. For example, suppose the inner edge is clamped while the outer edge is free. Then [16]

$$\begin{aligned} &u=\frac{\partial u}{\partial r}=0, \qquad \text{at } r=a_1,\\ &M_r=0, \qquad \text{at } r=a_m,\\ &Q_r-\frac{1}{r}\frac{\partial M_{r\theta}}{\partial \theta}=0, \qquad \text{at } r=a_m. \end{aligned} \tag{9}$$

This latter condition reduces to

$$\frac{\partial}{\partial r}\left(\frac{\partial^2 u}{\partial r^2}+\frac{1}{r}\frac{\partial u}{\partial r}+\frac{1}{r^2}\frac{\partial^2 u}{\partial \theta^2}\right)+\frac{(1-\nu)}{r^2}\frac{\partial^2}{\partial \theta^2}\left(\frac{\partial u}{\partial r}-\frac{u}{r}\right)=0, \qquad \text{at } r=a_m. \tag{9a}$$

Substituting equation (7) into equations (9) and (9a) then gives

$$\begin{aligned} &\text{at } r=a_1: \qquad W=\frac{\mathrm{d}W}{\mathrm{d}r}=0,\\ &\text{at } r=a_m: \qquad \frac{\mathrm{d}^2 W}{\mathrm{d}r^2}+\nu\left(\frac{1}{r}\frac{\mathrm{d}W}{\mathrm{d}r}-\frac{n^2}{r^2}W\right)=0,\\ &\qquad \frac{\mathrm{d}}{\mathrm{d}r}\left(\frac{\mathrm{d}^2 W}{\mathrm{d}r^2}+\frac{1}{r}\frac{\mathrm{d}W}{\mathrm{d}r}-\frac{n^2}{r^2}W\right)-\frac{n^2(1-\nu)}{r^2}\left(\frac{\mathrm{d}W}{\mathrm{d}r}-\frac{W}{r}\right)=0. \end{aligned} \tag{10}$$

The natural frequencies of vibration correspond to the eigenvalues of the differential system of equations (8) and (10). Since the boundary conditions (10) are homogeneous there will be a set of eigenvalues for the natural frequency p.

There are design advantages which result when the natural frequencies are as large as possible; in this investigation, therefore, it was attempted to maximize a linear combination of the natural frequencies by choosing a suitable representation for the shape function in an optimal way subject to the satisfying of the behaviour equations (8) and (10) and the design constraints (2) and (3). The mathematical formulation of this problem as an optimal control problem is given below.

4. OPTIMAL CONTROL PROBLEM

Introduce the transformation relations

$$\begin{aligned} &x_i=\frac{\mathrm{d}^{(i-1)}W}{\mathrm{d}r^{(i-1)}}, \qquad i=1,2,3,4,\\ &x_{i+4}=\frac{\mathrm{d}^{(i-1)}h}{\mathrm{d}r^{(i-1)}}, \qquad i=1,2,\\ &u=\frac{\mathrm{d}^2 h}{\mathrm{d}r^2}, \end{aligned} \tag{11}$$

so that the control function is represented by $\mathrm{d}^2h/\mathrm{d}r^2$ and is a measure of the curvature of the thickness profile of the disc. The state variables are the thickness $h(r)$, the radial deformation $W(r)$ and their derivatives. Substituting equations (11) into equations (8) gives

$$\frac{\mathrm{d}x_i}{\mathrm{d}r}=x_{i+1}, \qquad i=1,2,3,$$

$$\frac{dx_4}{dr} = \left[\frac{12(1-\nu^2)\rho p^2}{Ex_5^2} + \frac{3n^2\nu u}{x_5 r^2} - \frac{9n^2 x_6}{x_5 r^3} + \frac{6n^2 \nu x_6^2}{x_5^2 r^2} - \frac{n^2(n^2-4)}{r^4}\right] x_1$$
$$- \left[\frac{3\nu u}{x_5 r} - \frac{6n^2+3}{x_5 r^2} x_6 + \frac{6\nu}{x_5^2 r} x_6^2 + \frac{2n^2+1}{r^3}\right] x_2$$
$$- \left[\frac{3u}{x_5} + \frac{6+3\nu}{x_5 r} x_6 + \frac{6x_6^2}{x_5^2} - \frac{2n^2+1}{r^2}\right] x_3 - 2\left(\frac{3}{x_5} x_6 + \frac{1}{r}\right) x_4,$$
$$\frac{dx_5}{dr} = x_6,$$
$$\frac{dx_6}{dr} = u. \tag{12}$$

These correspond to the state equations for which the state and control variables are defined by equations (11). The appropriate state and control vectors are as follows:

$$\textit{state vector: } \mathbf{x} = (x_1, \ldots, x_6) = \left(W, \frac{dW}{dr}, \frac{d^2 W}{dr^2}, \frac{d^3 W}{dr^3}\middle| h, \frac{dh}{dr}\right);$$
$$\textit{control vector: } \mathbf{u} = \frac{d^2 h}{dr^2};$$
$$\textit{control parameter vector: } \mathbf{p} = (p_1, \ldots, p_l). \tag{13}$$

These are the first l natural frequencies of the disc, arranged in ascending order $0 < p_1 < p_2 < \ldots < p_l$.

Substituting equations (11) into equations (10) gives the following:

$$\theta^{(1)}: x_1(a_1) = x_2(a_1) = 0;$$
$$\theta^{(m)}: x_3(a_m) + \nu\left[\frac{x_2(a_m)}{a_m} - \frac{n^2}{a_m^2} x_1(a_m)\right] = 0;$$
$$x_4(a_m) + \frac{x_3(a_m)}{a_m} - \frac{x_2}{a_m^2}(a_m) - \frac{n^2}{a_m^2} x_2(a_m) + \frac{2n^2 x_1(a_m)}{a_m^3}$$
$$+ \frac{n^2(1-\nu)}{a_m^2}\left[x_2(a_m) - \frac{x_1(a_m)}{a_m}\right] = 0. \tag{14}$$

These correspond to the initial and terminal transversality conditions. The state inequality constraints are given by [see equations (2), (3) and (11)]

$$x_5 \geqslant \epsilon, \forall r \in [a_2, a_{m-1}],$$
$$\int_{a_1}^{a_m} 2\pi\rho r x_5 \, dr \leqslant W_0. \tag{15}$$

The merit criterion is defined by a function of the form

$$G(\mathbf{p}) = \sum_{i=1}^{l} c_i p_i, \tag{16}$$

where the coefficients c_i are weighting factors based on the Gaussian distribution function

$$c_i = \phi\left(\frac{p_i - p_1}{p_1}\right), \qquad i = 1, \ldots, l,$$
$$\phi(t) = \frac{1}{\sqrt{2\pi}} e^{-(t^2/2)}. \tag{17}$$

Hence,

$$c_1 > c_2 > \ldots > c_l > 0$$

and

$$0 < p_1 < p_2 \ldots < p_l.$$

The Gaussian distribution function was selected to give principal priority to the fundamental frequency p_1 and decreasing priorities to the higher frequencies $p_2, \ldots, p_l$. The initial values for the p_l used in equations (17) are obtained from experimental data for standard turbine disc configurations. These determine the coefficients c_l which are subsequently held constant during the synthesis. The merit criterion (16) gives a synthesis problem which appears to be closely allied in a dual sense, to a problem considered earlier [2, 5], whereby the weight of the turbine disc idealization was minimized subject to a constant on the natural frequencies of vibration, the frequencies being constrained to lie outside specified resonance bands. The establishment of this type of dual relationship could lead as a next step to a consideration of the more difficult but industrially important problem of designing a turbine disc to avoid certain critical frequency bands, while exhibiting optimal weight-frequency characteristics.

5. PONTRYAGIN FORMULATION

The optimal control problem consists in maximizing the merit criterion (17) subject to the state differential equations (12) in conjunction with the transversality conditions (14) and the state constraints (15). The state and control vectors are defined by equations (13). The solutions are based on the maximum principle of Pontryagin, the main results of which are summarized below for purposes of ready reference. For further details the reader is referred to reference [10].

Suppose that a dynamical system with state variables $\mathbf{x} = (x_1, \ldots, x_n)$ has equations of motion described by

$$\frac{d\mathbf{x}}{dr} = \mathbf{f}(\mathbf{x}, \mathbf{u}, \mathbf{p}, \mathbf{r}), \tag{12a}$$

where $\mathbf{u}(r) \in U$, defined over some interval $r_0 \leqslant r \leqslant r_1$, is a vector of controls and $\mathbf{p}$ is a vector of control parameters. The state variables are assumed to satisfy initial and terminal conditions of the form

$$\mathbf{x}(r_0) \in \theta^{(0)}; \qquad \mathbf{x}(r_1) \in \theta^{(1)}, \tag{14a}$$

where $\theta^{(0)}$ and $\theta^{(1)}$ are specified end manifolds in state space. Thus, for a given $\mathbf{u} \in U$, and a given $\mathbf{p}$, the state equations (12a) in conjunction with the transversality conditions (14a) possess a unique continuous solution $\mathbf{x}(r)$ which defines a trajectory in state space along which the states of the system are transferred between the end manifolds $\theta^{(0)}$ and $\theta^{(1)}$.

In addition, suppose that the system states are constrained to lie in a given region B of state space defined by

$$B \equiv \{\mathbf{x} \,|\, g(\mathbf{x}) \leqslant 0\}; \qquad B \subset E^n. \tag{15a}$$

This means that only those paths from the initial manifold $\theta^{(0)}$ to the terminal manifold $\theta^{(1)}$ which lie entirely in B are admissible. The object of the analysis is to determine an optimal control $\mathbf{u}(r) \in U$ for $r_0 \leqslant r \leqslant r_1$ and an optimal control parameter $\mathbf{p}$ which effects such a transfer while extremizing a merit criterion of the form

$$G = G(\mathbf{p}). \tag{17a}$$

The necessary conditions for an extremal solution are contained in Pontryagin's maximum principle which calls for the maximization with respect to $\mathbf{u} \in U$ of the Hamiltonian function defined by the scalar product

$$H = \boldsymbol{\lambda}.\mathbf{f}, \tag{18a}$$

where $\boldsymbol{\lambda} = (\lambda_1 \ldots \lambda_n)$ are the adjoint variables satisfying the differential equations

$$\frac{\mathrm{d}\boldsymbol{\lambda}}{\mathrm{d}r} = -\nabla_x H, \tag{20a}$$

where ∇_x denotes the gradient operator with respect to the state variables. This form of the maximum principle is applicable to arcs of the optimal trajectory which lies within the interior of the state constraint domain (15a), $g(\mathbf{x}) < 0$. For arcs of the optimal trajectory which lies on the boundary of B,

$$g(\mathbf{x}) = 0, \qquad \text{for } r_e \leqslant r \leqslant r_l,$$

where $r_0 \leqslant r_e < r_l \leqslant r_1$. The points $\mathbf{x}(r_e)$, $\mathbf{x}(r_l)$ are called the entry and leaving points respectively. The extremal conditions are now described by the restricted maximum principle (see chapter 4 of reference [10]), whereby

$$p(\mathbf{x}, \mathbf{u}, \mathbf{p}) \equiv \nabla_x g.\mathbf{f} = 0, \qquad \text{for } \forall r \in [r_e, r_l]$$

provided $\nabla_x g.\mathbf{f}$ does not contain r. Controls $\mathbf{u} \in U$ which satisfy the above conditions are said to belong to the restricted control set.

These results are now applied to the disc problem for which the Hamiltonian is defined by [see equations (12) and (18a)]

$$\begin{aligned} H(\boldsymbol{\lambda}; x; r; u) = \sum_{i=1}^{3} \lambda_i x_{i+1} + \lambda_4 \Bigg[& \left(\frac{12(1-\nu^2)}{Ex_5^2} \rho p^2 + \frac{3n^2 \nu u}{x_5 r^2} - \frac{9n^2 x_6}{x_5 r^3} + \frac{6n^2 \nu x_6^2}{x_5^2 r^2} - \frac{n^2(n^2-4)}{r^4} \right) x_1 \\ & - \left(\frac{3\nu u}{x_5 r} - \frac{6n^2+3}{x_5 r^2} x_6 + \frac{6\nu x_6^2}{x_5^2 r} + \frac{2n^2+1}{r^3} \right) x_2 - \\ & - \left(\frac{3u}{x_5} + \frac{6+3\nu}{x_5 r} x_6 + \frac{6x_6^2}{x_5^2} - \frac{2n^2+1}{r^2} \right) x_3 - 2 \left(\frac{3}{x_5} x_6 + \frac{1}{r} \right) x_4 \Bigg] + \lambda_5 x_6 + \lambda_6 u, \end{aligned} \tag{18}$$

where $\lambda_i(r)$; $i = 1, \ldots, 6$ are the components of the adjoint vector, the state and control vectors and parameters being given by equations (13). The solutions are based on the following configurations for the optimal trajectory: (i) arcs of the optimal trajectory which lies within the interior of the state constraint region $x_5 > \epsilon$; (ii) arcs of the optimal trajectory which lies on the boundary $x_5 = \epsilon$ for which the restricted maximum principle [10] is applicable.

The composite representation for the optimal trajectory between the end manifolds $\theta^{(1)}$ and $\theta^{(m)}$ defined by equations (14) is obtained by matching these separate arcs at the entry and leaving points. From equations (13), the optimal trajectory determines the optimal shape and deformation functions for the disc.

A detailed consideration of the above cases is presented in sections 6 and 7.

6. INTERIOR OF CONSTRAINT REGION

The configuration of interest here corresponds to arcs of the optimal trajectory lying in the interior of the state constraint region (15), $x_5 > \epsilon$. The control $u(r)$ is unbounded and continuous in $[a_2, a_{m-1}]$, so that, from the maximization condition,

$$\frac{\partial H}{\partial u} = \lambda_4 \left[\frac{3n^2 \nu x_1}{x_5 r^2} - \frac{3\nu x_2}{x_5 r} - \frac{3x_6}{x_5} \right] + \lambda_6 = 0. \tag{19}$$

With the Hamiltonian as defined in equation (18), the adjoint equations (20a) reduce to

$$
\begin{aligned}
\frac{d\lambda_1}{dr} &= -\frac{\partial H}{\partial x_1} = -\lambda_4 A, \\
\frac{d\lambda_2}{dr} &= -\frac{\partial H}{\partial x_2} = -\lambda_1 + \lambda_4 B, \\
\frac{d\lambda_3}{dr} &= -\frac{\partial H}{\partial x_3} = -\lambda_2 + \lambda_4 C, \\
\frac{d\lambda_4}{dr} &= -\frac{\partial H}{\partial x_4} = -\lambda_3 + \lambda_4 D, \\
\frac{d\lambda_5}{dr} &= -\frac{\partial H}{\partial x_5} = -\lambda_4 E, \\
\frac{d\lambda_6}{dr} &= -\frac{\partial H}{\partial x_6} = -\lambda_4 F - \lambda_5,
\end{aligned}
\tag{20}
$$

where

$$
\begin{aligned}
A &= \frac{12(1-\nu^2)\rho p^2}{Ex_5^2} + \frac{3n^2 \nu u}{x_5 r^2} - \frac{9n^2 x_6}{x_5 r^3} - \frac{n^2(n^2-4)}{r^4}, \\
B &= \frac{3\nu u}{x_5 r} - \frac{6n^2+3}{x_5 r^2} x_6 + \frac{6\nu x_6^2}{x_5^2 r} + \frac{2n^2+1}{r^3}, \\
C &= \frac{3u}{x_5} + \frac{6+3\nu}{x_5 r} x_6 + \frac{6x_6^2}{x_5^2} - \frac{2n^2+1}{r^2}, \\
D &= 2\left(\frac{3x_6}{x_5} + \frac{1}{r}\right), \\
E &= \left[-\frac{24(1-\nu^2)\rho p^2}{Ex_5^3} - \frac{3n^2 \nu u}{x_5^2 r^2} + \frac{9n^2 x_6}{x_5^2 r^3} - \frac{12n^2 \nu x_6}{x_5^3 r^2}\right] x_1 \\
&\quad - \left(-\frac{3\nu u}{x_5^2 r} + \frac{6n^2+3}{x_5^3 r^2} x_6 - \frac{12\nu x_6^2}{x_5^3 r}\right) x_2 \\
&\quad - \left(-\frac{3u}{x_5^2} - \frac{6+3\nu}{x_5^2 r^2} x_6 - \frac{12x_6^2}{x_5^3}\right) x_3 + \frac{6x_6}{x_5^2} x_4, \\
F &= \left(-\frac{9n^2}{x_5 r_3} + \frac{12n^2 \nu x_6}{x_5^2 r^2}\right) x_1 - \left(-\frac{6n^2+3}{x_5 r^2} + \frac{12\nu x_6}{x_5^2 r}\right) x_2 \\
&\quad - \left(\frac{6+3\nu}{x_5 r} + \frac{12x_6}{x_5^2}\right) x_3 - \frac{6x_4}{x_5}.
\end{aligned}
$$

Complete analytical solutions to the differential system (20) are very difficult to obtain and recourse is made to the following approximate technique. The validity of this method is justified *a posteriori*.

Consider series solutions of the form

$$
\lambda_i(r) = \sum_{j=0}^{\infty} \lambda_{ij}(r)\,\eta^j, \qquad i = 1, 2, \ldots, 6, \tag{21}
$$

where η is a small parameter which has essentially a mathematical rather than physical significance. Suppose λ_4 is small. This means $\lambda_{40} = 0$, so that $\lambda_4 = O(\eta)$. Substitute equations (21) into equation (19) and equate to zero the lowest power of η, giving $\lambda_{60} = 0$. Similarly substitute equations (21) into equations (20) and equate the corresponding coefficients of η^0. This gives, on solving the resulting differential equations, the zero-order solutions for $\boldsymbol{\lambda}$:

$$\begin{aligned}\lambda_{10} &= \lambda_1^0,\\ \lambda_{20} &= -\lambda_1^0 r + \lambda_2^0,\\ \lambda_{30} &= \lambda_1^0(r^2/2) - \lambda_2^0 r + \lambda_3^0,\\ \lambda_{40} &= \lambda_{50} = \lambda_{60} = 0.\end{aligned} \tag{22}$$

Therefore the adjoint vector is given by

$$\begin{aligned}\lambda_1 &= \lambda_1^0 + O(\eta),\\ \lambda_2 &= -\lambda_1^0 r + \lambda_2^0 + O(\eta),\\ \lambda_3 &= \lambda_1^0(r^2/2) - \lambda_2^0 r + \lambda_3^0 + O(\eta),\\ \lambda_4 &= O(\eta),\\ \lambda_5 &= O(\eta),\\ \lambda_6 &= O(\eta).\end{aligned} \tag{23}$$

Equations (22) are obtained by excluding the equation $\mathrm{d}\lambda_4/\mathrm{d}r = -\lambda_3 + \lambda_4 D$ in equations (20). Therefore from equations (22), $|D|$ must be large for consistency. From equations (13), and the definition of D,

$$D \equiv 2\left(\frac{3x_6}{x_5} + \frac{1}{r}\right) = 2\left(\frac{3}{h}\frac{\mathrm{d}h}{\mathrm{d}r} + \frac{1}{r}\right) \approx k \tag{24}$$

where

$$|k| \gg 0. \tag{25}$$

Therefore,

$$\begin{aligned}h(r) &\approx \frac{C}{r^{1/3}}\mathrm{e}^{kr/3}, \qquad C > 0,\\ h'(r) &\approx \frac{k}{3}h,\\ h''(r) &\approx \frac{k^2}{9}h.\end{aligned} \tag{26}$$

These determine the optimal thickness for sub-intervals of $[a_2, a_{m-1}]$ for which $h(r) \neq \epsilon$. The proof of condition (25) that $|k|$ is large is given in section 8. This is the justification for the earlier assumption that λ_4 is small. Therefore equations (23) and (26) determine a compatible set of solutions for the adjoint equations (20).

The optimal deformation $W(r)$ is obtained by substituting equations (26) into equation (8), and simplifying by using the condition (25), to give the differential equation

$$\frac{\mathrm{d}^4 W}{\mathrm{d}r^4} + 2k\frac{\mathrm{d}^3 W}{\mathrm{d}r^3} + k^2\frac{\mathrm{d}^2 W}{\mathrm{d}r^2} + \frac{\nu k^2}{r}\frac{\mathrm{d}W}{\mathrm{d}r} - \left[\frac{12(1-\nu^2)\rho p^2}{Eh^2} + \frac{n^2 \nu k^2}{r^2}\right]W = 0. \tag{27}$$

The solutions to this equation are given below for the cases when k is large and negative, and k is large and positive. These, together with condition (25) determine the interior arcs of the optimal trajectory, which are subsequently matched with the boundary arcs (at the entry and leaving points) to give the composite shape function for the disc.

Case 1a: $k < 0$

This corresponds to k large and negative.

Put $x=-k(r-a_2)$, in equation (27) and let $|k| \to \infty$. This gives, after simplification, the following differential equation:

$$\frac{d^4 W}{dx^4} - 2\frac{d^3 W}{dx^3} + \frac{d^2 W}{dx^2} - \Lambda^4 f(x) W = 0, \tag{28}$$

where

$$\Lambda^4 = e^{-2ka_2/3} \qquad \text{(large)},$$

$$f(x) = \frac{12(1-\nu^2)\rho p^2}{EC^2|k|^{14/3}}(-ka_2+x)^{2/3} e^{2/3x} > 0.$$

Put $W = e^{x/2}u(x)$ in equation (28). This gives the following differential equation for $u(x)$:

$$\frac{d^4 u}{dx^4} - \frac{1}{2}\frac{d^2 u}{dx^2} + \left[\frac{1}{16} - \Lambda^4 f(x)\right]u = 0. \tag{29}$$

Since the parameter Λ is large, this equation can be solved by using WKB expansions of the form

$$u(x) = g_0(x)\, e^{\Lambda\phi(x)}\left\{1 + \frac{g_1(x)}{\Lambda} + \frac{g_2(x)}{\Lambda^2} + \dots\right\}. \tag{30}$$

Substituting equation (30) into equation (29) and equating to zero coefficients of Λ^4, Λ^3, ... gives

$$\phi_s' = \{f(x)\}^{1/4} e^{is\pi/2}, \qquad s = 0, 1, 2, 3,$$

$$g_0 = \{f(x)\}^{-3/8}.$$

Therefore

$$W(x) = \sum_{s=0}^{3} \alpha_s e^{x/2}[f(x)]^{-3/8} \exp\left[\Lambda e^{is\pi/2} \times \int^x \{f(x)\}^{1/4} dx\right] \times \left(1 + O\left(\frac{1}{\Lambda}\right)\right), \tag{31}$$

where α_s, $s = 0,1,2,3$ are constants of integration. Finally, the form of equation (27) for large positive values of k is considered below.

Case Ib: $k > 0$

Put $x = k(r-a_2)$; $k \to \infty$ in equation (27). This gives, on simplification,

$$\frac{d^4 W}{dx^4} + 2\frac{d^3 W}{dx^3} + \frac{d^2 W}{dx^2} \approx 0.$$

Solving this results in

$$W(r) = \alpha_4 + \alpha_5 r + (\alpha_6 + \alpha_7 r)e^{-kr}, \tag{32}$$

where α_4, α_5, α_6, α_7 are constants of integration. Equations (32) and (31) determine the solutions to equation (27). The state and control variables are given by equations (13), (26), (32) and (31). These equations determine the complete representation for the system when the optimal trajectory belongs to the interior of the state constraint region.

The corresponding equations when the optimal trajectory belongs to the boundary are given below, in section 7.

7. BOUNDARY OF CONSTRAINT REGION

The restricted maximum principle is applied to arcs of the optimal trajectory lying on the state constraint boundary [10]. Let the boundary arc be defined by

$$x_5(r) = \epsilon, \forall r \in [r_e, r_l], \tag{33}$$

where $a_2 < r_e < r_l < a_{m-1}$, and $\mathbf{x}(r_e)$, $\mathbf{x}(r_l)$ are the entry and leaving points, respectively. The restricted control set described in section 5 is now formed:

$$\nabla_x(x_5 - \epsilon) = (0,0,0,0,1,0).$$

Therefore $p \doteq$ scalar product of $\nabla_x(x_5-\epsilon)$ with the right-hand sides of the state equations (12) is equal to x_6. Hence

$$x_6 = 0,$$
$$u = 0. \tag{33a}$$

This is to be expected since $h(r) \equiv x_5 = \epsilon$ implies $x_6 \equiv dh/dr = 0$ and $u \equiv d^2h/dr^2 = 0$.
Substituting into the state equations (12) or (8) and simplifying then gives

$$\frac{d^4 W}{dr^4} + \frac{2}{r}\frac{d^3 W}{dr^3} - \frac{2n^2+1}{r^2}\frac{d^2 W}{dr^2} + \frac{2n^2+1}{r^3}\frac{dW}{dr} + \left[\frac{n^2(n^2-4)}{r^4} - \frac{12(1-\nu^2)\rho p^2}{E\epsilon^2}\right] W = 0.$$

The solutions to this fourth-order equation are

$$W(r) = \alpha_8 J_n(\Omega r) + \alpha_9 Y_n(\Omega r) + \alpha_{10} I_n(\Omega r) + \alpha_{11} K_n(\Omega r) \tag{33b}$$

where $J_n(r)$ and $Y_n(r)$ are Bessel functions, $I_n(\Omega r)$ and $K_n(\Omega r)$ are modified Bessel functions, α_8, α_9, α_{10} and α_{11} are constants of integration and

$$\Omega^4 = 12(1-\nu^2)\rho p^2/E\epsilon^2.$$

State and control variables are given by equations (13), (33a) and (33b). This concludes the analysis for an optimal thickness $h^*(r) = \epsilon$.

8. OPTIMAL THICKNESS PATTERN

Equations (26), (31) and (32) corresponding to interior arcs of the optimal trajectory determine the optimal shape and deformation functions for $|k|$ large. These are merged at r_e and r_l with the corresponding solutions (33a), (33b) for the boundary arcs to yield the optimal design configuration.

The optimal thickness is given by (see Figures 2–4)

$$\begin{aligned} h^*(r) &= h^-(r), & a_2 \leqslant r \leqslant r_e,\\ &= \epsilon, & r_e \leqslant r \leqslant r_l,\\ &= h^+(r), & r_l \leqslant r \leqslant a_{m-1}, \end{aligned} \tag{34}$$

where $h^-(r)$, $h^+(r)$ correspond to the function (26) for values of $k<0$ and $k>0$, respectively. Figures 2 and 3 show the functions $h^-(r)$ and $h^+(r)$, respectively, corresponding to interior arcs of the optimal trajectory. For $k<0$, $h^-(r)$ is a monotonic decreasing function of r, so that in the interval $a_2 \leqslant r \leqslant r_e$, $h^-(r)$ decreases monotonically from b_1 and reaches its lower limit ϵ at $r = r_e$. At this point, the optimal trajectory enters the boundary of the state constraint domain, leaving it finally at $r = r_l$, so that $h^*(r) = \epsilon$ for $r_e \leqslant r \leqslant r_l$. From Figure 3 it is seen that in the interval $r_l \leqslant r \leqslant a_{m-1}$, the optimal thickness is given by $h^+(r)$. $h^+(r)$ has a minimum at

$$r = 1/k^+,$$

so that $r_l \geqq 1/k^+$. This result is used in equation (38) in obtaining the side constraints. In the interval $[r_l, a_{m-1}]$, $h^*(r) = h^+(r)$ increases monotonically from its limiting value ϵ to b_m.

But from physical continuity conditions

$$\begin{aligned} h^-(a_2) &= b_1, & h^-(r_e) &= \epsilon,\\ h^+(r_l) &= \epsilon, & h^+(a_{m-1}) &= b_m. \end{aligned} \tag{35}$$

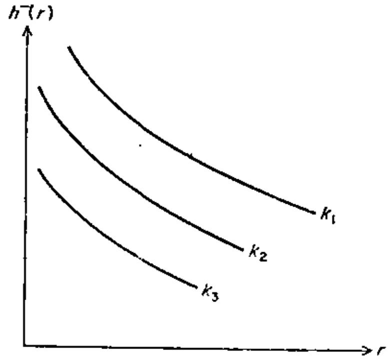

Figure 2. Thickness for $k < 0$. $|k_1| < |k_2| < |k_3|$.

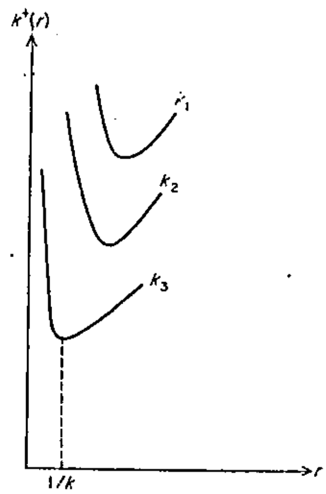

Figure 3. Thickness for $k > 0$. $k_1 > k_2 > k_3$; $h^+(r) = (C^+/r^{1/3})\exp(k^+r/3)$; $dh^+/dr = (C^+/3r^{1/3})(k^+ - 1/r)$ $\exp(k^+r/3)$.

Therefore, substituting equation (35) into equation (26) yields

$$b_1 = (C^-/a_2^{1/3})\,e^{k^-a_2/3},$$
$$\epsilon = (C^-/r_e^{1/3})\,e^{k^-r_e/3}.$$

Eliminating C^- gives

$$k^- = \frac{3}{a_2 - r_e}\ln\left|\frac{b_1}{\epsilon}\left(\frac{a}{r_e}\right)^{1/3}\right| \tag{36}$$

and therefore

$$|k^-| \to \infty \text{ as } \epsilon \to 0+. \tag{36a}$$

Again

$$b_m = (C^+/a_{m-1}^{1/3})\,e^{k^+a_{m-1}/3},$$
$$\epsilon = (C^+/r_l^{1/3})\,e^{k^+r_l/3}.$$

Eliminating C^+ gives

$$k^+ = \frac{3}{a_{m-1} - r_l}\ln\left|\frac{b_m}{\epsilon}\left(\frac{a_{m-1}}{r_l}\right)\right|, \tag{37}$$

and so

$$|k^+| \to \infty \text{ as } \epsilon \to 0+. \tag{37a}$$

Conditions (36a) and (37a) establish the validity of condition (25), which is the justification for the assumption of λ_4 small in section 5.

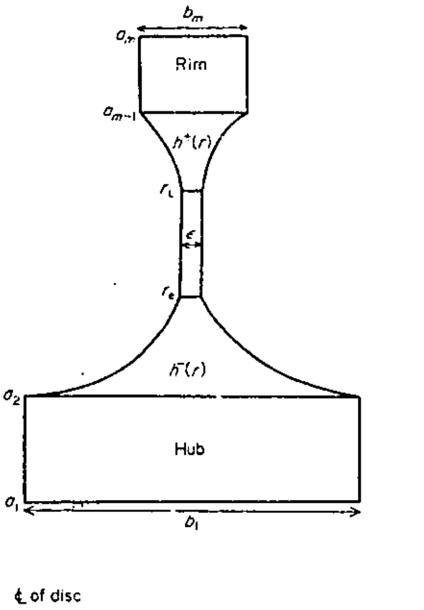

Figure 4. Optimal thickness. $h^+(r) \triangleq h(r), k > 0$; $h^-(r) \triangleq h(r), k < 0$.

Equations (35–37) and (26) also establish the continuity of $x_5 \equiv h$ and $x_6 \equiv \mathrm{d}h/\mathrm{d}r$ at $r = r_e, r_l$, which is a necessary condition for the analysis to be valid.

9. SIDE CONSTRAINTS

These represent constraints on the geometrical configuration of the disc. From Figures 3 and 4, with equation (37) being used since $h^+(r)$ has a minimum at $r = 1/k^+$

$$r_l \geqslant \frac{1}{k^+} = \frac{a_{m-1} - r_l}{3}\left[\ln\frac{b_m}{\epsilon}\left(\frac{a_{m-1}}{r_l}\right)^{1/3}\right]^{-1},$$

$$r_l \geqq \frac{a_{m-1}}{3\ln\{(b_m/\epsilon)(a_{m-1}/r_l)^{1/3}\}+1} \to 0 \text{ as } \epsilon \to 0+.$$

Therefore this inequality reduces to

$$0 \leqslant r_l < a_{m-1}. \tag{38}$$

But, for compatibility,

$$a_2 < r_e < r_l. \tag{39}$$

The weight is given by equations (3) and (34):

$$\begin{aligned}
\int_{a_1}^{a_m} 2\pi\rho r h^*(r)\,\mathrm{d}r &= \int_{a_1}^{a_2} 2\pi\rho r b_1\,\mathrm{d}r + \int_{a_2}^{r_e} 2\pi\rho r h^-(r)\,\mathrm{d}r + \int_{r_e}^{r_l} 2\pi\rho r\epsilon\,\mathrm{d}r \\
&\quad + \int_{r_l}^{a_{m-1}} 2\pi\rho r h^+(r)\,\mathrm{d}r + \int_{a_{m-1}}^{a_m} 2\pi\rho r b_m\,\mathrm{d}r \\
&= \pi\rho b_1(a_2^2 - a_1^2) + \pi\rho b_m(a_m^2 - a_{m-1}^2) + \pi\rho\epsilon(r_l^2 - r_e^2) \\
&\quad + 2\pi\rho\int_{a_2}^{r_e} r h^-(r)\,\mathrm{d}r + 2\pi\rho\int_{r_l}^{a_{m-1}} r h^+(r)\,\mathrm{d}r.
\end{aligned}$$

Therefore the constraint on the weight is given by

$$f_1(a_2, r_e, r_l) \leqslant 0, \tag{40}$$

where

$$f_1(a_2, r_e, r_i) \equiv \pi p b_1(a_2^2 - a_1^2) + \pi p b_m(a_m^2 - a_{m-1}^2) + \pi p \epsilon(r_i^2 - r_e^2)$$
$$+ 2\pi p \int_{a_2}^{r_e} r h^-(r)\,dr + 2\pi p \int_{r_i}^{a_{m-1}} r h^+(r)\,dr - W_0.$$

These integrals are evaluated by using standard numerical integration procedures [17].

The side constraints are given by equations (38)–(40) and their two-dimensional representation in the (r_e, r_i) plane is shown in Figure 5.

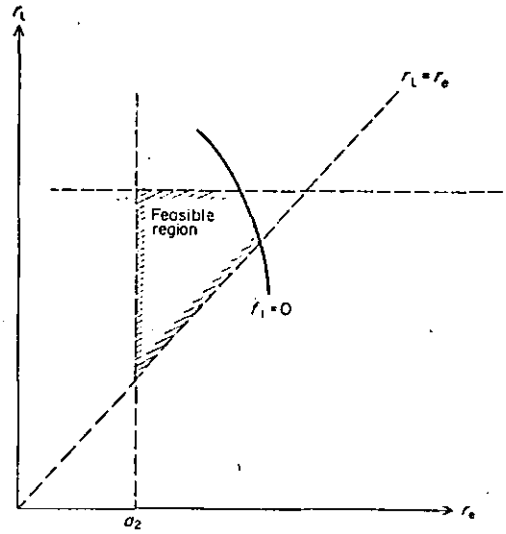

Figure 5. Optimal control problem → non-linear programming problem. $(r_e - r_i)$ design parameter subspace. ----, Portions of the boundary on which solutions cannot lie; ——, portions of the boundary on which solutions can lie.

10. BEHAVIOURAL CONSTRAINTS

The radial deformations within the subintervals $[a_1, a_2]$, $[a_{m-1}, a_m]$ are

$$W(r) = \alpha_{12} J_n(\Omega r) + \alpha_{13} Y_n(\Omega r) + \alpha_{14} I_n(\Omega r) + \alpha_{15} K_n(\Omega r), \qquad a_1 \leqslant r \leqslant a_2,$$
$$W(r) = \alpha_{16} J_n(\Omega r) + \alpha_{17} Y_n(\Omega r) + \alpha_{18} I_n(\Omega r) + \alpha_{19} K_n(\Omega r), \qquad a_{m-1} \leqslant r \leqslant a_m, \tag{41}$$

where $\alpha_{12}, \ldots, \alpha_{19}$ are constants of integration [see equation (33)]. The behavioural requirements are given by eliminating the constants of integration $(\alpha_0, \alpha_1, \ldots, \alpha_{19})$ from equations (32), (33), (36) and (41). The boundary conditions are obtained from equation (10) and the continuity of W, dW/dr, d^2W/dr^2 and d^3W/dr^3 at $r = a_2, r_e, r_i, a_{m-1}$. These arise from continuity requirements for the state vector (12). They are also necessary physical conditions for the continuity of deflection, slope, bending and shear forces. The elimination process gives a 20×20 determinantal equation of the form

$$f_2(a_2, r_e, r_i, p) \equiv \begin{vmatrix} \mathbf{A}_{11} & 0 & 0 & \mathbf{A}_{14} & 0 \\ \mathbf{A}_{21} & 0 & \mathbf{A}_{23} & 0 & 0 \\ 0 & \mathbf{A}_{32} & \mathbf{A}_{33} & 0 & 0 \\ 0 & \mathbf{A}_{42} & 0 & 0 & \mathbf{A}_{45} \\ 0 & 0 & 0 & 0 & \mathbf{B}_1 \\ 0 & 0 & 0 & 0 & \mathbf{B}_2 \end{vmatrix} = 0, \tag{42}$$

where the $\mathbf{A}_{ij}$ are 4×4 submatrices, while $\mathbf{B}_1$ and $\mathbf{B}_2$ are of order 2×4.

The non-zero elements of (42) correspond to the different types of Bessel functions used in section 7. The arguments of these functions are proportional to p_2 so that on evaluation the determinant (42) gives for f_2 a polynomial in the frequency so that

$$f_2 \equiv \sum_i \mu_i(a_2, r_e, r_i)\, p^i = 0.$$

The frequencies are given by the roots of this polynomial, so that

$$\mathbf{p} = \mathbf{p}(a, r_e, r_i), \tag{43}$$

where $\mathbf{p}$ is the vector of the first l roots of the polynomial f_2 and corresponds to the control parameter vector (13).

From equation (43) the merit criterion (17) must also be a function of a_2, r_e and r_i:

$$G(\mathbf{p}) \rightarrow f_0(a_2, r_e, r_i). \tag{44}$$

The vibrational frequencies are introduced into the synthesis procedures through equation (42) which is computed numerically by using standard triangularization procedures.

11. NON-LINEAR PROGRAMMING FORMULATION

The non-linear programming formulation is, formally, as follows:

$$\text{Maximize } G(\mathbf{p}) \text{ subject to } f_1(a_2, r_e, r_i) \leqslant 0,\ L \leqslant a_2 \leqslant U,\ 0 \leqslant r_i < a_{m-1},$$
$$a_2 < r_e < r_i,\ f_2(a_2, r_e, r_i, \mathbf{p}) = 0. \tag{45}$$

This is solved by transforming the problem into a series of unconstrained optimization problems by using the Heaviside penalty function transformation [12, 13]. These unconstrained problems are solved by using Rosenbrock's method [14].

12. RESULTS AND DISCUSSION

The numerical computations were performed on an English Electric KDF 9 computer using ALGOL. The computational effort was characterized by extremely large and complex programming procedures which imposed severe limitations on storage and test facilities. A substantial amount of the time was consumed in the Bessel function calculations [18]. In addition, considerable numerical difficulties arose in the calculation of the determinantal function $f_2(a_2, r_e, r_i, p)$ due to the presence of very large numbers, giving rise to local regions of instability in the synthesis.

The program was initiated by a set of values for a_2, r_e, r_i and p which satisfied the side constraints. However it was not possible to ensure the vanishing of f_2. This was not a serious disadvantage since the Heaviside penalty function transformation [12] always generates a feasible point as the solution to the equivalent unconstrained problem.

For these reasons the available computational experience is limited, although an examination of the preliminary results indicates that the synthesis is progressing in the right direction. The really effective utilization of the numerical procedures requires a more powerful range of computers than was available at the time of this investigation.

13. CONCLUSION

Powerful synthesis procedures based on the methods of mathematical programming have been developed for solving a highly complex structural optimization problem. Considerable progress has been made in solving the problem by using purely analytical techniques based on the maximum principle of Pontryagin which transforms the problem into a non-linear programming problem.

Available computational experience indicates the possibilities of developing a highly systematic synthesis capability when used in conjunction with *very* large, high-speed digital computers. The available evidence appears to warrant further investigation and development in this direction, with particular emphasis on more automatic software packages for handling very large problems.

14. ACKNOWLEDGMENT

This research was sponsored and supported by the Mechanical Engineering Laboratories of the English Electric Company, Whetstone, under project No. 420041, and is published by permission of the Company.

Acknowledgment is also made to Professor T. V. Davies, Department of Mathematics, University of Leicester, England, for many constructive suggestions during this investigation.

REFERENCES

1. B. M. E. de Silva 1969 In *Optimization* (R. Fletcher, ed.) p. 115–150. London: Academic Press. The application of nonlinear programming to the automated minimum weight design of rotating discs.
2. B. M. E. de Silva 1969 *Transactions of the American Society of Mechanical Engineers, Journal of Engineering for Industry* **91**, 1091–1099. Minimum weight design of discs using a frequency constraint.
3. B. M. E. de Silva 1965 *English Electric Co. Report No. W/M (6B) p. 1126.* On the application of nonlinear programming to the automatic structural synthesis of turbine discs.
4. B. M. E. de Silva 1967 *English Electric Report No. W/M (4B) p. 1323.* The minimum weight design of turbine discs.
5. B. M. E. de Silva 1968 *English Electric Co. Report No. W/M (4B) p. 1452.* Automated weight minimisation based on a frequency constraint.
6. B. M. E. de Silva 1970 *Transactions of the American Society of Mechanical Engineers, Journal of Basic Engineering* **92**, 245–250. Application of Pontryagin's principle to a minimum weight design problem.
7. B. M. E. de Silva 1968 *English Electric Co. Report No. W/M (4B) p. 1382.* Nonclassical variational problems in minimum weight structural optimization theory.
8. B. M. E. de Silva 1968 *English Electric Co. Report No. W/M (4B) p. 1442.* Variational methods in minimum weight design problems.
9. L. A. Schmit, T. P. Kicher and W. M. Morrow 1963 *American Institute of Aeronautics and Astronautics* **1**, 2820–2836. Structural synthesis capability for integrally stiffened waffle plates.
10. G. Leitmann 1966 *Introduction to Optimal Control.* New York: McGraw-Hill. See chapter 4.
11. H. Jeffreys and B. Jeffreys 1956 *Methods of Mathematical Physics.* Cambridge University Press. See pp. 522–525.
12. J. Kowalik 1966 *Acta polytechica scandinavica, Series d* **13**, 1–47 Nonlinear programming procedures and design optimization.
13. L. A. Schmit and R. L. Fox 1964 *American Institute of Aeronautics and Astronautics* **3**, 1109–1112. An integrated approach to structural synthesis and analysis.
14. H. H. Rosenbrock 1960 *Computation Journal* 3, 175–184. An automatic method for finding the greatest or least value of a function.
15. G. Capriz 1961 *English Electric Co., Nelson Research Laboratories, Report No. NS V* 207. Axial vibrations of turbine discs, Part I.
16. S. Timoshenko 1940 *Theory of Plates and Shells.* New York: McGraw-Hill. See chapter VII.
17. *Notes on Applied Science No. 16.* Modern computing methods. See chapter VII.
18. D. F. Barnard 1967 *English Electric Co., Technical Memorandum No. W/M, U. 9076.* A Whetstone Algol program to calculate Bessel functions of real argument and integral order.

Int. J. Math. Educ. Sci. Technol., VOL. 2, 171–181 (1971)

An Eigenvalue Analysis for Calculating the Vibrational Modes of Steam Turbine Discs

B. M. E. DE SILVA

Department of Mathematics, University of Technology, Loughborough, Leicestershire, England

Summary

This paper describes the application of numerical procedures to an engineering design problem of considerable practical importance. The problem is that of calculating the natural frequencies of vibration of steam turbine discs. The analysis is based on a variational formulation in conjunction with finite difference procedures to transform the problem to an eigenvalue problem. This is characterized by a symmetric band matrix, and the vibrational frequencies which correspond to the eigenvalues are computed using standard eigenvalue programming packages. The analysis includes a description of both natural and forced boundary conditions for the problem.

An essential feature of this investigation is the relative simplicity in elasticity theory used and the associated computational procedures. As such it should be of interest to teachers of final year engineering mathematics courses and to mechanical engineering students embarking on an M.Sc. programme.

From a research standpoint, the paper offers the possibility of extending the analysis to include shear correction effects and thick discs. These again are of considerable practical interest.

Introduction

The formulation of efficient analytical and computational procedures for determining the natural modes of vibration of steam turbine discs is of considerable importance in the development of an automated turbine design capability.[1,2] These vibrational problems, by their very nature, preclude the use of purely analytical methods of solution which, on the whole, are applicable only to discs of constant thickness[3] or of parabolic shape.[4] Therefore recourse must be made to approximate numerical procedures. Such procedures used in conjunction with digital computers have led to the development of highly systematic programs for studying the vibrational characteristics of turbine discs.

Prominent amongst these are the transfer matrix methods[5,6] in which the frequencies are given by the roots of a certain polynomial. The roots are determined using interpolation or spline function techniques.[7] The spline function techniques consist essentially in calculating successive values of the polynomial for different values of the frequency (ω) and a plot of the polynomial against ω is made. Those values of ω for which the polynomial is zero are the required natural frequencies. Alternatively, an interpolation procedure, based on an initial ω and an increment $\Delta\omega$, can be used. These must operate near the actual frequency in order to obtain rapid convergence.

The transfer matrix methods, though relatively simple from a mathematical standpoint, involve the programming of extremely long and complex routines and impose considerable limitations on storage facilities. However, they are efficient for most calculations in

Received 13 November 1970

which the designer uses his intuition, judgement and experience to reduce the number of polynomial calculations thereby obtaining rapid convergence.

They become significantly less efficient when coupled with synthesis programs[8,9] for optimizing the design process by generating a sequence of trial designs of improving merit. Most of these correspond to designs significantly different from standard disc configurations. So that it is extremely difficult, if not impossible, to obtain realistic starting procedures for use in conjunction with interpolation or spline function techniques. Consequently convergence is slow and unstable and often converges to a root of different order.

These difficulties can be overcome by using a variational formulation in conjunction with finite difference techniques to transform the problem to an eigenvalue problem. This is characterized by a symmetric band matrix, the eigenvalues of which correspond to the vibrational frequencies. These computations can be carried out efficiently and rapidly using standard matrix usercode programs.[10] Mathematically, the problem is represented by the eigenvalue equation

$$\mathbf{A}\mathbf{w} = \omega^2 \mathbf{B}\mathbf{w} \tag{1}$$

where

ω = natural frequency of vibration

$\mathbf{w}$ = deformation vector at the nodal points

$\mathbf{A}$ = symmetric band matrix of width 5

$\mathbf{B}$ = positive diagonal matrix

Therefore ω^2 are the eigenvalues of the symmetric band matrix $\mathbf{B}^{-\frac{1}{2}}\mathbf{A}\mathbf{B}^{-\frac{1}{2}}$. The analysis is capable of describing all possible combinations of boundary conditions.

From a teaching standpoint, the analysis is both concise and elegant, and should be of interest to teachers of final year engineering mathematics courses and to mechanical engineers embarking on an M.Sc. programme.

Variational Formulation

The turbine disc is idealized as a rotating circular disc of variable thickness (Figure 1). The thickness distribution is given by

$$\left.\begin{aligned} h(r) &= b_1, \quad a_1 \leqslant r \leqslant a_2 \\ &= \text{variable}, \quad a_2 < r \leqslant a_{M-1} \\ &= b_M, \quad a_{m-1} \leqslant r \leqslant a_M \end{aligned}\right\} \tag{2}$$

where $b_1, b_M, a_1, a_2, a_{M-1}, a_M$ are constants. The radial distance is measured from the axis of rotation along the normal direction, while $h(r)$ is measured parallel to the axis of rotation.

The strain and kinetic energies due to the bending deformation are given by Timoshenko.[11]

$$V = \iint \frac{D}{2}\left\{\left(\frac{\partial^2 u}{\partial r^2}+\frac{1}{r}\frac{\partial u}{\partial r}+\frac{1}{r^2}\frac{\partial^2 u}{\partial \theta^2}\right)^2 - 2(1-\nu)\left[\frac{\partial^2 u}{\partial r^2}\left(\frac{1}{r}\frac{\partial u}{\partial r}+\frac{1}{r^2}\frac{\partial^2 u}{\partial \theta^2}\right)-\left(\frac{\partial}{\partial r}\frac{1}{r}\frac{\partial u}{\partial \theta}\right)^2\right]\right\} r\,\mathrm{d}r\,\mathrm{d}\theta \tag{3}$$

$$T = \iint \tfrac{1}{2}\rho h\left(\frac{\partial u}{\partial t}\right)^2 r\,\mathrm{d}r\,\mathrm{d}\theta \tag{4}$$

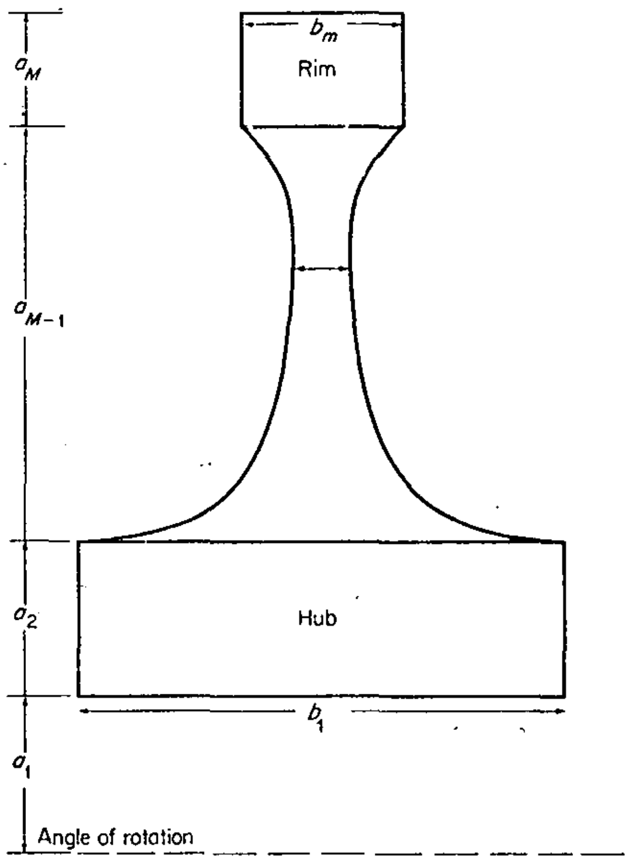

Figure 1. *Cross section of typical turbine disc*

where $u(r, \theta, t)$ = axial displacement at time t of section whose initial co-ordinates are r, θ.

$$D = \frac{\mathrm{Eh}^3(r)}{12(1-\nu^2)} g \quad \text{(bending stiffness)}$$

E = Young's modulus

ν = Poisson's ratio

g = acceleration due to gravity

The work done by the centrifugal forces is calculated as follows (Figure 2):
Let ϕ = slope in radial plane on disc, therefore

$$\phi = \frac{\partial u}{\partial r}$$

Centrifugal force on element $\rho \, \mathrm{d}V$ is given by

$$\begin{aligned} F &= \rho \, \mathrm{d}V\Omega^2(r - u\phi) \\ &= \rho\Omega^2(r-u\phi)\, hr \, \mathrm{d}r \, \mathrm{d}\theta \end{aligned}$$

$$\text{Work done on this element} = F \sin \phi u = Fu\phi$$

$$= \rho\Omega^2\left(r - u\frac{\partial u}{\partial r}\right) h \frac{\partial u}{\partial r} ur \, \mathrm{d}r \, \mathrm{d}\theta$$

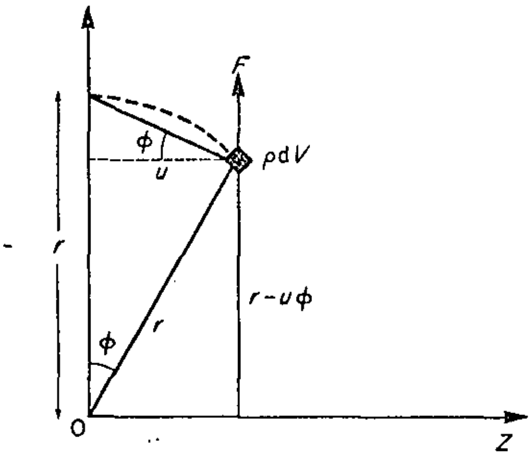

Figure 2. *Centrifugal effects on disc deformation*

Therefore

$$A = \iint \rho\Omega^2 h\left(r - u\frac{\partial u}{\partial r}\right)\frac{\partial u}{\partial r}\, ur\,\mathrm{d}r\,\mathrm{d}\theta$$

$$\approx \iint \rho\Omega^2 hr\frac{\partial u}{\partial r}\, ur\,\mathrm{d}r\,\mathrm{d}\theta \tag{5}$$

where

$$\Omega = \text{rotational speed of disc}$$

This is derived on the assumption of small bending deformations. Therefore from Hamilton's principle

$$\delta\int_{\text{initial}}^{\text{final}} (T - V + A)\,\mathrm{d}t = 0 \tag{6}$$

Finite Difference Formulation

Consider deflections harmonically dependent on both θ and t.

$$u = W(r)\sin(n\theta + pt) \tag{7}$$

where

$$n = \text{number of nodal diameters.}$$

Substituting equations (3), (4), (5) and (7) in equation (6) gives

$$\delta\int rL(r)\,\mathrm{d}r = 0 \tag{8}$$

where

$$L(r) = \frac{D}{2}\left\{\left(\frac{\mathrm{d}^2 W}{\mathrm{d}r^2} + \frac{1}{r}\frac{\mathrm{d}W}{\mathrm{d}r} - \frac{n^2}{r^2}W\right)^2 - 2(1-\nu)\left[\frac{\mathrm{d}^2 W}{\mathrm{d}r^2}\left(\frac{1}{r}\frac{\mathrm{d}W}{\mathrm{d}r} - \frac{n^2}{r^2}W\right)\right.\right.$$

$$\left.\left. - \frac{n^2}{r^2}\left(\frac{\mathrm{d}W}{\mathrm{d}r} - \frac{W}{r}\right)^2\right]\right\} + \rho\Omega^2 hr\, W\frac{\mathrm{d}W}{\mathrm{d}r} - \frac{\omega^2}{2}\rho h W^2 \tag{9}$$

This is discretized using the central difference approximations

$$\left.\begin{aligned}\left(\frac{dW}{dr}\right)_i &= \frac{W_{i+1}-W_{i-1}}{2\Delta}\\ \left(\frac{d^2 W}{dr^2}\right)_i &= \frac{W_{i+1}-2W_i+W_{i-1}}{\Delta^2}\end{aligned}\right\} \tag{10}$$

obtained by dividing the interval $[a_1, a_m]$ into finite increments by points $(r_0, r_1, \ldots, r_n)$ selected at equally spaced intervals of length Δ. Therefore

$$\left.\begin{aligned}&a_1 = r_0 < r_1 < r_2 < \ldots < r_{m-1} < r_m = a_M\\ &r_i = r_0 + i\Delta, \quad i = 0, 1, \ldots, m\end{aligned}\right\} \tag{11}$$

The function $L(r)$ defined by equation (9) is calculated at the points $(r_0, r_1, \ldots, r_m)$ using equation (10). Therefore

$$\begin{aligned}L_i &= L(r_i)\\ &= a_{i-1} W_{i-1}^2 + b_i W_i^2 + c_{i+1} W_{i+1}^2 + d_i W_{i-1} W_i + e_i W_i W_{i+1} + f_i W_{i+1} W_{i-1} - \frac{\omega^2}{2} \rho r_i h_i W_i^2\end{aligned} \tag{12}$$

where

$$a_{i-1} = \frac{D_i r_i}{2\Delta^4}\left[\left(1-\frac{\Delta}{2r_i}\right)^2 + 2(1-\nu)\left(\frac{\Delta}{2r_i}+\frac{n^2\Delta^2}{4r_i^2}\right)\right]$$

$$b_i = \frac{D_i r_i}{2\Delta^4}\left[\left(2+\frac{n^2\Delta^2}{r_i^2}\right)^2 - 2(1-\nu)\left(\frac{2n^2\Delta^2}{r_i^2}-\frac{n^2\Delta^2}{r_i^4}\right)\right]$$

$$c_{i+1} = \frac{D_i r_i}{2\Delta^4}\left[\left(1+\frac{\Delta}{2r_i}\right)^2 - 2(1-\nu)\left(\frac{\Delta}{2r_i}-\frac{n^2\Delta^2}{4r_i^2}\right)\right]$$

$$d_i = -\frac{D_i r_i}{\Delta^4}\left[\left(1-\frac{\Delta}{2r_i}\right)\left(2+\frac{n^2\Delta^2}{r_i^2}\right) + (1-\nu)\left(\frac{\Delta}{r_i}-\frac{n^2\Delta^2}{r_i^2}-\frac{n^2\Delta^3}{r_i^3}\right)\right] - \frac{1}{2\Delta}\rho\Omega^2 r_i^2 h_i$$

$$e_i = -\frac{D_i r_i}{\Delta^4}\left[\left(1+\frac{\Delta}{2r_i}\right)\left(2+\frac{n^2\Delta^2}{r_i^2}\right) + (1-\nu)\left(-\frac{\Delta}{r_i}-\frac{n^2\Delta^2}{r_i^2}+\frac{n^2\Delta^3}{r_i^3}\right)\right] + \frac{1}{2\Delta}\rho\Omega^2 r_i^2 h_i$$

$$f_i = \frac{D_i r_i}{2\Delta^4}\left[2\left(1-\frac{\Delta^2}{4r_i^2}\right) - (1-\nu)\frac{n^2\Delta^2}{2r_i^2}\right]$$

Discretizing the integral (8) using a trapezoidal type approximation in conjunction with equation (12) gives

$$\begin{aligned}\int_{r_0}^{r_m} L\,dr &= \Delta\left(\frac{L_0}{2}+\sum_{i=1}^{m-1} L_i + \frac{L_m}{2}\right)\\ &= \Delta\left(\sum_{i=-1}^{m+1}\alpha_i W_i^2 + \sum_{i=-1}^{m}\beta_i W_i W_{i+1} + \sum_{i=-1}^{m-1}\gamma_i W_i W_{i+2} - \frac{\omega^2}{4}\rho r_0 h_0 W_0^2\right.\\ &\qquad \left. - \frac{\omega^2 \rho}{2}\sum_{i=1}^{m-1} r h_i W_i^2 - \frac{\omega^2}{4}\rho r_m h_m W_m^2\right)\end{aligned} \tag{13}$$

where

$$\alpha_i = \frac{a_{-1}}{2}, \quad i = -1$$

$$= \frac{b_0}{2} + a_0, \quad i = 0$$

$$= \frac{c_1}{2} + a_1 + b_1, \quad i = 1$$

$$= a_i + b_i + c_i, \quad 2 \leqslant i \leqslant m-2$$

$$= \frac{a_{m-1}}{2} + b_{m-1} + c_{m-1}, \quad i = m-1$$

$$= \frac{b_m}{2} + c_m, \quad i = m$$

$$= \frac{c_{m+1}}{2}, \quad i = m+1$$

$$\beta_i = \frac{d_0}{2}, \quad i = -1$$

$$= \frac{e_0}{2} + \mathrm{d}_1, \quad i = 0$$

$$= \mathrm{d}_{i+1} + e_i, \quad 1 \leqslant i \leqslant m-2$$

$$= \frac{d_m}{2} + e_{m-1}, \quad i = m-1$$

$$= \frac{e_m}{2}, \quad i = m$$

$$\gamma_i = \frac{f_0}{2}, \quad i = -1$$

$$= f_{i+1}, \quad 0 \leqslant i \leqslant m-2$$

$$= \frac{f_m}{2}, \quad i = m-1$$

Eigenvalue Formulation

The stationary condition (8) transforms to

$$\frac{\partial}{\partial W_i}\int_{r_0}^{r_m} L(r)\,\mathrm{d}r = 0, \quad i = -1, 0, \ldots, n+1$$

Therefore from equation (13)

$$\left.\begin{aligned}
&2\alpha_{-1} W_{-1}+\beta_{-1} W_0+\gamma_{-1} W_1 = 0, \quad i=-1\\
&\beta_{-1} W_{-1}+2\alpha_0 W_0+\beta_0 W_1+\gamma_0 W_2 = \frac{\omega^2}{2}\rho r_0 h_0 W_0, \quad i=0\\
&\gamma_{-1} W_{-1}+\beta_0 W_0+2\alpha_1 W_1+\beta_1 W_2+\gamma_1 W_3 = \omega^2 \rho r_1 h_1 W_1, \quad i=1\\
&\gamma_{i-2} W_{i-2}+\beta_{i-1} W_{i-1}+2\alpha_i W_i+\beta_i W_{i+1}+\gamma_i W_{i+2} = \omega^2 \rho r_i h_i W_i, \quad i=2,\ldots,m-2\\
&\gamma_{m-3} W_{m-3}+\beta_{m-2} W_{m-2}+2\alpha_{m-1} W_{m-1}+\beta_{m-1} W_m+\gamma_{m-1} W_{m+1}\\
&\qquad\qquad\qquad\qquad = \omega^2 \rho r_{m-1} h_{m-1} W_{m-1}, \quad i=m-1\\
&\gamma_{m-2} W_{m-2}+\beta_{m-1} W_{m-1}+2\alpha_m W_m+\beta_m W_{m+1} = \frac{\omega^2}{2}\rho r_m h_m W_m, \quad i=m\\
&\gamma_{m-1} W_{m-1}+\beta_m W_m+2\alpha_{m+1} W_{m+1} = 0, \quad i=m+1
\end{aligned}\right\} \qquad (14)$$

Eliminating the redundant variables W_{-1}, W_{m+1}, these equations can be written in the matrix form

$$\mathbf{A}\mathbf{w} = \omega^2 \mathbf{B}\mathbf{w} \qquad (15)$$

where

$$\mathbf{w} = \begin{pmatrix} w_0 \\ w_1 \\ \vdots \\ w_m \end{pmatrix} \qquad (16)$$

$$\mathbf{B} = \rho \begin{bmatrix} \frac{1}{2}r_0 h_0 & & & & \bigcirc \\ & r_1 h_1 & & & \\ & & \ddots & & \\ & \bigcirc & & r_{m-1} h_{m-1} & \\ & & & & \frac{1}{2}r_m h_m \end{bmatrix} \qquad (17)$$

Therefore $\mathbf{B}$ is a positive diagonal matrix while $\mathbf{A}$ is a symmetric matrix which has the special form given by

$$\mathbf{A} = \begin{bmatrix}
2\alpha_0-\frac{\beta_{-1}^2}{2\alpha_{-1}} & \beta_0-\beta_{-1}-\frac{\gamma_{-1}}{2\alpha_{-1}} & \gamma_0 & & & & \bigcirc \\
\beta_0-\beta_{-1}-\frac{\gamma_{-1}}{2\alpha_{-1}} & 2\alpha_{-1}-\frac{\gamma_{-1}^2}{2\alpha_{-1}} & \beta_1 & \gamma_1 & & & \\
\gamma_0 & \beta_1 & 2\alpha_2 & \beta_2 & \gamma_2 & & \\
\cdot & \cdot & \cdot & \cdot & \cdot & \cdot & \cdot \\
 & & & & 2\alpha_{m-2} & \beta_{m-2} & \gamma_{m-2} \\
 & & & & \beta_{m-2} & 2\alpha_{m-1}-\frac{\gamma_{m-1}^2}{2\alpha_{m+1}} & \beta_{m-1}-\frac{\beta_m \gamma_{m-1}}{2\alpha_{m+1}} \\
 & \bigcirc & & & & \beta_{m-1}-\frac{\beta_m \gamma_{m-1}}{2\alpha_{m+1}} & 2\alpha_m-\frac{\beta_m}{2\alpha_{m+1}}
\end{bmatrix} \qquad (18)$$

All the elements are zero except those in the principal diagonal and four adjacent diagonals. This is called a band matrix of width five. From equation (15)

$$\det(\mathbf{A}-\omega^2\mathbf{B}) = 0$$

Therefore

$$\det(\mathbf{B}^{-\frac{1}{2}}\mathbf{A}\mathbf{B}^{-\frac{1}{2}}-\omega^2\mathbf{I}) = 0 \tag{19}$$

Therefore ω^2 are the eigenvalues of the symmetric band matrix $\mathbf{B}^{-\frac{1}{2}}\mathbf{A}\mathbf{B}^{-\frac{1}{2}}$. They are calculated using standard matrix usercode programs (English Electric Marconi KDF9).

Boundary Conditions

This analysis is based on the natural boundary condition and corresponds to the inner and outer radii of the disc being free. The other physical boundary conditions correspond to the forced boundary conditions for the problem, so that the minimization must be carried out subject to these constraint conditions. The modified matrices are readily obtained from the original **A**, **B** matrices by deleting either the first row and column, the last row and column, or both, and changing the first or last or both elements of the resulting matrices.

For example, suppose the inner radius is clamped and the outer radius free. Therefore

$$W = \frac{dW}{dr} = 0 \quad \text{at} \quad r = a_1$$

From equations (10) and (11)

$$W_0 = 0$$

$$W_{-1} = W_1$$

Using these results in equations (13) and (14) gives

$$\mathbf{A}^{(1,1)}\mathbf{w}^{(1)} = \omega^2\mathbf{B}^{(1,1)}\mathbf{w}^{(1)} \tag{20}$$

where

$$w^{(1)} = \begin{pmatrix} w_1 \\ \vdots \\ w_m \end{pmatrix}$$

$\mathbf{A}^{(1,1)}$, $\mathbf{B}^{(1,1)}$ are matrices of order m obtained by deleting the first row and column of the original matrices **A**, **B** defined by equations (17) and (18), and such that

$$A^{(1,1)}_{(11)} = 2(\alpha_{-1}+\alpha_1+\gamma_{-1})$$

For different boundary conditions different submatrices of **A**, **B** are chosen for the eigenvalue calculations. Table I gives these submatrices for the various boundary conditions.

Conclusions

This eigenvalue analysis is admirably suitable for programming on a digital computer and enables the rapid calculation of the natural frequencies of vibration and the modal shape matrix.

The eigenvalue calculations are based on reducing the matrix to tridiagonal form by Householder's method.[12] The eigenvalues of this matrix are found by a modified Sturm sequence method.[13] The corresponding eigenvectors are found by the Wielandt inverse iteration method.[13]

The program was written in usercode for use on an English Electric KDF9 computer. The flow chart for the program is given in Figure 3.

Table I. Modified matrices $\mathbf{A}^{pq}$, $\mathbf{B}^{pq}$ and associated elements for various boundary conditions

Inner radius \ Outer radius	Free	Clamped	Simply supported
Free	$\mathbf{A}, \mathbf{B}$	$\mathbf{A}^{(m+1,\, m+1)}, \mathbf{B}^{(m+1,\, m+1)}$ $A_{m,m}^{(m+1,\, m+1)} = 2(\alpha_{m+1}+\alpha_{m-1}+\gamma_{m-1})$	$\mathbf{A}^{(m+1,\, m+1)}, \mathbf{B}^{(m+1),\, m+1)}$ $A_{m,m}^{(m+1,\, m+1)} = 2\left[\alpha_{m+1}\left(\frac{2r_m-\nu\Delta}{2r_m+\nu\Delta}\right)^2+\alpha_{m+1}-\left(\frac{2r_m-\nu\Delta}{2r_m+\nu\Delta}\right)\gamma_{m-1}\right]$
Clamped	$\mathbf{A}^{(1,\,1)}, \mathbf{B}^{(1,\,1)}$ $A_{11}^{(1,\,1)} = 2(\alpha_{-1}+\alpha_1+\gamma_{-1})$	$\mathbf{A}^{(1,\,1;\, m+1,\, m+1)}$ $\mathbf{B}^{(1,\,1;\, m+1,\, m+1)}$ $A_{11}^{(1,\,1;\, m+1,\, m+1)} = 2(\alpha_{-1}+\alpha_1+\gamma_{-1})$ $A_{m-1,\, m-1}^{(1,\,1;\, m+1,\, m+1)} = 2(\alpha_{m+1}+\alpha_{m-1}+\gamma_{m-1})$	$\mathbf{A}^{(1,\,1;\, m+1,\, m+1)}$ $\mathbf{B}^{(1,\,1;\, m+1,\, m+1)}$ $A_{11}^{(1,\,1;\, m+1,\, m+1)} = 2(\alpha_{-1}+\alpha_1+\gamma_{-1})$ $A_{m-1,\, m-1}^{(1,\,1;\, m+1,\, m+1)} = 2\left[\alpha_{m+1}\left(\frac{2r_m-\nu\Delta}{2r_m+\nu\Delta}\right)^2+\alpha_{m-1}-\left(\frac{2r_m-\nu\Delta}{2r_m+\nu\Delta}\right)^2\gamma_{m-1}\right]$
Simply supported	$\mathbf{A}^{(1,\,1)}, \mathbf{B}^{(1,\,1)}$ $A_{11}^{(1,\,1)} = 2\left[\alpha_1\left(\frac{2r_0+\nu\Delta}{2r_0-\nu\Delta}\right)^2+\alpha_1-\left(\frac{2r_0+\nu\Delta}{2r_0-\nu\Delta}\right)^2\gamma_{-1}\right]$	$\mathbf{A}^{(1,\,1;\, m+1,\, m+1)}$ $\mathbf{B}^{(1,\,1;\, m+1,\, m+1)}$ $A_{11}^{(1,\,1;\, m+1,\, m+1)} = 2\left[\alpha_{-1}\left(\frac{2r_0+\nu\Delta}{2r_0-\nu\Delta}\right)^2+\alpha_1-\left(\frac{2r_0+\nu\Delta}{2r_0-\nu\Delta}\right)\gamma_{-1}\right]$ $A_{m-1,\, m-1}^{(1,\,1;\, m+1,\, m+1)} = 2(\alpha_{m+1}+\alpha_{m-1}+\gamma_{m-1})$	$\mathbf{A}^{(1,\,1;\, m+1,\, m+1)}$ $\mathbf{B}^{(1,\,1;\, m+1,\, m+1)}$ $A_{11}^{(1,\,1;\, m+1,\, m+1)} = 2\left[\alpha_{-1}\left(\frac{2r_0+\nu\Delta}{2r_0-\nu\Delta}\right)^2+\alpha_1-\left(\frac{2r_0+\nu\Delta}{2r_0-\nu\Delta}\right)^2\gamma_{-1}\right]$ $A_{m-1,\, m-1}^{(1,\,1;\, m+1,\, m+1)} = 2\left[\alpha_{m+1}\left(\frac{2r_m-\nu\Delta}{2r_m+\nu\Delta}\right)+\alpha_{m-1}-\left(\frac{2r_m-\nu\Delta}{2r_m+\nu\Delta}\right)\gamma_{m-1}\right]$

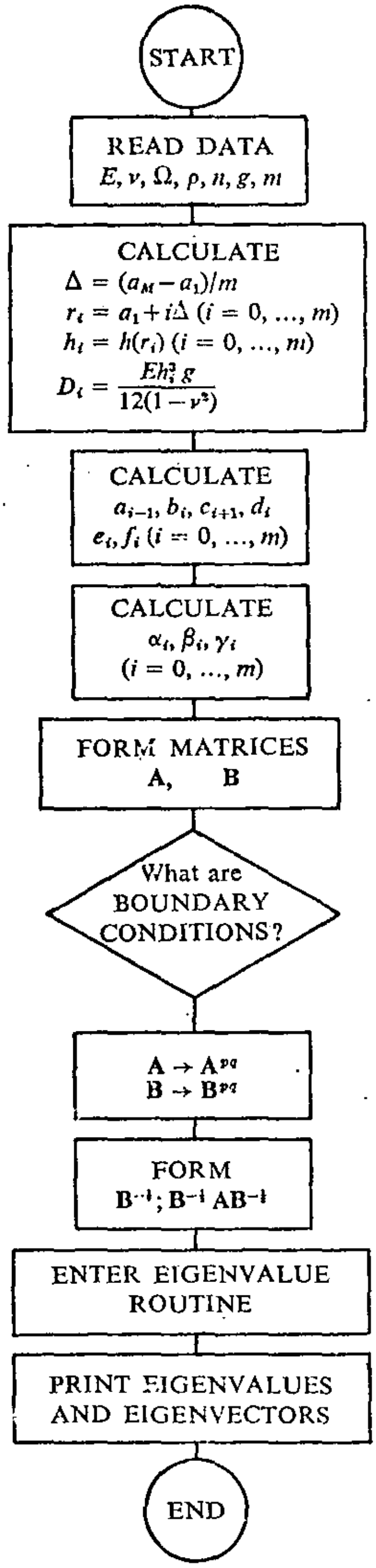

Figure 3. *Flow chart for disc eigenvalue calculations*

From a research standpoint, the analysis includes the possibilities of generalizations to include shear correction terms and the effects of large thickness theory, giving rise to non-linear eigenvalue problems.

Acknowledgements

This investigation was sponsored and supported by the Mechanical Engineering Laboratories of the English Electric Company, Whetstone, Leicester, under project numbers 420029/30 and is released by permission of the Company.

The computer program was written by J. W. Ward, MEL/Service programming section.

REFERENCES

1. O. P. T. Kantorowicz, 'Of steam turbine wheel, batch and blade vibrations', *Trans. NE. Cst Instn Engrs Shipbldrs*, 79, 51–93 (1962).
2. H. J. Thomas, 'Vibration problems of steam turbines', *A.E.G. Prog.* 3, 125–135 (1966).
3. R. V. Southwell, 'On the free transverse vibrations of a uniform circular disc clamped at its centre; and on the effects of rotation', *Proc. R. Soc.* A101, 133–153 (1922).
4. G. Z. Harris, 'The normal modes of a circular plate of variable thickness', *Q. Jl Mech. appl. Math.* **21**, 321–327 (1968).
5. F. F. Ehrich, 'A matrix solution for the vibration of modes of non-uniform discs', *Trans. ASME. J. appl. Mech.* **23**, 109–115 (1956).
6. P. S. Brass, *Disc and Blade Vibrations*, English Electric Co. Report No. W/M (6B), 1965, p. 1022.
7. H. M. Gibbs, *Disc and Blade Vibration Problems—Spline Control Flowchart for the Location of Natural Frequencies*, English Electric Co. Internal memorandum, February 1967.
8. B. M. E. de Silva, *Automated Weight Minimization Based on a Frequency Constant*, English Electric Co. Report No. W/M (4B), 1968, p. 1452.
9. B. M. E. de Silva, 'Minimum weight design of discs using a frequency constraint', *Trans. ASME. J. Engng Ind.* **91**, 1091–1099 (1969).
10. 'Latent roots and vectors of symmetric matrix', Subroutine No. L 235, in *English Electric Leo Marconi KDF 9 usercode Matrix Scheme Users' Manual* (A4-27-1).
11. S. Timoshenko, *Theory of Plates and Shells*, McGraw–Hill, 1940, Chap. 2 and 7.
12. J. H. Wilkinson, 'Householder's method for the solution of the algebraic eigenproblem', *Comput. J.* 3, 23–27 (1960).
13. J. H. Wilkinson, *Algebraic Eigenvalue Problems*, Oxford University Press, 1965.

Chapter 8

Feasible Direction Methods in Structural Optimization

B.M.E. de Silva

8.1 Introduction

This chapter describes procedures in the class of feasible direction methods which have been applied to structural optimization problems. A feasible direction method was perhaps the first of the nonlinear programming procedures to be employed in structural optimization by Schmit in 1960[1], and methods in this class enjoyed intensive development during the subsequent six years. They continue to be under development, but at a less rapid pace, and to be applied effectively to significant engineering problems, some of which are described in this chapter.

The basis of feasible direction methods was outlined by Fletcher in Section 5.4. They are in the class of direct search algorithms and therefore address themselves to the determination of the distance α^k and direction $\underset{\sim}{d}^k$ of travel from the k^{th} to the $(k+1)^{th}$ point in design space, i.e.

$$\underset{\sim}{x}^{k+1} = \underset{\sim}{x}^k + \alpha^k \underset{\sim}{d}^k \tag{8.1}$$

The direction $\underset{\sim}{d}^k$ is feasible if a move in that direction does not cause constraint violation, i.e.

$$g_j(\underset{\sim}{x}^k + \alpha^k \underset{\sim}{d}^k) \leq 0, \; j = 1,2,\ldots,m \tag{8.2}$$

for a system with m constraints. This requires a negative dot product of the move direction and the gradient to each active constraint. Denote $\tilde{\nabla} g_{\ell}$ as the gradient of one of the p active constraints $1,\ldots,\ell,\ldots,p$. Collecting these in an $n \times p$ matrix designated as $[\tilde{\nabla} g]$, where n is the number of design variables, we have as the condition of feasibility

$$[\tilde{\nabla} g]^T \tilde{d}^k \leq 0 \qquad (8.3)$$

A desirable condition upon the direction of move is that it also results in a reduction of the merit function, i.e. be useable. In this case, the mathematical condition is stated as

$$(\tilde{\nabla} W)^T \tilde{d}^k \leq 0 \qquad (8.4)$$

Furthermore, note should be taken of the side constraints, which define upper (U_j) and lower (L_j) bounds on each design variable x_j, i.e.

$$L_j \leq x_j \leq U_j, \; j = 1,\ldots,n \qquad (8.5)$$

Nearly all the applications to be described here employ an accelerated steepest descent mode (see Section 5.2), to travel from an initial feasible design point (or steepest ascent if the initial point is infeasible) to a constraint. When the constraint is reached it is impossible to move in the steep descent direction without piercing the constraint. An alternate redesign procedure is therefore required which insures continuation of the optimum design process. The development of efficient directions and distances of search from the boundary of the constraint set constitutes a central phase of the feasible direction procedure; it is studied in this chapter under the following categories:

1. Constant merit redesign (Section 8.2).

2. Travel on the constraint surface, with the direction of travel $\underset{\sim}{d}^{q}$ being a projection of the merit function gradient on the constraint boundary (Section 8.3).

3. Travel in a direction between the limits defined in (1) and (2), with the direction chosen "optimally" via utilization of a linear programming algorithm (Section 8.4).

These alternative procedures will now be discussed in turn.

8.2 <u>Constant Merit Redesign</u>

8.2.1 <u>Method of Alternate Base Planes</u>

Amongst the first successful attempts at the boundary redesign problem was the method of <u>alternate base planes</u> used by Schmit, et al[1-3] for the minimum weight design of trusses and waffle plates. This ~~method~~ is a quasi-random method which seeks a feasible design on the constant weight contour through a main constraint. The problems were characterized by linear side constraints which were handled separately to ensure designs, most of which lie within the lower (L_j) and upper (U_j) bounds on the design variables. The basic steps of the algorithm are as follows (Figure 8.1):

(i) The program begins by generating random search directions $\underset{\sim}{d}^{i}$ in planes normal to the coordinate lines OX_1, OX_2,..., OX_n in turn. This scanning is controlled by a counter i which is initially set to unity.

(ii) Generate the direction cosines of the straight line of travel,

$$d_j^i = R_j / \left(\sum_{j \neq i}^{n} R_j^2\right)^{1/2} \quad ; \; j = 1,2,\ldots,n, \; j \neq i$$

$$= 0 \qquad ; \; j = i$$

where R_j are random numbers.

(iii) Calculate the distance to the side constraints

$$\alpha_j^i = (L_j - x_j^k)/d_j^i \quad j = 1,2,\ldots,n, \; j \neq i$$

$$\alpha_{n+j}^i = (U_j - x_j^k)/d_j^i \quad j = 1,2,\ldots,n, \; j \neq i$$

This ensures that the proposed designs satisfy most of the side constraints. From this set of values $\underset{\sim}{\alpha}^i$ the smallest positive value is selected and designated λ^i and the negative value having the smallest absolute value is designated μ^i.

(iv) Six random numbers R_q ($q = 1,2,\ldots,6$) between 0 and 1 are generated in two sets of three and are multiplied by λ_i and μ_i to give the distance of travel in the base plane, designated by α_q^i, i.e.

$$\alpha_q^i = R_q \lambda^i \quad q = 1,2,3$$

$$= R_q \mu^i \quad q = 4,5,6$$

(v) The proposed new designs are given by

$$\underset{\sim}{x}_q^i = \underset{\sim}{x}^k + \alpha_q^i \underset{\sim}{d}^i$$

where $x_{q_i}^i$ is calculated from the constant weight condition

$$W(\underset{\sim}{x}^k) = W(x_1^k + \alpha_q^i d_1^i, \ldots, x_{i-1}^k + \alpha_q^i d_{i-1}^i, x_{q_i}^i,$$

$$x_{i+1}^k + \alpha_q^i d_{i+r}^i \ldots x_n^k + \alpha_q^i d_n^i)$$

(vi) Check the six proposed designs against the behavioral constraints in the order $q = 1,2,\ldots,6$. If any one of $\underset{\sim}{x}_q^i$ is feasible, steepest descent motion continues as before. Otherwise go to step (vii).

(vii) Replace $i \rightarrow i+1$, go to step (ii) and repeat iterations.

Step (vii) is equivalent to changing the base plane. If still no feasible design is forthcoming, the boundary point is taken as the optimal.

8.2.2 A Hill-Climbing Procedure

The above method was applied by deSilva[4,5] to the minimum weight design of discs subject to stress and vibration constraints. The method consumed considerable computer time in searching through the random directions to determine a feasible point on the constant weight contour and deteriorated rapidly for high dimensional design spaces. Schmit and Fox[6] used a simple hill-climbing technique based on a zig-zag concept to determine the optimal response of a spring-mass-damper system characterized by merit contours with a sharp ridge. This is a more rational method, based on an understanding of the problem, and a modification of this procedure by deSilva[5] is as follows:

$\underset{\sim}{x}^{k-2}$, $\underset{\sim}{x}^{k-1}$, $\underset{\sim}{x}^{k}$ are three successive designs generated by gradient mode of travel with $\underset{\sim}{x}^{k}$ a boundary point on a behavioral constraint

$$W(\underset{\sim}{x}^k) < W(\underset{\sim}{x}^{k-1}) < W(\underset{\sim}{x}^{k-2}) \tag{8.6}$$

where

$$g_j(\underset{\sim}{x}^k),\ g_j(x^{k-1}),\ g_j(x^{k-2}) \leq 0 \quad j = 1,\ldots,m \tag{8.7}$$

and $\quad g_\ell(\underset{\sim}{x}^k) = 0$ for at least one ℓ in $1 \leq \ell \leq m$

For the disc problem to be discussed in further detail subsequently, the g_ℓ corresponds to the vibration constraints in which the fundamental frequencies are required to exceed specified lower bounds. Let $\underset{\sim}{x}$ be the foot of the perpendicular from $\underset{\sim}{x}^k$ onto the gradient mode vector $\underset{\sim}{d}^{k-2}$ from $\underset{\sim}{x}^{k-2}$ (Figure 8.2).

$$\therefore\ \underset{\sim}{x} = (1 + \frac{\alpha^{k-1}}{\alpha^{k-2}} \cos\,\theta)\underset{\sim}{x}^{k-1} - \frac{\alpha^{k-1}}{\alpha^{k-2}} \cos(\theta)\underset{\sim}{x}^{k-2} \tag{8.8}$$

where

$$\cos\,\theta = \underset{\sim}{d}^{k-2}.\underset{\sim}{d}^{k-1}$$

This is the scalar product of the (normalized) steepest descent vectors $\underset{\sim}{d}^{k-2}$, $\underset{\sim}{d}^{k-1}$ with associated step lengths α^{k-2}, α^{k-1}. The angle θ measures the amount of zig-zag. In the absence of a sharp ridge on the merit contours, θ is small, $\cos\,\theta > 0$ and the point $\underset{\sim}{x}$ will be close to, but seldom on, the behavioral constraint g_ℓ which is essentially a numerical or non-analytic constraint.

Consider a direction with direction ratios defined by

$$\begin{aligned} \underset{\sim}{d}_\ell^k &= \underset{\sim}{x} - \underset{\sim}{x}^k \text{ if } g_\ell(x) < 0 \\ &= \underset{\sim}{x}^k - \underset{\sim}{x} \text{ otherwise} \end{aligned} \tag{8.9}$$

Under suitable conditions, $\underset{\sim}{d}^k$ approximates a tangent move towards the interior of the feasible set. In the disc problem the weight is a quadratic in x_n but linear in the remaining variables $x_1, x_2, \ldots, x_{n-1}$. The proposed direction of search is obtained by projecting the normalized direction (8.9) onto the constant weight hyperplane.

$$W(x_1, \ldots, x_{n-1}, x_n^k) = W(x_1^k, \ldots, x_{n-1}^k, x_n^k) \quad (8.10)$$

The distance of travel yields an alternate step within the design variable bounds (8.5):

$$\alpha^k = \min_{1 \leq j \leq n} \{(x_j^k - L_j), (U_j - x_j^k)\} \quad (8.11)$$

For a design violating a main constraint the step length (8.11) is progressively reduced. For multiple constraints, p in number, the direction (8.9) is replaced by the weighted sum

$$\underset{\sim}{d}^k = \sum_{\ell=1}^{p} c_\ell \underset{\sim}{d}_\ell^k \quad (8.12)$$

where c_ℓ are non-negative weighting factors determined using Zoutendijk-type procedures[7].

A different alternate step mode uses the distance of travel (8.11) to generate the direction of bounce into the feasible regions. The direction cosines d_i^k, $i = 1,2,\ldots,n$, are constrained by the condition that the objective function remain constant

$$W(\underset{\sim}{x}^k) = W(\underset{\sim}{x}^k + \alpha^k \underset{\sim}{d}^k) \quad (8.13a)$$

and the condition that $\underset{\sim}{d}^k$ be normalized

$$(\underset{\sim}{d}^k)^T \underset{\sim}{d}^k = 1 \quad (8.13b)$$

where α^k is the step length defined by (8.11). The system

(8.13) is indeterminate for $n > 2$. Complete solutions are obtained by using the physics of the problem to specify (n-2) components of $\underset{\sim}{d}^k$ and calculating the rest from Equations (8.13).

The method was applied to the minimal weight design of discs[4] in which the stresses were constrained to lie below the yield stress for the material. One such turbine disc to be optimized is shown in Figure 8.3. The problem is discretized using a piecewise linear representation for the disc profile (Figure 8.4). The shape function h(r) (where r is the radial distance from the axis of rotation) is therefore approximated by a sequence of discrete thickness variables $\{b_j, j \in J\}$ at specified radial distance $\{a_j, j \in J\}$. From engineering design considerations the width of the hub and the rim shape are specified while the hub radius a_2 is variable. Thus, the design variables are $\{b_j, j \in J; a_2\}$. The weight is linear in b_j but quadratic in a_2.

The stress computations were based on Donath's method (see Ref. 4), and cannot be expressed as analytically defined functions of the design variables. The behavior variables are functions only in the sense that they are computer oriented rules for determining the behavior associated with a given design and are not given in a closed analytical form in terms of the design variables. The behavior variables may be regarded as a "black box" into which are put the design variables representing a given design and out of which comes the corresponding behavior variables for that design. These are then checked against the behavioral constraints. The side constraints are essentially linear and are of the form $b_j \leq \varepsilon$; $j \varepsilon J$; $L \leq a_2 \leq U$ where ε, L and U are specified positive tolerances.

The computer program starts from an initial feasible design and enters an accelerated steepest descent mode of travel, continuing in this mode until a constraint is encountered. It is then no longer possible to move in this mode without piercing the constraint. In this problem, this situation occurs when a section b_ℓ, $\ell \varepsilon J$ of the disc is at the yield stress. A feasible design is sought by thickening this section and thinning the section b_s, $s \varepsilon J$ furthest from the yield stress in such a manner as to leave the weight unchanged. All other thicknesses remain unchanged. Thus,

$$\begin{aligned} d_i &= 0; \quad & i &\neq \ell, s \\ &> 0; \quad & i &= \ell \\ &< 0; \quad & i &= s \end{aligned} \tag{8.14}$$

d_ℓ, d_s were calculated from the simultaneous equations (8.13) and gave polynomial equations consistent with (8.14). The step size was determined by (8.11) to ensure designs within the design variable bounds. Initially, a feasible point was obtained at the first redesign attempt and thereafter as the designs became more highly constrained, a feasible design was still forthcoming after the first few attempts. The synthesis was programmed to successively reduce the step length (8.11) of no feasible design was forthcoming after a specified number of redesign attempts. If still no feasible design was forthcoming, the next section furthest from yield was thinned and the above process repeated. As a last resort, the program enters the alternate base plane redesign procedure.

Optimum designs for the turbine disc of Figure 8.3 were accomplished for design spaces which ranged from four to eleven design variables. The initial design for an eleven-dimensional representation is illustrated in Figure 8.4. Results are shown for the random and selective search procedures, respectively, in Figures 8.5 and 8.6. Figure 8.7 shows the variation of the design weight as a function of the number of redesign attempts. Other results for this problem and complete details of the method are presented in Reference 4.

8.2.3 Structural Analysis-Influenced Travel

The alternate step modes studied hitherto do not utilize the mechanisms inside the structural analysis packages to influence the design optimizations from a main constraint. Gellatly and Gallagher[8] use constraint merit redesign techniques for the minimum weight design of trusses subject to stress and deflection constraints. The design variables are the cross-sectional areas, giving rise to a linear merit functions. The behavior variables are the element stresses and nodal deflections. They direct the boundary search by calculating the normals to the behavioral constraints in static and dynamic response regimes. To describe the associated formulations, we designate the relevant equations of matrix displacement analysis as

$$\begin{aligned} \underset{\sim}{P} &= \underset{\sim}{K}\,\underset{\sim}{\Delta} \\ \underset{\sim}{\sigma} &= \underset{\sim}{S}\,\underset{\sim}{\Delta} \end{aligned} \tag{8.15}$$

where $\underset{\sim}{K}$, $\underset{\sim}{S}$, and $\underset{\sim}{P}$ are, respectively, the stiffness, stress, and design load matrices. The stiffness matrix at a given point in the design sequence ($\underset{\sim}{K}_o$) will be altered due to the change in the element stiffness matrix ($\underset{\sim}{K}_i$) associated with the i^{th} design variable. Thus, the new stiffness ($\underset{\sim}{K}$) is represented by

$$\underset{\sim}{K} = \underset{\sim}{K}_o + \sum_i \delta x_i \underset{\sim}{K}_i \tag{8.16}$$

where δx_i is the change in the associated design variable. Reference 8 demonstrates that a local approximation to the normals to the behavioral constraints is then given by

$$\begin{aligned} \frac{\partial \underset{\sim}{\Delta}}{\partial x_i} &= -\underset{\sim}{K}_o^{-1} \underset{\sim}{K}_i \underset{\sim}{\Delta} \\ \frac{\partial \underset{\sim}{\sigma}}{\partial x_i} = \underset{\sim}{S} \frac{\partial \underset{\sim}{\Delta}}{\partial x_i} &= \underset{\sim}{S}^k \underset{\sim}{K}_o^{-1} \underset{\sim}{K}_i \underset{\sim}{\Delta} \end{aligned} \tag{8.17}$$

In the method of reference 8, the direction of bounce is obtained by projecting the normal onto the constant weight hyperplane. For points on multiple constraints, Gellatly[9] suggests a constraint direction based on the weighted sum of constraint normals, of the same form as Equation (8.12). The direction on the weight hyperplane is a linear combination of the form

$$\underset{\sim}{d}_W^k = c\underset{\sim}{d}_W^k + \sum_{\ell=1}^{p} c_\ell \underset{\sim}{d}_\ell^k \tag{8.18}$$

where c is a constant and $\underset{\sim}{d}_D^k$ is the normal to the constant weight hyperplane, i.e.

$$\underset{\sim}{d}_W^k \cdot \underset{\sim}{d}_D^k = 0 \tag{8.19}$$

For bounce back into the feasible regions, the direction

$\underset{\sim}{d}_W^k$ must make acute angles with all constraint normals. This condition is expressible in the form

$$\underset{\sim}{d}_\ell^k \cdot \underset{\sim}{d}_W^k = \varepsilon_\ell > 0 \qquad (8.20)$$

where ε_ℓ are specified tolerances, usually selected to be unity. From (8.18)

$$\begin{aligned} c\underset{\sim}{d}_W^k \cdot \underset{\sim}{d}_D^k + \sum_{\ell=1}^{p} c_\ell \underset{\sim}{d}_\ell^k \cdot \underset{\sim}{d}_D^k &= 0 \\ c\underset{\sim}{d}_W^k \cdot \underset{\sim}{d}_m^k + \sum_{\ell=1}^{p} c_\ell \underset{\sim}{d}_\ell^k \cdot \underset{\sim}{d}_m^k &= \varepsilon_m \text{ for all } m \end{aligned} \qquad (8.21)$$

These equations form a determinate system for c_ℓ. The matrix of coefficients tends to be ill-conditioned in the neighborhood of an optimal.

8.3 Constrained Boundary Motion

8.3.1 Best's Method[10,11]

One of the earliest applications of travel along the constraints in the context of the structural design problem is due to Best[10,11]. His method starts from a trial design in the feasible region and steeply descends to the nearest (main) constraint. From a boundary point the method moves on the constraint surface in a direction in which the merit decreases most rapidly.

Suppose the point lies at the intersection of p constraint hypersurfaces. The normals are determined using techniques similar to Equation (8.17) and are collected in the matrix $[\underset{\sim}{\nabla} g]$. The direction of travel $(\underset{\sim}{d}^k)$ is orthogonal to $[\underset{\sim}{\nabla} g]$.

$$[\underset{\sim}{\nabla} g]^T \underset{\sim}{d}^k = 0 \qquad (8.22)$$

and is assumed normalized, i.e. Equation (8.13b) applies. The rate of decrease of the weight in the direction $\underset{\sim}{d}^k$ is determined by

$$-\frac{d}{d\alpha^k} W[\underset{\sim}{x}^k + \alpha^k \underset{\sim}{d}^k] = -\sum_{i=1}^{n} \frac{\partial W}{\partial x_i} \underset{\sim}{d}_i^k = -(\underset{\sim}{d}^k)^T \underset{\sim}{\nabla} W \qquad (8.23)$$

The problem consists in maximizing (8.23) subject to the constraint conditions (8.13b, 8.22) so as to give the optimal direction of travel, $\underset{\sim}{d}^k$. We can accomplish this by the Lagrange multiplier technique. Introduce the Lagrange multipliers $\lambda_o, \lambda_1, \ldots, \lambda_p$. Then

$$-\underset{\sim}{\nabla} W + [\underset{\sim}{\nabla} g]\underset{\sim}{\lambda} + 2\lambda_o \underset{\sim}{d}^k = 0 \qquad (8.24)$$

where $\underset{\sim}{\lambda} = \{\lambda_1, \ldots, \lambda_p\}$.

From (8.13b, 8.22, and 8.24), the direction of travel is given by

$$\underset{\sim}{d}^k = \frac{\underset{\sim}{H}\underset{\sim}{\nabla} W}{2\lambda_o} \qquad (8.25)$$

where

$$\begin{aligned} \underset{\sim}{H} &= \underset{\sim}{I} - [\underset{\sim}{\nabla} g]\{[\underset{\sim}{\nabla} g]^T[\underset{\sim}{\nabla} g]\}^{-1}[\underset{\sim}{\nabla} g]^T \\ \lambda_o &= -\tfrac{1}{2}[(\underset{\sim}{H}\underset{\sim}{\nabla} W)^T(\underset{\sim}{H}\underset{\sim}{\nabla} W)]^{1/2} \end{aligned} \qquad (8.26)$$

The operator $\underset{\sim}{H}$ plays a central role in the gradient projection method as will be shown subsequently in Section 8.3.2.

The distance of travel is estimated to the nearest constraint, so that, to first order

$$g_j(\underset{\sim}{x}^k) + \alpha^k (\underset{\sim}{d}^k)^T \nabla g_j(\underset{\sim}{x}^k) = 0 \qquad (8.27)$$

The required step length is then

$$\alpha^k = \min_j \{ \frac{-g_j(\underset{\sim}{x}^k)}{(\underset{\sim}{d}^k)^T \underset{\sim}{\nabla} g_j(\underset{\sim}{x}^k)} \} \tag{8.28}$$

The method was applied by Best[10,11] to the minimum weight design of cantilever box structures in the presence of stress and deflection constraints. The method is primarily applicable to problems with very flat constraints in which movement in the direction $\underset{\sim}{d}^k$ does not give rise to significant constraint violation. This condition is usually not satisfied by behavioral constraints in structural mechanics. A modification was proposed by Schmit[12] where condition (8.22) is replaced by (8.3). This reduces the problem to one with inequality constraints with a corresponding increase in complexity.

Constrained boundary motion in conjunction with a dynamic constraint was used by Zarghamee[13] to maximize the frequency subject to a linear weight constraint. The frequency is calculated from the eigenvalue equation

$$[\underset{\sim}{k} - \omega^j \underset{\sim}{M}]\underset{\sim}{\Delta}^j = \underset{\sim}{0} \tag{8.29}$$

where $\underset{\sim}{K}$, $\underset{\sim}{M}$ are the stiffness and mass matrices respectively and $\underset{\sim}{\Delta}^j$ is here the modal shape corresponding to the eigenfrequency ω^j. The modified stiffness matrix is given by (8.16) and for the modified mass matrix

$$\underset{\sim}{M} = \underset{\sim}{M}_o + \sum_i \delta x_i \underset{\sim}{M}_i \tag{8.30}$$

Differentiating (8.29) partially with respect to x_i and using (8.16) and (8.30)

$$[\underset{\sim}{k}_i - \omega^j \underset{\sim}{M}_i]\underset{\sim}{\Delta}^j - \frac{\partial \omega^j}{\partial x_i} \underset{\sim}{M}\underset{\sim}{\Delta}^j + [\underset{\sim}{k} - \omega^j \underset{\sim}{M}]\frac{\partial \underset{\sim}{\Delta}^j}{\partial x_i} = 0 \tag{8.31}$$

Assume the eigenvectors $\underset{\sim}{\Delta}^j$ to form a complete set so that we can express their gradients as

$$\frac{\partial \underset{\sim}{\Delta}^j}{\partial x_i} = \sum_k \beta_{k_{i,j}} \underset{\sim}{\Delta}^k \qquad (8.32)$$

where $\beta_{k_{i,j}}$ are constants.

Also, we take note of the orthogonality property of the eigenvalues with respect to $\underset{\sim}{M}$ as a weighting matrix:

$$(\underset{\sim}{\Delta}^i)^T \underset{\sim}{M} \underset{\sim}{\Delta}^j = \delta_{ij} \qquad (8.33)$$

where δ_{ij} is the Kronecker delta ($\delta_{ij} = 0$ if $i \neq j$ and $\delta_{ij} = 1$ if $i = j$).

From (8.31-8.33)

$$\frac{\partial \omega^j}{\partial x_i} = (\underset{\sim}{\Delta}^j)^T [\underset{\sim}{k}_i - \omega^j \underset{\sim}{M}_i] \underset{\sim}{\Delta}^j \qquad (8.34)$$

This measures the rate of change of the frequency in terms of the corresponding eigenvector. The constraint on the total weight is of the form

$$W(\underset{\sim}{x}) = W_o + \sum_{i=1}^{n} W_i x_i \qquad (8.35)$$

where $W(\underset{\sim}{x}) \leq W_o$. Hence we have the linear constraint

$$\sum_{i=1}^{n} W_i x_i \leq 0 \qquad (8.36)$$

The problem therefore consists in maximizing the frequency $\omega^j(\underset{\sim}{x})$ subject to the linear constraint. The solution was based on the gradient projection method for linear constraints, in which the gradient direction (8.34) is projected on the linear constraint using the projection operator $\underset{\sim}{H}$. This gradient projection method is again taken up below. Generalizations of the analysis to more complex structures are given by Turner[14,15].

8.3.2 Gradient Projection Method

The gradient projection method, due to Rosen[16], has proved to be of value in the structural optimization area and applications to various structural systems are given by Brown and Ang[17].

For nonlinear constraints, the method offers considerable flexibility and scope and consists in orthogonal projection of the gradient into the linear manifold of the supporting hyperplanes to the active constraints. The basic steps of the algorithm are summarized as follows:

Suppose $\underset{\sim}{x}^k$ lies on p constraint surfaces. Using prior symbolism, the n × p matrix of normals is designated as $[\nabla \underset{\sim}{g}]$, where each column is assumed linearly independent of the rest. The projection operator, $\underset{\sim}{H}$, for the linear manifold spanned by the supporting hyperplanes is given by Equation (8.26). The normalized direction of travel (d^k) is therefore defined by

$$\underset{\sim}{d}^k = \frac{\underset{\sim}{H}\nabla \underset{\sim}{W}}{|\underset{\sim}{H}(\nabla \underset{\sim}{W})|} \tag{8.37}$$

The gradient vector $\underset{\sim}{\nabla} W(\underset{\sim}{x}^k)$ can be written as a linear combination of the projected gradient and the normals $\underset{\sim}{\nabla} g_j(\underset{\sim}{x}^k)$ to the active constraints

$$-\underset{\sim}{\nabla} W(\underset{\sim}{x}^k) = -\underset{\sim}{H}\underset{\sim}{\nabla} W(\underset{\sim}{x}^k) + \sum_{i=1}^{p} r_i \underset{\sim}{\nabla} g_i(\underset{\sim}{x}^k) \tag{8.38}$$

where the r_i are constants. It can be shown that if $-\underset{\sim}{H}\underset{\sim}{\nabla} W = \underset{\sim}{0}$ and $\underline{r} \leq 0$ then $\underset{\sim}{x}^k$ is a local optimum. Whenever $|\underset{\sim}{H}\underset{\sim}{\nabla} W| > 0$ a small step length α^k is taken in the projected direction (8.37) to a point of improved merit. Because of the curvature of the boundary, this will be a non-feasible point and an interpolation procedure, as detailed in Reference 17.

When $-\tilde{H}\nabla W = 0$ and $r_i > 0$ for some i (i = 1,...,p) the constraints for which $r_i > 0$ are removed and the analysis is performed on the intersection of the remaining constraints. This is represented by sets of recursion relations on $\tilde{H}$, $\tilde{r}$, and are given in Reference 16.

8.4 Linear Programming-type Methods

Another method of boundary redesign is Zoutendijk's method of feasible directions [7] which has been applied by Pope(18) to static problems and by Fox and Kapoor(19,20) to minimum weight design problems which include inequality constraints on the natural frequencies. The method consists in reducing the problem to a series of linear programs. We describe the method with reference to the problem treated by Fox and Kapoor.

The method first requires calculation of gradients to the active constraints. Equation (8.34) can be adapted to the calculation at the normal to the frequency constraint. The normals to the deflection constraints are given by the derivatives to the eigenvectors, as follows:

By differentiation of Equation (8.30) with respect to x_i and using Eq. (8.33), we have

$$[\tilde{k} - \omega^j \tilde{M}] \sum_k \beta_{k_{i,j}} \tilde{\Delta}^k + [\frac{\partial \tilde{k}}{\partial x_i} - \omega^j \frac{\partial \tilde{M}}{\partial x_i} - \frac{\partial \omega^j}{\partial x_i} \tilde{M}] \tilde{\Delta}^j = \tilde{0} \quad (8.39)$$

Premultiplying by $(\tilde{\Delta}^k)^T$ and using the orthogonality condition (Equation 8.33), we have for $k \neq j$

$$(\underset{\sim}{\Delta}^k)^T[\underset{\sim}{k} - \omega^j \underset{\sim}{M}]\sum_k \beta_{k_{i,j}} \underset{\sim}{\Delta}^k + (\underset{\sim}{\Delta}^k)^T[\frac{\partial \underset{\sim}{k}}{\partial x_i} - \omega^j \frac{\partial \underset{\sim}{M}}{\partial x_i}]\underset{\sim}{\Delta}^j = 0 \quad (8.40)$$

from which

$$\beta_{k_{i,j}} = (\underset{\sim}{\Delta}^k)^T[\frac{\partial \underset{\sim}{k}}{\partial x_i} - \omega^j \frac{\partial \underset{\sim}{M}}{\partial x_i}]\underset{\sim}{\Delta}^j/(\omega^j - \omega^k) \quad (8.41)$$

Also, for $k=j$, we have by differentiation of (8.33) with respect to x_i and other operations

$$\beta_{k_{i,j}} = -\frac{1}{2}(\underset{\sim}{\Delta}^j)^T \frac{\partial \underset{\sim}{M}}{\partial x_i} \underset{\sim}{\Delta}^j \quad (8.42)$$

Equations (8.34, 8.41 and 8.42) determine the normals to the behavioral constraints. The linear program for the problem is now formulated as the determination of a direction $\underset{\sim}{d}^k$ which minimizes the linear function $(\underset{\sim}{d}^k)^T \underset{\sim}{\nabla W}$ subject to the constraints represented by Equations (8.3) and (8.4), except that α^k is determined by (8.11) for linear side constraints.

8.5 Closure

This chapter has described some of the more commonly used boundary redesign techniques for structural problems. Many of these have structural analysis packages which, although relatively simple from a mathematical standpoint, involve extremely long and complex programming routines which consume considerable computer space and time. This limits a fuller utilization of classical nonlinear programming algorithms. The objective of structural optimization is not the determination of the numerical optimum to the constrained problem but rather improving the efficiency of existing structural systems. As a result of these considerations there is a growing tendency to utilize the structural analysis procedures to solve the boundary redesign problem. Analysis procedures based on finite element procedures enable a more automatic coupling of the analysis and synthesis phases of the design process.

REFERENCES

1. Schmit, L.A., "Structural Design by Systematic Synthesis," Proc. 2nd Conf. on Elect. Comp., ASCE, Pittsburgh, 1960.
2. Schmit, L.A. and Morrow, W.M., "Structural Synthesis with Buckling Constraints," J. Struct. Div. 89, ASCE, 1963, pp. 107-126.
3. Schmit, L.A., Kicher, T.P., and Morrow W.M., "Structural Synthesis Capability for Integrally Stiffened Waffle Plates," AIAA J. 1, 1963, pp. 2820-2836.
4. de Silva, B.M.E., "Application of Nonlinear Programming to the Automated Minimum Weight Design of Rotating Discs; in Optimization," (R. Fletcher, ed.), Academic Press, 1969, pp. 115-150.
5. de Silva, B.M.E., "Minimum Weight Design of Discs, Using a Frequency Constraint," Trans. ASME, J. Eng. Ind. 91, 1969, pp. 115-150
6. Schmit, L.A. and Fox, R.L., "Synthesis for a Simple Shock Isolator," NASA CR-55, 1964.
7. Zoutendijk, G., "Methods of Feasible Directions," Elsevier, 1960.
8. Gellatly, R.A. and Gallagher, R.H., "A Procedure for Automated Minimum Weight Structural Design; Part I: Theoretical Basis," Aeron. Quart. 17, 1966, pp. 332-342.
9. Gellatly, R.A., "Development of Procedures for Large Scale Automated Minimum Weight Structural Design," AFFDL-TR-66-180, December 1966.
10. Best, G., "A Method of Structural Weight Minimization Suitable for High Speed Digital Computers," J. Aircraft 1,

1964, pp. 129-133.

11. Best, G., "Completely Automatic Weight Minimization Method for High Speed Digital Computers," J. Aircraft 1, 1964, pp. 129-133.

12. Schmit, L.A., "Comments on 'Completely Automatic Weight Minimization Method for High Speed Digital Computers,'" J. Aircraft 1, 1964, pp. 375-376.

13. Zarghamee, M.S., "Optimum Frequency of Structures," AIAA J. 6, 1968, pp. 749-750.

14. Turner, M.J., "Design of Minimum Mass Structures with Specific Natural Frequencies," AIAA J. 5, 1967, pp. 406-412.

15. Turner, M.J., "Optimization of Structures to Satisfy Flutter Requirements," AIAA J. 7, 1969, pp. 945-951.

16. Rosen, J.B., "The Gradient Projection Method for Nonlinear Programming; Part I: Linear Constraints," SIAM J. 8, 1960, pp. 181-217. Part II: Nonlinear Constraints, SIAM J. 9, 1961, pp. 514-532.

17. Brown, D.M. and Ang, A.H.S., "Structural Optimization by Nonlinear Programming," J. Struct. Div. 92, ASCE, 1966, pp. 319-340.

18. Pope, G.G., "The Design of Optimum Structures of Specified Basic Configuration," Int. J. Mech. Sci. 10, 1968, pp. 251-263.

19. Fox, R.L. and Kapoor, M.P., "Structural Optimization in the Dynamic Response Regime: A Computational Approach," AIAA J. 8, 1970, pp. 1798-1804.

20. Fox, R.L. and Kapoor, M.P., "Rates of Change of Eigenvalues and Eigenvectors," AIAA J. 6, 1968, pp. 2426-2429.

Figures. Chapter 8

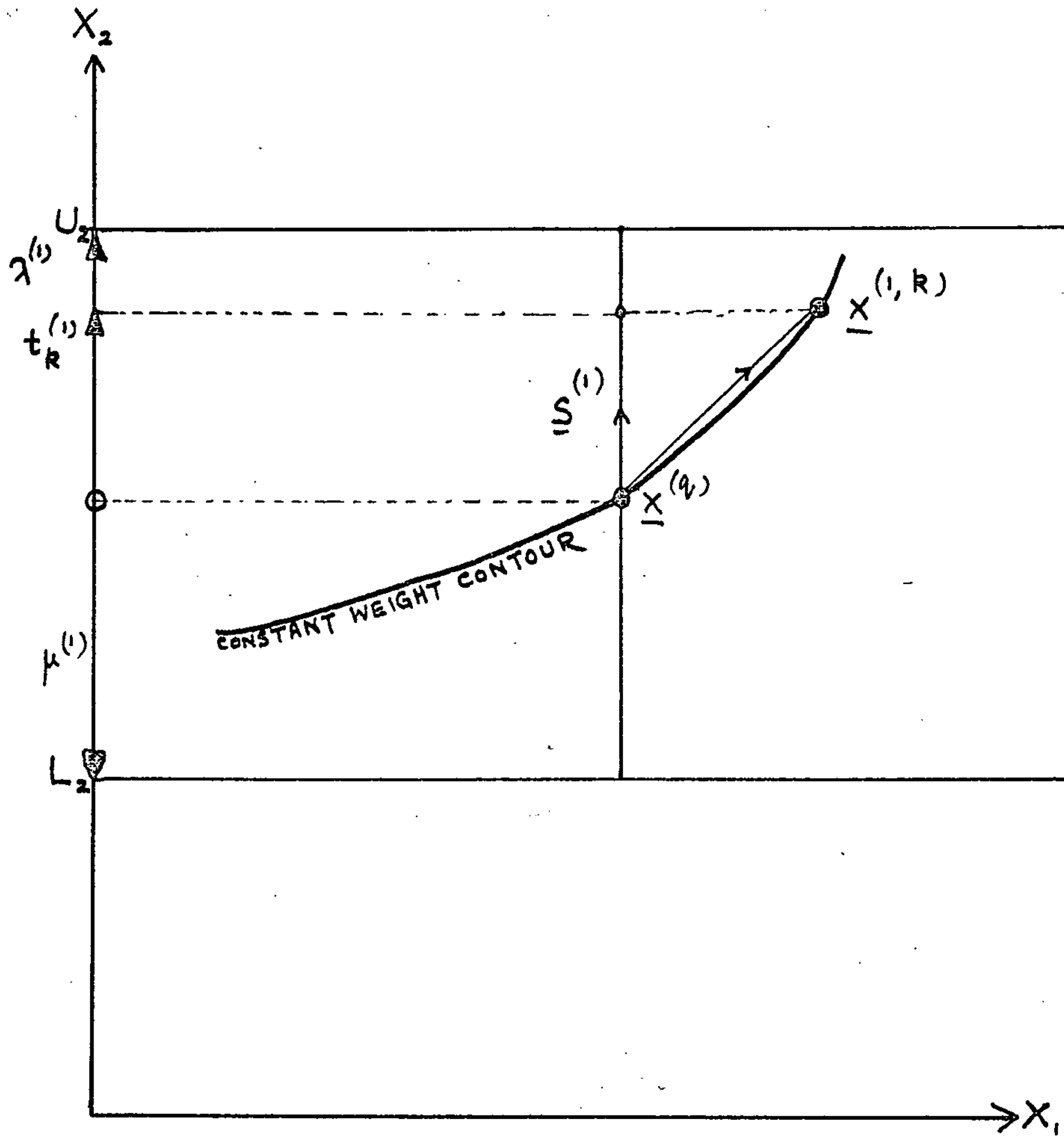

FIG. 8.1 METHOD OF ALTERNATE BASE PLANES.

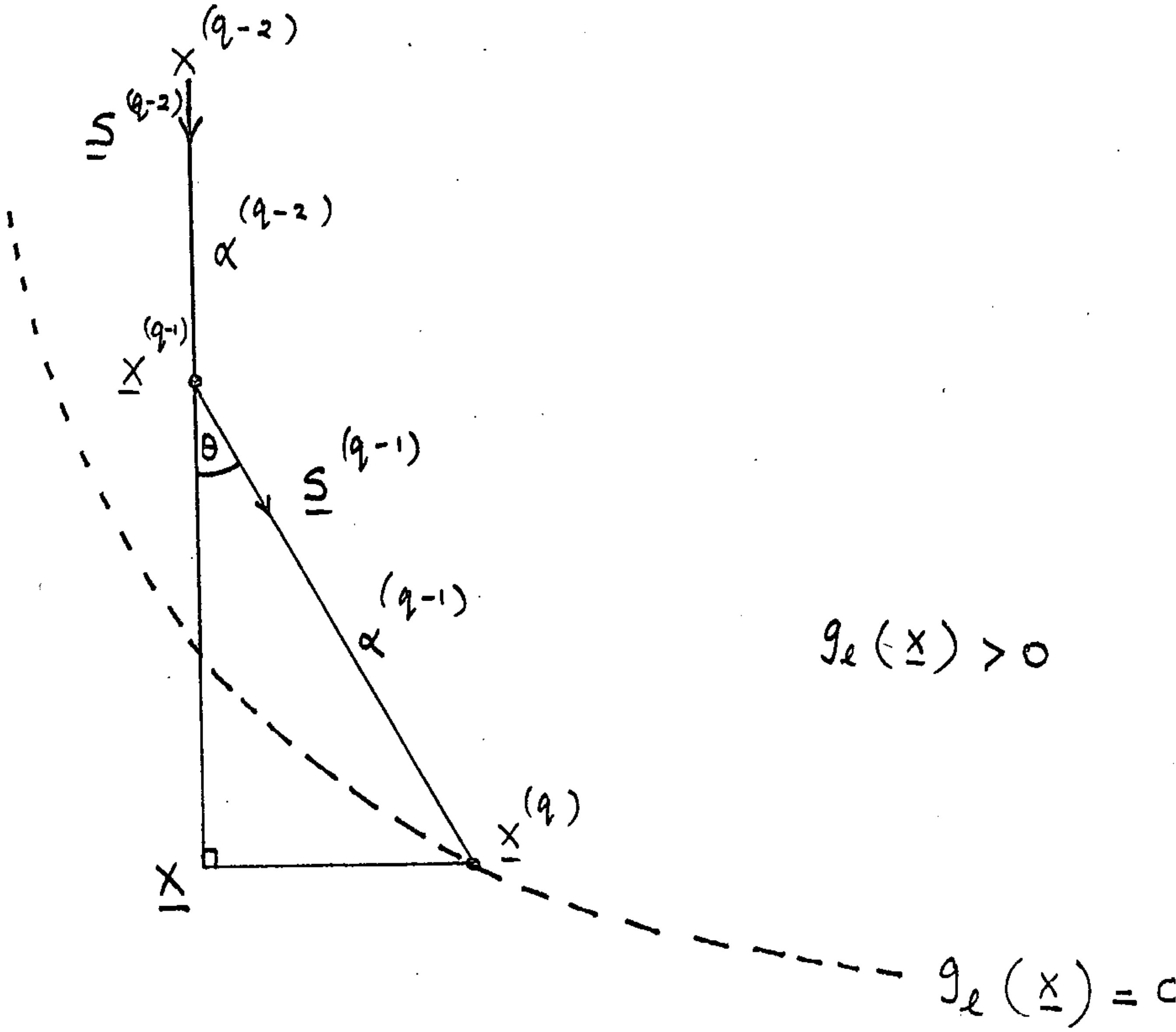

FIG 8.2 ESTIMATE FOR DIRECTION OF BOUNCE GIVEN THREE SUCCESSIVE STEEPEST DESCENT MODE DESIGNS.

THE ENGLISH ELECTRIC COMPANY LIMITED
MECHANICAL ENGINEERING LABORATORY
WHETSTONE

Report No. W/M (6B) p. 13

Fig Sht No. 8.3

CROSS SECTION OF TYPICAL TURBINE DISC

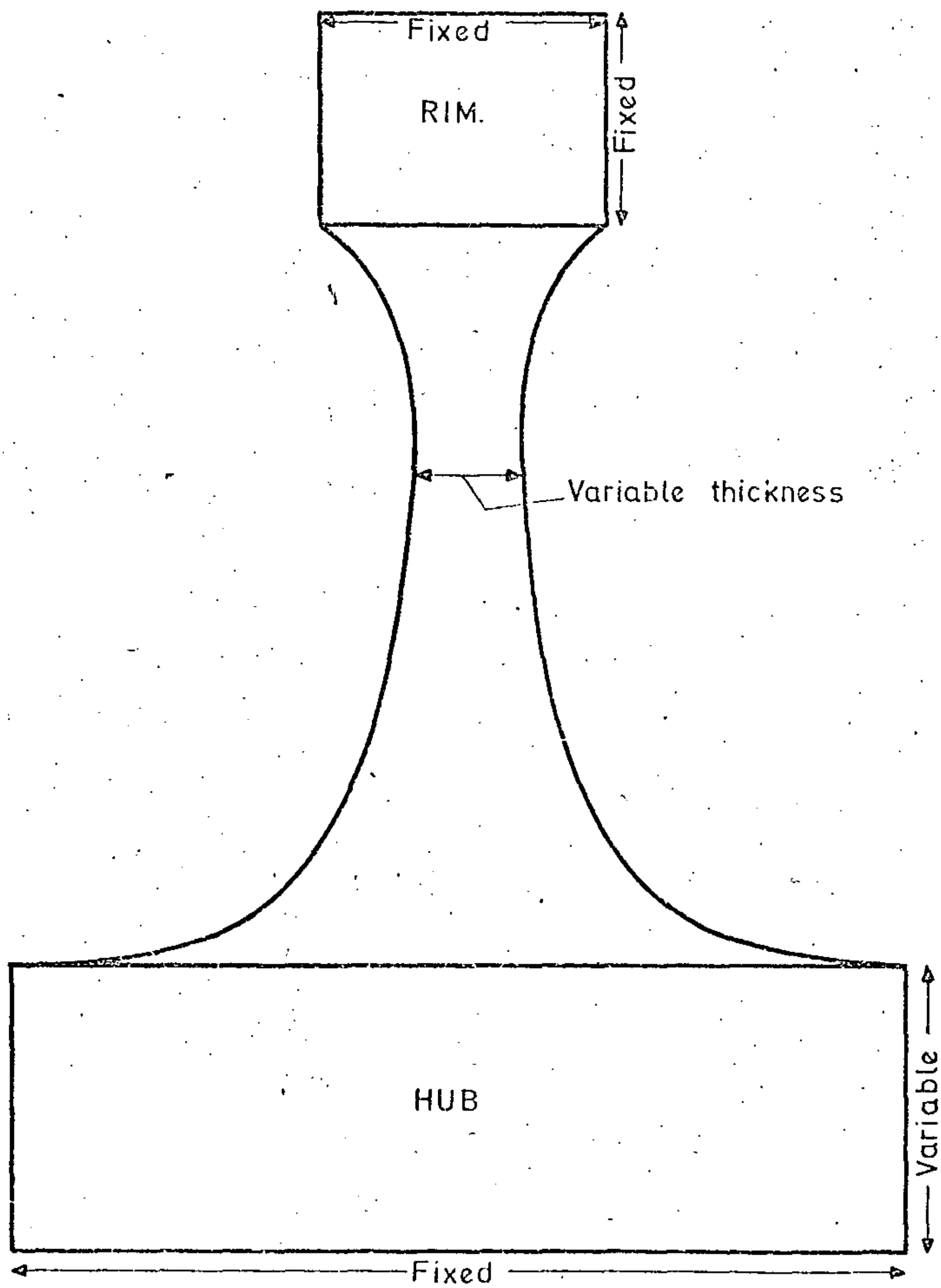

g No. R20172-7447 Date. June 1967

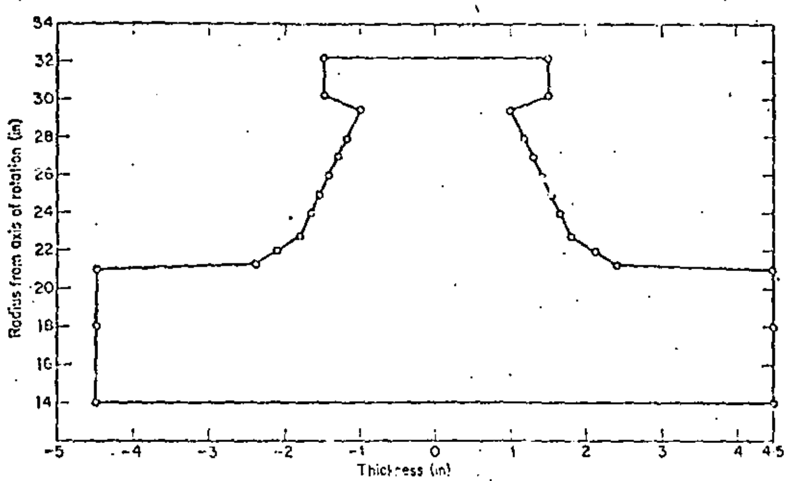

Fig. 8.4

Cases 3a, 3b. Initial design. Weight = $3{\cdot}58973 \times 10^3$ lb.

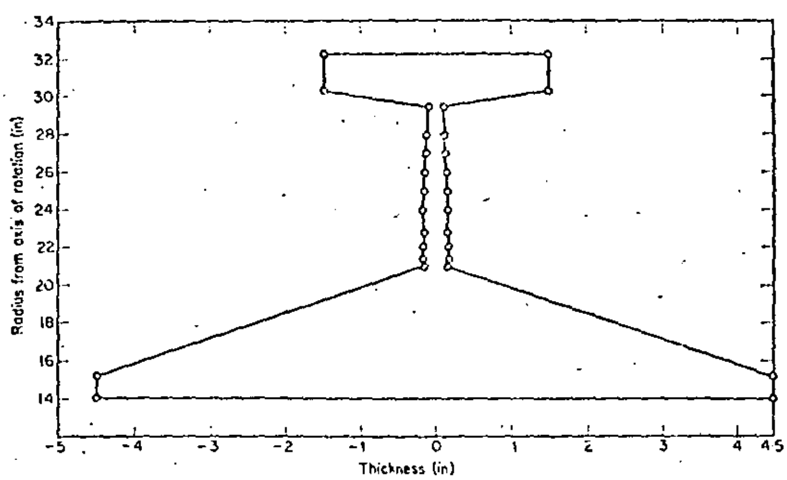

Fig. 8.5

Case 3a; 186 cycles. Final design. Weight = $1{\cdot}61401 \times 10^3$ lb

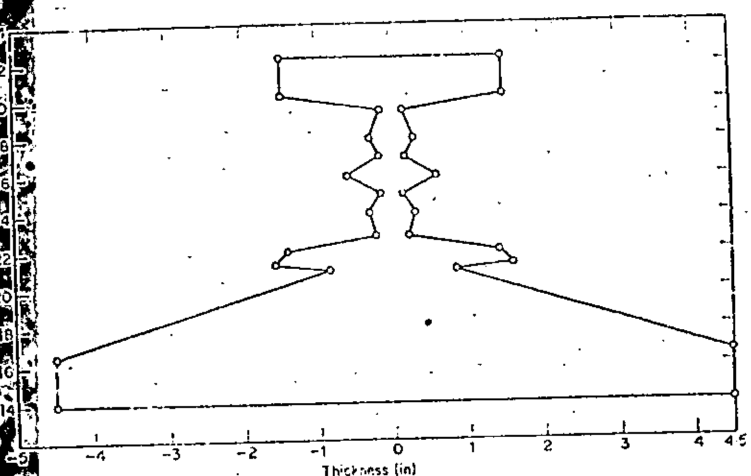

Case 3b. Final design. Weight = $2{\cdot}14537 \times 10^3$ lb.

Fig. 8.6

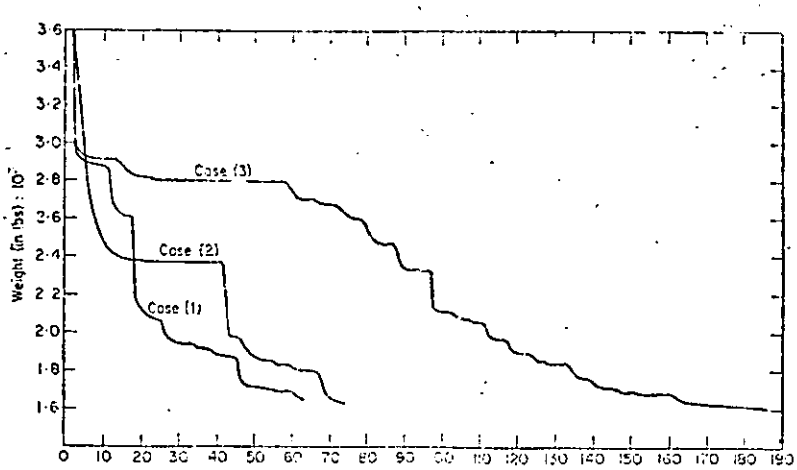

Weight *versus* total redesign attempts. Based on selective search techniques for moving away from a bound point.

Fig. 8.7

NOMENCLATURE

PART I: Chapter 1

a	radius of plate; also weight parameter in beam analysis
a_1, a_m	inner and outer radii respectively of disc
a_2	outer radius of hub
a_{m-1}	inner radius of rim
$\underline{B}F(\underline{x})$	behaviour matrix
b_i	elements of the behaviour matrix
$b_i^{(b)}$	bounds on the b_i
b_1, b_m	width of the disc hub and rim respectively
b	weight parameter
$\underline{C}$	submatrix of normals to active constraints
$c_i(\underline{x})$	general form for inequality constraints
D	dissipation rate per unit volume
E	Young's modulus
e_{ij}	components of strain tensor
e_r, e_θ	radial and tangential components of strain
$e_{\alpha\beta}$	strain components in generalised coordinates
$e^{\theta}_{\alpha\beta}$	maximum value of $e_{\alpha\beta}$
$\underline{F}$	flexibility matrix
F_i	body forces per unit volume
f	yield function
$\underline{f}$	fatigue susceptibility coefficient
g	gradient vector
$H(t)$	Heaviside unit step function

h	thickness of disc at a radial distance r
$\underline{K}_i$	stiffness of the i-member of structure
$\underline{K}_o$	stiffness matrix
k	yield constant
$k_{\alpha\beta}$	curvature in generalised coordinates
$\underline{L}$	lower bound on design variable vector
$\underline{L}^*$	lower bound on behaviour matrix
ℓ	length of beam
$\underline{M}$	mass matrix
M_o, M	fully plastic bending moment
M_r, M_θ	radial and tangential components of bending moment
$M_{\alpha\beta}$	bending moments in generalised coordinates
m	beam weight per unit length
$\underline{m}^{(q)}$	steepest descent vector for studying ridge effects in merit contours
m_j	coefficients of the linearised weight function
$\underline{P}$	load matrix
p	transverse load per unit area
Q_i, q_i	generalised stress and strain components respectively
q	design cycle counter
$\underline{R}$	matrix of the normals to constraints
R_1, R_2	radii of curvature in the circumferential and meridianal plane
r	radial distance measured from axis of disc
r_{ij}	elements of $\underline{R}$
r_o	intermediate radial point in hub
S	closed surface in the material under consideration
S_T	part of S on which the surface forces T_i are specified
S_U	part of S on which the velocity components u_i vanish

$\underline{S}$	stress matrix
s,S	radial stresses at inner and outer radii respectively
T	tensile load per unit circumferential length
T_i	surface tractions per unit area
t	distance of travel in design parameter space
U	strain energy per unit area
$\underline{U}$	upper bound on design variable vector
$\underline{U}^*$	upper bound on behaviour matrix
u	deflection
u_i	compatible velocity field components
$u_i^{(c)}$	velocity field for a structure on the point of collapse
$\underline{u}$	optimal boundary search vector
V	volume enclosed by S
V_C	volume of structure on the point of collapse
V_m	absolute minimum weight volume
V_S	volume of structure which is safe
W	transverse velocity field in plastic case; radial component of displacement in elastic case; also used in certain instances to denote weight
W_o	initial optimal weight estimation
W_s	draw down weight
$\underline{x}$	design variable vector
z	plate thickness measured from undeformed middle surface
α_1, α_2, β_1, β_2	coefficients used in a penalty function formulation based on exponential functions
Δb_i	gap vector
ΔW	weight reduction
$\underline{\delta}^{(max)}$	upper bound on deflection vector

$\underline{\delta}$	matrix with element δ_j
δ_j	deflections in structure
$\underline{\delta}^{(i)}$	i-eigenvector for standard vibration equation
ε	control parameter on step length
$\varepsilon_1{}^i$	± 1
θ	hinge rotation, also angular coordinate
λ	constant of proportionality
$\lambda^{(i)}$	i-eigenvalues for standard vibration equation
ν	Poisson's ratio
$\phi(\underline{x})$	penalty function component of $\psi_s(\underline{x})$ in the Heaviside transformation
$\underline{\psi}$	direction of travel
$\psi_s(\underline{x})$	modified objective function incorporating constraints using penalty function techniques
ρ	density of material
$\underline{\sigma}$	matrix with element σ_i
σ_i	stresses in structure
σ_{ij}	component of stress tensor
σ_o	yield stress
σ_r	radial component of stress
σ_θ	tangential component of stress
$\sigma_1 \quad \sigma_2$	principal circumferential and meridianal stress

Chapter 2

a_j	radial coordinate at standard sections of disc
b_j	thickness coordinates at standard sections of disc
$b_j(\underline{x})$	behaviour constraint functions
G^*	union of G_k
G_k	constraint hypersurfaces in design space
$g_k(\underline{x})$	equivalent representation for design constraints
H	system Hamiltonian
I	index set for i
J	index set for j
K_j	upper bound on element thickness
L	bounds on the behaviour variables
N	normalisation factor
n	total number of points of division of disc
p_i	radial coordinates at intermediate sections of disc
q_i	thickness coordinates at intermediate sections of disc
R	feasible region
$S_i(\underline{x})$	side constraint functions
U	bounds on the behaviour variables
u	control function
W_k	modified weight functional
α	coefficient of thermal expansion
$\beta^{(i)}$	variable metric type step length
ε	lower bound on step length
Δ	step length along $\underline{\lambda}$

η_k	control parameter for modified weight functional
λ_1, λ_2	adjoint variables
$\underline{\lambda}$	search direction from boundary point
ϕ	temperature difference
τ_1, τ_2, τ_3	principal shearing stresses

Chapter 3

a_i	amplitude for the displacements
L	Lagrangian function
ℓ	Lagrangian energy density
n	number of nodal diameters round disc
p	natural frequency of vibration
p_o	critical frequency
Q_r, Q_θ	shear forces
T	kinetic energy
T_{ij}	elements of quadratic form for T
t	kinetic energy density
u	axial displacement as a function of polar coordinates r, θ and time t
$\underline{u}$	control vector
V	potential energy
V_{ij}	elements of quadratic form for V
v	potential energy density
W(r)	radial form of function which describes axial displacement
$\underline{x}$	state vector

ε	phase factor for the displacements
δ_{mj}	additional mass elements
η	efficiency coefficient
η_i	(small) displacements from equilibrium configuration
Ω	speed of rotation of disc

PART II: Chapter 4

F	integrand of J
$\underline{f}$	vector of state differential equations
f_o	integral component of I
G	non-integral component of I
g_k	inequality constraints
H	Hamiltonian incorporating inequality constraints
$\hat{H}$	Hamiltonian in the absence of inequality constraints
I	merit criterion
J	modified functional for first variation analysis
ℓ	order of vector $\underline{w}$
m	order of vector $\underline{u}$
n	order of vector $\underline{x}$
p	scalar product of the state differential equations with the normals to the active constraints
p'	suffix denoting active constraints
t	independent variable
t_o, t_1	initial and final values of t
$\underline{u}$	control parameter vector
$\underline{u}_c$	partitioned control vector
V	Bellman optimality function
$\underline{w}$	control vector
$\underline{x}$	state vector
$\theta^{(o)}$, $\theta^{(1)}$	initial and final manifolds
$\lambda(t)$	generalised Lagrange Multiplier associated with the state differential equations
$\mu(t)$	generalised Lagrange multiplier associated with inequality constraints

Chapter 5

C_1, C_2	arbitrary constants of integration
F	yield condition for material
r_o, r_1	intermediate radial points
$\theta^{(1)}$, $\theta^{(m)}$	initial and final manifolds
$\eta(r)$	function of class C^2
$\underline{\lambda}$	adjoint vector

Chapter 6

a_i	coefficients of G
A,B,C,D,E,F	coefficients of the adjoint equations
f_o	transformed objective function
f_1	constraint function on weight
f_2	locator polynomial for frequency
$G(p)$	merit functional
k	large parameter
p_k	k-natural frequency of vibration
W_o	upper bound on weight
α_i	arbitrary constants of integration
η	small parameter for power series expansion of $\underline{\lambda}$
Λ	large parameter
μ	coefficients of f_2
Φ	Gaussian distribution function
Ω	arguments of the Bessel functions